AMERICAN ASSOCIATION FOR THE ADVANCEMENT OF SCIENCE

SCIENCE

13 OCTOBER 1995 $7.00
VOL. 270 • PAGES 205–348

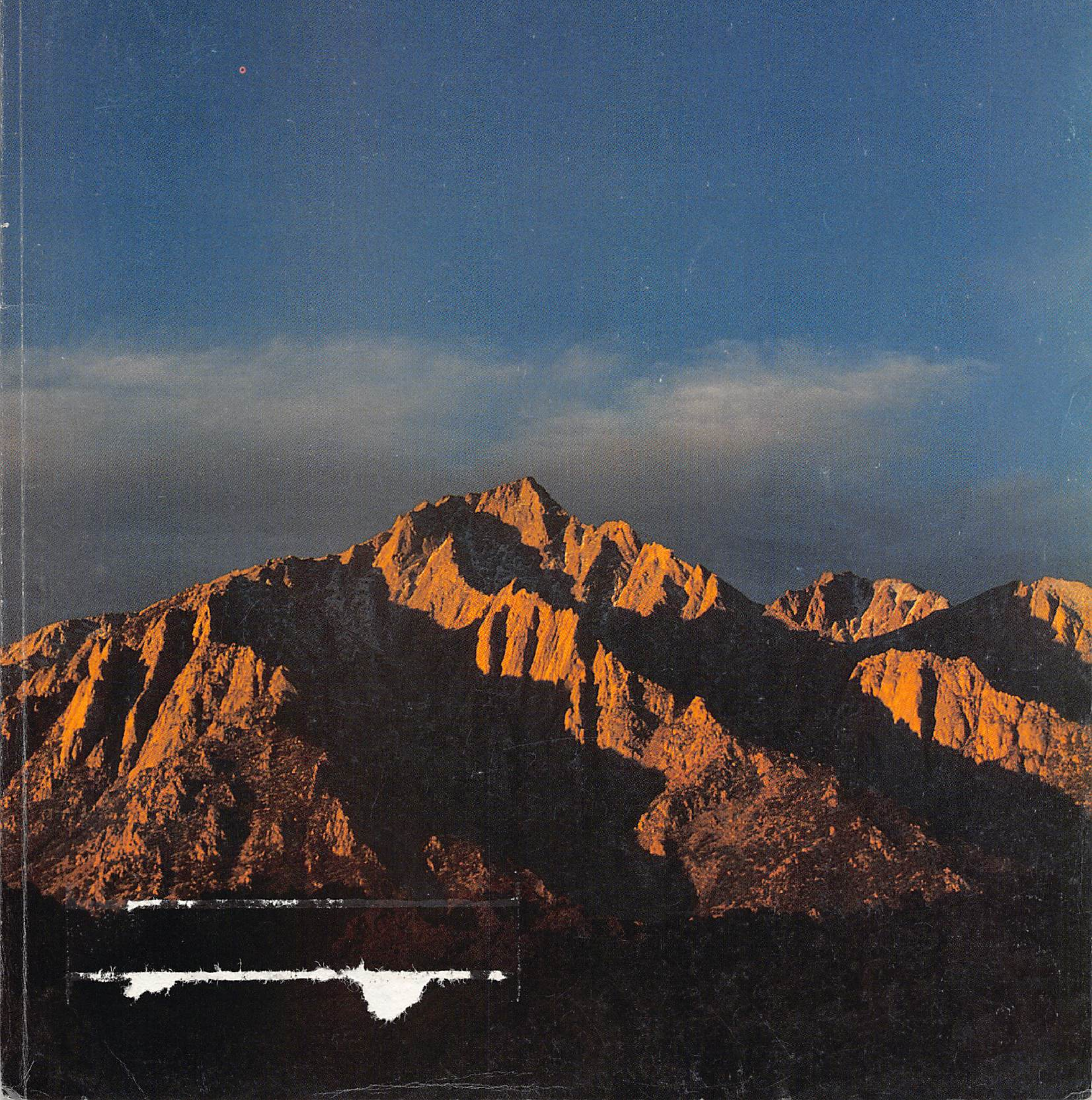

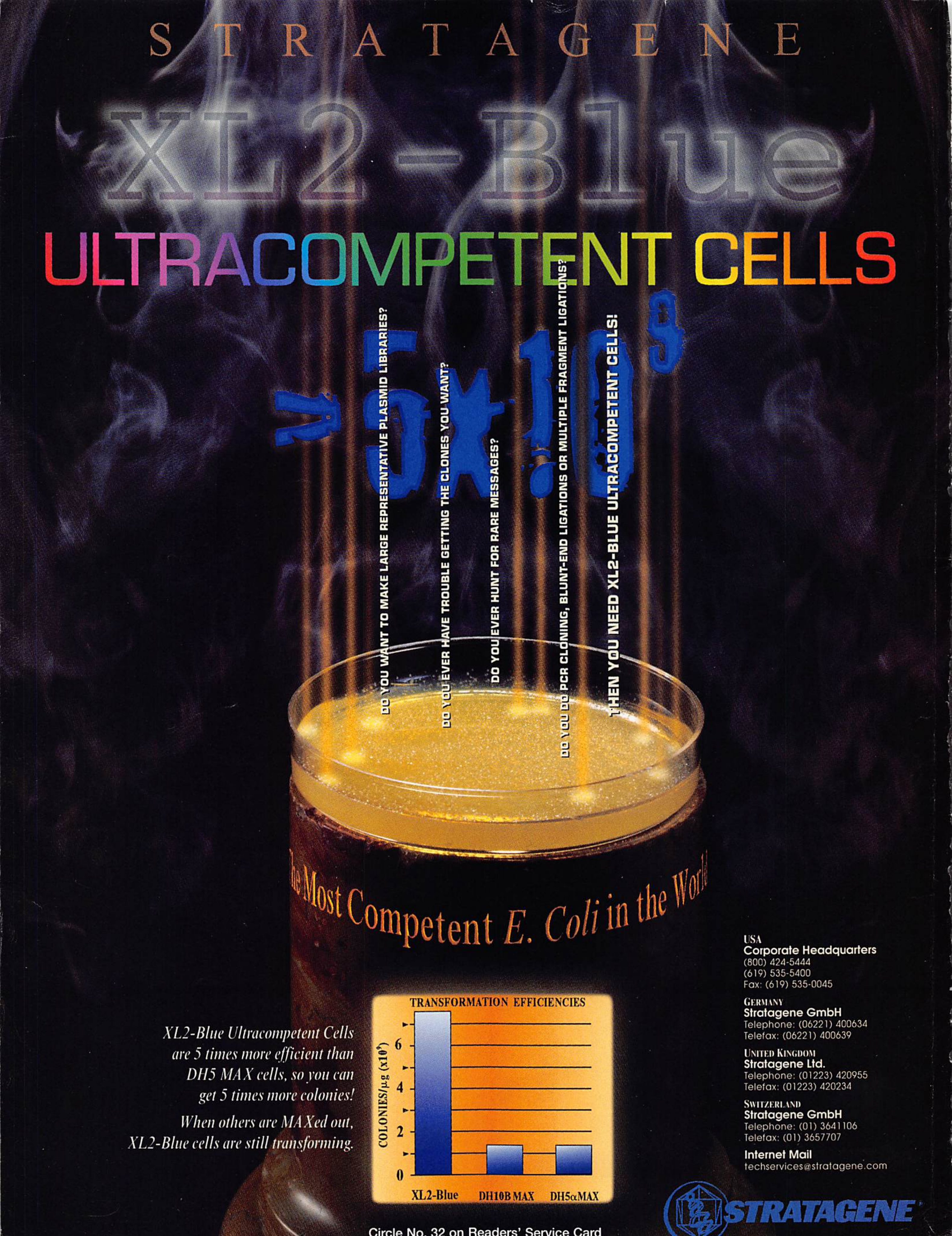

Circle No. 32 on Readers' Service Card

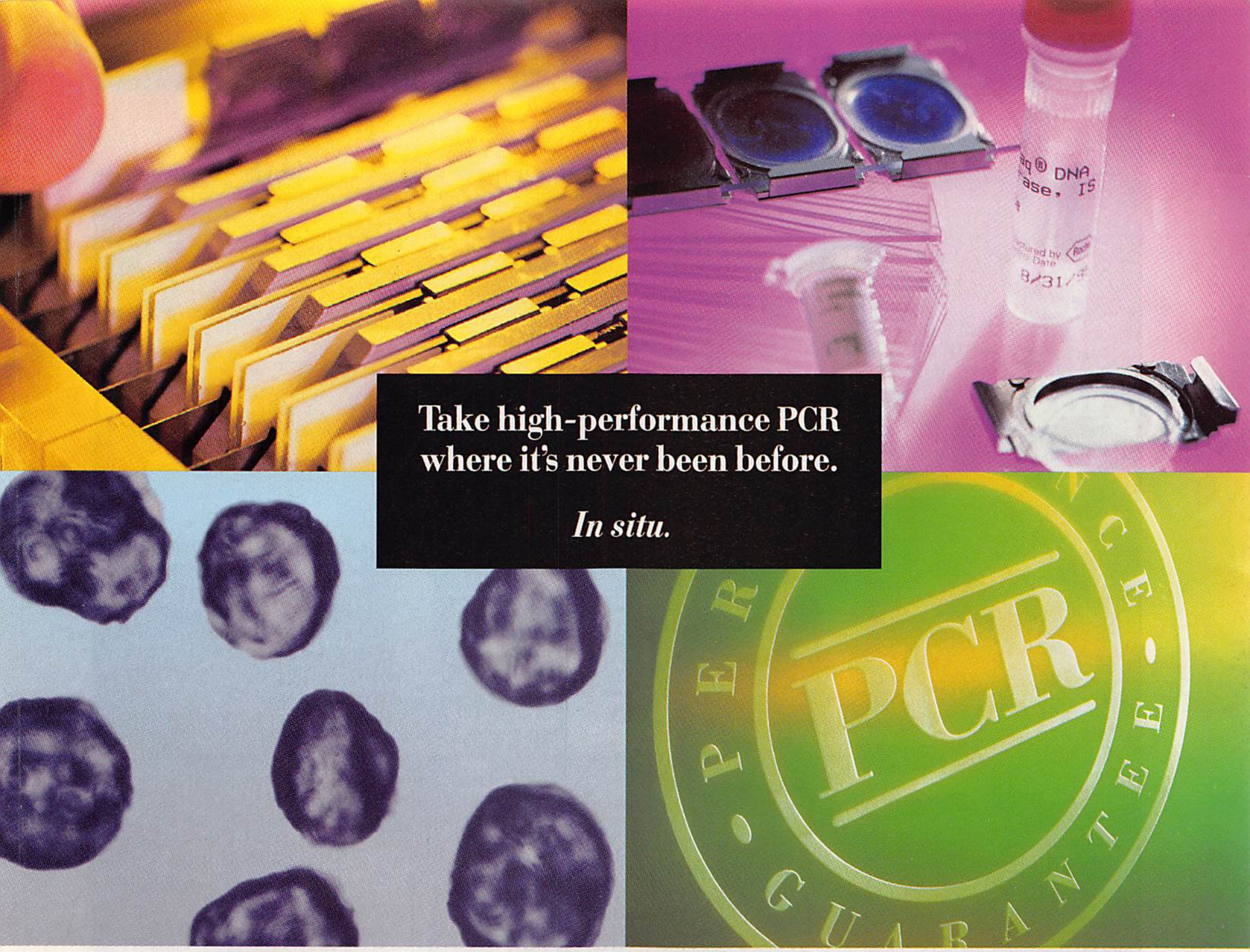

GeneAmp In Situ *PCR System 1000 (left). Localization of varciella zoster virus (VZV) by* in situ *PCR in human brain tissue (right).*

Now *in situ* PCR is everything it should be. Robust. Reproducible. Convenient. The new GeneAmp® *In Situ* PCR System 1000,* with co-optimized reagents and accessories, expands the power of PCR into the cell. This innovative system streamlines the entire process and provides consistently superior results.

Engineered for *In Situ* PCR Excellence.

Our novel sample block, accessories and proven thermal cycler design ensure cycle-to-cycle, slide-to-slide uniformity for highly reproducible results. The 10-slide block with vertical slots maximizes thermal contact—without mineral oil—to guarantee optimal PCR performance. Up to 30 samples can be amplified each run.

Setup is convenient with our AmpliCover™ Discs and Clips and silane-treated glass slides, which create a standardized reaction chamber, without messy adhesives. This complete system includes our AmpliTaq® DNA Polymerase, *IS*, specifically formulated for efficient *in situ* PCR.

Take high performance PCR where it's never been before with the GeneAmp *In Situ* PCR System 1000 and our line of *in situ* PCR reagents and accessories. To request information, call 1-800-345-5224. Outside the U.S. and Canada, contact your local Perkin-Elmer representative.

PERKIN ELMER

Europe Langen, Germany Tel: 49 6103 708 301 Fax: 49 6103 708 310
Japan Tokyo, Japan Tel: (0473) 80-8500 Fax: (0473) 80-8505
Latin America Mexico City, Mexico Tel: 52-5-651-7077 Fax: 52-5-593-6223
Australia Melbourne, Australia Tel: (03) 9212-8585 Fax: (03) 9212-8502

Perkin-Elmer PCR reagents are developed and manufactured by Roche Molecular Systems, Inc., Branchburg, New Jersey, U.S.A.

Roche

* patents pending

ISO 9001 CERTIFIED

Circle No. 43 on Readers' Service Card

Your research is already full of "unknowns."

Can your sera "take the heat"?

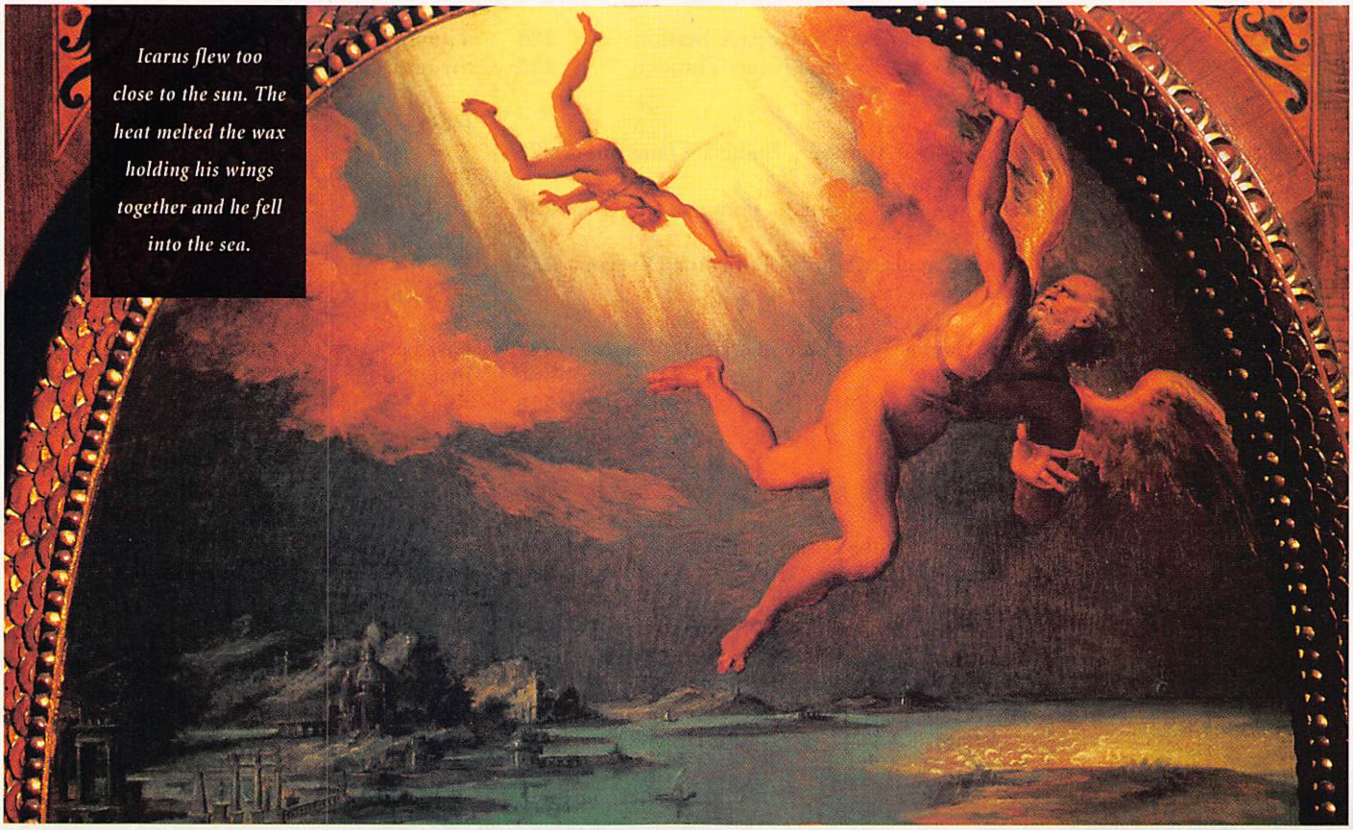

The use of non-domestic fetal bovine sera for your cell culture research may be introducing unknowns that will be costly. Non-domestic sera can carry environmental contaminates which are not tested for, antibiotics and pesticides that are not screened for, as well as other metabolic and evolutionary aberrations. They may offer a tempting price and attractive packaging, right down to a "USDA approved" label. Unfortunately, that label is often applied to non-domestic, uncontrolled sera lots. The truth is, unless your fetal bovine serum actually comes from domestic stock that have been raised and processed in the United States, you are gambling with sera that can bring your research to a crashing halt.

Research Sera eliminates these "unknowns." Research Sera is harvested exclusively from U S stock that are owned by our parent company, ConAgra, Inc., a $10.5 billion food products company that produces a very large portion of the world's beef products. You can be guaranteed that Research Sera is 100% U S Origin.

To further diminish the unknowns, Research Sera is accompanied with assays of biochemistries of current relevance. Research Sera is assayed for TGF-ß1 – probably the most important cytokine in cell culture, Insulin – perhaps the most important hormone, and Estradiol – one of the most studied estrogens. Furthermore, the IgG levels in Research Sera are reported. And since Research Sera can be reserved, you can finish a multi-year research project with a single lot of sera.

Don't settle for inferior materials. We'll send you a free sample of Research Sera, and you'll know what you are bringing into your lab. Call 1-800-933-0909.

RESEARCH SERA ™

Another Peak of Excellence Product from Summit Biotechnology 701 Centre Ave. Fort Collins, CO 80526-1843

Circle No. 17 on Readers' Service Card

ISSN 0036-8075
13 October 1995
Volume 270
Number 5234

Science

American Association for the Advancement of Science

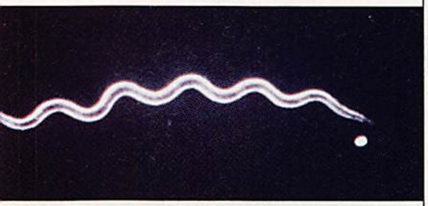

228

Does the Lyme spirochete cause chronic infections?

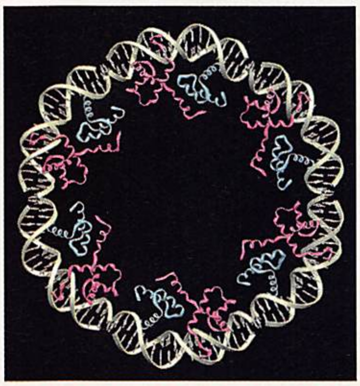

251, 262 & 290

Opposites attached

NEWS & COMMENT

RESEARCH NEWS

POLICY FORUM

PERSPECTIVES

ARTICLE

DEPARTMENTS

Board of Reviewing Editors

COVER

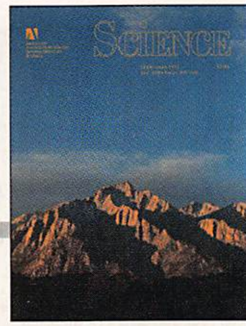

View westward of Lone Pine Peak (elevation 3945 meters), located on the southern Sierra Nevada crest 10 kilometers southeast of Mount Whitney. Differential rock uplift across the Sierra Nevada fault system has generated more than 2500 meters of relief between Lone Pine Peak and Owens Valley to the east. Erosion and deposition may be responsible for a large fraction of Cenozoic rock uplift in the Sierra Nevada. See page 277. [Photo: R. S. Anderson]

RESEARCH ARTICLE

REPORTS

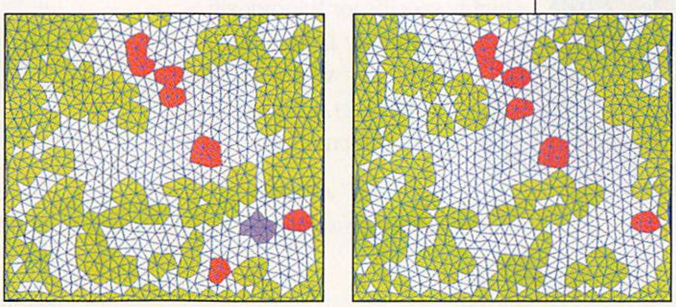

270
Superfluid flux lines

Indicates accompanying feature

■ **SCIENCE (ISSN 0036-8075) is published weekly on Friday, except the last week in December, by the American Association for the Advancement of Science, 1333 H Street, NW, Washington, DC 20005.** Second-class postage (publication No. 484460) paid at Washington, DC, and additional mailing offices.

Domestic individual membership and subscription (51 issues): $97 ($50 allocated to subscription). Domestic institutional subscription (51 issues): $228. Foreign postage extra: Mexico, Caribbean (surface mail) $53; other countries (air assist delivery) $93. First class, airmail, student and emeritus rates on request. Canadian rates with GST available upon request, GST #1254 88122. **Printed in the U.S.A.**

Change of address: allow 4 weeks, giving old and new addresses and 8-digit account number. **Postmaster:** Send change of address to *Science*, P.O. Box 1811, Danbury, CT 06813–1811. **Single copy sales:** $7.00 per issue prepaid includes surface postage; bulk rates on request.

Science is indexed in the *Reader's Guide to Periodical Literature* and in several specialized indexes.

edited by PHIL SZUROMI

Quantum computation

One approach for making smaller integrated circuits would be a quantum computer in which the logic states 0 and 1 would be replaced by wave functions and the logic operations by superpositions of quantum states. Theory suggests that quantum computers could be very powerful for tasks such as in Shor's factorization of prime numbers. In a review, DiVincenzo (p. 255) notes that a working quantum computer would be extremely demanding and would require a huge extension of the rudimentary quantum computing possible today.

Binding of homeodomain heterodimers to DNA

The MAT $\alpha 2$ homeodomain protein of yeast regulates transcription by binding DNA with either MAT $\alpha 1$ or MCM1. Each of the complexes, **a**1/$\alpha 2$ and $\alpha 2$/MCM1 bind to distinct sites in the yeast genome and repress transcription of the adjacent genes in a cell type–specific manner. Li *et al.* (p. 262; see the Perspective by Andrews and Donoviel, p. 251) present the crystal structure of the **a**1/$\alpha 2$ heterodimer bound to DNA. The $\alpha 2$ COOH-terminal tail is disordered when $\alpha 2$ binds DNA alone but becomes ordered in the ternary complex and contacts the **a**1 homeodomain. Such flexible protein recognition domains may mediate contact between many other heterodimeric transcription factors. Jin *et al.* (p. 209) examine the requirements for proper spacing between the **a**1/$\alpha 2$ DNA binding sites and the length of the $\alpha 2$ tail.

Magnetoresistive materials

In seeking new materials, combinatorial libraries can be used to synthesize and screen a large number of samples rapidly. Briceño *et al.* (p. 273) used this method to search for materials that exhibit strong magnetoresistance, a property of great interest for downsizing magnetic recording heads. They found a class of cobalt oxides that have large magnetoresistance, and further determined that in contrast to manganese-based compounds, the effect increases as the material is doped with larger alkaline earth ions.

Lifting mountains

What forces cause the uplift of large mountain ranges? Small and Anderson (p. 277; see cover) examine the interplay of erosion and generation of relief, which removes load and induces isostatic uplift, on the formation of the Sierra Nevada, California. Their model shows that coupled erosion along the crest of the range and deposition in the Great Valley could have produced the observed tilting of the range to the west and apparent uplift on the east. Summit elevations may have increased while the mean elevation of the range may have decreased in the past 10 million years.

Rock vein pursuit

Pseudotachylites are veins or larger bodies of melted rock formed by frictional melting, most commonly during asteroid impacts or faulting. The conditions responsible for their formation have been obscure because analogous features have been difficult to produce in the lab. Fiske *et al.* (p. 281) generated pseudotachylites in high-velocity shock experiments in which they used an aluminum container that deformed with the sample, facilitating strain heating. Strain heating may thus complement shock heating in melting and altering rocks in impact events.

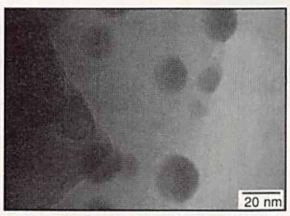

Glucocorticoid mechanism

Although they have been used for years as immunosuppressive and anti-inflammatory agents, little is known about the mechanism of glucocorticoid (GC) action. Scheinman *et al.* (p. 283) and Auphan *et al.* (p. 286; see news story by Marx, p. 232) show that the nuclear factor kappa B (NF-κB) transcription factor, a regulator of genes involved in the immune response, is repressed by GCs, and that GCs induce increased synthesis of IκBα, the inhibitor of NF-κB. This additional IκBα binds to NF-κB, preventing its action.

Hearty protein

How large is large? For proteins, most lie within the range of 180 to 900 amino acid residues per molecule (masses of 20,000 to 100,000 daltons). Labeit and Kolmerer (p. 293; see the news story by Barinaga, p. 236) present the molecular cloning and sequencing of titin, a protein from human heart of 26,926 residues (3 million daltons). Analysis of the sequence domains, the messenger RNA splicing patterns in various tissues, and the structural organization of other muscle proteins suggests that titin serves two functions. First, it specifies the global arrangement of thick, mysoin-containing filaments in muscle and, second, selective expression of domains explains the different elasticity of muscles.

Peroxide pathway

Binding of platelet-derived growth factor (PDGF) to its receptor initiates a number of events that transmit signals within the cell. Sundaresan *et al.* (p. 296) report that treatment of vascular smooth muscle cells with PDGF increases the intracellular concentration of hydrogen peroxide (H_2O_2). Responses of the cells to PDGF, such as enhanced DNA synthesis and chemotaxis, were inhibited when the this increase in H_2O_2 was blocked. Thus H_2O_2, like nitric oxide, may function in signal transduction.

Parts of speech

Speech conveys information through both the frequency distribution of sounds (spectral information) as well as timing for making different sounds (temporal cues). Shannon *et al.* (p. 303) show that speech can be recognized with high accuracy even if the spectral information is highly degraded. They added white noise to spoken words and sounds in a way that preserved temporal cues but reduced frequency information into only a few broad bands. Vowels and consonants could be recognized with only three bands of modulated noise. Such results bear not only on how speech is processed in the human brain but can also be useful in designing hearing aids.

SCIENCE

http://www.aaas.org

Publisher: Richard S. Nicholson
Editor-in-Chief: Floyd E. Bloom
Editor: Ellis Rubinstein
Managing Editor: Monica M. Bradford
Deputy Editors: Philip H. Abelson *(Engineering and Applied Sciences)*; John I. Brauman *(Physical Sciences)*; Thomas R. Cech *(Biological Sciences)*

Editorial Staff
Assistant Managing Editor: Dawn Bennett
Senior Editors: Eleanore Butz, R. Brooks Hanson, Pamela J. Hines, Barbara Jasny, Katrina L. Kelner, Paula A. Kiberstis, Linda J. Miller, L. Bryan Ray, Phillip D. Szuromi, David F. Voss
Associate Editors: Gilbert J. Chin, Suki Parks, Linda R. Rowan
Letters: Christine Gilbert, *Editor;* Steven S. Lapham
Book Reviews: Katherine Livingston, *Editor;* Jeffrey Hearn, *Editorial Assistant*
Editing: Valerie Jablow, *Supervisor;* Cara Tate, *Senior Copy Editor;* Jeffrey E. Cook, Harry Jach, Erik G. Morris, Christine M. Pearce
Copy Desk: Ellen E. Murphy, *Supervisor;* Joi S. Granger, Daniel T. Helgerman, Melissa Q. Rosen, Beverly Shields, Kameaka Williams, *Assistant*
Editorial Support: Sherryf Farmer, *Supervisor;* Brent Gendleman, Carolyn Kyle, Michele Listisard, Diane Long, Patricia M. Moore, Ted Smith
Administrative Support: Sylvia Kihara, Charlene King
Telephone: 202-326-6501; **FAX:** 202-289-7562; **TDD:** 202-408-7770

News Staff
News Editor: Colin Norman
Features Editor: John M. Benditt
Deputy News Editors: Tim Appenzeller, Joshua Fischman, Jean Marx, Jeffrey Mervis
News & Comment/Research News Writers: Linda B. Felaco (copy), Constance Holden, Jocelyn Kaiser, Richard A. Kerr, Andrew Lawler, Eliot Marshall, Rachel Nowak, Robert F. Service, Richard Stone, Lori Wolfgang (intern)
Bureaus: Marcia Barinaga (Berkeley), Jon Cohen (San Diego), James Glanz (Chicago), Dennis Normile (Tokyo), Wade Roush (Boston)
Contributing Correspondents: Barry A. Cipra, Elizabeth Culotta, Ann Gibbons, Anne Simon Moffat, Virginia Morell, Robert Pool, Gary Taubes
Administrative Support: Fannie Groom
Telephone: 202-326-6500; **FAX:** 202-371-9227; **Internet Address:** science_news@aaas.org

Art & Production Staff
Production: James Landry, *Director;* Wendy K. Shank, *Manager;* Lizabeth A. Harman, *Assistant Manager;* Laura A. Creveling, Scherraine B. Mack, Stephen E. Taylor, *Associates;* Leslie Blizard, *Assistant*
Art: Amy Decker Henry, *Director;* C. Faber Smith, *Associate Director;* Katharine Sutliff, *Scientific Illustrator;* Holly Bishop, *Graphics Associate;* Elizabeth Carroll, Preston Morrighan, *Graphics Assistants*

Europe Office
Editorial: Richard B. Gallagher, *Office Head and Senior Editor;* Stella M. Hurtley, Julia Uppenbrink, *Associate Editors;* Belinda Holden, *Editorial Associate*
News: Daniel Clery, *Editor;* Nigel Williams, *Correspondent;* Michael Balter *(Paris)*, Patricia Kahn *(Heidelberg)*, *Contributing Correspondents*
Administrative Support: Janet Mumford; Anna Sewell
Address: 14 George IV Street, Cambridge, UK CB2 1HH
Telephone: (44) 1223-302067; **FAX:** (44) 1223-302068
Internet address: science@science-int.co.uk

EDITORIAL

Flaws in Risk Assessments

Chemical risk assessment studies conducted with rodents have helped to justify expenditures of more than a trillion dollars over the past 20 years. Large additional outlays are planned, although it has not been shown that such studies have substantially benefited human health. In fact, it has become increasingly clear that the main causes of untimely human death are smoking and diet. For example, a recent article in the *New England Journal of Medicine** indicates that excess weight has a wide range of deleterious effects on health.

The risk assessment procedures used by the Environmental Protection Agency (EPA) have been criticized for many years and for many reasons. Their quality has recently come under intensified criticism, as is evident in the proceedings of a July 1995 meeting sponsored by Toxicology Forum of Washington, D.C., and in a recently published book, *Dietary Restriction.*† The critics point out that rodent risk assessment studies lack reproducibility because of genetic drift in the test animals and because of a failure to control their consumption of food.

Most standard risk assessment experiments expose rodents to large doses of a test chemical for about 2 years, which is approximately their natural life-span. For most tests, one or more of three strains of rodents are used: Sprague-Dawley (SD) rats, Fischer (F-344) rats, and B6C3F1 mice. These animals have a higher natural incidence of tumors than do humans, and some of the tumors are not common to humans. These rodent strains were adopted in the belief that they would exhibit less variability than wild-type animals do. On the basis of this assumption, enormous effort has been expended in studies of about 500 different chemicals. Each experiment has involved comparison between dosed and nondosed animals (controls). Thus a large database is available concerning the weight, longevity, and pathology of control animals. Data cited in the Toxicology Forum proceedings and in *Dietary Restriction* indicate that, during the past 25 to 30 years, the adult body weight of rodents from most of the strains used in toxicity testing has increased 20 to 30%. Degenerative diseases and tumor incidence also have increased. Rodent survival has decreased. At the Merck Research Laboratory in the 1970s, the survival rate at age 2 of SD rats used as controls was 58%. In the 1980s it was 44%, and in the 1990s it had dropped to 24%. A different laboratory compiled data on F-344 rats. In 1970, 80% of males survived for 2 years. In 1981, 60% survived. Their current survival rate is 36%. The incidence of tumors in control rodents has also changed with time. For example, the number of liver tumors in control B6C3F1 mice increased from an average of 32% in 1980 to about 50% in 1984. In tests at various laboratories, liver tumor incidence in male B6C3F1 mice has varied between 10 and 76%.

A partial explanation for this variability in longevity and health lies in practices at the breeder companies. Apparently, they have unwittingly caused genetic drift by their methods of selecting breeding stock. The standardized procedure at risk assessment laboratories has also been a factor. In general, animals are fed ad libitum (ad lib); that is, they are given as much food as they want to eat. As a result of overeating, the health of ad lib animals is impaired. This is clearly shown by the fact that if the food intake of littermates of ad lib animals is reduced to 70% or less of ad lib amounts, rodent health and longevity are much improved. A recent experiment using SD rats compared the longevity of control rats fed ad lib with that of rats fed 65% of the ad lib amounts. At maturity, the ad lib males weighed 60% more than did the diet-restricted males. Only 7% of the ad lib males lived as long as 2 years. In contrast, 72% of the diet-restricted rats survived for more than 2 years. They were sleek and healthy. Although this phenomenon has been widely observed and well known for many years, the standard protocol still calls for ad lib feeding, so that in effect, when animals are exposed to chemicals in risk assessments, they simultaneously receive one potential carcinogen and one known carcinogen—their food.

When scientists plan experiments, they seek to control the important variables and to achieve time-invariant reproducible results. Those at EPA with the responsibility for establishing protocols for risk assessment experiments have acted as if they did not share these goals.

Philip H. Abelson

*J. E. Manson *et al.*, *N. Engl. J. Med.* **333**, 677 (1995). †R. W. Hart, D. A. Neumann, R. T. Robertson, Eds., *Dietary Restriction: Implications for the Design and Interpretation of Toxicity and Carcinogenicity Studies* (ILSI Press, Washington, DC, 1995).

SCIENCE

http://www.aaas.org

Published by the **American Association for the Advancement of Science (AAAS),** *Science* serves its readers as a forum for the presentation and discussion of important issues related to the advancement of science, including the presentation of minority or conflicting points of view, rather than by publishing only material on which a consensus has been reached. Accordingly, all articles published in *Science*—including editorials, news and comment, and book reviews—are signed and reflect the individual views of the authors and not official points of view adopted by the AAAS or the institutions with which the authors are affiliated.

The American Association for the Advancement of Science was founded in 1848 and incorporated in 1874. Its objectives are to further the work of scientists, to facilitate cooperation among them, to foster scientific freedom and responsibility, to improve the effectiveness of science in the promotion of human welfare, to advance education in science, and to increase public understanding and appreciation of the importance and promise of the methods of science in human progress.

LETTERS

Hard questions

The environmental effects of dioxin-contaminated herbicides such as Agent Orange, sprayed by the U.S. military during the Vietnam War (mangrove forests south of Ho Chi Minh City in 1970, left, unsprayed; right, after spraying), have long been the subject of debate. A letter recommends follow-up study of those effects. Other letters discuss electronic publishing, the academic job market, and fusion.


AAAS


AAAS

Dioxins in Vietnam

With reestablishment of full diplomatic recognition of Vietnam by the U.S. government finally accomplished, it seems appropriate to ask why no studies of the environmental effects of dioxin [TCDD (tetrachlorodibenzodioxin)] in Vietnam have been undertaken by the U.S. government. In fact, the National Academy of Sciences in 1974 recommended that studies "be started immediately" (*1*). This apparent lack of concern on the part of our government contrasts with actions of Canada, Japan, and other countries. Canada has an extensive pilot program operating in the south of Vietnam helping to assist and further train Vietnamese scientists in methods of assessing degrees of dioxin contamination. The Canadians calculate that Vietnam, a country one-third the size of British Columbia, was subjected to annual environmental loadings of dioxin more than 150 times greater than annual worst-case loadings to the British Columbia environment as a result of pulp mill discharges (*2*).

As a recent editorial (*3*) stated

> Many in the United States may feel a special responsibility to join the ongoing research efforts by inadequately funded investigators from Europe and other countries, especially those from France and the World Health Organization. It is also the case that scientific information about TCDD effects gleaned from studies in Vietnam will help industrialized nations to deal with widespread contamination by dioxin in their own environments.

We believe the AAAS would contribute to a truly significant follow-up to the work of its Herbicide Assessment Commission (*4*) by urging Congress to fund a full-scale study of dioxin in Vietnam, offering its good services as desired.

A. H. Westing*
Westing Associates,
Putney, VT 05346, USA
E. W. Pfeiffer†
University of Montana,
Missoula, MT 59812–1002, USA

*Former director, AAAS Herbicide Assessment Commission. †Professor emeritus of zoology.

References

1. Committee on the Effects of Herbicides in Vietnam, *The Effect of Herbicides in South Vietnam, Part A—Summary and Conclusions* (National Academy of Sciences, Washington, DC, 1974), p. 514.
2. Hatfield Consultants, Ltd., personal communication to E. W. Pfeiffer.
3. J. Dwyer and D. Flesch-Janyo, *Am. J. Publ. Health* **85**, 476 (1995).
4. J. D. Constable, R. E. Cook, M. Meselson, A. H. Westing, *Science* **186**, 584 (1974); AAAS Herbicide Assessment Commission, *Congr. Rec.* **118**, 6806 (3 March 1972).

Electronic Publishing

In their editorial " 'Wired' science or whither the printed page?" (4 Aug., p. 615), Shmuel Winograd and Richard N. Zare state that the scientific community must ask "some very hard questions" about electronic publishing. One point made by Winograd and Zare may lead readers to believe that electronic publishing precludes peer-review and that this results in rapid publishing. The speed of dissemination of electronic journals comes not from bypassing the peer-review process, but from

bypassing the print process; it can save on the order of 3 to 6 months.

This new medium allows for strictly refereed journals as well as free-wheeling discussion groups. Hence, the Web contains reviewed journals such as *Psycholoquy* (**http://www.princeton.edu/˜harnad/psyc.html**), which is reviewed to standards most print journals are hard-pressed to meet, and preprint journals, such as the high energy physics e-print archive (http://xxx/lanl.gov/), which dominates its field because of rapid dissemination and universal free access.

Jeffrey H. Boatright
John M. Nickerson
Robert L. Church
Editors, Molecular Vision,
c/o Emory Eye Center, Emory University, Atlanta, GA 30322, USA
URL at **http://www.cc.emory. edu/MOLECULAR_VISION/index. html**

My colleagues and I in the American Society for Biochemistry and Molecular Biology (ASBMB), which publishes the *Journal of Biological Chemistry*, welcome the timely editorial on electronic publication by Winograd and Zare. We share both the enthusiasm and the concerns expressed in the editorial about issues such as quality control, authorship, intellectual property and archivability. We also agree that technical capabilities, while impressive, are an insufficient guide to electronic presentation of scientific information. It is for this reason that our successful efforts to publish the *Journal of Biological Chemistry* electronically (**http:/www-jbc.stanford.edu/jbc/**) have required a truly collaborative effort between the ASBMB, the scientist-editors of the journal, the Stanford University Libraries, Stanford Academic Information Resources, and Cadmus, publisher of the print version of the journal.

Robert D. Simoni
Associate Editor,
Journal of Biological Chemistry,
c/o Department of Biological Sciences, Stanford University, Stanford, CA 94305–5020, USA

The examples cited by Winograd and Zare as electronic publication of scientific journals online that are "already a reality" (*Journal of Biological Chemistry* and *Astrophysical Journal Letters*) are both actually expensive demonstration projects, offered free to all Internet users to evaluate the delivery technology. More realistic examples of online publications can be found at the OCLC Electronic Journals Online server (**http://www.oclc.org/oclc/promo/ejo_list.htm**), where users must be paying subscribers. A critical evaluation of the history of the *Online Journal of Current Clinical Trials* (sold last year by the AAAS, the publisher of *Science*, to Chapman and Hall) would be a valuable lesson in how economics affected a technically excellent electronic publication.

As the U.S. government involves itself with the fledgling electronic publication efforts (*1*), those of us attempting to make economic sense of an evolving market can only wonder what its long-term role will be.

The most important issues are no longer about technology or quality, but economics. Of the thousands of peer-reviewed research serials published in the world, only a few dozen are available in an electronic format, most on CD-ROM. Many publishers balk at spending even a small fraction of their printing budgets on the production of electronic versions and fear that electronic subscriptions will further erode revenues from their declining subscriber base. Thus, they postpone making a closer evaluation of the survival value of their product in a changing marketplace.

Pete Goldie
President, Lightbinders, Inc., 2325 Third Street—Suite 324, San Francisco, CA 94107, USA
E-mail: pg@lbin.com
URL at **http://bin.com**

Notes

1. For example, the National Science Foundation's (NSF's) grant to theoretical physicist Paul Ginsparg and his colleagues at Los Alamos National Laboratory to maintain a server of high energy physics data, the NSF grant of $450,000 to launch *Astrophysical Journal Letters* online, and the funding of the Mosaic program by the National Center for Supercomputing Applications.

■

Worthy Pursuits

In his editorial "Degrees of freedom" (18 Aug., p. 903), Don S. Doering eloquently describes the plight of new Ph.D. researchers who, in trying to adapt to a tight academic job market, face a strong prejudice against any career other than academic research. To answer his question, "How do we fix a system that . . . has produced many more Ph.D.'s than the market can bear?" I suggest that academic scientists who espouse that prejudice be limited to training only enough Ph.D.'s to replace themselves (or even fewer, if budgets in their field are shrinking). How can they ethically train any more than that, when they knowingly condemn the additional ones to a professional life they regard as inferior?

Academic scientists typically supervise Ph.D. theses from their thirties to their sixties; allowing for those who die early, switch to administrative positions, or otherwise leave the field sooner, each needs to train a replacement no more than once every 20 years or so. When the issue is put to academic scientists this way, some will stand by their beliefs and ease the imbalance on the supply side. The others, faced with giving up most of their cheap labor supply, will probably come to realize that for a student to pursue a career outside the academy maybe isn't so unworthy after all.

William Lockeretz
School of Nutrition Science and Policy, Tufts University, Medford, MA 02155, USA

■

Asymmetrical Ability

Oliver Sacks (Letters, 5 May, p. 621) suggests that the development of exceptional musical abilities in some individuals with neurodevelopmental disorders such as autism and Williams syndrome constitutes a "savant" talent and as such might represent a "neuromodule." He speculates that the exaggerated leftward asymmetry of the planum temporale area of the brain recently reported in a group of professional musicians by Gottfried Schlaug *et al.* (Reports, 3 Feb., p. 699) may reflect the neuromorphological substrate of such a neuromodule.

In fact, we have carried out analyses (*1*) of the planum temporale in individuals with Williams syndrome. The surface area of the left and right planum temporale of four subjects was measured with magnetic resonance images (MRI) with the same anatomical criteria used by Schlaug *et al.* The planum temporale asymmetry for these individuals with Williams syndrome was on par with that of the group of musicians studied by Schlaug *et al.* (mean, −0.23; standard deviation, 0.24). Three of the four individuals with Williams syndrome had greater asymmetry than that of the musicians, but less than that of musicians with perfect pitch. In contrast, five normal control subjects had an asymmetry coefficient that was consistent with the nonmusician control group in the study by Schlaug *et al.* (mean, −0.34; standard deviation, 0.14). In addition, subjects with Williams syndrome did not differ from normal subjects in total planum temporale surface area (1000.8 versus 962.1 square millimeters, respectively), despite significant overall reduction of cerebral volume reported in subjects with Williams syndrome (*1*), suggesting dispro-

portionate growth of the entire posterior supratemporal region.

These preliminary data suggest that disproportionate growth, and perhaps exaggerated asymmetry, occur in the posterior supratemporal region in individuals with Williams syndrome. However, establishing whether this asymmetry is a source of musical ability will have to await more detailed analyses. Also, the fact that individuals with Williams syndrome typically possess exceptional language abilities relative to other cognitive domains and despite mental retardation (2) introduces the possibility that planum temporale asymmetry is related to linguistic abilities rather than, or as well as, musical abilities.

Gregory Hickok
Ursula Bellugi
Wendy Jones
Laboratory for Cognitive Neuroscience, Salk Institute for Biological Studies, 10010 North Torrey Pines Road, La Jolla, CA 92037, USA

References

1. T. L. Jernigan, U. Bellugi, E. Sowell, S. Doherty, J. Hesselink, *Arch. Neurol.* **50**, 186 (1993).
2. U. Bellugi, P. P. Wang, T. L. Jernigan, in *Atypical Cognitive Deficits in Developmental Disorders: Implications for Brain Function*, S. H. Broman and J. Grafman, Eds. (Erlbaum, Hillsdale, NJ, 1994), pp. 23–56.

Fusion Progress

We disagree strongly with the letter by David Montgomery (8 Sept., p. 1328) in which he criticizes the fusion program for an alleged lack of scientific culture and content. He characterizes the field as it was in its infancy, approximately 20 years ago. He does not acknowledge the program's success and degree of scientific maturation in the intervening two decades.

It is important to understand the implications of the fact that the fusion process requires high temperatures, on the order of 10 kilovolts, and that the behavior of matter at these temperatures takes on special properties, well outside those typical of terrestrial experience. Investigating these properties has led to the development of the subfield of high-temperature plasma physics. Facilities have been developed that are capable of producing plasmas of fusion temperature and density, and, as well, the science governing the behavior of these plasmas has also been developed. This science base has three parts: (i) a much increased and continually expanding understanding of the underlying physics; (ii) an ability to test this understanding with specialized diagnostics routinely producing detailed time-resolved profiles of density, temperature, magnetic field, current, and so forth; and (iii) the development of sophisticated computer codes that translate fundamental understanding into practical tools for experimental testing of theory and for fusion facility design.

Montgomery criticizes, in particular, fusion plasma diagnostics. His characterization is out of date. Diagnostic instruments have been developed and widely deployed to measure the spatial and temporal profiles of *all* the internal plasma variables he says are largely lacking. Comparison of these measurements with theory indicates a mature, first-principles understanding of plasma stability, control, and current flow. Plasma transport, being driven by low-level turbulent processes, is less well understood from first principles and is the subject of intense current research. An empirical description is also being developed through a "wind tunnel" approach to design new machines.

Montgomery also criticizes the technical review processes of the fusion program. However, with the increased internationalization of fusion research over the past two decades, American plasma physics and fusion research have experienced much wider and more intense assessments than could be had earlier through the "rough-and-tumble

atmospheres of university seminars."

Fusion is being pursued for its promise as an environmentally benign energy source. This mission orientation should not, and does not, lower its scientific standards. Indeed, the scientific progress of fusion is a subject of which we are most proud.

David E. Baldwin
Thomas C. Simonen
General Atomics,
3550 General Atomics Court,
San Diego, CA 92121–1194, USA

■

CO Binding and Bending Energetics

Robert F. Service (Research News, 18 Aug., p. 920) provides a lively sketch of the debate over the geometry of carbon monoxide (CO) binding to myoglobin and its importance for understanding the protein's ability to discriminate CO from O_2. While Service focuses on the conflicting structural interpretations of spectroscopic and x-ray diffraction data, I would like to highlight the argument from energetics. Because electronic forces strongly favor an upright geometry, it takes more energy to bend the Fe-CO bond significantly than the protein can muster through steric forces. The estimation of this energy from vibrational spectroscopy (*1*) was one of the first of the "chinks . . . in the armor" of the bent-CO dogma.

The energy argument has an important corollary: The absence of significant bending does *not* mean that steric forces play no role in discriminating between CO and O_2 (*2*). Precisely because of CO's strong preference for upright binding, steric forces may well lower the CO affinity, even if they are not strong enough to bend the CO once it binds. Site-directed mutagenesis provides some support for this view. When the distal histidine residue, the side chain of which is positioned to interfere with upright binding, is replaced (*3*) by the sterically undemanding glycine, the CO affinity *increases*, by 1.0 kilocalories per mole. At the same time, the O_2 affinity *decreases*, by 1.6 kilocalories per mole, reflecting the importance of the attractive force of the hydrogen bond, mentioned by Service, between the distal histidine and the bound O_2. These changes suggest that steric repulsion of CO and H-bond attraction of O_2 are *both* important in discriminating CO from O_2. However, other influences may also be at play, including changes in the occupancy of the binding pocket by water molecules (*4*). Further work is needed to delineate the various contributions to the binding energies.

Thomas G. Spiro
Department of Chemistry,
Princeton University,
Princeton, NJ 08544, USA

References

1. X.-Y. Li and T. G. Spiro, *J. Am. Chem. Soc.* **110**, 6024 (1988); G. B. Ray, X.-Y. Li, J. A. Ibers, J. L. Sessler, T. G. Spiro, *ibid.* **116**, 162 (1994).
2. J. P. Collman, J. I. Brauman, T. R. Halbert, K. S. Suslick, *Proc. Nat. Acad. Sci. U.S.A.* **73**, 3333 (1976)
3. J. S. Olson *et al.*, *Nature* **336**, 265 (1988).
4. T. Li, M. L. Quillin, G. N. Phillips Jr., J. S. Olson, *Biochemistry* **33**, 1433 (1994).

Letters to the Editor

Letters may be submitted by e-mail (at science_letters@aaas.org), fax (202-289-7562), or regular mail (*Science*, 1333 H Street, NW, Washington, DC 20005). Letters will not be routinely acknowledged. Full addresses, signatures, and daytime phone numbers should be included. Letters should be brief (300 words or less) and may be edited for reasons of clarity or space. Beginning in October 1995, our previous policy of consulting with all letter authors before publication will be discontinued.

edited by Jocelyn Kaiser

Chimp Finally Shows AIDS Symptoms

Another AIDS truism is heading for the trashbin: the belief that no animal other than humans develops AIDS from HIV infection.

According to two well-connected AIDS researchers, a chimpanzee at Atlanta's Yerkes Regional Primate Research Center that was first infected with HIV in 1986 has become seriously ill with symptomatic AIDS. Although it's unclear what impact if any this will have on attempts by AIDS researchers to use chimps to understand and prevent the disease, the finding may alter how people view existing data from HIV-infected chimps.

As first reported in the 9 October *U.S. News and World Report*, a chimp named Jerome has developed acute diarrhea and critically low levels of CD4 cells, the key immune system warriors that steadily decline in HIV-infected people. A spokesperson says Yerkes researchers decline to discuss Jerome until they present their data in a scientific forum.

The news is no surprise to the University of Alabama, Birmingham's, Patricia Fultz, who works with HIV in chimps and who first infected Jerome 9 years ago when she was at the Centers for Disease Control and Prevention. Fultz co-wrote a paper in the March 1991 *Journal of Infectious Disease* that described how HIV was unraveling Jerome's immune system, predicting that he would succumb to AIDS.

Now that her prediction appears correct, Fultz believes the finding "will add weight" to the studies that have tested HIV vaccines in chimps. Yet she cautions that the 9-year lag between infection and disease suggests the chimp model still has serious drawbacks. "I don't think it will make any difference at all on vaccine development," she concludes. For similar reasons, she doubts that chimps can illuminate human HIV pathogenesis.

Still, as Fultz acknowledges, those truisms could change, too, if a strain of HIV is found that causes disease in chimps more quickly. Fultz and other scientists are searching for such strains.

Summit Aims to Save Ukrainian Science

Hoping to rescue his fellow scientists from calamity, a prominent Ukrainian cell biologist has organized an international summit next month to propose reforms in Ukraine's science establishment.

Ukrainian scientists are growing desperate. The National Academy of Sciences of Ukraine (UNAS), which pays the bills for Ukraine's 150-odd research institutes, since April has received almost none of the $54 million budget the government has promised. Yet there is a "frightening apathy within the academy," writes summit organizer Yuri Gleba in a 17 September letter to invitees. Most Ukrainian researchers agree that the UNAS "cannot continue in its present form, but ... no proposals for change or calls for reforms have been forthcoming," says Gleba, head of the International Institute of Cell Biology in Kiev and a senior researcher at American Cyanamid in Princeton, New Jersey.

Gleba hopes to jump-start reform in talks between Ukrainian science leaders and about a dozen Westerners—including Sherwood Rowland, foreign secretary of the U.S. National Academy of Sciences, and British pharmacologist Sir Arnold Burgen, former president of Academia Europaea. The meeting, set for 6 to 7 November, may influence a new Special Commission on Science of the Ukrainian government. Gleba, a commission member himself, warns that "without some external pressure," the bureaucratic panel may do little to avert the crisis.

At least one Ukrainian scientist believes Gleba's summit—sponsored by the Soros Foundation and endorsed by the UNAS—is on the right track. "I totally support his approach," says biophysicist Oleg Krishtal, who will attend the meeting. How to reform Ukrainian science, he says, "is a question of the historical future of Ukraine."

STEVEN DICKMAN

Help wanted. Scientists are seeking advice on budget crisis at Ukraine's National Academy of Sciences.

Newt's Science Breakfast Club?

Now that Congress has abolished its science think tank, House Speaker Newt Gingrich (R–GA) may be looking for a way to create a new one. The Office of Technology Assessment (OTA), a policy analysis shop, officially went out of business on 1 October, but it's already missed.

Gingrich is thinking about inviting some of his colleagues to a breakfast later this fall to talk science, says an aide to Representative Amo Houghton (R–NY). The purpose, the aide says, would be "to discuss what the House should do in place of" the OTA. Former OTA Director Roger Herdman said last month that Houghton, an OTA champion, had spoken with him about the meeting, but that the agenda "is up to the Speaker."

According to an OTA source, Herdman recently asked senior staffers to suggest policy experts to speak at what apparently could become a series of breakfast meetings. Not a bad idea, the ex-staffer says—except that Herdman indicated Gingrich would likely nix some obvious choices and would favor conservative themes. Says one OTA staffer, "It would make a great tombstone: OTA, 1972–1995, replaced by the Science Breakfast Club. No liberals need apply."

Agencies Envision Unified Grant System

Navigating the federal bureaucracy to win research grants is no easy matter. But now a small band of bureaucrats say they want to help. Officials from the three armed services, the National Science Foundation (NSF), the Department of Energy, the National Institutes of Health, and other agencies are quietly putting together a plan to simplify the way universities conduct business with the federal government.

The goal, says one NSF manager, is to create an electronic database that would allow universities to make proposals to any federal research office using a common set of rules. Such interagency coordination could be a boon to university researchers and accountants overwhelmed by the paperwork required to handle grants from different sources, as it would lead to a single accounting system for all federally funded extramural research, he says.

The automated system would also have a spin-off benefit for investigators: If a proposal didn't meet the mission of the agency to which it was submitted, it could be routed to one pursuing that line of research, says Helmut Hellwig, director of the Air Force Office of Scientific Research: "Right now, there is no formal interagency coordination to do this." Gerald Iafrate, director of the Army Research Office, adds that referrals today depend on personal relationships among research directors. Backers say the system could also save time and money by resulting in more joint projects, thereby eliminating duplication of research.

Proponents of the idea will meet in November to work out details of their plan, which then must win approval from agency chiefs. For now, they want to keep a low profile, lest they get caught up in the unwieldy bureaucracy that typically orchestrates such interagency initiatives. "If it gets political, it will fall apart," says one.

Europeans Clash Over Space Station

The ministers who oversee the European Space Agency meet next week in Toulouse, France, to strike a bargain on their participation in the space station program. So far, an agreement has proved elusive

More than a decade has gone by, many millions of dollars have been spent, and thousands of scientists and engineers have labored on the project. But not a single piece of European hardware has yet been built for the international space station. Nor does the European Space Agency (ESA) even have approval from its 14 member states to do so, as they have not been able to decide what should be built or how to divide up the bill. Now, with just 2 years to go before the first element of the space station is launched into orbit, there's no more time for delay. "If there is no decision, we will have a big difficulty in delivering hardware on time," says Jorg Feustel-Buechl, director of ESA's human space program.

Yet that is looming as a real possibility, just a week before the government ministers who oversee ESA meet in Toulouse, France, to agree on major parts of the organization's budget for the next 5 years. ESA officials hoped that the meeting would finally see an agreement on Europe's commitment to the station. But as *Science* went to press, Italy had reneged on an earlier commitment of funds, and government negotiators were struggling to hold the program together. ESA officials fear that if a decision is not made now, the other partners in the project—the United States, Canada, Japan, and Russia—will go ahead without them. "We will really miss the train," says Feustel-Buechl.

The fate of Europe's contribution to the orbiting platform is not the only thing at stake. The space station decision is part of a larger debate over the scope of ESA and its future mix of launcher development, engineering, and science programs. Each large member state has a different idea. Germany and Italy want a vibrant space station program, as their industries would largely build the hardware, while France is eager to continue modernizing the Ariane rocket fleet, which is largely French-built. The British, meanwhile, are criticizing ESA's science program and demanding major cuts (see box)—part of a growing pressure from member states for ESA to reform its management, trim its staff, and be tougher on industry in awarding contracts.

At a meeting in Munich last month to celebrate ESA's 20th birthday, Roy Gibson, a former director general of the agency, remarked dryly: "The European spirit has become rather diluted recently." In that context, the do-or-die decision about the space station is a test of the organization's ability to reach consensus.

Big plans

There was plenty of European spirit at the beginning. When U.S. President Ronald Reagan invited Europe to participate in the space station effort in 1984, ESA managers came up with an ambitious blueprint that would make Europe a formidable space power. Its main elements were the Hermes spaceplane, a small version of the shuttle which would give Europe independent access to the station, and two Columbus laboratory modules, one permanently attached to the station and the other a human-tended free-flyer orbiting separately from the station and serviced by Hermes. Just building the hardware alone would have cost more than $6 billion.

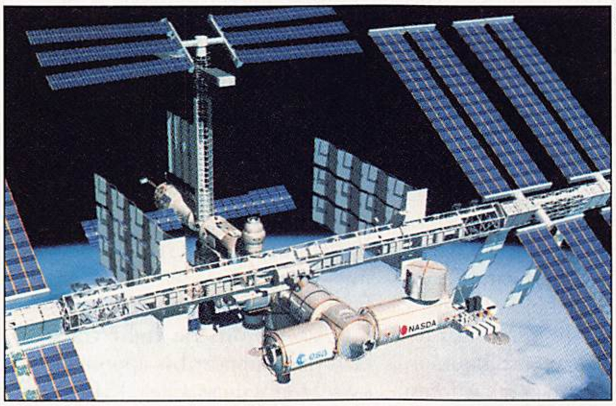

Hanging together. Lab modules from the United States, Europe, Japan, and Russia form the core of the planned international space station.

In the recession years of the early 1990s, however, European nations began to rethink their space budgets. When ministers convened at Granada in southern Spain in 1992, the knives were out: The free-flyer module and, most painfully for the French, the Hermes spaceplane were cut from the program. The plan that emerged consisted of three elements: a smaller attached Columbus module; the automatic transfer vehicle (ATV), a "space tug" which would carry payloads lofted into space by Europe's Ariane 5 rocket to the station; and the crew return vehicle (CRV), an "escape pod" for the station crew, to be developed jointly with Russia.

The ESA council, which is made up of delegations from each member country, was slated to approve this revamped plan in March. In late 1994, however, France and Germany demanded cuts on the order of $2 billion from the total $4.8 billion space station plan, a figure that includes both development and operations through 2003, when the station is completed. ESA's proposed solution was to drop the CRV from the program. But that proposal immediately ran into difficulties because it would have cost French jobs: French companies were pegged to take the leading role in ATV and CRV work.

The council deferred its decision until October. During the spring France proposed dropping Columbus—which would be built largely by German industry—and concentrating funds on the ATV and CRV. "The French were not turned on by Columbus," says Johan Bleeker, director of the Netherlands' National Space Research Institute. Their plan was seriously discussed, says Feustel-Buechl; in July France and Germany ordered ESA to make a detailed study of the two options.

Dropping Columbus would, however, have had serious implications for space station partners outside ESA. The module would provide between 10% and 15% of the total laboratory space on the station, and half of the experiment racks in Columbus will go to U.S. researchers in exchange for the services provided by the U.S. parts of the station. U.S. and German officials say Columbus is Europe's "entrance card" into the space station project.

The council concluded in late August that dropping Columbus was not feasible, but they did abandon the CRV. "France and Germany have come to an agreement," says Bleeker. But France demanded concessions: first, that $66 million be provided for continuing design studies on the CRV, and that Germany agree to support a program to continue development of the Ariane 5 rocket after its scheduled first launch next spring. "All things are linked," admits Feustel-Buechl. "There was an understanding between the two countries on both these elements."

Thus all seemed to be set for a decision at Toulouse—until Italy dropped a bombshell at the end of last month. Italian officials said

U.K. Concerns Send Jitters Through ESA Space Science

The European Space Agency's (ESA's) science program is on the crest of a wave. Over the past 20 years it has launched around 17 missions without a single failure and currently has three missions—a total of six spacecraft—simultaneously being prepared for launch over the next few months. But the ESA science wave could be about to break on an immovable rock: the United Kingdom.

Next week, government ministers from ESA's 14 member nations will meet in Toulouse, France, to decide on the agency's budget for several programs, including science, over the next 5 years. ESA science program director Roger Bonnet is not asking for any extra money, just the same budget, about $450 million per year, adjusted for inflation—roughly 4% annually. Most national delegations, in the run-up to the Toulouse meeting, seem quite content with this deal, although Germany wants a frozen budget without increases for inflation.

ARMY TIMES

Hot seat. ESA Director General Jean-Marie Luton faces opposition from Britain.

Not the United Kingdom. Citing its own budget problems and arguing that ESA needs to boost efficiency, it has stubbornly insisted that the program should be cut each year by 5%, for a total cut of 25% by 2000. "This would be the most dramatic decrease we could imagine. … The program would be ruined," says Bonnet.

U.K. officials say they are in a bind. "Our lack of funding is acute," said Ken Pounds, chief executive of the U.K. Particle Physics and Astronomy Research Council (PPARC), at ESA's 20th birthday meeting in Munich, Germany, last month. The problem is that PPARC's budget is fixed, so if international program budgets continue to rise with inflation, it will have to cut domestic research—including funding for scientific instruments to fly on ESA missions. "The U.K. government is down on big science, and the squeeze has hit," says David Southwood of London's Imperial College, who is currently chair of ESA's influential Science Program Committee.

Indeed, signs of the squeeze were already evident last year, when PPARC was forced to pull out of supplying instruments for Integral, ESA's planned orbiting gamma-ray observatory—a mission British researchers helped to design. The move angered ESA partners and disappointed some British researchers. "It's like being a member of a golf club but not being able to afford the green fees," says space scientist Mike Cruise of the University of Birmingham.

But Pounds argues that ESA could blunt the impact of any cuts by becoming more efficient. "It is vital for ESA to carry out its ambitious program, but like NASA [the U.S. National Aeronautics and Space Administration], it must find a cheaper way to carry out missions," says Pounds. He isn't the first to say so. Under pressure from its member states, ESA managers last fall invited the firms Andersen Consulting and Price Waterhouse to look at its management and accounting methods. The Andersen report, presented to ESA in the spring, criticized ESA's complex bureaucracy, the lack of competition in its procurement policy, and the huge infrastructure set up to handle an extensive human space flight program—a program that has been scaled back dramatically (see main text). Among its 14 recommendations: a 20% staff cut.

Southwood defends ESA's tendency to play it safe, and hence expensive, when designing spacecraft. "ESA missions have worked, and they serve a large community—success is more expensive. If you buy a car once every 20 years, what sort do you buy?" But Birmingham's Cruise concluded there is room for improvement after conducting an independent analysis of a proposed ESA mission called STEP, designed to test whether gravitational mass is identical to inertial mass. "I have a fair degree of confidence that you could take 10% from projects and ESA would still be OK. I'm not so sure about a 25% cut," he says.

As ESA's science program is mandatory for member countries, the budget decision at Toulouse has to be unanimous, and national officials interviewed by *Science* seem divided over what will happen. Some think delegates will compromise on Germany's zero-inflation option. Others favor an ESA proposal which would temporarily reduce the budget by up to 7.5% over the next 3 years. Whatever happens, most agree that the United Kingdom will have to moderate its stance. "The convoy can't wait for the slowest member," says Southwood. But when it moves science may not be riding as high as in the past.

–D.C.

they could not meet their $400 million share of station costs. Italy's space agency, ASI, has been in a state of administrative chaos for some years and is heavily committed to a wide range of projects, including an independent contribution to the space station of a pressurized logistics module that would sit in the shuttle hold to carry supplies. Last month ASI declared that it wanted to pay just $133 million in cash with an additional "in-kind" payment of extra work by Italian industry.

That arrangement would give Italian companies a far greater share of the work than Italy's financial contribution entitles it to—an arrangement unlikely to be palatable to other ESA partners. And Italy's cash shortfall, coupled with the reluctance of several smaller contributors to the space station program to meet their obligations, leaves the total sum declared so far several hundred million dollars short of the $1.86 billion space station budget proposed by ESA for the 5 years 1996 to 2000.

This budget confusion is making ESA's international partners twitchy, and station opponents in the United States like Representative Tim Roemer (D–IN) argue that Italy's proposal shows the program is falling apart. U.S. station supporters are upbeat publicly, but privately they are unhappy with Europe's jittery stance. White House officials in recent months have been urging European politicians to get on board quickly.

Ministers and government officials are now locked in negotiations to find a solution. But if a deal cannot be made, members of national delegations hint that France may cancel the meeting—or dissatisfied delegations simply may not turn up, a situation that ESA dreads. "Opportunities will fade away. This is an important meeting for us," says Feustel-Buechl.

Given their huge investment in money and political chits, however, sources on both sides of the Atlantic say it is unlikely that European politicians will walk away from the space station effort. Such a move would infuriate their aerospace industries, damage European relations with the United States and Japan, and mark a clear retreat on a high-profile, high-technology program. And with the pressure on, the ministers may have run out of time-outs.

–Daniel Clery

With additional reporting by Robert Koenig in Berlin and Andrew Lawler in Washington.

BIOTECHNOLOGY

Yellowstone Managers Stake a Claim on Hot-Springs Microbes

YELLOWSTONE NATIONAL PARK, WYOMING—National parks like Yellowstone may themselves be national treasures, but the government now wants to convert some of their natural riches into working capital and knowledge that will benefit the park, the public, and science. In a meeting here last month that drew representatives of such big biotechnology and pharmaceutical names as Promega, New England Biolabs, Novo Nordisk, Eli Lilly, and DuPont, Yellowstone National Park managers said they intend to seek a share of commercial profits generated by hot-water microbes, or thermophiles, incubated by the park's bubbling hot springs.

The meeting, to discuss the latest research on thermophiles (see box), marked the latest step in the National Park Service's efforts to see that taxpayers reap dividends on their investment in maintaining the park. Without such a payback, said John Varley, Yellowstone's resource management chief, microbe prospecting might assume the image of public lands mining, logging, and grazing as "yet another giant rip-off of the people who have been paying their tax money to support this park" since it was established in 1872.

Large sums could be at stake. Take Taq polymerase, the driving ingredient of the polymerase chain reaction (PCR). Taq gets its name from its parent bacterium *Thermus aquaticus*, identified in 1965 in a 73-degree Celsius Yellowstone pool. Two decades later, its enzyme proved useful in high-heat PCR cycles that multiply a few DNA strands into millions—and earns millions of dollars for Swiss drug giant Hoffmann-La Roche, which owns patents on PCR and Taq polymerase. Other companies are now searching out newer, better thermophiles in springs where 99.9% of the microscopic inhabitants may remain unknown. The talents of those few found so far run from churning out sturdy enzymes that strip old paint off airplane wings to erasing byproducts from gold ore in a high-heat reaction that would weaken other bacteria.

Park managers made their first move earlier this year, when federal attorneys interpreted the laws governing research in national parks to mean that park micro-organisms remain government property even after they are carted around the globe and cultured in the lab. Park collecting permits now sanction commercial development of Yellowstone microbial strains, but only with an agreement that cuts the government in on any revenue. (Purely academic researchers won't have to pay anything.) While no rate structure has been set, Varley said, options run from fees or royalties to a request that companies donate 1% of profits from Yellowstone discoveries back to the park.

Varley's suggestions drew a mixed response. David H. Gelfand, a Roche scientist who first applied the Yellowstone enzyme to PCR when he worked for Cetus Corp., said that Taq polymerase was a one-time windfall the government is now unfairly using as a "whipping boy." Biotech companies already hand over plenty of cash to Uncle Sam through income taxes, he said, and the greatest public benefit comes through knowledge of the microbial world.

Taq polymerase is a whipping boy, Varley responded, because it's a prime example of the value of preserving national parks. If a profit-sharing mandate puts collectors off, he said: "Go somewhere else. You're not going to find what you find here." Indeed, Yellowstone's 10,000 or more hot-water features may be the most diverse collection of springs anywhere. Micro-organism prospectors argue, however, that they do not harm the resource. "I don't come with a backhoe," said Jeff Braman of Stratagene, a California biotech company. "I'm not prospecting in the same way the strip miners are prospecting for ore."

Many at the meeting were eager to back the park, financially or otherwise, although they did not agree how. Jay Short, chief technology officer of Recombinant BioCatalysis Inc., said the environment and its prized microbes will be protected only if industry shows they have value. Roche has, in fact, offered donations to Yellowstone, but officials, previously unsure of their legal standing, turned them down. Now the park is on the brink of closing facilities due to short budgets, and Yellowstone Superintendent Michael Finley said: "We'll take money from anyone who wants to give it to us."

–Michael Milstein

Michael Milstein is a science writer in Cody, Wyoming.

A Glimpse of Early Life Forms

M. MILSTEIN

Microbe hunters. Susan Barns and Siegfried Burggraf prospecting in Obsidian Pool.

Fizzling and bubbling furiously, spitting bursts of steam and black sand, Obsidian Pool looks a bit primordial. That's fitting: The oblong hot spring, in a backcountry nook of Yellowstone National Park, contains living relics of Earth's early life, if Indiana University microbiologist Norman R. Pace is right. Pace announced at a meeting in Yellowstone last month (see main text) that he and his colleagues have found two microbes from Obsidian Pool and one from another Yellowstone spring that appeared early in the evolution of life on Earth and have undergone relatively little change since then.

Discovered by Susan M. Barns of Pace's lab and Anna-Louise Reysenbach, a colleague of Pace's now at Rutgers University, the microbes belong to the domain Archaea, which includes microscopic organisms distinctly different from true bacteria, or eubacteria. But their gene sequences are so different from those of familiar archaeal species that Pace proposed they be classified in a new, third kingdom within the Archaea. He and his colleagues have named the proposed new kingdom Korarchaeota, using the Greek word for youth.

A computer-generated evolutionary tree based on their genetic variations suggests "they are the most primitive organisms so far discovered," said Pace. "They have the shortest [branch] from the common ancestor of all life." Montana State University microbiologist David M. Ward, who also works in Yellowstone and is familiar with the data, says, "The idea that these may be close relatives of the primordial archaea seems like a good one."

To learn more about these primitive organisms, microbiologist Siegfried Burggraf has replicated Obsidian Pool's chemistry in Karl O. Stetter's lab at the University of Regensburg in Germany, in hopes of growing enough of them to study. If the microbes cooperate, Barns says, "we may get some idea of what the common ancestor was like."

–M.M.

SPACE SCIENCE

A Focal Point for Diverse Disciplines

Thanks to the persistence of a Swiss physicist and his political allies, space scientists are about to get their own institute devoted to stitching together the field's scattered disciplines. The new International Space Science Institute, located in Bern, the Swiss capital, will be inaugurated on 6 November, when it plays host to its first event: a workshop on the outer reaches of the solar system, where particles streaming from the sun meet the interstellar medium.

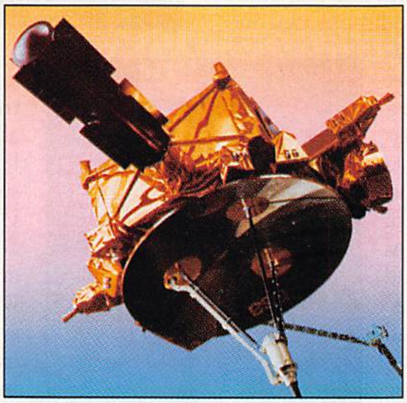

ESA

Data factory. Institute will analyze data from missions like Ulysses.

The institute offers "a place to compare notes among disciplines," says its founder and co-director, Johannes Geiss. It also provides a much-needed venue for scientists of different nationalities to meet, space scientists say. And for the European Space Agency (ESA)—which is funding half the organization's $1.5 million annual costs—it provides an opportunity to say thank you to Switzerland, which lacks any ESA facility but has been consistently supportive of its space projects, according to ESA officials.

The new institute will concentrate on data gathered by international missions studying the physics of the sun, the solar wind, and other space plasmas, interactions between the sun and Earth, and comets, says Geiss. ESA scientists have focused on such research rather than the planetary science that is the mainstay of the U.S. and Russian programs.

The institute will have fewer than a dozen scientists and support staff, but by bringing in visiting researchers, Geiss and his colleagues intend to organize study groups and workshops of up to 40 theoreticians and experimentalists. The emphasis will be on sifting through the huge amounts of data from these missions that remain largely unexplored. "There are so many open questions left; the challenge is to organize them and find the time to explore them," says Geiss, who teaches at the University of Bern and participated in the Ulysses mission.

The institute will not duplicate work now done by ESA, says Martin Huber, who directs ESA's space science department. "It will do pure research based on satellite data and will not be involved with operations and planning," he says. Bringing together the different disciplines will provide great synergy, Huber adds.

The 5-day November workshop will bring together astronomers familiar with the heliosphere, a region dominated by the solar wind that extends 100 astronomical units from the sun, and physicists who have been gathering data on the effects of the sun around Earth. Western European, American, Russian, Polish, and Japanese scientists will participate in the effort. The response to the workshop has been enthusiastic, says Geiss, who will co-direct the institute with Bengt Hulqvest, former director of the Swedish Institute of Space Research in Kiruna: "Only one person didn't accept who was invited, and he has health problems."

The enthusiasm is no surprise to Geiss: He received lots of encouragement for his idea from a diverse group of scientists, ranging from Roald Sagdeev, former chief of the Soviet Union's space science program, to Reimar Luest, former ESA director general. Finding the money, however, was not so easy.

ESA science managers at first balked at participating, given the tight squeeze on funding. But, thanks to lobbying from Swiss politicians such as Peter Criolla, who heads that country's ESA delegation, the Paris-based ESA agreed in December to support the proposed institute. The governments of Switzerland and the canton of Bern will kick in half the required funding. The Swiss aerospace company Contraves, which helps build part of the European Ariane rocket, also stepped in to provide some endowment money.

In addition to supporting the small staff, the money will finance visits to the facility primarily from European space scientists. "We feel at this point that financing Europeans is our priority," says Geiss, although he adds that others are welcome. The institute is unlikely to cover travel costs for non-Europeans, but the Swiss National Science Foundation has an international account that they could turn to for support.

If the upcoming workshop proves a success, Geiss says he hopes it will set the pattern for future efforts. "We are trying to play the role of an institute of advanced studies—but, of course, Princeton already is using that name."

–Andrew Lawler

NATIONAL LABORATORIES

Los Alamos Wins One in Tritium Race

Adopting what Energy Secretary Hazel O'Leary calls "the old belt-and-suspenders approach," the Department of Energy (DOE) has settled on a two-track strategy for making tritium for the United States' nuclear arsenal. DOE will recommend that Congress allocate $45 million in fiscal year 1996 for a multiyear study of the feasibility of making the radioactive isotope in an advanced proton accelerator. It will also call for another $5 million to be spent on a parallel track: a study of tritium production in a commercial nuclear power reactor, either leased from a utility or purchased outright.

The announcement, which at press time was scheduled for 10 October, will please officials at Los Alamos National Laboratory, where the bulk of the research and development for a tritium-producing accelerator will be pursued. But it represents a loss for proponents of an alternative approach: building an all-new reactor specifically for making tritium. It will also disappoint scientists who hoped that the accelerator could be explicitly dedicated to making both tritium and beams of neutrons for basic science (*Science*, 18 August, p. 914). "I've got one obligation, and that's to produce tritium" for defense purposes, says O'Leary.

Even though the U.S. nuclear stockpile is shrinking, the supply of tritium—the thermonuclear explosive in a hydrogen bomb—is shrinking even faster. This radioactive isotope of hydrogen, which decays at 5.5% a year, hasn't been produced by the United States in significant quantities since 1988. Even if the government makes the stockpile cuts specified by the still-unratified START-II treaty, new tritium would be needed by 2011. The dual-track approach, says O'Leary, should ensure that DOE won't "get halfway down the path and stop" because of technical or political obstacles.

The accelerator approach poses the chal-

SAM KITTNER

Keeping options open. DOE's Hazel O'Leary.

lenge of reliably generating a tightly focused 130-megawatt proton beam—the most powerful ever created by a linear accelerator. The beam would smash into a tungsten target, producing neutrons and other particles that would be slowed in water and sprayed into a gas stream containing helium-3, which the neutrons would convert into tritium. Paul Lisowski, director of the Accelerator Production of Tritium program at Los Alamos, doesn't think the technical challenge is overwhelming: "What we're talking about is building up a system from parts that have already been tested." Counting the 1996 expenditure, DOE is now prepared to spend roughly $350 million for Los Alamos to build and test a lower energy prototype; a full-scale accelerator would cost in the vicinity of $2 billion and would probably be located at Savannah River, DOE officials say.

Reactor production of tritium is a more familiar technology: The current tritium stock was produced by bombarding lithium rods with neutrons in the cores of now-defunct reactors at Savannah River. At a total cost of about $250 million, the reactor studies will look at the safety of running a reactor with a full load of lithium bars and at regulatory issues. The actual cost of purchasing and converting a commercial reactor might be between $1 and $2 billion, say DOE sources.

O'Leary believes that the conversion or dual use of a fission reactor would have "the lowest incremental environmental impact," as the reactor would be operating anyway to produce electricity. Still, any reactor produces long-lived radioactive byproducts, and blurring the long-standing distinction between civilian and military plants raises questions "that would need to be resolved at the highest levels of government," says Jon Ventura, a legislative and public affairs specialist for defense programs at DOE. The accelerator, in contrast, would produce no long-lived waste and wouldn't suffer from the public fears surrounding fission reactors.

DOE has decided not to exploit what some scientists see as another strength of the accelerator option, however: the possibility of using it as the world's most intense source of neutron beams for probing materials and molecules. In times of thin funding, says Burton Richter, director of the Stanford Linear Accelerator Center, such dual use would yield "an accelerator for research built on military money."

O'Leary's announcement offers no encouragement to Richter and others who hoped to share the facility. But John Browne, director of the neutron-science center at Los Alamos National Laboratory, offers a small consolation prize. Even if the defense accelerator isn't open to basic researchers, future neutron sources for civilian research "will benefit from the R&D."

–James Glanz

LYME DISEASE

NIH Gears Up to Test a Hotly Disputed Theory

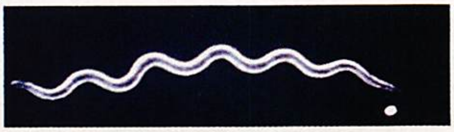

CHARLES W. STRATTON/VISUALS UNLIMITED

The National Institutes of Health (NIH) is preparing to fund a $1-million-a-year study that it hopes will settle a dispute that has riven a segment of the medical community in the past few years. At issue: Is there a chronic form of Lyme disease that sometimes persists after conventional antibiotic treatment, inflicting a variety of symptoms such as muscle pain, fatigue, and memory loss on its victims? A group of physicians and patient advocates believes the answer is an emphatic "yes," and they have been agitating for the medical establishment to take them seriously. The upcoming NIH study means that their claims will finally be put to the test. But many Lyme disease researchers are skeptical of the need for this project.

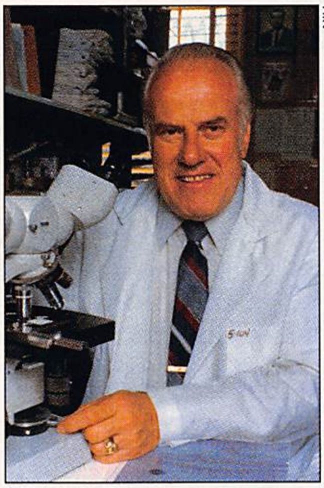

NIH

Eponymous spirochete. Willy Burgdorfer and *B. burgdorferi.*

The very existence of the trial is testimony to the persistence of patient advocacy groups. They have lobbied Congress for many years to support research into chronic Lyme symptoms, promoting the need for long-term therapy. Their tactics have angered research leaders such as Allen Steere of Tufts University, who was the first to identify the U.S. Lyme syndrome in the 1970s. The multimillion-dollar trial that NIH is planning, he says, "would never have been funded" through the "normal mechanisms" of investigator-initiated research. But Greg Folkers, a spokesperson for the National Institute of Allergy and Infectious Diseases, says, "This trial has been under discussion for several years"—well before Congress recommended that NIH study new antibacterial strategies.

Steere, Alan Barbour—a microbiologist at the University of Texas, San Antonio—and other researchers believe that there's little evidence to support the notion that there is an epidemic of chronic infection by Lyme disease. Most so-called chronic cases, they believe, are not Lyme disease at all; NIH's study could be a waste of money. But advocate groups—particularly the Lyme Disease Foundation (LDF) of Hartford, Connecticut, which includes physicians who treat Lyme patients—argue that the disease is more elusive, more malignant, and more difficult to treat than academic scientists have acknowledged. They believe that the traditional treatment advocated by physicians at leading medical schools such as Yale, Tufts, and the University of Connecticut—2 to 4 weeks of oral antibiotics and, in rare cases when the central nervous system is infected, 4 weeks of intravenous antibiotics—is in many cases insufficient to wipe out the disease.

Joseph Burrascano Jr., a Long Island physician who specializes in treating Lyme disease and has served as board member of the LDF, argues that more aggressive therapy is often needed. He prescribes months-long courses of antibiotics for many of his Lyme patients, including intravenous therapy. Kenneth Liegner, a physician in Armonk, New York, has also written that clinicians should expect "a revolution in our conceptualization of this disease." Evidence is mounting, Liegner says, that "subsets of patients" with as-yet-unconfirmed immune system weaknesses do not benefit from routine therapy and may require "prolonged antibiotic treatment."

Patient activists have seized on these arguments and are pushing for studies which they believe will confirm a more radical attack on the disease than has been recommended by the establishment so far. One objective, says patient advocate Kenneth Fordyce, chair of the governor's Lyme disease advisory committee in New Jersey, is to get insurance companies to reimburse patients for antibiotic therapy that lasts longer than the standard 28 days.

Disagreement between the activists and the medical establishment erupted 3 years ago, when abstracts of a dozen papers submitted by clinicians to a Lyme disease conference were rejected by the program committee as lacking in scientific merit. The papers—most of which discussed chronic Lyme cases—were reinstated over the objections of several researchers after patient advocacy groups protested (*Science*, 5 June 1992, p. 1384).

After failing to convince the establish-

ment of its scientific views, LDF took a route that has been well trodden by AIDS and breast cancer activists: It mounted a lobbying campaign. NIH is now accepting proposals for a trial that will examine whether patients with long-lasting symptoms are truly infected with Lyme, and whether they benefit from prolonged antibiotic therapy.

Origins: Old Lyme. The tussle between the activists and the Lyme disease establishment stems in large part from inadequate diagnostic tests and limited understanding of how the culprit organism survives in humans. The symptoms of Lyme disease in the United States were first identified during the 1970s through Steere's studies of children in New England who were suffering from swollen knees and joints. Steere determined that the syndrome—which was heavily focused around Old Lyme, Connecticut—is a form of arthritis associated with bites from deer ticks and a strange, bulls-eye rash, erythema migrans. It soon became apparent that Lyme syndrome was similar to an infection that had been described in Europe in the 19th century. In 1982, biologist Willy Burgdorfer at NIH's Rocky Mountain lab in Montana nailed the infectious agent: a spiral-shaped bacterium (a spirochete) of the Borrelia family, mainly found in a small deer tick, *Ixodes scapularis*. In honor of the discoverer, the bacterium was named *Borrelia burgdorferi*.

Today, Burgdorfer says that the Lyme organism and other spirochetes—slow-growing but potent organisms responsible for a variety of diseases including syphilis—deserve more attention from researchers. Syphilis, for example, "has been known for ages. ... But with all our advanced technology, we are not in a position to 100% prove that the manifestations shown by a patient are due to chronic spirochetosis [ongoing infection] or something else," such as late-appearing damage from an infection that may have stopped much earlier. The same uncertainties plague the diagnosis and treatment of Lyme disease, Burgdorfer says.

The weak understanding of the organism's biology is compounded by the lack of a good diagnostic test. Blood tests for human Lyme infection have been unreliable, often yielding false positives, and, some physicians say, many false negatives. It was only in October 1994, Barbour notes, that leaders of public health agencies from around the United States met in Michigan to establish common standards for testing and confirming the presence of Lyme infection.

Because it was hard to diagnose cases with certainty, it was also hard to sort out the effects of different therapies. The confusion has been increased by the widening spectrum of symptoms attributed to Lyme infection. Initially, Steere focused on clear-cut indicators—the rash and swollen joints. But subtler effects have now been added to the list, including injury to the eyes, the heart, the nervous system, and the brain.

A polarized community. As the list of possible ill effects grew, so did the number of patients who felt they were suffering from Lyme disease. Their ranks stood at fewer than 1000 in 1982, but, according to the Centers for Disease Control and Prevention, rose to more than 13,000 in 1994. To Steere, the increase is a sign that Lyme disease "has become an overdiagnosed and overtreated illness." To back up this contention, Steere conducted a study, published in the *Journal of the American Medical Association* in 1993, in which he reported that 57% of 788 cases referred to the clinic as Lyme disease patients by other physicians were not infected with *Borrelia*.

Many other academics—such as Durland Fish and Eugene Shapiro of Yale—agree with Steere that clinical practice has gone overboard. They believe many physicians are classifying vaguely defined illnesses as Lyme disease and selecting antibiotic therapy as the most convenient solution, particularly for prolonged and ill-defined ailments, such as diffuse pain (fibromyalgia) and fatigue. One of the major problems in this field, says Shapiro, "is not Lyme disease itself but the misdiagnosis of Lyme disease and anxiety about Lyme disease."

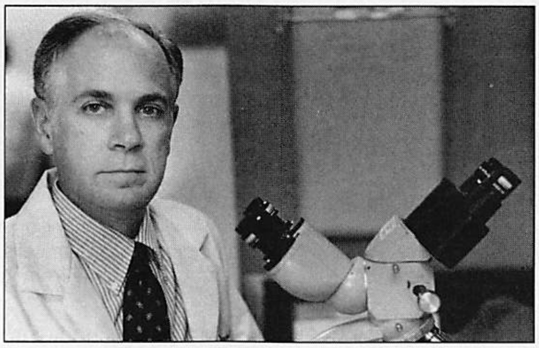
BRADFORD F. HERZOG

Skeptic. Allen Steere believes Lyme disease is "an overdiagnosed and overtreated illness."

At the other pole are physicians who think Steere and his medical school colleagues ignore the subtlety and persistence of *B. burgdorferi*. Burrascano, in a 1993 Senate hearing, denounced the "conspiracy ... of university-based" scientists who he said were using their clout to promote the "outdated" idea that "Lyme is a simple, rare illness that is ... easily cured by 30 days or less of antibiotics." Burrascano points out that the Lyme bacterium is difficult to detect in the blood after the initial infection even if it has been left untreated. The aggressive treaters of Lyme disease have long argued that the spirochete hides within cells, deep in joints and connective tissue, in the eyes, and in the relative isolation of the cerebrospinal nerve system. These locations are inaccessible to routine antibiotic therapy, they argue, and long-term infections require the use of intravenous, potent antibiotics over many months.

Somewhere in the middle of the Lyme battleground are physicians like neurologist Patricia Coyle, a clinician at the Health Sciences Center of the State University of New York, Stony Brook, who see merit in Burrascano's arguments but doubt that many patients are afflicted with chronic infections. Coyle, who works in a special clinic at Stony Brook that sees 1600 Lyme patients a year, says key questions about Lyme infection remain unanswered.

First, Coyle asks: "Does the spirochete go into the cells or not? We don't know." However, she says in vitro studies suggest that it does, and that it may escape antibiotics that way. Second, Coyle would like to know to what extent and how often the spirochete penetrates the central nervous system. Also, she would like to confirm which antibiotics are best at attacking it there. Third, she would like to learn whether the organism enters a quiescent period after infection. While scientists have been exploring these issues in laboratory studies, Coyle argues that it is important and "very practical" to carry out a large clinical trial, because it's risky in dealing with infections to extrapolate from bench to bedside.

These are just the kinds of questions that NIH's clinical trial will address. The aim is to recruit patients who have previously been diagnosed and given routine therapy for Lyme disease, but whose symptoms persist. They will be carefully screened to fit criteria—as yet undefined—of confirmed Lyme patients. And they will be assigned blindly to one of several treatment regimens, including a placebo group, to be followed for several years, probably at more than one center. "One of the big unanswered questions," says John LaMontagne of the National Institute of Allergy and Infectious Diseases, "is whether or not *Borrelia* produces some sort of permanent neurologic damage that cannot be reversed with antibiotic therapy."

Researchers such as Barbour and Steere are concerned that the trial—if not well designed—could end up an expensive disappointment. But Barbour agrees it may serve a useful purpose. The debate among clinicians about what causes long-term symptoms and how to cure them "needs to be settled," he says. "People are spending millions of dollars on antibiotics," hoping to be rid of all kinds of symptoms. Adds Burgdorfer: "Once we have the answers to these questions, all the other stuff ... the politics ... the quarreling among the scientists, will disappear." In a community so split, that may be a forlorn hope.

–Eliot Marshall

Designer Tissues Take Hold

By engineering polymers that attract and bind liver, nerve, and other cells, scientists are beginning to create artificial organs that are biologically "real"

There's nothing simple about the liver. The organ's many different cell types are arranged in precise three-dimensional patterns to filter toxins from the blood, convert nutrients into forms usable by body tissues, and perform a broad range of other functions. Now scientists are taking basic steps toward growing this complicated organ in the lab.

Tissue engineering, as this field is known, has been around for a little more than a decade. Its researchers have already developed laboratory-grown versions of tissues such as skin and cartilage that are now being tested as replacements for damaged tissues. These are, however, comparatively simple body parts, consisting of one or two cell types layered on a synthetic polymer scaffold or a mesh made of the structural protein collagen (see box).

A lab-grown liver, however, calls for a new level of sophistication and control: A variety of cells need to be arranged and grown in particular orientations. That means a scaffold with a high degree of selectivity, something polymer and collagen scaffolds lack. But by attaching specific cellular recognition molecules, such as protein fragments, to synthetic scaffolds, biologists and chemists have been able to demonstrate that such feats are indeed possible.

Linda Griffith-Cima, a chemical engineer at the Massachusetts Institute of Technology (MIT), and her colleagues have designed a scaffold that attracts liver cells called hepatocytes while rejecting other cell types. Scientists are using similar hybrid technology to direct the growth of nerve cells on biocompatible materials in hopes of eventually repairing damaged nerves, and to create synthetic blood vessels lined with cells that minimize the formation of dangerous blockages.

Although the work on these hybrid scaffolds is still of a preliminary nature, "it's definitely where the field is going," says David Mooney, an assistant professor of chemical engineering and dentistry at the University of Michigan. The dual nature of the devices is allowing researchers to take advantage of the ability to precisely control the structure of synthetic materials while at the same time camouflaging their foreign nature, minimizing conflicts with the body's immune system. "We not only remove the foreign surface, but we replace it with one that promotes directed growth of the tissue we're interested in," says David Clapper, a cell biologist at BSI Corp., an Eden Prairie, Minnesota–based company working to improve the performance of blood vessels and other implants.

Although the destination is exciting, the field still has to negotiate some bumps before it gets there. One possible barrier, points out Martin Yarmush, a bioengineer at Rutgers University in New Jersey, is that once cells attach themselves to a matrix, hybrid or otherwise, they begin to excrete proteins which may interfere with the carefully laid plans by binding unwanted cells in that region.

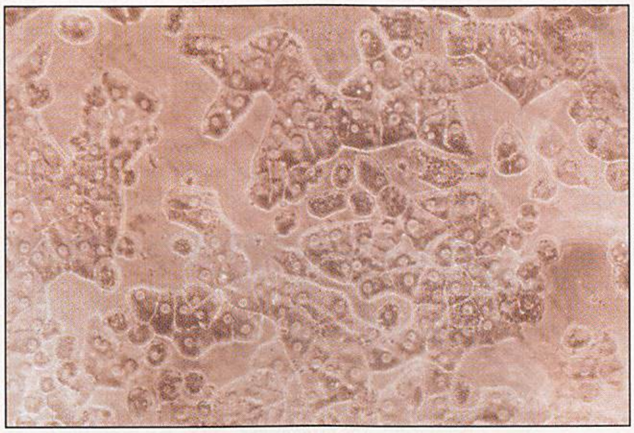

BIOMATERIALS/ELSEVIER SCIENCE LTD.

Liver in a lab. Researchers attached cellular recognition molecules to this polymer mesh, selectively binding these liver cells, known as hepatocytes, which remove damaged proteins from the blood.

Liver under construction

Selection of specific cell types is a crucial issue in tissue design. Natural and synthetic scaffolds for body tissues, by themselves, are not terribly picky hosts. "Synthetic scaffolding materials are easy and cheap to make and form into a desired structure," says Mooney. But they typically provide holdfasts for many different types of cells, he adds; collagen is similarly undiscriminating. And, notes Mooney, collagen is "hard to isolate in large quantities." So researchers have tried to take advantage of the mass-production capacity of synthetics, but modify them with a biological ability to select specific cell types.

The efforts to bind liver cells illustrate the potential power of such a combination. Thus far, most researchers have been trying to design polymers to selectively bind hepatocytes, the most common and important cell type in the liver. These cells carry out more metabolic functions than any other group of cells in the body. One of their duties is to remove damaged proteins from the blood. The cells can do this because they recognize specific carbohydrate sequences, attached to these proteins, that mark these complexes as damaged goods. In the late 1970s Paul Weigel and his colleagues at Johns Hopkins University made synthetic versions of the carbohydrate sequences and used them as lures for the cells: The scientists attached the carbohydrates to a polymer surface made from polyacrylamide, and saw that the hepatocytes engulfed the lures and remained stuck to the polymer surface.

Although successful at binding hepatocytes, polyacrylamide isn't a viable scaffold for tissue engineering, because the material provokes a strong immune response in the body. So more recently Griffith-Cima and her colleagues decided to try attaching the same carbohydrates to a more biocompatible synthetic surface. But they had to choose their material carefully, as many synthetics, such as polypropylene, can be tolerated by the body but quickly become coated with proteins which attract all kinds of cells—exactly what the scientists didn't want.

The researchers decided to build their scaffold with a meshed, water-filled network of polyethylene oxide, or PEO, which is resistant to protein adsorption. PEO molecules are star-shaped, with several arms emanating from a central core. When linked in a network in a water-based solution, the end of each arm floats free.

These ends contain reactive hydroxyl groups, to which the researchers attached carbohydrate molecules as lures for hepatocytes. Griffith-Cima and her colleagues report in the journal *Biomaterials* (in press) that when they added rat hepatocytes, the cells went right for the lures and ended up bound to the polymer mesh. But other cells, such as fibroblasts, failed to bind to the mesh when Griffith-Cima's group added them to the solution. "[Griffith-Cima] has solved one of the big problems—getting a receptor that is unique for hepatocytes," says Kevin Healey, a biomedical engineer at the Chicago campus of Northwestern University.

The next step is to build cell-specific scaffolds in three dimensions. A normal liver,

Out of the Lab, Into the Body

Although efforts to make hybrid cellular scaffolds for tissue engineering have barely begun (see main text), projects that use natural or synthetic matrix material alone—or nothing at all—have forged further along. Attempts to engineer structural tissues, such as skin and cartilage, have scored the greatest successes, with several new products on or nearing the market.

During one recent study, a Swedish team engineered a patient's own cartilage-producing cells, or chondrocytes, to treat damaged knee cartilage. Joint cartilage normally does not regenerate in the body; hence, damage from injury or illness tends to become more severe over time. More than 500,000 patients undergo surgery in the United States each year to alleviate the pain and restricted movement that accompany cartilage damage. But such procedures typically provide only short-lived symptomatic relief.

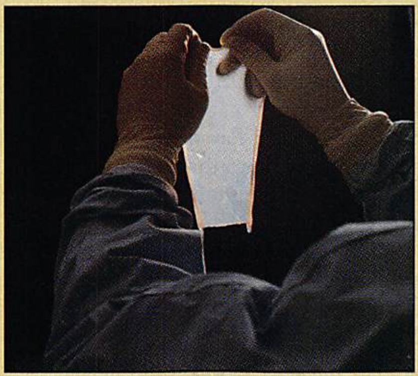

ORGANOGENESIS

Ready to wear. Lab-grown skin such as this patch, grown on a collagen scaffold, has proven successful in clinical trials.

So researchers at the University of Göteborg and Sahlgrenska University Hospital in Sweden extracted chondrocytes from 23 patients, multiplied the cells in a bioreactor, and implanted the new tissue in the patients' damaged knee joints. In the 6 October 1994 issue of the *New England Journal of Medicine*, the researchers, led by Lars Peterson and Anders Lindahl, reported "good to excellent" results for 14 out of 16 patients in which the lab-grown cartilage was implanted to repair damage at the upper end of the joint; the new cartilage cells displayed the consistency of healthy cartilage. The other seven patients, treated to repair defects in the cartilage surrounding the kneecap, fared less well, in part because cartilage there experiences greater mechanical stress, says Lindahl.

This technique is somewhat time-consuming, however: It took the Swedish team a few weeks to collect, grow, and transplant these cells. So other researchers want to develop engineered tissues that are more ready-made. For instance, a team at Organogenesis, a Massachusetts-based biotech company, has had success growing sheets of artificial skin on natural matrix materials that form ready-to-use grafts. This May, they finished a clinical trial of skin grown on collagen, a natural material in the extracellular matrix that binds cells to form tissues. The Organogenesis team reported that the engineered skin was 60% better than conventional bandaging treatments at healing venous ulcers, skin lesions that typically affect the elderly.

To grow this skin, a team led by cell biologist Nancy Parenteau multiplied cells from neonatal foreskin tissue donated after circumcisions. Parenteau's team uses two cell types that don't seem to trigger an immune reaction in the graft. The first type, fibroblasts, make up the "dermal" or underlying skin layer. The second, keratinocytes, constitute the top or epidermal covering. The team first seeds fibroblasts on collagen purified from bovine tendons, and then after about a week adds keratinocytes. Another 2 weeks of incubation yields a replacement skin ready for transplant. Over a period of weeks, successive layers of lab-grown skin are placed over a patient's ulcerated skin, and blood vessels grow into and sustain the new tissue. After 3 months, Parenteau says, none of the implanted skin has shown signs of rejection. Another approach—developed by Advanced Tissue Sciences in La Jolla, California—grows skin cells on a biodegradable polymer mesh; it has also fared well in early human trials.

Other tissues being explored by these biological engineers include bone, tendon, intestine, heart valves, bone marrow, and trachea. Researchers are also working to implant insulin-producing cells into diabetics to help these patients regulate their blood sugar without the need for regular injections of the hormone, and to implant dopamine-producing cells into Parkinson's disease victims to treat the symptoms of this neurological disorder. Says David Mooney, a tissue engineer at the University of Michigan: "The range of applications people are looking at is rather immense."

–R.F.S.

which has the largest volume of any organ in the body, consists of a mass of cells tunneled through with blood vessels. The organ's size enables it to filter toxins continuously from the large volume of blood in the body as well as perform its myriad of other functions. To do so, however, the variety of liver cells have to be precisely interspersed. Griffith-Cima's group is taking on these 3D challenges as well. The researchers recently devised a way to use computer-controlled printing techniques to lay down polymers known as polylactic acid (PLA) in specific patterns, one paper-thin layer at a time. That allows them to build up a porous 3D scaffold with a precisely controlled architecture.

The researchers are now working to attach PEO molecules (with the carbohydrate lures) to their PLA scaffolds. And over the next couple of years, says Griffith-Cima, they hope to attach other recognition molecules, such as antibodies, to the PEO arms in order to fix liver cells called bile duct cells. They also plan to use the amino acid sequence arginine, glutamic acid, aspartic acid, and valine—known as the REDV sequence—to specifically attract endothelial cells. Eventually, with the proper lures, they hope to fix the right mix of cells for a functioning liver.

Gathering nerve

Hybrid scaffolds are also useful because they can influence the direction of cell growth. At the State University of New York, Buffalo, Joseph Gardella and his colleagues are using the technique on nerve cells. Ultimately, they and other researchers hope to direct growing neurites—the cell arms that carry nerve impulses—across gaps caused by accidents or illness in the central and peripheral nervous systems. One possibility now being explored by Gardella and his colleagues involves organizing cellular adhesion molecules on a polymer surface.

Gardella, John Ranieri—who recently moved from Brown University to CarboMedics in Austin, Texas—and a group of Swiss colleagues led by Patrick Aebischer at the Lausanne University Medical School and Hans Mathieu at the Ecole Polytechnique Fédérale de Lausanne, start with a Teflon fabric mesh. Teflon is considered safe for a variety of biological implants. The researchers then prepare a pattern on it to guide neurites, using a segment of the extracellular matrix protein laminin, which binds to nerve cells, as that guide. They begin by covering the polymer mesh with a mask made of nickel with tiny slits cut in the metal. The researchers then expose the nickel-masked Teflon to a hot ionized gas, which penetrates the slits in the nickel and converts fluorine atoms in the fabric to reactive hydroxyl groups. These

hydroxyl groups then act as links to which the researchers attach peptide sequences—known as YIGSR sequences—from laminin.

In the December issue of the *International Journal of Developmental Neuroscience*, the researchers reported that when they placed mouse nerve cells on their scaffold, the cells bound selectively to regions with the YIGSR-modified Teflon. Moreover, when new neurite branches grew from these cells, they followed the patterned surface. "This is a critical demonstration that you can pattern polymers and nerves will follow the patterns," says MIT's Christine Schmidt, who is researching directed nerve-cell growth. Now the researchers are working to roll their modified fabrics into tubes that can be wrapped around damaged nerves in the body.

Designer liners

Teflon has a long history as another type of implant: artificial blood vessels. But here its history is somewhat spotty. Although the synthetic works well on large-diameter vessels—wider than 6 mm—smaller vessels develop problems. These vessels typically clog up within 2 years after implantation—platelets and smooth muscle cells in the blood begin sticking to the surface of the polymer mesh, occluding the opening. This wouldn't happen if the implant walls more closely resembled natural blood vessels, so scientists are re-engineering them to do just that.

INT'L JOURNAL OF DEVELOPMENTAL SCIENCE/ELSEVIER SCIENCE LTD.

Nerves grown in a row. *(Top)* By attaching cell adhesion molecules in patterns on a Teflon sheet, researchers have been able to bind nerve cells to the sheet (scale bar = 100 microns). Growing neurites from these cells *(right)* follow these patterns.

"We're trying to take surfaces that are recognized [by the body] as foreign and change them into something the body really likes," says BSI's Clapper. What the body likes in the case of blood vessel inner walls are endothelial cells, which normally create a slippery surface on those walls that prevents platelets and smooth muscle cells from adhering. The strategy Clapper and several other researchers are pursuing is to induce those cells to bind to the inner walls of polymer vessels.

Researchers have long known that extracellular matrix proteins such as fibronectin and laminin promote endothelial cell binding to different surfaces. Since the early 1980s researchers have identified a number of different peptide sequences of these proteins that are responsible for the adhesion. One, the REDV sequence, was singled out in 1986 by Martin Humphries and Kenneth Yamada at the National Institutes of Health in Bethesda, Maryland. And in 1991 Jeffrey Hubbell, a chemical engineer at the California Institute of Technology in Pasadena, showed that in vitro, the sequence enhances endothelial cell binding to the common graft polymers PTFE and polyethyleneterephthalate.

At the same time work has also progressed with polymers modified with other peptides. In the July issue of the journal *Heart Valve Disease*, researchers report the first in vivo results on a polymer coated with the RGD sequence, made up of arginine, glycine, and aspartic acid. Catherine Tweden and her colleagues at St. Jude Medical, an implant company in St. Paul, Minnesota, along with William Craig and collaborators at Integra Life Sciences in La Jolla, California, report that they implanted RGD-coated polymer patches in the aortas of dogs. After 33 weeks, endothelial cells covered 75% of the RGD coated patches, three times more area than was covered in controls without the peptide coating. The Integra researchers are now implanting RGD-coated synthetic vessels into animals to see if grafts show the same benefit.

The blood vessels, researchers hope, are harbingers of implants to come. Implant researchers are modifying surfaces of a host of other devices, including those for hip joints and breast and dental implants. But like the research on assembling cells into complex tissues, this work remains in its earliest stages. Most of the promising results come from lab studies of how cells interact with hybrid scaffolds. In large part, it remains to be seen how such materials will behave in the bodies of animals, let alone humans. And before that final step can be taken, researchers must convince health officials that any implanted material and its byproducts are safe. Says Rutger's Yarmush, "a lot of detailed work needs to be done."

–Robert F. Service

IMMUNOLOGY

How the Glucocorticoids Suppress Immunity

If you are diagnosed with a disorder caused by an overactive immune system, such as an allergic skin reaction or a serious inflammatory disease like rheumatoid arthritis, chances are your physician will prescribe one of a class of steroid drugs called glucocorticoids. But ask how these drugs suppress immune reactions, and you are likely to get a shrug. Even though they have been mainstays of clinical immunology for decades, researchers have had few clues about how the glucocorticoids suppress immune and inflammatory reactions—until now, that is.

Work described on pages 283 and 286 by two research teams, one led by Albert Baldwin of the University of North Carolina, Chapel Hill, and the other by Michael Karin of the University of California, San Diego, points to what could be a major immunosuppressive mechanism of the drugs. Researchers have known for several years that the drugs, which are derivatives of hormones whose effects include helping the body respond to stress, work by interfering with immune cells' ability to turn on many of the genes needed to mount effective immune responses. The new work suggests that a large part of this effect occurs because the drugs stimulate production of a protein called IκBα, which locks up a key activator of the genes known as NF-κB, so that it can't do its job. "We understood [the glucocorticoids'] end effects, but we didn't understand the path through which they work," says immunologist Jeffrey Leiden of the University of Chicago School of Medicine. These papers, he adds, provide "a simple and elegant explanation of at least one pathway."

The explanation they offer may do more than satisfy immunologists' curiosity about how the glucocorticoids suppress the immune system. Many of the conditions for which they are prescribed require long-term treatment, and that can lead to undesirable side effects, such as cataracts, weakened bones, and abnormal fat accumulation. "The glucocorticoids are a really fantastic development for treating many human diseases. The problem is the side effects," says Anthony Cerami of the Picower Institute in Manhasset, New York, whose team is also studying the drugs' mechanism of action. But if they do indeed work by inhibiting NF-κB activity, chemists might be able to design

new immunosuppressive drugs that do the same job with fewer side effects.

The glucocorticoid drugs and hormones haven't been an entirely closed book. They regulate many other genes besides those needed for immune responses, and researchers have developed a clear picture of how they perform this function. When the drugs or hormones enter the cell, they bind to a receptor in the cytoplasm and form a complex that moves into the nucleus, where it acts as a transcription factor that turns genes either on or off. Among the genes turned on, for example, are those involved in stress reactions, such as the genes that make the enzymes needed to produce the sugar glucose, which gives cells a quick energy boost.

But many of the immune-system genes turned down by the glucocorticoids appear to lack a necessary feature for that regulation. These include genes encoding cytokines such as the interferons and interleukins, which activate immune cells, as well as those for cell adhesion molecules that draw immune cells into inflammatory sites. And very few of those genes carry the DNA sequence the glucocorticoid-receptor complex binds to when it regulates genes. That suggested the complex works indirectly. But how?

Researchers thought they had a clue 5 years ago, when several teams, including Karin's, found that glucocorticoids prevent another transcription factor, AP-1, from binding to its target genes and turning them on. Among the genes so inhibited, Karin and his colleagues found, is the one for the protein-dissolving enzyme collagenase, which is a major contributor to the tissue damage of inflammation. Indeed, Karin describes collagenase as "the number-one enzyme for destruction of connective tissue in rheumatoid arthritis patients." Despite that, he says that not all of the glucocorticoids' immune effects are likely to be explained by blocking AP-1 activity. For one thing, most of the steroids' potential target genes lack AP-1 binding sites, just as they lack binding sites for the glucocorticoid-receptor complex.

What they do have binding sites for, however, is still another transcription factor—NF-κB, which in the past several years has emerged as a regulator of many cytokine and cell adhesion genes. That discovery prompted researchers, including Karin and Baldwin, to see if glucocorticoids might somehow interfere with NF-κB activity. About a year ago, four research teams, Baldwin's among them, got the first inkling that they might do so: They showed that the glucocorticoid receptor complex binds to NF-κB and prevents it from binding to DNA and increasing gene activity. While that presented another possible mechanism by which the glucocorticoids might suppress the immune system, Baldwin says that other observations made during the course of those experiments suggested that direct binding of the complex to NF-κB was not the only, and perhaps not even the major, way the glucocorticoids were working.

In unstimulated immune cells, NF-κB is held in the cytoplasm in complexes with another protein, either IκBα or the structurally related protein IκBβ. Stimulation of the cells by any of a variety of immune signals results in the addition of phosphate groups to the IκBs, a chemical change that triggers their breakdown and releases NF-κB. The NF-κB then migrates to the nucleus, where it activates its target genes. But the researchers found, Baldwin says, "that in the presence of glucocorticoids the amount of NF-κB that went into the nucleus was significantly diminished," while IκBα concentrations were higher than expected.

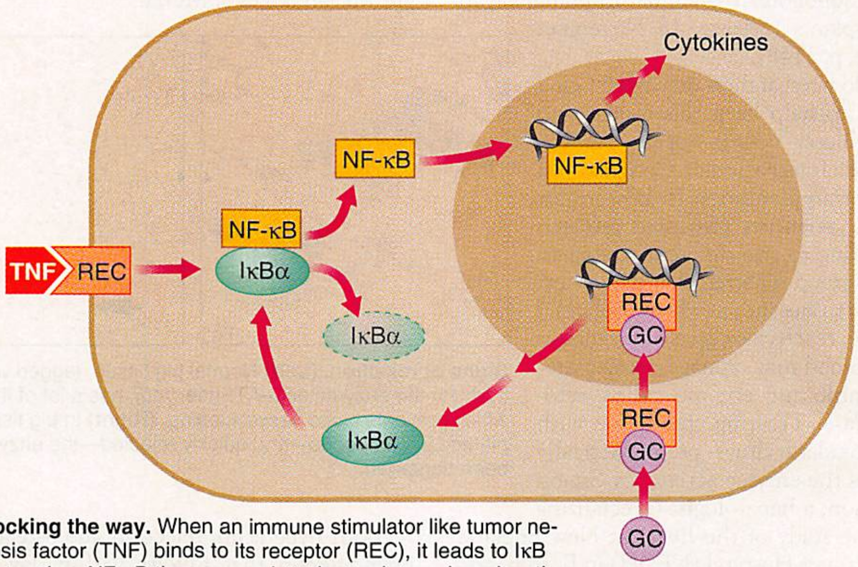

Blocking the way. When an immune stimulator like tumor necrosis factor (TNF) binds to its receptor (REC), it leads to IκB destruction. NF-κB then moves into the nucleus, where it activates cytokine and other genes. By stimulating IκBα production, the glucocorticoids (GC) may prevent this.

This suggested that the glucocorticoids were working through IκBα.

Meanwhile, Karin and his colleagues were coming to a similar conclusion. They showed that the glucocorticoid dexamethasone inhibits activation of the interleukin-2 gene by both AP-1 and NF-κB—but that only the NF-κB effect requires new protein synthesis. This result suggested that the glucocorticoid stimulates production of another protein that inhibits NF-κB action, and the likely candidate was an IκB. And that's what both groups have now shown directly.

They've found that glucocorticoids increase transcription of the IκBα gene into RNA, the first step of protein synthesis. As a result, IκBα concentrations go up within the cell, allowing the protein to hold NF-κB in inactive form in the cytoplasm even under conditions when it would normally be released to move into the nucleus.

And the effect is not just limited to cultured cells, as Karin's team showed that it also occurs in mice. "As far as I can tell," says Karin, the increased production of IκBα and consequent block in NF-κB activity "can explain the major effects of glucocorticoid, which is shutting off cytokine production." Indeed, agrees Baldwin, "by inhibiting NF-κB, you can really knock the legs out of an immune response." The North Carolina worker suggests, however, that direct binding of the glucocorticoid-receptor complex to NF-κB may still play a role in the immunosuppression. Should any of the transcription factor escape from IκBα, the complex could bind NF-κB in the nucleus and prevent it from reaching the DNA.

But however NF-κB's activity is blocked, its inhibition is turning out to be an important mechanism of action for anti-inflammatory drugs generally. Last year Sankar Ghosh, a Howard Hughes Medical Institute investigator at Yale University School of Medicine, and his colleagues obtained results suggesting that aspirin, a nonsteroidal anti-inflammatory drug, exerts some of its effects by inhibiting NF-κB activity, although only at very high concentrations (*Science*, 12 August 1994, p. 956).

And the central role of NF-κB inhibition in suppressing immunity could point the way to improved immunosuppressant and anti-inflammatory drugs. "Once you know the mechanism, you can begin to set up rational screens for other [NF-κB] inhibitors," says Leiden. "What you are looking for is a better safety–side effect profile." Whether such drugs can in fact be found remains to be seen. But researchers are already encouraged by what they are learning about glucocorticoid action. "I think the findings are very significant," says Ghosh. "This just makes sense in many ways."

–Jean Marx

XENOTRANSPLANTATION

New Ways to Avoid Organ Rejection Buoy Hopes

BOSTON—The body's first reaction to truly foreign tissue is not a subtle one. Organs transplanted from pigs into nonhuman primates often swell and blacken within minutes, as blood cells called platelets rush in and seize on the inner walls of blood vessels, clumping together to strangle blood flow. This gruesome phenomenon, called hyperacute rejection, is one of the biggest roadblocks obstructing what many see as a route to alleviating the dire shortage of human donor organs—animal-to-human organ transplants (*Science*, 18 November 1994, p. 1148).

Now researchers may have found ways to help keep this route—and the blood vessels—open. At the Third International Congress on Xenotransplantation in Boston last week, scientists presented research pointing to two different strategies. One group reported that when host blood rushes into newly transplanted tissue, reactive oxygen molecules in the blood may damage a key platelet-inhibiting enzyme called ecto-ATPase. Treating this tissue with antioxidant drugs prophylactically keeps the enzyme active, say Simon Robson, a hepatologist (specializing in the study of the liver) at New England Deaconess Hospital (NEDH) in Boston, and his colleagues, immunologist Fritz Bach, surgeon Daniel Candinas, and pathologist Wayne Hancock.

Another group of researchers described a different strategy that focuses on genetics. Immunologist David White, a founder of the British transplant company Imutran, gave the first detailed accounts of his experiments, announced in a press conference 3 weeks ago, showing that donor pig organs genetically engineered to express human immune regulators have survived in monkeys for up to 8 weeks with no signs of rejection. By inhibiting the activation of key immune proteins called complement, White says, this approach makes hyperacute rejection "a thing of the past."

The NEDH research drew a largely positive response, because it implies that hyperacute rejection could be controlled without suppressing the host's immune system, which also contributes to rejection. "It could be very important work," says immunologist David Sachs, director of the Transplantation Biology Research Center at Massachusetts General Hospital (MGH) and editor of the journal *Xenotransplantation*. "With a specific way of inhibiting [hyperacute rejection] that doesn't require a lot of immunosuppression, we'll be much better off." Participants took a more cautious view of White's work, noting that natural variations in immune response in transgenic animals could help account for enhanced survival. Still, conference attendees were heartened by these signs of progress. "One by one we're going to overcome the major obstacles," says immunologist Megan Sykes of MGH.

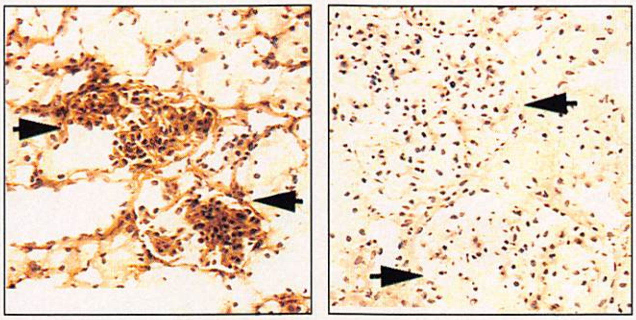
S. ROBSON AND W. HANCOCK

Signs of rejection. (Left) Normal pig tissue, tagged with an antibody for the enzyme ecto-ATPase *(red)*, has a lot of the enzyme, which prevents blood vessel clotting. **(Right)** In pig tissue transplanted into baboons—and quickly rejected—the enzyme has been degraded.

Both hyperacute rejection and a related phenomenon that follows within days or weeks, called delayed xenograft rejection, are triggered at the surface of the endothelial cells that line blood vessels. Under normal conditions, these cells help keep blood in a liquid state by producing proteins and surface enzymes that inhibit the aggregation of platelets. But they fail to do so where host blood meets the vessel walls in a donor organ. Researchers have pinned much of the blame on immune system warriors such as xenoreactive natural antibodies (XNAs) and complement proteins, which cause endothelial cells to shrivel, exposing platelet-activating molecules in the tissues below.

But studies over the last several years by Robson, Bach, and colleagues at NEDH indicated that injured endothelial cells undergo changes that actually accelerate clotting without involving the immune system. Robson exposed cultured pig endothelial cells to inflammatory mediators and discovered that the cells lost their usual ability to inhibit clotting.

At last week's conference, Robson provided an explanation for this lost ability: The enzyme ecto-ATPase, which inhibits platelet aggregation, was missing or inactivated on the injured cells. He had exposed cultured pig endothelial cells to inflammatory mediators such as reactive oxygen intermediates, and within 30 minutes, ecto-ATPase activity dropped by more than 50%. And because the inflammatory agents Robson used were rich in oxygen, he fingered the element as the ecto-ATPase destroyer.

White blood cells called neutrophils generate highly reactive oxygen radicals, which underlie many forms of inflammation. So Robson and his colleagues speculated that oxygen-generating neutrophils in blood rushing into a newly transplanted organ can change the shape of ecto-ATPase, rendering it inactive or making it more likely to be sheared off.

Indeed, Robson found that when he treated endothelial cells with antioxidant drugs such as catalase and superoxide dismutase before exposure to inflammatory agents, they didn't lose their ecto-ATPase. Such drugs might be used to stabilize ecto-ATPase in the organs of donor animals before transplantation. Bach also raises the possibility of inserting the gene encoding human ecto-ATPase into pig embryos to produce animals that express the enzyme in greater amounts or in a more oxidation-resistant form.

Other researchers applaud the work because it underscores warnings that therapies directed at eliminating immune responses to transplantation may not be enough to control hyperacute rejection. "It may not be enough to focus on inhibiting antibodies and complement. Regulation of clotting and coagulation may also be very important," says MGH's Sykes. "That's why what Robson is doing is very interesting."

At least one researcher, however, was not at all interested in modifying endothelial cell responses. "What my data say is, you don't need it," says Imutran's White. Clotting simply doesn't occur in hearts transplanted into cynomolgus monkeys from Imutran's genetically modified pigs, he contends.

In Imutran's recent experiment, detailed at the congress to the intense interest of participants, researchers placed one copy of the gene encoding a human complement-regulating protein, decay accelerating factor (DAF), into pig embryos. Adult pigs then expressed DAF in tissues and endothelial cells at three to four times human levels. Without immunosuppressive drugs, monkeys receiving hearts from these transgenic pigs survived for a median of 5.1 days, compared to 1.6 days for controls receiving nontransgenic hearts. And with immunosuppression, the monkeys receiving transgenic hearts survived for a median of 40 days, weeks longer than previously achieved in a cross-species transplant.

"With immunosuppression, we can get long-term survival," White says. "I can envisage a scenario where, 12 months from now, our data will have achieved the 'comfort factor' where we think we are justified in going to clinical trials in humans." DAF in the transgenic hearts may inhibit complement proteins from attacking endothelial cells, so that platelets never come into contact with subendothelial clotting factors.

Other researchers at the congress praised Imutran's advance, but called White's timetable overoptimistic. "This work potentially makes an important contribution, but it certainly does not indicate to me that we are ready to use these transgenic hearts clinically," says MGH's Sachs. "We still have to worry about delayed rejection and [long-term] T cell immunity." Sachs is also concerned because some of the donor pigs had unexpectedly low levels of an antigen that binds to XNAs. This could have helped avoid hyperacute rejection. White responds that data on antigen levels are "not robust," and the contrast between healthy transgenic hearts and unhealthy control hearts is "amazing."

Many researchers believe that only a combination of donor- and recipient-based therapies, both pharmaceutical and genetic, will eventually make xenotransplantation routine. "This is a big problem, and people are going to have to work together to solve it," says Sachs. "The exciting thing is that every step looks as if it is amenable to being dealt with. I believe it eventually will work."

–Wade Roush

ATMOSPHERIC RESEARCH

Lofty Flashes Come Down to Earth

Walter Lyons had a mystery right in his backyard, which lies at the foot of the Rocky Mountains and commands a view over the Great Plains. So last summer he threw a little garden party, inviting over a few friends and colleagues—16 research groups in all, with their instruments—to help him solve it. The mystery was what could be creating the menagerie of exotic flashes that can be detected from his yard as they light up the atmosphere high above giant thunderstorms on the plains. And last summer's gathering at Lyons's home on Yucca Ridge near Fort Collins, Colorado, along with research efforts from other vantage points, has gone a long way toward providing an answer.

"There's so much data it's almost overwhelming," says Lyons, a meteorologist at Mission Research Corporation's ASTER Division in Fort Collins. Most of the observations are still being digested, but they are already showing how exceptional lightning strokes that drain storm clouds of huge amounts of electrical charge could spark the flashes. By analyzing spectra of the flashes and measurements of their timing, researchers have traced two different mechanisms for setting the upper atmosphere aglow, one driven by a quick pulse of energy from the lightning stroke and the other by a slower change in the atmosphere's electric field.

A year ago, observations from Lyons's yard and elsewhere had shown that the flashes come in forms ranging from carrot-shaped "red sprites" at altitudes of 40 to 90 kilometers to a fainter, broader glow at still higher altitudes (*Science*, 5 August 1994, p. 740). Analyzing the data, Dennis Boccippio and Earle Williams of the Massachusetts Institute of Technology and Lyons found that the sprites, at least, coincide with the huge, positively charged cloud-to-ground lightning bolts from the biggest thunderstorms (*Science*, 25 August, p. 1088). Although that pointed to lightning as the sprites' ultimate cause, researchers did not know the mechanism.

The colors of the sprites offered a clue, however. Rare visual sightings and color video images of these brief flashes had shown that they have a red hue reminiscent of the aurora. That suggested that the light of a sprite, like that of the aurora, comes from oxygen or nitrogen molecules excited by collisions with high-energy electrons. Now two groups—Stephen Mende of Lockheed Palo Alto Research Laboratory in California and his colleagues working at the Fort Collins site and Davis Sentman and colleagues at the University of Alaska, who made their observations from the top of Colorado's Mount Evans—have recorded spectra of sprite light and found that its source is molecular nitrogen excited by electron collisions.

But how could lightning only 5 to 10 kilometers above the ground unleash electrons at altitudes 10 times higher? One possibility relied on the 100-microsecond pulse of electromagnetic energy broadcast by a lightning stroke. Moving upward at the speed of light into thinner regions of the atmosphere, it might eventually be able to rip electrons from atmospheric molecules and accelerate them unhindered by too many collisions with other molecules.

S. B. MENDE AND R. L. RAIRDEN

High lights. Changes in the atmosphere's electric field above a thunderstorm spawned these sprites.

Researchers had also considered a slower, "electrostatic" mechanism that depends on the charge a cloud induces in the atmosphere above it as it electrifies before unleashing a lightning stroke. The cloud's own charge is annihilated when the lightning suddenly transfers upwards of 1000 coulombs of charge to the ground, while the field above the cloud lingers. And because the field is no longer nullified by the cloud charge, for a few milliseconds it's strong enough to ionize molecules and accelerate the resulting electrons.

Measurements of the precise timing of lightning strokes and flashes now imply that both mechanisms may be at work—in different parts of the upper atmosphere. Mende and his colleagues found that sprites lag the huge positive lightning strokes triggering them by several milliseconds. That's much longer than it would take for the electromagnetic pulse from a lightning stroke to arrive at the altitude of a sprite. But the timing is about right for the slower electrostatic mechanism, notes Williams.

Electromagnetic pulses could still have a role, however, in the fainter, broader flashes sometimes recorded at around 90 kilometers in the lowermost ionosphere. Working in Lyons's yard, Hiroshi Fukunishi of Tohoku University and his colleagues found that these flashes appeared less than 1 microsecond after the lightning—about the right interval for an electromagnetic pulse to reach the ionosphere. The finding also fits theoretical calculations made by Umran Inan and his colleagues at Stanford University, who had pointed out that a pulse was far more likely to trigger a flash in the ionosphere, where molecules are already ionized, than at the lower altitudes where sprites appear.

Although researchers have tentatively sorted out mechanisms for two upper-atmosphere phenomena, many questions remain. Theorists have yet to publish even a hand-waving explanation of yet another species of flash, the "blue jets" that explode from storm-cloud tops. And the menagerie of middle-atmosphere flashes may contain even more strange beasts. There will be plenty more work for the next yard party on Yucca Ridge.

–Richard A. Kerr

MOLECULAR BIOLOGY

Titanic Protein Gives Muscles Structure and Bounce

An athlete with a biological bent may pause a moment while lifting weights or taking a jog to appreciate the molecular choreography that takes place when muscles contract: the ratchetlike sliding actions of filaments made of actin and myosin molecules. But few athletes are likely to know the identity of another key muscle protein, the molecule responsible for their muscles' ability to spring back into shape after being stretched. While this protein does not have the name recognition of actin and myosin, it does have its own claim to fame. It is the largest protein known, a single chain of nearly 27,000 amino acids, with a molecular weight of about 3 million. Few other proteins have molecular weights greater than 200,000.

Fittingly, the muscle protein is called titin, and its size has made determining its entire sequence difficult. But on page 293 of this issue, molecular biologist Siegfried Labeit and his student Bernhard Kolmerer, of the European Molecular Biology Laboratory in Heidelberg, Germany, report that they have accomplished the feat.* And their achievement is drawing high praise. "This is really a fascinating work, not only because they were able to complete the sequence … but also because of the information that was revealed," says Jeffrey Chamberlain, who studies muscle proteins at the University of Michigan Medical School in Ann Arbor.

Indeed, the sequence reveals a brand-new type of structural motif that may account for the protein's springiness. What's more, the length of this motif can vary, and that may explain why some muscles are more elastic than others. Other parts of the protein's sequence suggest how it may perform another key function, acting as a ruler to aid the precise placement of proteins within muscle fibers.

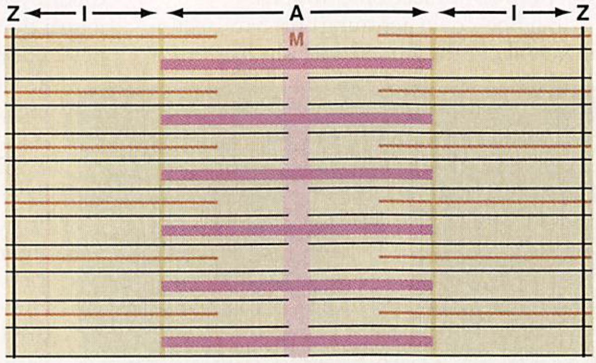

Ratchets and springs. Each titin molecule *(black)* spans half a sarcomere, from Z line to M line. The sliding filaments of actin *(tan)* and myosin *(red)*, on the other hand, meet midway.

Labeit and Kolmerer determined titin's structure in the usual way, making DNA copies of the messenger RNA that directs titin's synthesis, sequencing that DNA, and converting that sequence into the amino acid sequence of the protein. Because of the huge size of the messenger RNA, they couldn't make a single copy, but had to piece the sequence together from roughly 50 overlapping copies.

Their efforts reveal that 90% of the titin protein consists of 244 copies of two well-known protein motifs, known as the fibronectin type III (FN3) and immunoglobulin (Ig) domains for the proteins in which they were first discovered. Researchers already knew from partial sequences of titin that these motifs were there, and even suspected that they might comprise virtually all of the protein. But Labeit and Kolmerer found, in the center of titin, a new protein motif that has never been seen before. They call it PEVK, from the symbols for the amino acids proline, glutamate, valine, and lysine, which make up 70% of the motif.

With titin's complete sequence in hand, the researchers could begin to develop a better picture of the roles titin plays in the structure and function of sarcomeres, the repeating units of which muscles are made. Microscopic studies in the 1980s had revealed that individual titin molecules span half the length of the sarcomere, from the Z line that marks the border between sarcomeres to the M line, which runs down the center of the sarcomere. Between these two endpoints, the stringlike titin molecules pass through two distinct zones of the sarcomere, the I band, dominated by filaments made of actin, and the A band, where the actin filaments overlap with others made of myosin.

Because of its size, a single titin molecule can span that entire 1-micron distance; the actin and myosin filaments by contrast are made of hundreds of individual molecules. Indeed, because titin spans the distance from Z to M, it seemed a good candidate for controlling the layout of sarcomere proteins, especially in the highly ordered A band. That idea has been supported by the current work. "Now that we have the whole sequence, we can see that the primary structure of the molecule very nicely matches the complicated structure of the [A band]," says John Trinick, who studies titin at the University of Bristol, United Kingdom.

For example, a set of accessory proteins is arranged in 11 stripes that cross the myosin-containing A band in each half-sarcomere. And titin's structure correlates with that arrangement. In the part of the protein that spans the 11-stripe region, the Ig and FN3 motifs, which have the ability to bind other proteins, are ordered in a "super-repeat," a regular pattern of Ig and FN3 motifs, repeated 11 times. The super-repeats had already been discovered in titin, but the new work shows that they line up with the protein stripes. It also reveals other structural patterns in titin that correspond to the placement of other A-band proteins. That buttresses the idea that, for laying down A-band proteins, titin "probably is like a great big template," says Trinick.

The structure may also shed light on how titin contributes to the ability of muscles to spring back after they are stretched. As muscles expand and contract, the sarcomere changes length, mostly in the I band. That, says Michigan's Chamberlain, means that the part of titin that crosses the I band "has to be extremely flexible, because it is going to be moving in and out like an accordion." Earlier experiments suggested, however, that titin behaves more like a spring, pulling the muscle back into shape after being stretched, than like the passive bellows of an accordion. Labeit and Kolmerer now propose that the PEVK sequence may in fact be the spring. For one thing, it is located in the middle of the expandable I band, where the spring would be expected to be.

And, more suggestive yet, when the researchers compared titins from cardiac and skeletal muscle, they found that the PEVK region was only 163 amino acids long in the stiff cardiac muscle, whereas in the much more elastic skeletal muscle it was more than 2000 amino acids long. "That correlates nicely with elasticity," says Trinick, and may "start to explain how different muscles have different stiffnesses."

That tantalizing correlation suggests experiments to test the springiness of PEVK directly. For example, says Labeit, researchers can dot the titin protein with antibodies specific for different parts of the protein, then by watching the spacing of the antibodies when the muscle is stretched, they can pinpoint the stretchiest part of the protein and see if it indeed contains PEVK. And while researchers pursue such questions, athletes can play with a new imagery, visualizing within their muscles not just tiny molecular ratchets, but titanic molecular springs as well.

–Marcia Barinaga

* Sequence information is available at **http://www.aaas.org/science/science.html** (see "Beyond the Printed Page").

edited by CONSTANCE HOLDEN

Sensing Music

Playing music has transformative powers, not only on those listening to it, but also on the brains of the performers—especially, it appears, on the malleable brains of child musicians. On page 305, Thomas Elbert of the University of Konstanz in Germany and Edward Taub of the University of Alabama report that the agile left hands of string musicians—especially those who began training before age 12—are represented by larger brain areas than are the left hands of nonmusicians.

The researchers used a technique called magnetic source imaging to measure brain activity when a light touch was applied to the fingers of six violinists, two cellists, and a guitarist. Touching the left fingers of the string players activated a bigger portion of the somatosensory brain area in the musicians than it did in a control group of six nonmusicians.


CHRISTIAN STEINER

All those pulsing cells. Emerson string quartet at work, using hands and brains.

The difference suggests that musicians' brains had reorganized to devote more neurons to receiving sensations from the left fingers. Just how many more the researchers couldn't determine, but their data suggest it could be two to three times as many. What's more, musicians who started before the age of 12 showed an effect twice as large as did their peers.

An "interesting twist here is the youth," says neuroscientist Tim Pons of the Bowman Gray School of Medicine in Winston-Salem, North Carolina. "If you get them relatively young, you have this increased expansion." Taub says, though, that it is equally important that "plasticity has not disappeared in the older individual. It is just reduced."

This study adds to other work on reorganization of the brain following the learning of a skill. In 1993, for example, neuroscientist Alvaro Pasqual-Leone of the National Institute of Neurological Disorders and Stroke reported an expansion of the brain area receiving sensations from the Braille-reading finger in blind people. And Avi Karni, Leslie Ungerleider, and colleagues at the National Institutes of Health have shown in the brain's motor area what Elbert and Taub found for sensory neurons: When people tap out a well-practiced sequence with their fingers, they activate a greater area of the motor cortex than when tapping an unpracticed sequence (*Science*, 2 December 1994, p. 1475; the study was published in the 14 September *Nature*).

Does having all that cortex devoted to musical—and manual—dexterity make you a better player? "Presumably," says Taub. But "we haven't proved it."

The Violent Side of Low Cholesterol?

Numerous studies have shown that low levels of the neurotransmitter serotonin are associated with suicidal and other forms of impulsive violent behavior. But in just the past few years, researchers have fingered a possible third party in the picture: low cholesterol.

Low cholesterol levels tied to violence? It's "an issue which is real for sure and one that has been overlooked by the cardiovascular people to some extent," says psychiatrist Marku Linnoila of the National Institute on Alcohol Abuse and Alcoholism. That reality is debatable, however: "I'm skeptical about it," says epidemiologist David Gordon of the National Heart, Lung, and Blood Institute.

In the most extensive review to date of relevant literature (to be presented next month at a meeting of the Robert Wood Johnson clinical scholars), neurobiologist Beatrice A. Golomb of the University of California, Los Angeles, claims that "Low cholesterol may ... promote violence," and that this link may be mediated by serotonin.

The picture is still patchy. The evidence Golomb cites comes from research with both monkeys and humans. Work by Jay Kaplan of Bowman Gray School of Medicine in Winston-Salem, North Carolina, indicates that lowering dietary cholesterol in monkeys brings out more aggressive, less affiliative behavior. Serotonin levels also go down, he says. In humans, a meta-analysis of six large studies of cholesterol-lowering drugs, done by clinical pharmacologist Matthew Muldoon and colleagues at the University of Pittsburgh, found that people taking medication actually had the same death rates as the controls—compensating for fewer heart-related deaths with more violent deaths.

One explanation for this connection, says Golomb, is that fatty acids in the blood (related to cholesterol) compete with the serotonin precursor tryptophan for binding to serum albumin. Thus, the less fat in the blood, the more tryptophan binds to albumin, and the less tryptophan is available to get to the brain.

Skeptics such as Gordon, however, point out that the effect may not be real at all. The evidence gained was "post-hoc," he says, and was found only in primary and not secondary prevention trials—that is, trials with subjects who already have heart disease. Gordon says, however, that he hopes for more definitive evidence from a trial Muldoon is now just starting, which is specifically designed to evaluate the neurobehavioral correlates of low or lowered cholesterol.

It's a touchy subject, says Muldoon: "So many people have made their career on identifying what's bad about cholesterol."


ROY CALDWELL

Ready for battle. Maybe. Mantis shrimp performs threat display, baring dark purple spots on its appendages, to defend its home.

The Bluffing Shrimp

There are shrimp that fight and shrimp that lie. Twelve years ago researchers at the University of California (UC), Berkeley, reported that weaklings among the mantis shrimp *Gonodactylus bredini* bluff their way out of confrontations by putting on a threat display. Not only were other shrimp confused by the display—it scared them off—but researchers were puzzled as well. If the behavior is successful, they reasoned, all the shrimp would evolve to use it, and then no one would pay any attention to it. Useless, bluffing would be disregarded.

Now behavioral ecologist Eldridge Adams of the University of Rochester thinks he's learned why bluffing persists. In a paper published in the August issue of the *Journal of Theoretical Biology*, Adams and Michael Mesterton-Gibbons of Florida State University explain that the threat display is only cost-effective for some members of the species, and its intermittent use leads to its persistence.

Adams, who has observed more than 500 shrimp fights, explains that the threat display—which involves spreading "raptorial appendages" and showing off big spots on them—offers a large potential benefit for molting shrimp which, having soft shells, would lose any battle they got into. But there are also costs: Making a threat makes you more vulnerable to injury in the event

(continued on page 239)

(continued from page 237)

you are attacked. So "animals of intermediate strength" are usually better off not using threats. Thus only the strongest (who have the firepower to back up threats) and weakest use threat displays, and the behavior can persist. It turns out "you can have a stable communication system even if the very weakest is using the threat deceptively," Adams says.

Robert Gibson, behavioral ecologist at UC Los Angeles, calls the case of the fighting shrimp "one of the few well-documented cases of intraspecific deception." What the researchers found, he says, is that its persistence "can be explained by individual variation in costs and benefits."

Virtual Science Fair

NEWS FROM THE NET

Nils Peterson of Washington State University's (WSU's) College of Education is now running what he calls "the only virtual science fair on the planet."

The fair, which sprang out of attempts to get teachers-in-training hooked up to the Internet, was set up last April. The list of submissions, which closed at the end of September, stands at 109, from 19 schools. Simple-minded "show and tell"–style models won't do, says Peterson. Presenters instead have been instructed to prepare a scientific "poster" with an abstract, a hypothesis, and supporting data and images. It's better than a real poster session, notes Peterson, as "the attachments to the exhibit can be downloaded by the viewer." The youngest participants are second graders in Fairbanks, Alaska, who have two projects: "Snap, Crackle, Pop—Which Rice Krispie Treats Are Best" and "How Much Money Do I Save Turning Off Lights?" In the latter, second-grader Spark Estes draws a path of how he uses lights as he goes through his day. High school entries include "Effects of Music on Animal Learning Patterns," and there are submissions from three education colleges, including "Linear Equations and Rubber Bands." The fair (reachable at **http://www.educ.wsu.edu/fair_95/index.html**) will run from 6 November to 15 December. Project authors will be standing by their electronic posters for dialogues with visitors on Fridays during the exhibit. Biochemist Kevin Facemyer of the education school is already plotting next year's fair. "I think we may institute a more rigorous 'call for papers,'" with screening for merit and presentations like those at real scientific meetings, he says.

Report From School Science Front

Those who are pressing for public schools to join the information age may be discouraged to learn that in the U.S. "the average public school spent only $50 on science computer software and $100 on mathematics software in 1993–94." So says a report released last week, "State Indicators of Science and Mathematics Education,"* a biennial production of the Council of Chief State School Officers. It goes on to relate that yearly expenditures for science supplies are generally less than $1 per student.

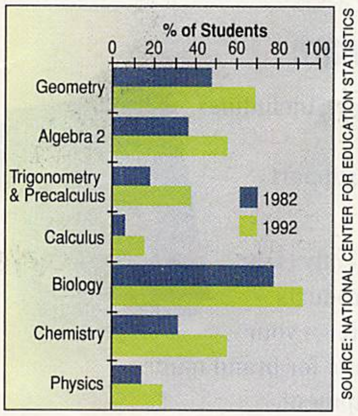

Getting numerate. Changes in percent of students taking math and science by high school graduation, 1982–92.

The report is designed to take the pulse of public science education through various indicators, including student achievement scores, course offerings and enrollments, and teacher qualifications. The picture that emerges is a mixed one, although the numbers reflect some of the actions that have been taken following the dire reports about science education and public science illiteracy that have come out during the past decade.

Among the findings, for example, are that "enrollments in science and mathematics have risen significantly from 1982 to 1992" (see chart). And the percentage of high school graduates who have taken math and science courses has gone up as well—from 48% to 70% in geometry, for example, and 32% to 56% in chemistry. "The reform process obviously is resulting in the diminution of low-level courses like 'consumer math' and transition to serious courses regardless of whether students are on an academic or vocational track," says Luther Williams, director of the education directorate of the National Science Foundation, which funded the report.

The report identifies factors it considers most important for student success: They include time spent doing textbook problems ("time on task"), "moderate" testing (somewhere in between daily and never), and "frequent use of calculators." But some indicators don't always tie in with student achievement: In 1994, for example, the District of Columbia led the nation in number of certified math teachers per 1000 students. But its 8th graders were at the bottom of the list on math proficiency.

*The report is available from the Council of Chief State School Officers, 202-408-5505.

Bending Light in Einstein Crosses

Operating in what astronomers call the "serendipity mode," the Hubble Space Telescope (HST) has discovered two gravitational lenses known as Einstein crosses, in which the light from a distant galaxy bends around a second galaxy, creating four images of the galaxy when the light reaches Earth. The four-lobed patterns should eventually prove useful for testing cosmological parameters such as the rate at which the universe is expanding.

"HST is the clear winner right now" in its ability to detect such crosses, says John Huchra of the Harvard-Smithsonian Center for Astrophysics, who discovered the first Einstein cross from the ground in 1984. With its penetrating vision, the orbiting telescope could eventually double or triple the "dozen good and dozen not-so-good" gravitational lenses known now, he says.

The two crosses were found by Kavan Ratnatunga, Eric Ostrander, Richard Griffiths, and Myungshin Im of Johns Hopkins University, who will report their results in the 1 November *Astrophysical Journal Letters*. The telescope detected the crosses when in serendipity mode, meaning the optical telescope searches star fields that happen to be in its view while other instruments are doing scheduled studies.

By combining measurements of the lobes' angular separation with other information—such as the speed at which both the source and lensing galaxy are receding from Earth—researchers can use the crosses to derive new estimates of the universe's expansion rate.

The Hopkins team still must follow up with ground-based spectroscopic measurements of the cross in order to verify that the four lobes in a given cross indeed come from the same galaxy. And follow-up, says Ratnatunga, will be "tough—even with the best [telescopes] in the world," as the crosses would likely never have been spotted in the first place without Hubble's keen vision.

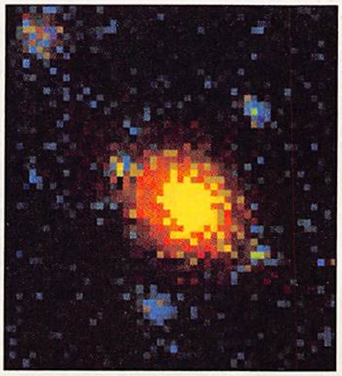

RATNATUNGA *ET AL.*

Crossroads. Four images of distant object surround galaxy.

THE NEW AVANTI™ J-25. GET READY FOR THE DRIVE OF YOUR LIFE.

No conventional centrifuge keeps pace with the new 25,000-rpm Avanti J-25 High-Performance Centrifuge Systems from Beckman. Everything about the Avanti J-25 series – from their innovative SR* drive to their new lightweight, large-volume rotors – helps you perform more separations in less time.

ACCELERATE YOUR THROUGHPUT... WHILE CUTTING RUN TIME

Now your lab can complete more separations, more quickly, than with any conventional high-speed. That's because the Avanti J-25 offers greater speeds and *g*-forces, with larger volumes, than any competitive model. A high-torque SR direct drive makes these benefits possible by accelerating and braking in up to *half the time* of conventional high-speeds. Set-up is quick and easy. And with the J-25I, you're freed from rotor ID by an innovative Instant Rotor Identification System (IRIS™).

SAFE FOR THE ENVIRONMENT...AND FOR YOU

Because Beckman shares your concerns about environmental safety, the Avanti J-25's brushless SR drive is air-cooled, and an advanced refrigeration system eliminates CFCs from its design. The Avanti J-25 also consumes much less power, produces less than half the heat, and is 50% quieter than conventional models. Compliance with some of the world's highest standards for quality and operator safety is guaranteed by CE marking, UL and CSA approval.

High-performance productivity is another part of the Beckman Plus, that extra level of personalized service and support available only from Beckman. For more information about the Avanti J-25 series, contact one of our sales offices worldwide.

** SR drives are manufactured by Beckman with technology licensed from Switched Reluctance Drives Limited.*

BECKMAN

Worldwide Offices: Africa, Middle East, Eastern Europe (Switzerland) (22) 994 07 07. **Australia** (61) 02 816-5288. **Austria** (2243) 7292164. **Canada** (800) 387-6799. **China** (861) 5051241-2. **France** (33) 1 43 01 70 00. **Germany** (49) 89-38871. **Hong Kong** (852) 814 7431. **Italy** (39) 2-953921. **Japan** 3-3221-5831. **Mexico** 525 575 5200, 525 575 3511. **Netherlands** 02979-85651. **Poland** 408822, 408833. **Singapore** (65) 339 3633. **South Africa** (27) 11-805-2014/5. **Spain** (1) 358-0051. **Sweden** (8) 98-5320. **Switzerland** (22) 994 07 07. **Taiwan** (886) 02 378-3456. **U.K.** (01494) 441181. **U.S.A.** 1-800-742-2345.

Circle No. 41 on Readers' Service Card

Circle No. 26 on Readers' Service Card

Quality, Precision, and Reliability –
The Leica Product Range for Histopathology

Whether for routine diagnostics in the biomedical or industrial quality assurance field: Leica offers an optimal solution, which is only to be expected from one of the leading world-wide manufacturers of microtomes and histology instruments.

LEICA VT 1000 E/M – Vibrating knife microtome for fresh tissues.

LEICA CM 1900 – Rapid sectioning cryostat for fast application results.

LEICA RM 2155 – Rotary microtome for fully automatic sectioning.

LEICA TP 1050 – Vacuum tissue processor for more efficiency and safety.

LEICA HISTOEMBEDDER – Compact, programable tissue embedding center.

LEICA AUTOSTAINER XL – High-throughput routine slide stainer.

Circle No. 20 on Readers' Service Card

Leica Instruments GmbH · P.O. Box 1120 · Heidelberger Strasse 17-19 · D- 69226 Nussloch · Germany · Telephone (0 62 24) 143-0 · Telefax (0 62 24) 143 200

Leica

Electronics and the Dim Future of the University

Eli M. Noam

By now, everybody knows about it—about the tremendous advances in computer networks as tools of inquiry; about the free communication links among researchers around the world; about the loss of stifling organizational hierarchy and coercive governmental controls; and about the ethic of sharing information instead of commercializing it. Technology, it seems, has created a new set of tools for academic endeavors, strengthening and enriching the existing research environment.

Parts of this exciting scenario are indeed coming true. Yet to conclude that the global academic village is all gain and no pain (beyond perhaps the need to protect against a few immature but creative youngsters) would be naïve. True, communications technology will link the information resources of the globe. But as one connects in new ways, one also disconnects the old ways. Thus, while new communications technologies are likely to strengthen research, they will also weaken the traditional major institutions of learning, the universities. Instead of prospering with the new tools, many of the traditional functions of universities will be superseded, their financial base eroded, their technology replaced, and their role in intellectual inquiry reduced. This is not a cheerful scenario for higher education.

Scholarly activity, viewed dispassionately, consists primarily of three elements: (i) the creation of knowledge and evaluation of its validity; (ii) the preservation of information; and (iii) the transmission of this information to others. Accomplishing each of these functions is based on a set of technologies and economics. Together with history and politics, they give rise to a set of institutions. Change the technology and economics, and the institutions must change, eventually.

The Old Direction of Information Flows

Information institutions started about 5000 to 8000 years ago when, at different places around the world, priests emerged as specialized preservers and producers of information. Collectively, they were also the primary information storage medium of their societies. Because reliance on individual and group memory to transmit information across time and space was inefficient, recording methods emerged. Writers had to be trained, and schools emerged. Writing, in turn, led to the establishment of formal information-storage institutions. Under the Assyrian king Assurbanipal (668 to 627 B.C.), the royal library in Nineveh stocked over 10,000 works. Documents were arranged by subject such as law, medicine, history, astronomy, biography, religion, commerce, legends, and hymns, each in a separate room in a compound. Wise men congregated there to use the information and to add to it. No doubt they also argued among themselves and were surrounded by disciples. Thus, knowledge and inquiry were already being organized along lines strikingly similar to today's university departments.

This model—centrally stored information, scholars coming to the information, and a wide range of information subjects housed under one institutional roof—was logical when information was scarce, reproduction of documents expensive and restricted, and specialization low. It became also the model for the most formidable of knowledge institutions of antiquity, the Great Library of Alexandria. At its peak, the library amassed nearly 700,000 volumes. Less recognized is its role as a graduate university. From the beginning, Ptolemy I Soter and his librarian, Demetrius, recruited some of the foremost scholars of the Hellenistic culture, such as the geometrician Euclid, to what was called the "museum." These scholars were surrounded by disciples and apprentices. Again, the pattern was similar. Scholars came to the information-storage institution and produced collaboratively still more information there, and students came to the scholars.

The New Direction of Information Flows

This system of higher education remained remarkably stable for over 2500 years. Now, however, it is in the process of breaking down. The reason is not primarily technological; technology simply enables change to occur. The fundamental reason is that today's production and distribution of information are undermining the traditional flow of information and with it the university structure, making it ready to collapse in slow motion once alternatives to its function become possible.

Most branches of science show an exponential growth of about 4 to 8% annually, with a doubling period of 10 to 15 years. As an illustration of this trend, *Chemical Abstracts* took 31 years (1907 to 1937) to publish its first 1 million abstracts; the second million took 18 years; the most recent million took only 1.75 years. Thus, more articles on chemistry have been published in the past 2 years than throughout history before 1900.

The response of organizations to the increased volume of information has been to improve processing capabilities by various means, such as better education, larger staffs, internal reorganization, and investment in technology. The main strategy, however, has been to increase specialization. As the body of knowledge grows, fields of expertise evolve into ever narrower slices.

The inexorable specialization of scholars means that even research universities cannot maintain coverage of all subject areas in the face of the expanding universe of knowledge, unless their research staff grows at more or less the same rate as scholarly output, doubling every 5 to 10 years. This is not sustainable either economically or organizationally, nor would it permit the existence of smaller-sized elite universities. As a result, universities no longer cover a broad range of scholarship. They might still have offerings in most of the major academic disciplines (whatever that means), but in only a limited set of the numerous subspecialities. For the same reason, many specialized scholars find fewer similarly specialized colleagues on their own campus for purposes of complementarity of work. Instead, scholarly interaction increasingly takes place with similarly interested but distant specialists, that is, in the professional rather than the physical realm.

None of this is new, of course. But as the information-induced pressures of specialization have grown, so have the means to make the invisible college the main affiliation. Air transport established the jet-setting professoriate. Even more so, electronic communications are now creating new electronic scholarly communities in response to the elementary need for intellectual collaboration. Ironically, it is the university that pays for the network connectivity that helps its resident scholars to shift the focus of their attention to the outside world—or, in the jargon of electronic communications, to join virtual communities in cyberspace. As this happens—and we are only at the beginning of convenient technology—the advantage of physical proximity of scholars in universities declines steeply.

The author is professor of Finance and Economics, and director, Columbia Institute for Tele-Information, Graduate School of Business, Columbia University, New York, NY 10025. Email: enoam@research.gsb.columbia.edu

The second function of the university is the storage of information. It has been said that a university is as strong as its library. But here, too, considerations of economics and technology change everything. As the production of scholarship increases exponentially, so does the cost of acquisition and reference. For example, in 1940 an annual subscription to *Chemical Abstracts* cost $12; in 1977 it was $3500; and in 1995 it was $17,400. As comprehensive library collections have become unaffordable, electronic alternatives have become powerful in their storage capacity, broad-ranging in content, and efficient in retrieval. Therefore, universities are gradually shifting from investment in the physical presence of information to the creation of electronic access. It is a logical response and undermines the fundamental role of the university as the repository for specialized information. Soon the combination of laptop computer and phone line will serve this function as well—and often better—anywhere, anytime.

The third function of the university is the transmission of information, its teaching role. It is hard to imagine that the present low-tech lecture system will survive. Student-teacher interaction is already under stress as a result of the widening gulf between basic teaching and specialized research. And the interaction also comes with a big price tag. If alternative instructional technologies and credentialing systems can be devised, there will be a migration away from classic campus-based higher education. The tools for alternatives could be video servers with stored lectures by outstanding scholars, electronic access to interactive reading materials and study exercises, electronic interactivity with faculty and teaching assistants, hypertextbooks and new forms of experiencing knowledge, video- and computer-conferencing, and language translation programs. While it is true that the advantages of electronic forms of instruction have sometimes been absurdly exaggerated, the point is not that they are superior to face-to-face teaching (though the latter is often romanticized), but that they can be provided at dramatically lower cost. A curriculum, once created, could be offered electronically not just to hundreds of students nearby but to tens of thousands around the world. It would be provided by universities seeking additional revenues in a period of declining cohorts, though probably not at first by elite colleges, which guard their scarcity value.

Already, electronic distance education is available for a wide range of educational instruction through broadcast, cable, online, and satellite technologies. Such forms of instruction appeal to motivated students with full-time jobs, family obligations, limited mobility, distant locations, and needs for specialized courses. An example is the Agricultural Satellite Network (AgSat), which allows two dozen agricultural colleges to exchange their course offerings and "reduce duplication." Such efforts at cost reduction are not likely to be welcomed by the beneficiaries of low-tech teaching, the university faculty, which finally defines the mission and structure of its institutions and is as resistant to change as any other profession.

In any event, the ultimate providers of an electronic curriculum will not be universities (they will merely break the ice) but rather commercial firms. Textbook publishers will establish sophisticated electronic courses taught by the most effective and prestigious lecturers. At present, tuition fees at private universities are nearly $50 per lecture hour per student, not counting most of the public and philanthropic support that universities receive or the opportunity cost of students' time. With such Broadway show–sized prices, alternative providers will inevitably enter the electronic education market. Today's students, if they seek prestigious jobs or entry-restricted professions, usually have no choice other than to attend university. However, this is a weak and mostly legal reed for universities to lean on, and is only as strong as their gatekeeper control over accreditation and over the public's acceptance of alternative credentials. When this hold weakens, we may well have in the future a "McGraw-Hill University" awarding degrees or certificates, just as today some companies offer in-house degree programs. If these programs are valued by employers and society for the quality of admitted students, the knowledge students gain, and the requirements that students must pass to graduate, they will be able to compete with many traditional universities, yet without bearing the substantial overhead of physical institutions. It is likely that commercial publishers will assemble an effective and even updated teaching package, making the traditional curriculum at universities look dull by comparison, just as "Sesame Street" has raised the expectations of pupils for a lively instructional style. Already available on video is the "Greatest Lectures by America's Superstar Teachers," distributed by a company advertising itself as "your own private university, staffed exclusively by a 'dream team' of America's best lecture professors." Degrees are granted by the all-electronic International University College, affiliated with the big cable TV company Jones Intercable. The same company also offers courses on its Mind Extension University channel that receive credit by the degree programs of several dozen colleges.

Commercial providers will offer primarily mainstream undergraduate and professional education. At the same time, some of the invisible colleges of interlinked specialists will be transformed from a wide-openness that is unmanageable, into more structured virtual departments that may offer graduate credentials, specialization, socialization, and apprenticeship, thus weakening these roles of the universities, too.

Of course, another reason to attend a university is to participate in a rite of generational passage into adulthood, and its associated social networking. While this is an important aspect of university experience, it could be replicated in other ways—as it was in the thousands of years preceding mass college attendance—and often in more attractive locations and climates.

If the university's dominance over higher education falters, its economic foundation will erode. In these times of budgetary squeezes, most universities will not be able to compensate for tuition losses by increased public funding. The role of the private sector will have to grow in order to fuel and maintain the existing system. Yet private donations are likely to decline, if anything, with the university's reduced central role in research and teaching and with increasing disillusionment about the ability of higher education to solve society's problems.

The Impact on the University

The problems affecting universities will not be uniform. In the area of teaching, the most negative impact will be on mass undergraduate and professional education and on highly specialized and advanced fields. Least affected will be contact-intensive programs such as selective and tutorial-based liberal arts education (especially if they are backed by healthy endowments), as well as skill training that requires hands-on instruction and feedback, and small but stable fields of graduate study that are not lucrative for commercial providers.

In the area of research, least affected will be fields that do not experience substantial growth and specialization, and where researchers share a strong core. (They will be financially squeezed, however, by the loss of cross-subsidies from previously grant-rich parts of the university.) Most affected will be highly specialized research, where keeping up to the minute is critical. This is not to say that research requiring teams and shared equipment will not necessarily be located on campus, but it will be connected primarily to other units elsewhere in academia, industry, and government. The university will then exist as a sort of office park of semiautonomous units, each a soft money tub on its own bottom. The administration of universities is then likely to be even more decentralized than today, and partly run from a distance by telecommuting staff and specialized subcontractors.

The Future Role of the University

In presenting this bleak scenario for the future of the university, it is easy to appear as yet another dismal economist or technological determinist, and to invite a response reaffirming the importance of quality education, academic values, the historic role of education in personal growth, and the human need for freewheeling exchange. Such arguments are correct, may make one feel good, but are beside the point. The question is not whether universities are important to society, to knowledge, or to their members—they are—but rather whether the economic foundation of the present system can be maintained and sustained in the face of the changed flow of information brought about by electronic communications. It is not research and teaching that will be under pressure—they will be more important than ever—but rather their instructional setting, the university system. To be culturally important is necessary (one hopes) but, unfortunately, not sufficient for a major claim on public and private resources. We may regret this, but we can't deny it.

This scenario suggests a change of emphasis for universities. True teaching and learning are about more than information and its transmission. Education is based on mentoring, internalization, identification, role modeling, guidance, socialization, interaction, and group activity. In these processes, physical proximity plays an important role. Thus, the strength of the future physical university lies less in pure information and more in college as a community; less in wholesale lecture, and more in individual tutorial; less in Cyber-U, and more in Goodbye-Mr.-Chips College. Technology would augment, not substitute, and provide new tools for strengthening community on campus, even beyond graduation. In research, the physical university's strength lies in establishing on-campus specialized islands of excellence that benefit from the complementarity of physical proximity. This requires the active management of priorities, and a significant unbundling of the credentialing, teaching, housekeeping, and research functions. In the validation of information, the university will become more important than ever. With the explosive growth in the production of knowledge, society requires credible gatekeepers of information, and has entrusted some of that function to universities and its resident experts, not to information networks. But to safeguard the credibility of this function requires universities to be vigilant against creeping self-commercialization and self-censorship.

The threats to universities may not appear overnight, but they will surely arrive. People often overestimate the impact of change in the short term, but they also underestimate it in the long term. They recall that earlier promises about the potential of broadcasting as a tool of distance education failed to materialize, and they now believe that even a vastly more effective interactive medium will meet the same fate, forever. Yet the fundamental forces at work cannot be ignored. They are the consequence of a reversal in the historic direction of information flow. In the past, people came to the information, which was stored at the university. In the future, the information will come to the people, wherever they are. What then is the role of the university? Will it be more than a collection of remaining physical functions, such as the science laboratory and the football team? Will the impact of electronics on the university be like that of printing on the medieval cathedral, ending its central role in information transfer? Have we reached the end of the line of a model that goes back to Nineveh, more than 2500 years ago? Can we self-reform the university, or must things get much worse first?

Fast Ferroelectric Liquid-Crystal Electrooptics

David M. Walba

Many emerging technologies, including remote learning and video teleconferencing, interactive television, desktop digital audio-video, and the World Wide Web, share a common problem: a need for ever higher data transfer rates. Owing to power dissipation limits of conventional electronics, it seems likely that optical encoding of data will be an important part of the solution. Nevertheless, the silicon chip will be here for a long time to come. Silicon by itself, however, is a poor choice for modulation of light with electronics. These facts of digital life are currently driving an exciting research area aimed at development of electrooptic (EO) materials capable of working with silicon to create a class of devices sometimes termed integrated optical chips (*1*).

Organic thin films are among the most promising such materials. Design and synthesis of organic optical chips involve three key tasks: (i) Molecules enabling the required EO performance must be created; (ii) the molecules must be assembled into a material with the correct supermolecular stereochemistry to afford the required optical quality and EO properties; and (iii) this material must be properly integrated with a semiconductor device—a key process requiring supermolecular organization on a more global level.

The grandparent of organic EO films is the nematic liquid crystal (LC). Nematic LC molecules are highly anisotropic with respect to interaction with electric fields at low frequencies and with optical fields, properties useful for EO modulation. Self-assembly provides an elegant solution to the problem of supermolecular organization (the second task for realizing organic integrated optics), and the excellent processibility of LCs provides an approach for accomplishing that crucial third task of integration on silicon. This powerful combination has enabled the production of first-generation optical chips: LCs on amorphous-silicon integrated chips, which have been incorporated into video-camera color viewfinders as well as some of the first consumer virtual reality headsets. In this application, the EO modulator converts digital electronic data into optical signals in a large number of channels running in parallel. Here the optical signals are not destined for another chip, but rather are beamed into the human brain through that most highly evolved EO receiver—the eye.

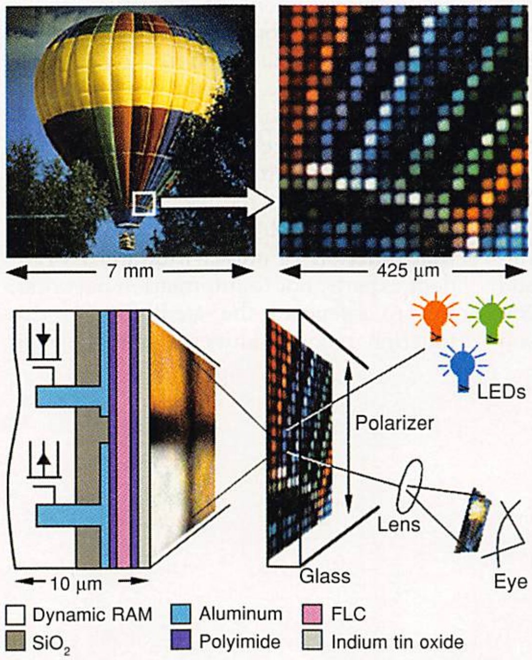

Prototype spatial light modulator. The 7 mm × 7 mm active area of the device is shown at upper left. The photomicrographs (of the same chip being driven by a computer) were taken with time-sequential illumination from red, green, and blue light-emitting diodes (LEDs) using a shutter speed of 1⁄60th second. [Photomicrographs courtesy Displaytech, Inc.]

For many applications, however, nematic LC modulators are either too slow, too large, or both. Enter chiral smectic-C ferroelectric LCs (FLCs) (*2*). FLCs are a unique state of matter: true liquids with a polar supermolecular structure (*3*). Thus, FLCs combine the processibility of LCs with many valuable properties of well-known inorganic polar-effect materials, such as lithium niobate and potassium titanyl phosphate, including many types of EO effects that do not occur in the nonpolar nematic LCs.

For example, the polar structure of the FLC self-assembly leads to a macroscopic electric dipole moment termed the ferroelectric polarization. Although the magnitude of this macroscopic dipole is typically relatively small on a per molecule basis (~0.01 D per molecule, although values as high as 3 D per molecule have been observed)—because the ferroelectric polarization scales with the number of molecules in the sample—in a film 1 µm by 1 cm^2, the macroscopic dipole moment is on the order of 10^{15} D. Even a single ferroelectric domain on the order of 1 µm by 5 µm by 5 µm in size has a dipole moment on the order of 10^8 D. It is therefore not surprising that FLC films respond more strongly to applied electric fields than conventional LCs. In the surface stabilized (SS) FLC device invented by Clark and Lagerwall (*4*), EO switching in thin films is fast, of very high contrast, and intrinsically digital (that is, the switches are either on or off, depending on the sign of the applied field, with a sharp switching threshold and bistable memory).

The size scale, speed, and power dissipation characteristics of SSFLC switches are well fitted to the ubiquitous VLSI (very large scale integration) silicon (*5*), leading to a new type of integrated optical chips (see figure) (*6*). These devices, referred to as spatial light modulators (SLMs), are essentially write-only silicon memory chips with optical read-out. With 256 × 256 = 64K channels running at 10 kHz, the prototype VLSI-FLC SLM pictured in the figure can convert electronic data to optical form at about 0.5 Gbit/s. One application of such devices is in projection or personal information display. The data rate of the SLM is directly visible in the figure: All of the perceived color and gray scale information seen in the photomicrographs results from time-averaging of one-bit digital frames; the high data rate enables display of 15-bit full-color images at 60 frames per second. Next-generation devices with 1280 × 1024 channels running at 10 kHz will drive 10 Gbits/s.

This is achieved by running many channels in parallel at a slow rate per channel. For information display and many other applications, this approach is ideal. For some applications, such as sending data along high-speed networks, a single channel running at 10 Gbits/s or faster is required. This kind of speed is impossible with standard LC switching, even for FLCs, because the EO effect derives from large motions of the molecules, which cannot occur at rates much faster than 1 MHz with the small driving fields available from standard VLSI silicon. Ultrafast EO modulation can be obtained, however, by taking advantage of another property of organic materials: electronic second-order nonlinear optics (NLO).

Thus, organic materials can exhibit an ultrafast EO effect caused not by motions of

The author is in the Department of Chemistry and Biochemistry and the Optoelectronic Computing Systems Center, University of Colorado, Campus Box 215, Boulder, CO 80309-0215, USA, and is a cofounder and member of the board of Displaytech, Inc., 2200 Central Avenue, Boulder, CO 80303, USA. E-mail: walba@colorado,edu

molecules or atoms but rather by motions of electrons. This effect is much weaker than LC molecular switching and typically requires much larger devices for the same degree of interaction with light at a given modulating field strength, but it can deliver blistering speed, an acceptable tradeoff for ultrafast single-channel modulators. In order to achieve useful NLO-based switching, however, supermolecular stereocontrol is again required, one in which very specific arrays of functional groups are oriented correctly in space. Because such materials are typically colored, these functional arrays are often termed NLO chromophores.

The most straightforward approach to organic NLO materials involves orientation of NLO chromophores along the polar axis of a sample with macroscopic polar symmetry. A very intensively studied approach for achieving this structure involves application of an external electric field to an organic polymer film containing NLO dye molecules with large dipole moments, using an external electric field, then freezing in the resulting polar structure by lowering the temperature of the sample to below the polymer glass transition. Great success in obtaining films with useful EO properties has been achieved in this way, and ultrafast optical circuits using such poled polymers are being demonstrated. However, problems remain, and several alternative approaches are under investigation.

Because FLCs spontaneously self-assemble into a polar structure, and techniques for processing FLC films on VLSI silicon are already relatively highly developed, FLC materials with useful NLO properties would complement poled polymers, providing increased flexibility in design and fabrication of NLO switches. Early NLO experiments with FLCs, however, showed that typical materials used in displays have NLO figures of merit on the order of 10^5 too small. Some understanding of the molecular origins of the polar structure occurring in FLCs has allowed the design of materials improved by about 10^4 in EO properties (*7*); however, at least an additional order of magnitude improvement is required in order to create useful ultrafast FLC NLO chips.

Until recently, this goal seemed elusive because of a very fundamental LC principle: LC molecules possess a large steric aspect ratio (that is, the molecules are long and skinny). Furthermore, in the FLC phase the long axis of the molecules is perpendicular to the polar axis of the material. Because most NLO chromophores are long functional arrays, they tend to orient perpendicular to the FLC polar axis as well, leading to incorrect supermolecular stereochemistry and poor NLO properties.

This problem now appears tractable, given the recent synthesis and characterization in our laboratories of FLC side-by-side dimer structures wherein the chromophore of the prototype NLO dye disperse red 1 (DR1) orients along the polar axis (normal to the LC long axis) in the FLC phase (*10*). The materials possess excellent liquid crystallinity; polarized light spectroscopy, ferroelectric polarization measurements, and powder x-ray scattering combine to show that the materials self-assemble to give the proper supermolecular stereochemistry for NLO. Thus, it seems reasonable to hope that FLCs with NLO properties on a par with poled polymers will be achievable, paving the way for the creation of ultrafast VLSI-FLC EO modulators similar in basic structure to the device shown in the figure.

Several key issues need addressing before realization of this goal, however. These issues revolve around the fact that it will likely be necessary for the light to propagate parallel to the plane of the FLC film in NLO-based devices, requiring guided wave optics. Very little work on FLC wave guiding has been accomplished to date, and key aspects of the problem such as temperature sensitivity and optical clarity have not yet been addressed. However, it is clear that because their unique supermolecular structure, FLCs offer a highly attractive potential approach to both highly parallel and ultrafast transmission of information with light.

References and Notes

1. B. W. Wessels *et al.*, Eds., *Thin Films for Integrated Optics Applications*, vol. 392 (Materials Research Society, Pittsburgh, PA, in press).
2. R. B. Meyer, L. Liebert, L. Strzelecki, P. Keller, *J. Phys. Lett. (France)* **36**, L69 (1975).
3. D. M. Walba, in *Advances in the Synthesis and Reactivity of Solids*, T. E. Mallouk, Ed. (JAI Press, Greenwich, CT, 1991), vol. 1, pp. 173–235.
4. N. A. Clark and S. T. Lagerwall, *Appl. Phys. Lett.* **36**, 899 (1980).
5. L. K. Cotter, T. J. Drabik, R. J. Dillon, M. A. Handschy, *Opt. Lett.* **15**, 291 (1990).
6. M. A. Handschy *et al.*, in *One-Transistor DRAM Ferroelectric-Liquid-Crystal Spatial Light Modulator*, D. P. Casesant and T.-H. Chao, Eds., *Optical Pattern Recognition V* (International Society for Optical Engineers, Bellingham, WA, 1994).
7. D. M. Walba *et al.*, *J. Am. Chem. Soc.* **113**, 5471 (1991); D. M. Walba *et al.*, *Ferroelectrics* **121**, 247 (1991); K. Schmitt *et al.*, *Liq. Cryst.* **14**, 1735 (1993).
8. D. M. Walba *et al.*, in (*1*); D. M. Walba *et al.*, in *Organic Thin Films for Photonics Applications*, 1995 OSA Technical Digest Series (Optical Society of America, Washington, DC, 1995), vol. 21, pp. 272–274.

9. I thank N. A. Clark for critical reading of the manuscript, and M. H. Handschy and M. Meadows for helpful discussions.

A Heterodimeric Transcriptional Repressor Becomes Crystal Clear

Brenda J. Andrews and Michael S. Donoviel

Over the past decade or so, studies of cell-type determination in budding yeast have consistently affirmed the predictive power of genetics—complex hypotheses, based solely on the analysis of mutants, have largely withstood the scrutiny of biochemists and molecular biologists. Now, the crystal structure of a1/α2 repressor, solved by Li *et al.* and described in this issue (*1*), provides a decisive molecular view of interactions suggested by genetic functional studies in vivo. In addition, the structure provides a first glimpse at what is likely to be a common mechanism by which the activity of transcriptional regulatory proteins is altered by interaction with different partners.

Saccharomyces cerevisiae exists as three cell types with distinct physiological properties and specialized roles during the yeast life cycle (*2*). Haploid cell type is determined by a single genetic locus, *MAT*, which encodes master regulatory proteins that dictate the expression of sets of cell type–specific genes. Haploid **a** cells carry the *MAT***a** allele and express a set of **a**-specific genes. In the other haploid cell type, α, which carries the *MAT*α allele, **a**-specific genes are turned off while another set of genes (α-specific genes) is turned on. Haploid **a** and α cells can mate to form the third specialized cell type, the **a**/α diploid cell.

Transcriptional repression is crucial in controlling the expression of cell type–specific gene sets (*3*, *4*). First, in both α and **a**/α cells, the MAT α2 gene product α2 collaborates with the ubiquitous transcription factor Mcm1 to form a heterodimeric repressor which binds to the **a**-specific gene operator that lies upstream of **a**-specific genes. As a result of α2-Mcm1 binding, **a**-specific genes are turned off (*5*, *6*). Second, in **a**/α diploid cells, α2 performs another function; it binds cooperatively with the *MAT***a** gene product a1 to the haploid-specific gene operator to turn off haploid-specific genes (*6*, *7*). The a1 and α2 proteins are related: They belong to the homeodomain family of proteins that regulate transcription in a wide range of eukaryotic organisms (*8*). Like some other homeodomain

The authors are in the Department of Molecular and Medical Genetics, University of Toronto, Toronto M5S 1A8, Canada.

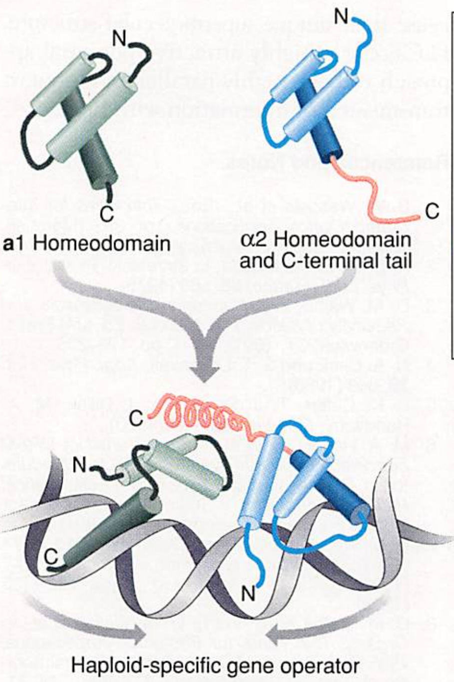

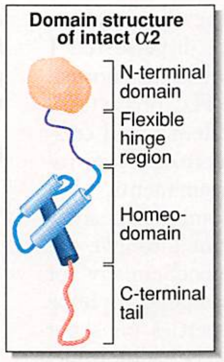

ILLUSTRATION: K. SUTLIFF

The yeast a1/α2 repressor bound to DNA. In the **a**1/α2 heterodimer, the carboxyl terminal (C-terminal) tail of α2 (pink) forms an amphipathic helix that contacts the homeodomain of **a**1. Binding of **a**1/α2 induces a bend in the DNA that is important for correct repressor-DNA interaction. Cylinders, helical regions.

proteins, the specificity and affinity with which α2 binds to DNA are enhanced by interaction with a partner protein. In particular, association with Mcm1 or **a**1 endows α2 with the appropriate binding specificity to repress two distinct classes of target genes. On its own, the **a**1 homeodomain protein cannot bind DNA.

We know how α2 interacts with DNA (*9*). As in other homeodomain proteins, the homeodomain of α2 folds into three helices, the most carboxyl-terminal of which inserts into the major groove of DNA (see figure; *8-10*). Genetic experiments have defined two regions of α2, adjacent to the homeodomain, that specify formation of a complex with different partners. Mutations in the so-called "flexible hinge" region of α2, located amino terminal to the homeodomain, diminish the cooperative interaction with Mcm1 and reduce the repression of **a**-specific genes (*11*). In contrast, mutations in a "tail" domain, which lies carboxyl terminal to the homeodomain, specifically impair both the cooperative interaction with **a**1 and the repression of haploid-specific genes (*12*). These hinge and tail regions are sufficient to confer dimerization specificity: A heterologous homeodomain can be directed to interact with Mcm1 simply by adding the flexible hinge and will interact with **a**1 if fused to the carboxyl terminal tail. An important piece of structural information adds to the picture: When α2 alone is bound to DNA, or is uncomplexed in solution, the carboxyl terminal tail is disordered. However, solution nuclear magnetic resonance studies show that the tail assumes a helical structure when it is bound to **a**1 (*9, 10, 13*). Together, these observations implicate the carboxyl terminal tail of α2 as the key interface with the **a**1 protein in the **a**1/α2 repressor complex.

The molecular picture of an active **a**1/α2 repressor complex impressively confirms this prediction. Li *et al.* have solved the structure of a ternary complex containing an **a**1/α2 heterodimer bound to a 21–base pair operator sequence. The carboxyl terminal tail of α2 indeed provides the sole contacts with **a**1 in the heterodimeric complex (*1*). A portion of the tail forms a short amphipathic helix with three leucine residues which project from the surface of the helix into a hydrophobic pocket on the **a**1 homeodomain. Mutation of these leucine residues, or another hydrophobic residue that stabilizes the tail helix, diminishes the ability of **a**1 and α2 to repress transcription in yeast. The precise correlation between an active repressor in vivo and a helical tail indicates that interactions of the carboxyl terminal tail of α2 and the homeodomain of **a**1 are crucial for creating a functional repressor complex.

How is the DNA binding activity of the **a**1/α2 complex affected by the heterodimer interface? The structure of the **a**1/α2–DNA ternary complex rules out the simple model that the contacts made between the α2 homeodomain and DNA are altered as a result of heterodimerization. Li *et al.* (*1*) found that contacts between the α2 homeodomain and DNA in the context of the heterodimer are virtually indistinguishable from those seen in the structure of an α2 monomer bound to DNA. Two observations make this finding somewhat surprising. First, although α2 alone binds to unbent DNA, binding of the **a**1/α2 heterodimer causes a pronounced bend in the DNA, making additional protein-DNA contacts possible (*9, 14*). Second, a version of α2 that is mutated in three key residues that contact the major groove of DNA binds DNA poorly on its own but still functions well in the **a**1/α2 heterodimer (*15*).

How then is the binding specificity of the **a**1/α2 heterodimer achieved? When interpreted in the context of in vivo studies, the structure of the ternary complex suggests that the increased DNA binding specificity of the heterodimer has several roots. First, the **a**1 homeodomain makes significant contacts with the DNA—the heterodimeric complex will bind only to sites that provide contacts required by both partners. Perhaps the **a**1-specific DNA contacts can compensate for defects in α2 binding, accounting for the relative resistance of the heterodimer to mutation of residues in α2 that contact DNA. If this were true, the DNA binding mutant of α2 protein might be exquisitely sensitive to mutation of key residues in **a**1 that contact the DNA. Second, noncontacted bases in the DNA sequence may also add to the stability of the complex because an **a**1/α2 operator sequence must accommodate a significant bend in order to form a productive repressor complex. Finally, interactions involving the carboxyl terminal tail of α2 and the homeodomain of **a**1 are clearly crucial for the specificity of repressor binding. As discussed above, the protein-protein contacts between **a**1 and α2 do not appear to alter notably their DNA binding helices. Rather, the heterodimer interface may increase specificity by dictating the precise spacing of the DNA binding helices of the two partners. In this regard, it is of particular interest that small alterations in spacing between the **a**1 and α2 binding sites within the operator sequence severely reduce both heterodimer binding in vitro and repression in vivo (*16*). Jin *et al.*, in experiments also described in this issue, extend this observation (*17*). They designed altered α2 proteins with small insertions into the tail of α2 between the homeodomain and the helix that contacts **a**1. These α2 insertion mutants allowed efficient repression of transcription through both wild-type **a**1/α2 sites as well as operator sequences with increased spacing between the half-sites. Increased flexibility at the heterodimer interface may allow increased flexibility in the binding site.

The structure of the **a**1/α2–DNA complex provides a detailed molecular view of the pairing of α2 with one of its partners. This pairing is clearly central to an elegant mechanism for the combinatorial control of gene expression. Yeast and other eukaryotic cells use highly related proteins to mediate combinatorial control. Li *et al.* (*1*) describe a number of other homeodomain proteins which may interact with partners by a flexible tail analogous to that found next to the α2 homeodomain. For example, interaction of the *Drosophila* extradenticle homeodomain protein with other homeodomain regulators requires short regions next to the homeodomain (*18*). Future structural studies may well reveal a highly conserved means of using heterodimerization to allow a small number of proteins to influence many regulatory decisions.

References

1. T. Li, M. R. Stark, A. D. Johnson, C. Wolberger, *Science* **270**, 262 (1995).
2. I. Herskowitz, J. Rine, J. N. Strathern, in *The Mo-*

lecular Biology of the Yeast Saccharomyces: *Gene Expression*, E. W. Jones, J. R. Pringle, J. R. Broach, Eds. (Cold Spring Harbor Laboratory Press, Cold Spring Harbor, NY, 1992), vol. 2, p. 583.
3. A. Johnson, in *Transcriptional Regulation*, S. L. McKnight and K. R. Yamamoto, Eds. (Cold Spring Harbor Laboratory Press, Cold Spring Harbor, NY, 1992), p. 975.
4. B. M. Herschbach and A. D. Johnson, *Annu. Rev. Cell Biol.* **9**, 479 (1993).
5. C. A. Keleher, C. Goutte, A. D. Johnson, *Cell* **53**, 927 (1988); C. A. Keleher, S. Passmore, A. D. Johnson, *Mol. Cell Biol.* **9**, 5228 (1989); S. Passmore, R. Elble, B.-R. Tye, *Genes Dev.* **3**, 921 (1989).
6. A. D. Johnson and I. Herskowitz, *Cell* **42**, 237 (1985).
7. C. Goutte and A. D. Johnson, *ibid.* **52**, 875 (1988); A. Bender and G. F. Sprague, *ibid.* **50**, 681 (1987); A. M. Dranginis, *Nature* **347**, 682 (1990).
8. W. J. Gehring, M. Affolter, T. Burglin, *Annu. Rev. Biochem.* **63**, 487 (1994).
9. C. Wolberger, A. K. Vershon, B. Liu, A. D. Johnson, C. O. Pabo, *Cell* **67**, 517 (1991).
10. C. L. Phillips, A. K. Vershon, A. D. Johnson, F. W. Dahlquist, *Genes Dev.* **5**, 764 (1991).
11. R. T. Sauer, D. L. Smith, A. D. Johnson, *ibid.* **2**, 807 (1988); A. K. Vershon and A. D. Johnson, *Cell* **72**, 105 (1993).
12. A. Mak and A. D. Johnson, *Genes Dev.* **7**, 1862 (1993); M. R. Stark and A. D. Johnson, *Nature* **371**, 429 (1994); J. Strathern, B. Shafer, J. Hicks, C. McGill, *Genetics* **120**, 75 (1988); K. Tatchell, K. A. Nasmyth, B. D. Hall, *Cell* **27**, 25 (1981).
13. C. L. Phillips, M. R. Stark, A. D. Johnson, F. W. Dahlquist, *Biochemistry* **33**, 9294 (1994).
14. D. L. Smith, A. B. Desai, A. D. Johnson, *Nucleic Acids Res.* **23**, 1239 (1995).
15. A. K. Vershon, Y. Jin, A. D. Johnson, *Genes Dev.* **9**, 182 (1995).
16. C. Goutte and A. D. Johnson, *EMBO J.* **13**, 1434 (1994).
17. Y. Jin, J. Mead, C. Wolberger, A. K. Vershon, *Science* **270**, 290 (1995).
18. F. B. Johnson, E. Parker, M. Krasnow, *Proc. Natl. Acad. Sci. U.S.A.* **92**, 739 (1995).

Unity in Transposition Reactions

Nancy L. Craig

The process of transposition, in which pieces of DNA move around the genome, was made famous by Barbara McClintock's discovery of "jumping genes" and the surprising plasticity of DNA (*1*). Other biological transactions also make use of this process: the acquisition of bacterial genes for antibiotic resistance, the replication of certain bacteriophages, the integration of retroviruses, and the intracellular movement of retroviral-like elements. New evidence points to unexpected parallels among these many transposition events: They all occur by similar DNA breakage and joining reactions. Moreover, the structures of transposition proteins from very different biological sources have remarkable overall structural similarity, even though they lack extensive primary sequence homology.

Central to all transposition reactions are breakage events that precisely expose the 3′ tips of the transposable element; these exposed 3′ tips are then joined to the target DNA (*2*). Sometimes DNA cleavage reactions also occur at the 5′ tips of the element; whether this occurs has a profound influence on the structure of the transposition products. Thus, although all transposition reactions involve DNA breakage and joining, several different types of recombination products can emerge, depending on which DNA strands are broken and joined (see figure).

The author is in the Howard Hughes Medical Institute, Department of Molecular Biology and Genetics, Johns Hopkins University School of Medicine, Baltimore, MD 21205, USA. Email: nancy_craig@qmail.bs.jhu.edu

Retroviral integration (*1–3*) and the replication of phage Mu (*1*, *2*, *4*) exhibit breakage and joining at only the 3′ ends of mobile elements. In retroviral integration, the viral RNA genome is converted to double-stranded DNA by reverse transcription. This DNA product is then cleaved by the retrovirally encoded integrase to expose 3′-OH ends at the embedded tips of the actual retroviral DNA. Strand transfer reactions then join these exposed 3′ ends to staggered positions on the target DNA, one transposon end joining to one target strand and the other end joining to a displaced position on the other target strand. As a result, the transposon is covalently joined to the target DNA but is flanked by short gaps that reflect the staggered positions of target joining; host DNA repair functions then repair these flanking gaps. The resulting product, in which the retroviral DNA is covalently joined to the target DNA, is called a simple insertion (see figure).

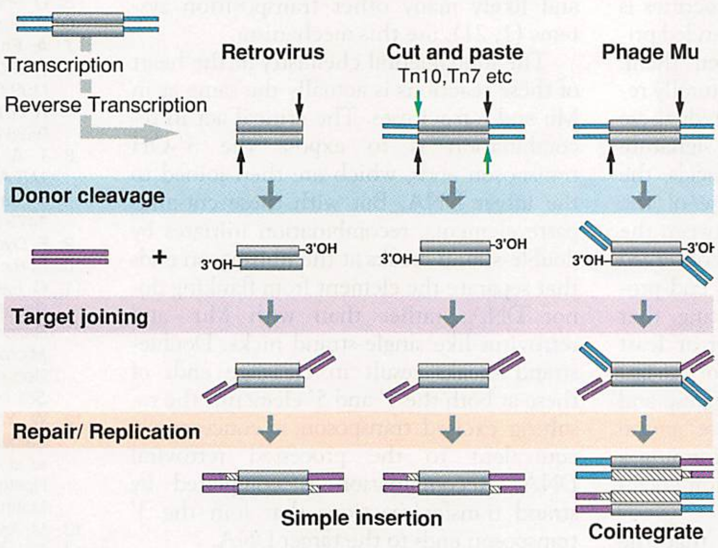

The DNA-processing reactions that underlie the translocation of three mobile elements. Gray boxes, mobile elements; blue lines, flanking donor DNA; black arrow, cleavage at the 3′-OH ends; green arrow, cleavage at the 5′ ends; red line, target DNA; cross-hatching, DNA replication.

In the case of bacteriophage Mu replication, the phage DNA is embedded in host chromosomal DNA. DNA cleavage reactions executed by MuA protein, the Mu-encoded transposase, introduce single-strand nicks at both tips of the element. These cleavages cleanly expose the 3′-OH ends of the transposon, separating them from flanking bacterial DNA but leaving the transposon covalently linked at its uncleaved 5′ ends to flanking DNA; the exposed 3′ ends of the transposon are then joined by strand transfer reactions to staggered positions on the target DNA. This transposition product is then replicated by host DNA replication to generate a product called a cointegrate in which the donor backbone, target, and two transposon copies are linked (see figure). In some cases, such as Tn3, another element-encoded recombination system further processes the cointegrate to generate a target molecule containing a simple insertion and regenerate the donor (*5*).

Identical chemical steps executed by element-encoded transposition proteins underlie retroviral integration and Mu replication: DNA cleavage reactions expose the 3′-OH ends of the elements, followed by strand transfer reactions that covalently join these 3′ element ends to the target DNA. Although the products of retroviral integration and Mu transposition are distinct, their differences arise not from the transposition reactions per se but rather from the state of the DNA substrate, in particular at the 5′ ends. Mu remains linked to the donor site while also inserting into the target site, because no cleavage occurs at the 5′ ends of the element; by contrast, in the retrovirus the substrate DNA contains only the transposable DNA segment.

The DNA cleavage and strand transfer reactions at the 3′ ends of retroviruses and phage Mu proceed by similar mechanisms. Both are Mg^{2+}-dependent reactions and likely result from direct, one-step transesterifications without covalent, protein-DNA intermediates (6). In DNA cleavage, H_2O is the nucleophile that attacks a phosphodiester bond at the transposon tip, resulting in phosphodiester bond hydrolysis and exposure of the 3′-OH transposon end. In strand transfer, the newly exposed 3′-OH transposon tip is the attacking nucleophile; attack by the 3′-OH transposon end on the target DNA results in the covalent linkage of the transposon end to a target strand. The chemical similarity of these reactions and the fact that mutation of the proteins that execute these reactions [retroviral integrases (7) and the MuA transposase (8)] block both the 3′ breakage and joining steps led to the suggestion that the same (or at least closely related) active sites execute both of these reactions.

That a retroviral integrase and a bacterial transposase are indeed fundamentally related has now been spectacularly demonstrated by the structures of the catalytic domains of these proteins at the atomic level. The overall topology of the HIV integrase (9) and MuA transposase (*10*) structures is similar, although there is little extended primary sequence homology between them. That these proteins might be structurally related was not entirely unanticipated; these and other recombinases contain a signature array of conserved acidic amino acids, the D,D(35)E motif, so-called because of the usually 35–amino acid spacing between the last two residues (*7, 11*) These conserved amino acids are critical for the 3′ end processing reactions (*7, 8*), suggesting that these amino acids are part of (or at least closely related to) the active sites of the enzymes. Moreover, in both the integrase and MuA transposase structures, these amino acids are close together (*9, 10*), forming a plausible binding site for a metal ion cofactor essential to recombination.

What was unanticipated was that the structures of the catalytic domains of these recombinases would also be so profoundly related to the structures of two other nucleic acid–processing enzymes, ribonuclease H (*12*) and the Holliday junction–resolving enzyme RuvC (*13*). All four proteins display the same central overall protein topology with clustering of acidic residues (*9, 10*). Thus, all of these proteins—of disparate biological function—are members of a superfamily that executes metal ion–dependent polynucleotidyl transferase reactions.

How are the DNA-processing reactions that underlie recombination coordinated so as to result in recombination rather than breakage? In Mu, a tetramer of transposase (that is, four metal-dependent phosphoryl transfer centers) actually executes recombination (*14*); the precise arrangement of these active sites and how they may communicate with each other is not yet known. Two of the active sites may mediate the strand cleavage steps and the other two the strand transfer steps. The central regulatory step in Mu recombination is the transition of MuA from the monomer to the active tetramer form (*15*), a step that depends on critical features of the substrate DNA and other protein cofactors. The retroviral integration system may, like Mu, use a tetramer of active sites, but the architecture of the retroviral system has not yet been directly established (16).

Many mobile elements translocate by a cut-and-paste mechanism that is seemingly distinct from that of retroviral integration and Mu replication—the introduction of double-strand breaks at the ends of an element to generate an excised transposon that is then inserted into a target site. This paradigm was first established for the bacterial transposons Tn10 and Tn7 (*1, 2, 17, 18*), but it is now clear that numerous elements, including the P element of *Drosophila* (*19*), the Tc elements of *Caenorhabditis elegans* and other organisms (*20*), and likely many other transposition systems (*1, 21*), use this mechanism.

The fundamental chemistry at the heart of these reactions is actually the same as in Mu and retroviruses. The critical act in recombination is to expose the 3′-OH transposon ends, which are then joined to the target DNA. But with these cut-and-paste elements, recombination initiates by double-strand breaks at the transposon ends that separate the element from flanking donor DNA, rather than with Mu- and retrovirus-like single-strand nicks. Double-strand breaks result in cleavage ends of these at both the 3′ and 5′ elements; the resulting excised transposon is conceptually equivalent to the processed retroviral DNA. Recombination is completed by strand transfer reactions that join the 3′ transposon ends to the target DNA.

As these double-strand break elements are processed by the same chemistry as the retroviruses, it is not surprising that double-strand break transposases can have amino acid similarities to the retroviral recombinases. Essential D,D(35)E motifs are present in recombinases that execute cut-and-paste reactions (*20–22*), and critical acidic amino acids that may function like the D,D(35)E motif have also been identified in other transposases (*17*). Indeed, clusters of acidic amino acids that can interact with metal ions may be present in many recombinases.

How do the double-strand break transposases execute cleavages at both 3′ and 5′ tips of mobile elements? In the case of Tn10, a single gene product, the Tn10 transposase, executes all the DNA processing and transfer reactions (*17*). Tn7, however, executes the initiating double-strand breaks through a collaboration of two Tn7-encoded D,D(35)E proteins (*22*). In an alternative pathway to replication, phage Mu displays a distinctive mechanism for element excision via double-strand breaks; following MuA-mediated cleavage and strand transfer at the 3′ ends of Mu DNA, an as yet unidentified nuclease distinct from transposase itself cuts the connections between the 5′ ends of Mu and the flanking donor DNA, resulting in a simple insertion (*2, 4*).

The biological and conceptual connections between many different mobile elements have long been recognized (*1*). It is now clear that biologically diverse systems also share fundamental biochemical and structural similarities.

References

1. D. E. Berg and M. M. Howe, *Mobile DNA* (American Society for Microbiology, Washington, DC, 1989).
2. K. Mizuuchi, *Annu. Rev. Biochem.* **61**, 1011 (1992).
3. S. Goff, *Annu. Rev. Genet.* **26**, 527 (1992).
4. B. D. Lavoie and G. Chaconas, *Curr. Top. Microbiol. Immunol.* **204**, 83 (1995).
5. D. Sherratt, in (*1*), pp. 163–184.
6. K. Mizuuchi, *J. Biol. Chem.* **267**, 21273 (1992).
7. A. Engelman and R. Craigie, *J. Virol.* **66**, 6361 (1992); J. Kulkosky *et al.*, *Mol. Cell Biol.* **12**, 2331 (1992); D. C. van Gent, A. A. M. Oude Groeneger, R. H. A. Plasterk, *Proc. Natl. Acad. Sci. U.S.A.* **89**, 9598 (1992).
8. T. A. Baker and L. Luo, *Proc. Natl. Acad. Sci. U.S.A.* **91**, 6654 (1994); K. Kim, S.-Y. Namgoong, M. Jayaram, R. M. Harshey, *J. Biol. Chem.* **270**, 1472 (1995).
9. F. Dyda *et al.*, *Science* **266**, 1981 (1994).
10. P. Rice and K. Mizuuchi, *Cell* **82**, 209 (1995).
11. O. Fayet *et al.*, *Mol. Microbiol.* **4**, 1771 (1990); P. Radstrom *et al.*, *J. Bacteriol.* **176**, 3257 (1994); R. Rezsohazy, B. Hallet, J. Delcour, J. Mahillon, *Mol. Microbiol.* **9**, 1283 (1993); T. G. Doak, F. P. Doerder, C. L. Jahn, G. Herrick, *Proc. Natl. Acad. Sci. U.S.A.* **91**, 942 (1994).
12. W. Yang, W. A. Hendrickson, R. J. Crouch, Y. Satow, *Science* **249,** 1398 (1990); K. Katayanagi *et al.*, *Nature* **347**, 306 (1990); J. F. Davies II, Z. Hostomska, Z. Hostomky, S. R. Jordan, D. A. Matthews, *Science* **252**, 88 (1991).
13. M. Ariyoshi *et al.*, *Cell* **78**, 1063 (1994).
14. T. A. Baker, E. Kremenstova, L. Luo, *Genes Dev.* **8**, 2416 (1994); B. D. Lavori, B. S. Chan, R. G. Allison, G. Chaconas, *EMBO J.* **10**, 3051 (1991).
15. M. Mizuuchi, T. A. Baker, K. Mizuuchi, *Cell* **70**, 303 (1992); T. A. Baker and K. Mizuuchi, *Genes Dev.* **6**, 2221 (1992).
16. A. B. Hickman *et al.*, *J. Biol. Chem.* **269**, 29279 (1994).
17. N. Kleckner *et al.*, *Curr. Top. Microbiol. Immunol.* **204**, 49 (1995); R. M. Chalmers and N. Kleckner, *J. Biol. Chem.* **269**, 8029 (1994).
18. N. L. Craig, *Mol. Microbiol.* **5**, 2579 (1991); *Curr. Top. Microbiol. Immunol.* **204**, 27 (1995).
19. P. D. Kaufman and D. C. Rio, *Cell* **69**, 27 (1992).
20. H. G. van Luenen, S. D. Colloms, R. H. A. Plasterk, *ibid.* **79**, 293 (1994); J. C. Vos and R. H. Plasterk, *EMBO J.* **13**, 6125 (1994).
21. B. R. Calvi, T. J. Hong, S. D. Findley, W. M. Gelbart, *Cell* **66**, 465 (1991).
22. E. May and N. L. Craig, unpublished data; R. Sarnovsky and N. L. Craig, unpublished data.

Quantum Computation

David P. DiVincenzo

If the bits of computers are someday scaled down to the size of individual atoms, quantum mechanical effects may profoundly change the nature of computation itself. The wave function of such a quantum computer could consist of a superposition of many computations carried out simultaneously; this kind of parallelism could be exploited to make some important computational problems, like the prime factoring of large integers, tractable. However, building such a quantum computer would place undreamed of demands on the experimental realization of highly quantum-coherent systems; present-day experimental capabilities in atomic physics and other fields permit only the most rudimentary implementation of quantum computation.

Often in science, fruitful results come from combining two seemingly unrelated ideas into one. Here I discuss such a combination, quantum mechanics and computers, which together make for a new subject, quantum computers, which is beginning to define itself and explore a path, albeit a rough and rather long one, toward reality. The idea of a quantum computer is simple, even if its realization is not. In a properly functioning ordinary computer, all of the bits always have a definite state at any instant in time, say 011100101 ... In a quantum computer, however, we will say that the state of the bits can be described by a wave function, which might look like

$$\Psi = a|011100101\ldots\rangle + b|111010001\ldots\rangle + \ldots \quad (1)$$

The coefficients a, b, ... are complex numbers, and the probability that the computer is in the state 011100101 ... is $|a|^2$, that it is in the state 111010001 ... is $|b|^2$, and so on. However, describing the state of the computer by a wave function does not merely imply the ordinary uncertainties of life that we use probabilities to describe. For instance, the phases of the complex coefficients a, b, ... have genuine significance: These coefficients can describe interference among different states of the computer, a very useful process for computation, as it turns out. The quantum wave function declares that the computer exists in all of its states simultaneously so long as that state is not measured; when we do choose to measure it, a particular state will be observed with the prescribed probability.

No computer now is very well described by such a wave function; our present-day machines accurately obey the laws of classical physics. But if someday the bits of a computer are shrunk to atomic scale, then a quantum description of the bit state and the dynamics of a computer may become plausible. Feynman considered this possibility in 1985 (*1*) and concluded optimistically, "it seems that the laws of physics present no barrier to reducing the size of computers until the bits are the size of atoms, and quantum behavior holds dominant sway." In this article, I will first discuss the main basis of Feynman's optimism, which is that the analog of computer "gates" can be implemented within the realm of some very well understood (but difficult) experimental physics. Then I will go on to discuss what Feynman did not know, that by cleverly using quantum dynamics to design computations that interfere constructively or destructively, remarkably powerful computations like Shor's prime factoring algorithm (*2*) become possible. The seeds of this idea also appeared in 1985, in a paper by Deutsch (*3*). Deutsch realized then that quantum mechanics strikes down one of the most cherished principles of theoretical computer science, that of a unique computational complexity for every mathematical problem. Going back to the work of Turing (*4*), it was believed that the answer to the question of whether any given problem could be solved in a time that was polynomial in the size of its inputs, or greater than polynomial, was independent of the physical apparatus used to perform the computations. This indeed seems to be true for all computers operating on the principles of classical physics, but quantum computers can solve in polynomial time problems that have no polynomial-time solution on any classical machine.

The author is with the IBM Research Division, Thomas J. Watson Research Center, Post Office Box 218, Yorktown Heights, NY 10598, USA.

Building Blocks of Quantum Logic

In this section I offer a bottom-up view of how a quantum computation might be reduced to practice, emphasizing that, at least in its first few steps, the required operations correspond to very well known procedures in experimental physics. At the very base of this construction is the qubit (or quantum bit) (*5*), a quantum system that, like an ordinary computer bit, has two accessible states but can, unlike an ordinary computer bit, exist in any superposition of those two states. Many two-state systems are known in physics, but throughout this article I will use as an example of this the spin-up (labeled $|1\rangle$) and spin-down (labeled $|0\rangle$) states of a spin-½ elementary particle like an electron or a proton. As in Boolean logic, we will build up operations in quantum logic using a small collection of logic gates, in which the states of input qubits (one or two qubits in the examples given below) are transformed in a specified fashion, leaving the qubits in a particular output state. In accordance with the laws of the quantum mechanics of isolated systems, we will take the allowable transformations to be unitary operations describing the time evolution of the input quantum state.

As an example, the quantum analog of the one-bit NOT or inverter gate can be implemented with spectroscopic techniques that have been well known in physics for over 50 years. As almost any elementary textbook of quantum mechanics shows (*6*), the time evolution of a spin-½ state can be accurately controlled by the judicious application of time-dependent magnetic fields. An inversion of the state, in which spin-up evolves to spin-down and vice versa, is accomplished by what is known as a tipping pulse. Suppose that we have an isolated spin in the presence of a combination of a stationary and a time-dependent magnetic field, described by the Hamiltonian

$$\mathbf{H} = \frac{1}{2}g\mu[H_0\sigma_z + H_1\sigma_y P(t)\sin(\omega t)] \quad (2)$$

Here, $g\mu$ is the magnetic dipole moment of the particle ($\mu = e\hbar/mc$, in centimeter-gram-second units, where e is the electron charge, $\hbar$ is Planck's constant divided by 2π, m is the particle mass, and c is the speed of light), the static magnetic field H_0 is along the z axis, and the ac magnetic field pulse with amplitude H_1 is along the y axis; σ_y and σ_z are the Pauli spin matrices, and $P(t)$ is the pulse envelope function, shown as a square pulse in Fig. 1. The time (t) evolution under this Hamiltonian is discussed fully in many places [for example, (*6*)]. During a tipping pulse, the ac field is in resonance with the energy difference between the two spin states: $\hbar\omega = g\mu H_0$. Under this condition, the 2 × 2 unitary matrix describing the time evolution of the spin in the spin-up–spin-down

basis, from the beginning $t = 0$ to the end $t = T$ of the pulse, simply has the form of a two-dimensional rotation matrix (except for phase factors)

$$U = \begin{pmatrix} e^{i\omega T/2} & 0 \\ 0 & e^{-i\omega T/2} \end{pmatrix} \cdot \begin{pmatrix} \cos\Omega T/2 & -\sin\Omega T/2 \\ \sin\Omega T/2 & \cos\Omega T/2 \end{pmatrix} \tag{3}$$

Here, $\Omega = g\mu H_1/4\hbar$ is the Rabi frequency; because both Ω and T are at the disposal of the experimentalist conducting the tipping-pulse procedure, any angle of rotation may be obtained. For a 180° tipping pulse, when $\Omega T = \pi$, this time evolution accomplishes the NOT operation: If the system is initially in the $|0\rangle$ state, it ends up in the $|1\rangle$ state, and vice versa. Of course this classical operation has the nonclassical feature that there are definite phase factors associated with the time evolution. They can in general be chosen to be unity, although because usually $\omega \gg \Omega$, setting these phases is probably the most difficult feature of the tipping-pulse unitary transformation to control accurately.

There is nothing special in this spin-resonance operation about the tipping angle π; a whole continuous (three-parameter) family of operations, corresponding to any SU(2) matrix (7), can be performed. It is this generalization that is the essence of quantum computing and gives it its great potential power.

For a coupled two-spin system, there is a similar spin-resonance protocol (8–10), familiar to the physics of double resonance, which can perform the exclusive-or (XOR) function (11, 12). The XOR of two bits is simply the sum of their two Boolean values, modulo 2. The only new ingredient that is needed to accomplish the XOR by spin-resonance techniques is a nonzero Hamiltonian coupling together the two spins. The protocol is easiest to explain if this coupling has the form of an Ising interaction (9), so that the Hamiltonian takes the form

$$H = \frac{1}{2} g_a \mu H_0 \sigma_{az} + \frac{1}{2} g_b \mu H_0 \sigma_{bz} + J\sigma_{az}\sigma_{bz} + \mathcal{H}(t) \tag{4}$$

although an XOR protocol can be constructed no matter what the form of the coupling term between the two spins a and b. Here, $\mathcal{H}(t)$ is the time-dependent Hamiltonian to be prescribed by a tipping-pulse protocol. Without the application of these tipping pulses, this Hamiltonian simply describes a stationary quantum system with exactly four energy eigenstates (Fig. 2A). Because of the spin-spin interaction, the energy spacing between every pair of levels in this four-level spectrum will generically be distinct. This permits a tipping-pulse protocol in which specific individual resonances can be selected. Thus, if a pulse is applied at time t_1 whose ac frequency is tuned to ω_1 [the energy spacing between the first and third energy levels in this spectrum (Fig. 2A)] and the tipping angle is chosen again to be π, then at the end of the pulse at time t_2, the desired XOR will be complete. That is, by flipping the state of the a spin if the b spin is $|1\rangle$, and doing nothing otherwise, this pulse leaves the final state of spin a in the XOR of the initial states of a and b, while leaving b in its original state, as summarized by the first two columns of the truth table in Fig. 2C. A gate symbol for this XOR operation is shown in Fig. 2D.

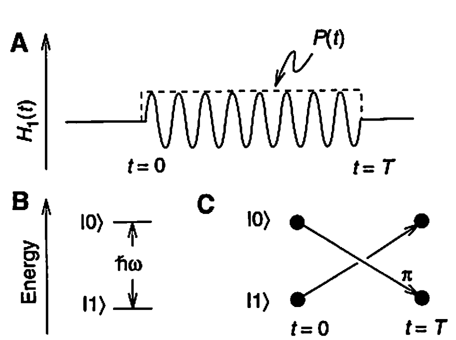

Fig. 1. The action of the NOT or inverter gate. The Hamiltonian describing the magnetic-resonance manipulation that results in the NOT operation is $\mathbf{H} = g\mu[H_0\sigma_z + H_1(t)\sigma_y]$. **(A)** The time dependence of the magnetic field of the tipping pulse, in this example a sinusoid at frequency ω multiplied by a square function $P(t)$ going from time $t = 0$ to $t = T$. **(B)** Energy level diagram for the qubit. The tipping pulse is tuned to be in resonance with the energy gap between the two stationary energy eigenstates $|0\rangle$ and $|1\rangle$. **(C)** State evolution diagram, showing the evolution paths of the two computational basis states. The π in this diagram denotes that on the path indicated, the state acquires a 180° phase shift (assuming the parameters are chosen such that $\omega T = 0$ and $\Omega T = \pi$).

The XOR protocol is very closely related to procedures invented long ago in the field of resonance spectroscopies (13). In 1956, Feher introduced a procedure for polarization transfer in electron-nucleus double resonance (ENDOR), which contains the XOR protocol just discussed. In Feher's initial experiments, the a spin was carried by the outermost unpaired electron of a P dopant in crystalline Si, and the b spin was carried by a nearby ^{29}Si nucleus (hence the name of the technique). The ENDOR and XOR protocols differ only in that Feher's procedure used a second π pulse applied at time t_2 at a different frequency ω_2 resonant with the transition between the first and second energy levels in the spectrum in Fig. 2A. At the end of the second pulse, at time t_3, the ENDOR operation is complete. The truth table for the ENDOR protocol is the first and third columns of Fig. 2C; like the one-pulse protocol, it leaves the a spin (the P electron spin in Feher's experiment) in the XOR of the initial states of a and b. In addition, it leaves b in the initial state of a, which is the polarization transfer that was of interest to Feher; for many purposes in physics, chemistry, and biology, it is highly desirable to move the spin state of an electron onto a nearby nucleus. The fact that this procedure also performs an interesting logical function, XOR, was not previously noted by ENDOR spectroscopists.

In either the one- or two-qubit gates, high-precision methods from experimental physics are required. It is necessary that the timing of the tipping pulses be precisely controlled, in order that the accumulated phase ωT be precisely zero (or some other chosen value). For the two-qubit operations, it is also necessary that the interaction Hamiltonian that determines the energy level splittings in the four-level spectrum be precisely known and controlled. In addition, the frequency content of the π pulses should be tailored in such a way that a pulse that nominally has ac frequency ω_1 has no small residual undesirable component at ω_2. This requires a careful choice of the pulse shape (in general, the square-pulse form in Fig. 1A would be undesirable). Many of these issues, especially those of pulse shaping and frequency stability, have been considered extensively in the science of magnetic resonance (14).

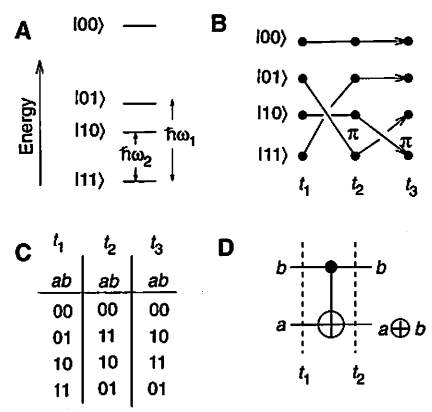

t_1 ab	t_2 ab	t_3 ab
00	00	00
01	11	10
10	10	11
11	01	01

Fig. 2. The action of the two-qubit XOR gate. **(A)** Energy level diagram for the two qubits, showing the four stationary states of the Hamiltonian in Eq. 4. The states are labeled by the two qubit values of the two spins $|ab\rangle$. **(B)** The time evolution pathways of the quantum states under the action of the tipping-pulse protocol described in the text. Again, the π's denote 180° phase shifts along the indicated pathways. **(C)** The truth table summarizing the result of the time evolution of the gate from the initial state (time t_1) to after the first (time t_2) and second (time t_3) tipping pulses. **(D)** The gate notation used for the XOR operation, obtained by using just the first of the two pulses of the ENDOR protocol. The resulting gate leaves qubit b unchanged and leaves a in the state given by the sum of a and b, modulo 2.

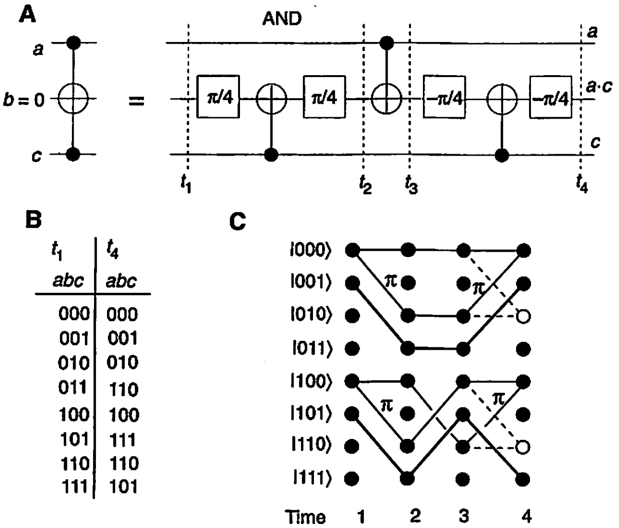

B

t_1 abc	t_4 abc
000	000
001	001
010	010
011	110
100	100
101	111
110	110
111	101

Fig. 3. Construction of the AND gate. **(A)** A notation for the three-qubit AND operation, and a gate construction of AND using three XOR gates and four single-qubit rotations. The $\pi/4$ gate corresponds to the operation in Eq. 3, with $\omega T = 0$ and $\Omega T = \pi/4$. When the work qubit b is initially set to $|0\rangle$, it ends up in the state $|a{\cdot}c\rangle$. **(B)** The full truth table of the three-qubit AND gate. **(C)** The state evolution diagram for the AND gate, showing the intermediate state along selected pathways at the times shown in (A). A new feature appears here: For some input states, the intermediate state is a superposition of two different computational pathways. The final state is definite again because constructive interference permits only one of the possible outcomes (the pathways that interfere destructively at the last step are dashed).

Quantum Circuits

Virtually any unitary operations on sets of qubits can be thought of as the universal gates of quantum computation (15, 16). What this means is that any unitary transformation in the 2^n-dimensional Hilbert space spanned by n qubits can be decomposed exactly (12) into a set of these universal operations applied in sequence to the n qubits. The two operations introduced above, one-bit rotations and the two-bit XOR, possess this universal property (12). Thus, even though it is beyond present-day experimental capabilities, we could build up any quantum computation (which includes all ordinary Boolean computations, and more) by applying these basic operations in sequence to selected qubits or pairs of qubits to build up a "circuit" of arbitrary complexity.

As an example of the use of this repertoire to efficiently construct a useful quantum computation, the construction of an AND gate is shown in Fig. 3 (12, 17). It involves three bits because the input bits a and c are left unchanged during the operation; the work bit b is set to $|0\rangle$ initially and is left in the state (a AND c) at the end. (The AND is the product of the two bit values.) It is well known in "reversible" logic (18, 19) that it is necessary to introduce a work bit because the AND operation by itself is irreversible; the same is true in quantum computing because all unitary operations are reversible (that is, have an inverse). The AND gate in Fig. 3A requires three XOR gates, in each case with the result placed in the b bit, along with four one-bit gates, all of which are just $\pm 45°$ tipping pulses. This particular implementation of the AND has phase factors that are all unity except for one: The state $|110\rangle$ is transformed to the state $-|110\rangle$. In many cases this change of phase may be acceptable for the operation of the gate (for example, if it is known that the input qubit b will always be set to $|0\rangle$). If it is necessary that all the phase factors be unity, then the implementation is somewhat more complicated, requiring six XORs and eight one-bit gates (12).

Diagrams such as Fig. 3A give a deceptively simple impression of the ease with which elementary quantum-mechanical manipulations might be assembled to perform a quantum computation. In the implementation of the AND gate, it is implied that we know how to "wire up" three XORs and a number of other gates. But consider what this "wiring up" means: While the XOR connecting qubits b and c is in operation, spins b and c should have some prescribed interaction (say, the Ising coupling of Eq. 4), whereas the couplings between a and b and between a and c should be zero. When the second XOR is in operation, the microscopic couplings should be rearranged, with the a-b coupling being nonzero. This is not a commonplace happening, and it certainly was not envisioned by Feher or any magnetic resonance experimentalists in the 1950s.

This "interconnection" problem can probably be solved, but it is one whose solution involves the most speculative and uncertain features of the quantum computer implementations suggested to date. The gedanken apparatus in Fig. 4 shows a possible future device that might solve the interconnection problem for a quantum computer. It depicts the tip of a specifically designed atomic force microscope (AFM) (20) approaching the surface of a crystal from above. It is imagined that both the tip and the surface are constructed with the following criteria in mind: (i) The spins of the H-atom nuclei, one of them placed at the very end of the tip and the others placed periodically on the surface, serve as the qubits. (ii) All the electrons are tied up in bonds, both in the bulk (crystalline Si is an insulator) and on the surface. This is done so that flipping an electron spin, or transporting it, is not an available quantum degree of freedom because such excitations require too much energy. (iii) Likewise, all other nuclei in the system have a spin of zero, so that only the H-atom proton spins are available for interaction. (I will say more at the end of this article about the undesirable consequences of stray quantum degrees of freedom in a quantum computer, principally concerning their role in the loss of quantum phase coherence.) (iv) Like any AFM, this one should be capable of moving the atom at the tip into contact with any atom on the surface at will. This property is

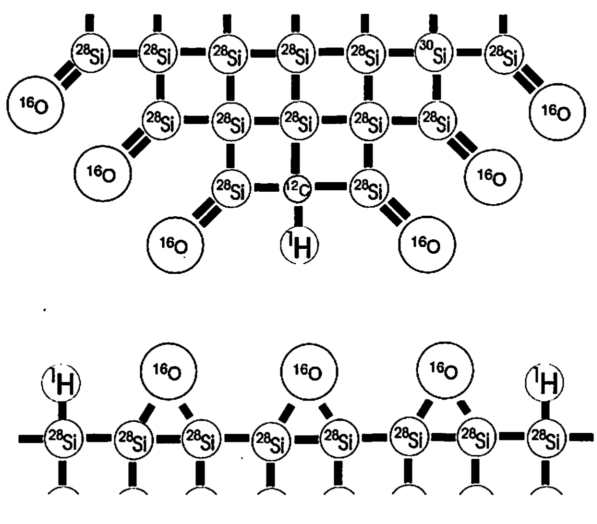

Fig. 4. Cartoon illustrating the kind of atomic-scale engineering that would be required to implement quantum computation with an AFM. It is imagined that an undoped crystalline Si tip is approaching a crystalline Si surface. The qubits are carried by the proton spin of the H atom at the very end of the tip and the H atoms arranged periodically along the surface. Interactions between the tip qubit and the other qubits can be turned on and off by the physical approach of the tip to various sites on the surface, permitting a gate protocol like the one of Fig. 3A to be carried out. By arranging for all the surface dangling bonds to be saturated, one can eliminate undesirable qubits carried by stray electron spins. Stray qubits carried by nuclear spins are likewise avoided by permitting only spin-zero isotopes in the vicinity of the H atoms. The tip qubit can be made spectroscopically distinct by bonding it to a different atom producing a chemical shift, which can be useful in devising selective magnetic resonance protocols.

the one that accomplishes the desired interconnection action: When the first XOR in Fig. 3A is to be performed, the microscope tip should be parked in contact with the H atom to the right on the surface in Fig. 4; for the second XOR, it should be parked in contact with the H atom on the left, and so on. Present-day AFMs cannot yet satisfy all of these design criteria. However, incredible strides have been made in the last few years in using AFMs to do spin-resonance manipulations and measurements on small groups of spins (*20, 21*).

Peter Shor's Prime Factorization

The AND gate constructed in Fig. 3A performs a classical Boolean operation. Still, its implementation is very nonclassical, in a way that is a prototype for the really powerful procedures (for prime factorization and the like) that are unique to quantum computation. Figure 3C shows how the various input states of the AND construction of Fig. 3A evolve in time through three of its stages to the final answer (we only follow the computations for which the work qubit b is set to $|0\rangle$). In any classical computation, each of these computations would follow a single, definite pathway in time from the beginning of the computation to the end, but in quantum computation, the computation can be split up into several (in this case just two) pathways that, by the quantum-mechanical principle of superposition, evolve in time in parallel. Because these pathways carry definite phases (note in the figure the points at which a 180° phase shift is introduced by the time evolution), these computations can, upon recombining at the end, interfere either constructively or destructively to produce definite outcomes. In the example shown, $|000\rangle$ evolves in time to itself, as required by the AND truth table, because the two computational pathways arriving at $|000\rangle$ at the end have the same phase (0 along one path, 2π along the other) and so interfere constructively. The incorrect outcome, $|010\rangle$, which the computational pathways also reach, is prevented because the phases are opposite (0 and π) and the interference is destructive. If the phases were not carefully controlled, then the incorrect outcome would occur half the time. It is by this means that a quantum computation, despite being in a very complex, indeterminate computational state in its intermediate stages, can be in a definite, computationally useful state at the end.

It is this general schema for quantum computation, first introduced by Deutsch (*3*), that is used to great effect in Shor's algorithm (*2, 4*) for efficiently solving a large-scale computational problem. Figure 5 illustrates a kind of architecture of the quantum computation that Shor uses to perform prime factorization. This diagram is a generalization of the one used to illustrate the operation of the AND in Fig. 3A, in that it shows the evolution pathways of the computational states as a function of time though the factoring procedure (time runs downward now, rather than to the right). As Deutsch and Jozsa envisioned in earlier work (*22*) [see also (*23*)], Shor divides the qubits of the computer into two registers labeled (somewhat misleadingly) input and output. The number of bits in each register needs to be of order the number of bits in the integer to be factored; for argument's sake (to be very ambitious), suppose that both registers contain $k = 1000$ bits. The rectangles in Fig. 5 depict the members of the entire Hilbert space of the input and output bits. This diagram is of necessity highly schematic because the dimension of this Hilbert space is huge: 2^{1000} for both the input and output registers. In fact, it is this exponential scaling of the size of the Hilbert space with respect to the number of particles in the system that is one of the reasons for the great potential power of quantum computing; unitary matrices can easily be constructed and multiplied on an ordinary digital computer, but their size cannot be exponential in the number of components of that computer (*24*).

The shading in Fig. 5 indicates the instantaneous state vector throughout the three main stages of Shor's computation. The first few steps are very simple: The starting state is fixed to be all zeros (all spins down). (The classical input, that is, the integer N to be factored, does not enter the procedure yet.) In stage 1, the computation is split up into 2^{1000} pathways, so that the wave function of the system becomes a linear superposition of all possible states, with equal phases, of the input register x. This highly nonclassical computation is very easy to prescribe spectroscopically: A 90° tipping pulse applied to each input spin places the wave function of the system in the desired state.

Stage 2 of computation is less trivial, requiring a single evaluation of a classical Boolean function

$$f(x) = c^x (\mathrm{mod}\ N) \qquad (5)$$

The value of this function is placed in the output register y. Here x is the value of the input register considered as an integer in binary representation, N is the integer to be factored, and the constant c is any other integer that has no prime factors in common with N; mod N indicates modular arithmetic, in which the result is the remainder after division by N. Because of the superposition principle, a single evaluation of $f(x)$ obtains every value of the output, given that the input is a superposition of all possible values. To evaluate $f(x)$ on a quantum computer, it should first be "compiled," in the usual classical sense, so that $f(x)$ is written as a sequence of operations of primitive Boolean functions like NOT and AND. Then one would implement this sequence of NOTs and ANDs as a quantum procedure, for example, in a sequence of magnetic-resonance tipping pulses.

I will not give a complete explanation of why the parallel evaluation of this particular $f(x)$ is useful for prime factorization. This requires some straightforward technicalities of number theory; good discussions may be found in the original literature (*2*) and in some recent reviews (*4*). In a nutshell, the important property of $f(x)$ is its periodicity with respect to x. If N is a prime number, then the period of $f(x)$ is $N - 1$, but if N is composite, the period of $f(x)$ is shorter, and knowledge of this period leads, after a straightforward (classical) calculation, to one of the prime factors of N.

Shor noted that a quantum computer is very well adapted to finding the periodicity

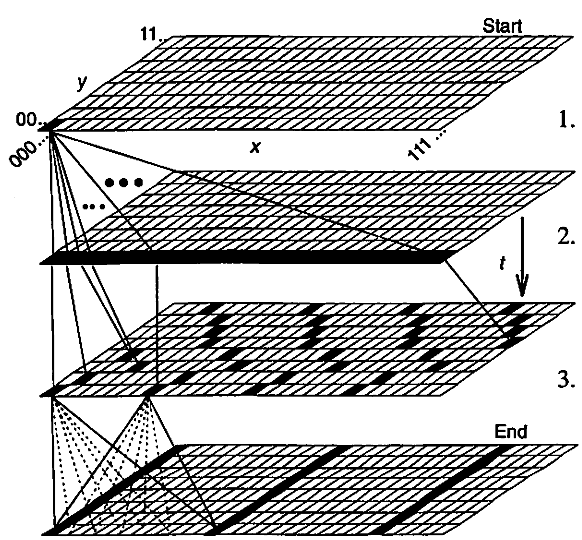

Fig. 5. A schematic depiction of the time evolution pathways in Shor's prime factoring procedure. The computational states appearing in the wave function at each selected instant in time are indicated by the filled rectangles. A few of the pathways are sketched out. Most of the pathways in the final step (dotted lines) interfere destructively, with only a few (solid lines) interfering constructively.

of $f(x)$, by means of the execution of a Fourier transform on the input register x (not the output register y); this is the third and final stage of computation depicted in Fig. 5. To be precise, the Fourier transform takes a wave function of the form

$$\Psi_i = \sum_{x=00...0}^{11...1} c_x |x\rangle \tag{6}$$

and evolves it in time so that it ends up as

$$\Psi_f = \sum_{x=00...0}^{11...1} \left(2^{-k/2} \sum_{x'=00...0}^{11...1} e^{2\pi i x x'/2^k} c_{x'} \right) |x\rangle \tag{7}$$

or in words, the final wave function coefficients are the discrete Fourier transform of their initial values. Shor observed that this transformation is a unitary operation and showed that it could be performed in a number of steps polynomial in k, the number of bits in the input register (which is in turn of order the number of bits needed to represent N, the number to be factored). Coppersmith (*25*) found a simple, explicit, robust gate construction (Fig. 6) for implementing the radix-2 Fourier transform of Eq. 7. It is a straightforward transcription of the steps involved in performing the Cooley-Tukey fast Fourier transform (FFT), with the individual "twiddle factors" of the FFT implemented by the two-qubit X_i gates shown. This procedure is very similar to the first step of Shor's computation, which just consists of the 90° tipping pulses applied to each bit in turn, without the twiddle-factor gates. Coppersmith noted that this sequence of operations takes on the order of k^2 steps.

This final FFT step is a very efficient way of obtaining the period of $f(x)$, in the same way that the scattering of x-rays from a crystal is a good way of obtaining its periodicity; a final measurement of the value of the register x is a measurement of the position of one of the "Bragg peaks" of this scattering process [although this measurement only obtains some unknown multiple of the fundamental period of $f(x)$, there are again some straightforward number-theoretic considerations that permit the fundamental period itself to be deduced reliably from this measurement]. Shor's procedure manages to be useful in the same way as the AND gate implementation; despite being in an indefinite, superposed computational state through the middle parts of the computation, destructive interference forbids almost all possible outcomes (just as in Bragg scattering, diffraction into almost every direction is forbidden), leaving the system in an (almost) definite, and thus computationally useful, state. Note that the diffraction process described here differs in a crucial respect from the diffraction of classical waves: the size of the diffraction grating used in Fig. 5 grows as an exponential of the size of the number to be factored. It is for this reason that classical wave optics cannot efficiently solve this problem.

A final tally of the number of steps required to perform Shor factoring reveals why this result has caused a stir in the computer science community. The result is polynomial in k, going as k^3 for small k and asymptotically approaching k^2 for large k. After many decades of effort, the best algorithms for factoring on an ordinary Boolean computer are nonpolynomial, scaling like $\exp(ak^{1/3})$, where a is some constant (*4, 26*). Although it is not known whether this particular problem might ultimately yield to a polynomial-time solution on an ordinary computer, Shor's result has made computer scientists realize that the algorithmic approaches available on a quantum computer are much more powerful than ordinary Boolean logic, and active work is under way in more fully defining the power of quantum mechanics to solve important mathematical problems.

The Decoherence Problem

Even though the formal results on the great capabilities of quantum computation are perfectly in accord with the laws of quantum physics, there are still several very fundamental physical obstacles that need to be overcome before quantum computation can be performed in the laboratory. These obstacles will make the path to constructing a quantum computer a long and arduous one, and one that will not be traversed before many years have elapsed. Two principal obstacles have been identified: the error correction problem and the decoherence problem. I will not discuss error correction, which may ultimately be very difficult in quantum computing because it seems that slight imperfections in the implementation of π pulses and other elements would ultimately lead a calculation off track (*27*). Other authors have explored the difficulties here (*28, 29*) and are beginning to define the rudiments of an error correction scheme (*30*). For the Shor algorithm, small errors can be defeated simply by running the computation repeatedly until the correct answer is obtained—prime factors can easily be confirmed by multiplication. (Actually, Shor's algorithm, like many other useful ones, is not guaranteed to give a correct answer in one run, even in the absence of errors.)

It seems to be the decoherence problem that makes even the initial investigation of modest-sized quantum computations difficult. Decoherence is this: If the quantum system is not perfectly isolated from its environment, the quantum dynamics of the surrounding apparatus will also be relevant to the operation of the quantum computer, and its effect will be to make the computer's evolution nonunitary. Because computational pathways separated at the beginning of the computation only recombine at the very end (Fig. 5), loss of phase coherence along these paths will spoil the constructive and destructive interference that is essential for quantum computing; therefore, the decoherence time t_ϕ needs to be much longer than the expected running time of the computation. Fortunately, the decoherence problem is one for which continuing advancement in the experimental art is likely to make a difference. Improving the isolation between the quantum system and its environment, which accompanies the steady advance of the technology used in high-precision quantum physics experiments, results in a lengthening of t_ϕ and a growing possibility to perform useful quantum computations.

Table 1 gives a survey of the current state of the art for t_ϕ's in a wide variety of two-state quantum systems (*16*). Because of the great disparity of energy scales, the available speeds range over 16 orders of magnitude. There is also a great disparity in the present technological capability for applying tipping pulses to each of these systems; the gamma-ray spectroscopy that would be needed for manipulating the Mössbauer nucleus does not exist, whereas the high-precision radio-frequency technol-

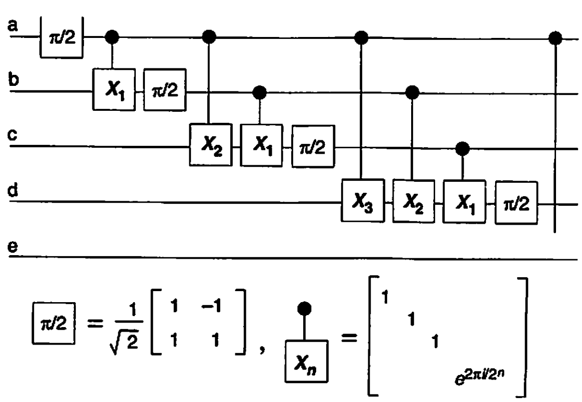

Fig. 6. The gate array introduced by Coppersmith (*25*) for performing the Fourier transform (step 3 of the Shor procedure in Fig. 5). The matrix unitary operators corresponding to the two types of quantum gates used in the figure are shown. The two-qubit X_n gate may be implemented by a simple combination of XORs and one-qubit gates (*12*). The X_n gate acts symmetrically on its two qubits. The process can be extended for inputs beyond a through e.

ogy for doing tipping pulses in nuclear magnetic resonance (NMR) is very mature. Also, the technology may not allow the potential speed of any given qubit to be fully utilized: For example, in the recent proposal for implementing quantum computation with a linear ion trap (*31*), the switching time would be 10^{-5} s rather than 10^{-14} s because it is limited by the qubit encoded in the quantized vibrations of the ions in the trap.

There is also a great disparity in the decoherence times available in these systems (Table 1). The ratio of the switching times to the decoherence times is an important figure of merit for quantum computation, being the number of steps of computation that might be performed before phase coherence is spoilt. Unruh's (*32*) calculations indicate that to perform computations like Shor factoring, this figure of merit should be something like the cube of the number of bits in the integer to be factored. If the object is to factor a 10^4-bit number (a task believed to be beyond the capability of any conceivable classical computer), it is evident that most of the present-day qubits are inadequately phase coherent to do the job. Nevertheless, several experiments have now been done in which actual, rudimentary quantum logic gates have been constructed, one involving optical microcavities (*33*) and another using trapped ions (*34*). The technology used in this last example is the one that is under development for the next generation of atomic clocks (*35*). This is significant because quantum computers require long dephasing times in addition to long decoherence times. Dephasing, loss of the accuracy of the phase factors of Eq. 3 because of the drift of the clock, must also be kept very small in quantum computation.

Table 1. Important times for various two-level systems in quantum mechanics that might be used as quantum bits, including prospective qubits ranging from nuclear physics, through atomic, electronic, and photonic systems, to electron and nuclear spins. The time t_{switch} is the minimum time required to execute one quantum gate; it is estimated as $\hbar/\Delta E$, where ΔE is the typical energy splitting in the two-level system; the duration of a π tipping pulse cannot be shorter than this uncertainty time for each system. The phase coherence time as seen experimentally, t_ϕ, is the upper bound on the length of time over which a complete quantum computation can be executed accurately. The ratio of these two times gives the largest number of steps permitted in a quantum computation using these quantum bits. See (*16*) for the original references.

Quantum system	t_{switch} (s)	t_ϕ (s)	Ratio
Mössbauer nucleus	10^{-19}	10^{-10}	10^9
Electrons: GaAs	10^{-13}	10^{-10}	10^3
Electrons: Au	10^{-14}	10^{-8}	10^6
Trapped ions: In	10^{-14}	10^{-1}	10^{13}
Optical microcavity	10^{-14}	10^{-5}	10^9
Electron spin	10^{-7}	10^{-3}	10^4
Electron quantum dot	10^{-6}	10^{-3}	10^3
Nuclear spin	10^{-3}	10^4	10^7

Outlook

It is evident from this survey of the current state of the art in quantum experimental physics that the construction of quantum computers is presently in the most rudimentary stage, and that to even think about a procedure like Shor factorization, which might require millions of operations (*14*) on thousands of qubits, might be absurdly premature. However, even a much more modest quantum computer will permit the study of effects that are of great scientific interest. For example (*10*), even a few bits of quantum computation will be very useful in performing so-called Bell measurements, which could be used to implement quantum teleportation (36), in which an unknown quantum state can be transported to a remote location. At perhaps the 10-qubit level, a quantum computer becomes capable of performing Schumacher's quantum coding (*5*), which would be of interest in the implementation of efficient quantum cryptography (*37*). And at perhaps the 100-qubit level, a quantum computer becomes an efficient repeater for a noisy (that is, partially decohered) quantum cryptographic link (*38*). In this application, it might become possible to create Einstein-Podolsky-Rosen pairs (*36*) at very remote locations, permitting new, stringent tests of the validity of the quantum theory. At this time, both physicists and computer scientists are actively searching for new ways to use quantum computers.

The quantum-gate approach outlined here appears to be a very arduous one for the ultimate implementation of a quantum computer, but other paradigms, which might ultimately provide an easier path to implementation, are being explored. For example, it might be that the natural time evolution of some simple quantum system, like the quantum states of a crystal, might itself perform some useful computation; preliminary work on this sort of "quantum cellular automaton" has been done (*9*, *39*). Perhaps our present understanding that stringent isolation is a requirement for quantum computation is untrue; it may be that the time evolution of the density matrix of an open quantum system is also a powerful computational tool, or that new approaches to error correction (*30*) will let noisy qubits compute. In any case, the next few years should be interesting ones for the quantum computer.

REFERENCES AND NOTES

1. R. P. Feynman, *Opt. News* **11**, 11 (February 1985).
2. P. W. Shor, in *Proceedings of the 35th Annual Symposium on the Foundations of Computer Science* (IEEE Computer Society, Los Alamitos, CA, 1994), p. 124 [this paper, "Algorithms for Quantum Computation: Discrete Log and Factoring," is available on the World Wide Web (*40*)].
3. D. Deutsch, *Proc. R. Soc. London Ser. A* **400**, 97 (1985).
4. For a review, see A. Ekert and R. Jozsa, in preparation; see (*41*); see also J. Brown, *New Sci.* **133** (no. 1944), 21 (1994).
5. The term "qubit" has been in circulation for the last several years: see B. Schumacher, *Phys. Rev. A* **51**, 2738 (1995) [available on the Web ("Quantum Coding") (*40*)].
6. G. Baym, *Lectures on Quantum Mechanics* (Benjamin-Cummings, Reading, MA, 1969), pp. 140 and 317–324.
7. See J. Mathews and R. L. Walker, *Mathematical Methods of Physics* (Benjamin, Menlo Park, CA, ed. 2, 1970), p. 464, for details of the SU(2) group.
8. A. Ekert, in *Atomic Physics 14: 14th International Conference on Atomic Physics, Boulder, CO, 1994* (AIP Conference Proceedings 323, AIP Press, New York, 1995), p. 450; see (*41*).
9. S. Lloyd, *Science* **261**, 1569 (1993); *ibid.* **263**, 695 (1994).
10. A. Barenco, D. Deutsch, A. Ekert, R. Jozsa, *Phys. Rev. Lett.* **74**, 4083 (1995) (available from the Los Alamos preprint archive as quant-ph/9503017); also see (*41*).
11. D. Deutsch, *Proc. R. Soc. London Ser. A* **425**, 73 (1989).
12. A. Barenco *et al.*, *Phys. Rev. A*, in press [available from Los Alamos preprint archive (quant-ph/9503016) and on the Web ("Elementary Gates for Quantum Computation") (*40*)]; T. Sleator and H. Weinfurter, *Phys. Rev. Lett.* **74**, 4087 (1995).
13. C. P. Slichter, *Principles of Magnetic Resonance* (Springer-Verlag, Berlin, ed. 3, 1992).
14. W. S. Warren and M. S. Silver, *Adv. Magn. Reson.* **12**, 247 (1988). These authors report the record pulse-sequence length in NMR to be 4096.
15. S. Lloyd, *Phys. Rev. Lett.* **75**, 346 (1995); D. Deutsch, A. Barenco, A. Ekert, *Proc. R. Soc. London Ser. A* **449**, 669 (1995) [available from Los Alamos preprint archive (quant-ph/9505018)]; see (*41*).
16. D. P. DiVincenzo, *Phys. Rev. A* **50**, 1015 (1995) [available from Los Alamos preprint archive (cond-mat/9407022) and on the Web ("Two-Bit Gates are Universal for Quantum Computation") (*40*)]. The sources of the numbers in the table are given here.
17. A related implementation of the so-called "Fredkin gate" (*19*) has been considered previously. See Y. Yamamoto, M. Kitegawa, K. Igeta, in *Proceedings of the 3rd Asia-Pacific Physics Conference* (World Scientific, Singapore, 1988); G. J. Milburn, *Phys. Rev. Lett.* **62**, 2124 (1989).
18. R. Landauer, *IBM J. Res. Dev.* **5**, 183 (1961); T. Toffoli, in *Automata, Languages and Programming*, J. W. de Bakker and J. van Leeuwen, Eds. (Springer, New York, 1980), p. 632.
19. E. Fredkin and T. Toffoli, *Int. J. Theor. Phys.* **21**, 219 (1982).
20. J. A. Sidles *et al.*, *Rev. Mod. Phys.* **67**, 249 (1995).
21. D. Rugar, C. S. Yannoni, J. A. Sidles, *Nature* **360**, 563 (1992); O. Züger and D. Rugar, *Appl. Phys. Lett.* **63**, 2496 (1993).
22. D. Deutsch and R. Jozsa, *Proc. R. Soc. London Ser. A* **439**, 554 (1992).
23. D. R. Simon, in (*2*), p. 116 [available on the Web ("On the Power of Quantum Computation") (*40*)].
24. This viewpoint on quantum computing was explored by R. P. Feynman [*Int. J. Theor. Phys.* **21**, 467 (1982)].
25. D. Coppersmith, *IBM Res. Rep. RC19642* (1994), and unpublished material; see also R. Cleve, unpublished material.
26. A. K. Lenstra, H. W. Lenstra Jr., M. S. Manasse, J. M. Pollard, in *Proceedings of the 22nd Annual ACM Symposium on the Theory of Computing* (ACM Press, New York, 1990), p. 564; an extended version appears in A. K. Lenstra and H. W. Lenstra Jr., Eds., *The Development of the Number Field Sieve*, vol. 1554 of *Lecture Notes in Mathematics* (Springer-Verlag, Berlin, 1993), p. 11.
27. However, see I. L. Chuang, R. Laflamme, P. Shor, W. H. Zurek, in preparation [available from Los Alamos

preprint archive (quant-ph/9503007) and on the Web ("Quantum Computers, Factoring, and Decoherence") (*40*)].
28. R. Landauer, in *Proceedings of the Drexel-4 Symposium on Quantum Nonintegrability—Quantum Classical Correspondence*, D. H. Feng and B.-L. Hu, Eds. (International Press, Boston, in press).
29. R. Landauer, *Philos. Trans. R. Soc. London Ser. A*, in press.
30. A. Berthiaume, D. Deutsch, R. Jozsa, *Proceedings of the Workshop on Physics and Computation, PhysComp '94* (IEEE Computer Society Press, Los Alamitos, CA, 1994), p. 60; A. Barenco, D. Deutsch, A. Ekert, C. Machiavello, unpublished material.
31. J. I. Cirac and P. Zoller, *Phys. Rev. Lett.* **74**, 4091 (1995).
32. W. G. Unruh, *Phys. Rev. A* **51**, 992 (1995) [available from Los Alamos preprint archive (hep-th/9406058)].
33. Q. A. Turchette, C. J. Hood, W. Lange, H. Mabuchi, H. J. Kimble, "Measurement of Conditional Phase Shifts for Quantum Logic," preprint (June 1995).
34. S. R. Jefferts, C. Monroe, E. W. Bell, D. J. Wineland, *Phys. Rev. A* **51**, 3112 (1995); C. Monroe, private communication.
35. R. S. Van Dyck Jr., in *Physics News in 1994*, April 1995 supplement of *APS News*, P. W. Schewe, Ed. (American Institute of Physics, College Park, MD, 1995), p. S6.
36. C. H. Bennett *et al.*, *Phys. Rev. Lett.* **70**, 1895 (1993).
37. C. H. Bennett, G. Brassard, A. Ekert, *Sci. Am.* **267** (no. 4), 50 (1992).
38. C. H. Bennett *et al.*, "Purification of Noisy Entanglement, and Faithful Teleportation via Noisy Channels," preprint (May 1995).
39. N. Margolus, in *Complexity, Entropy, and the Physics of Information*, vol. VIII of *Santa Fe Institute Studies in the Sciences of Complexity*, W. H. Zurek, Ed. (Addison-Wesley, Reading, MA, 1990), p. 273.
40. URL http://vesta.physics.ucla.edu/~smolin/(Quantum Information Page, Center for Advanced Accelerators).
41. URL http://eve.physics.ox.ac.uk/QChome.html (Quantum Computation and Cryptography page, Clarendon Laboratory, University of Oxford).
42. I am grateful to my colleagues N. Amer, C. H. Bennett, D. Coppersmith, N. Gershenfeld, R. Landauer, S. Lloyd, A. Peres, J. Smolin, and W. Wootters for many helpful discussions about this work. I thank the various audiences who heard me speak on this topic recently; they all helped me hone the story that I have written here.

Crystal Structure of the MATa1/MATα2 Homeodomain Heterodimer Bound to DNA

Thomas Li, Martha R. Stark, Alexander D. Johnson, Cynthia Wolberger*

The *Saccharomyces cerevisiae* MAT**a**1 and MATα2 homeodomain proteins, which play a role in determining yeast cell type, form a heterodimer that binds DNA and represses transcription in a cell type–specific manner. Whereas the α2 and **a**1 proteins on their own have only modest affinity for DNA, the **a**1/α2 heterodimer binds DNA with high specificity and affinity. The three-dimensional crystal structure of the **a**1/α2 homeodomain heterodimer bound to DNA was determined at a resolution of 2.5 Å. The **a**1 and α2 homeodomains bind in a head-to-tail orientation, with heterodimer contacts mediated by a 16-residue tail located carboxyl-terminal to the α2 homeodomain. This tail becomes ordered in the presence of **a**1, part of it forming a short amphipathic helix that packs against the **a**1 homeodomain between helices 1 and 2. A pronounced 60° bend is induced in the DNA, which makes possible protein-protein and protein-DNA contacts that could not take place in a straight DNA fragment. Complex formation mediated by flexible protein-recognition peptides attached to stably folded DNA binding domains may prove to be a general feature of the architecture of other classes of eukaryotic transcriptional regulators.

Homeodomain proteins constitute a superfamily of DNA binding proteins that play critical roles in gene regulation and development in many eukaryotic species. These proteins have in common a conserved 60–amino acid DNA binding domain that has been well characterized structurally, biochemically, and genetically (*1*, *2*), whereas other portions of the proteins are quite divergent. The fold adopted by the homeodomain, as uncovered in structural studies of *Drosophila* (*3*–*5*), yeast (*6*, *7*), and human (*8*) homeodomains, consists of three α helices and an NH_2-terminal arm. Homeodomains bind DNA by inserting the third of these three α helices into the major groove of the DNA, while the NH_2-terminal arm contacts bases in the adjacent minor groove. Biochemical studies have shown that isolated homeodomains, which typically bind DNA as monomers, often exhibit only a relatively modest degree of DNA sequence selectivity (*9*–*11*). In the case of the yeast α2 homeodomain protein, we know that the specificity and affinity with which α2 binds DNA is augmented by its association with either of two partner proteins: the product of the MAT**a** locus, **a**1, or the non–cell type–specific protein MCM1. The **a**1/α2 and α2/MCM1 complexes each bind to a distinct set of DNA sites in the yeast genome, causing repression of the adjacent genes. Combinatorial control by **a**1 and α2 provides a means to achieve cell type–specific regulation of a large set of genes since **a**1 and α2 are expressed together in only the **a**/α diploid yeast cell type (*12*).

One of the partner proteins of α2, **a**1, is also a member of the homeodomain superfamily (*13*). In the diploid **a**/α cell type, these two homeodomain proteins form a heterodimer that binds to sites upstream of haploid-specific genes (hsg) (*14*–*16*). In the absence of α2, the **a**1 protein exhibits no detectable specific binding to DNA (*11*). However, the presence of **a**1 in solution dramatically raises the affinity of α2 for hsg operators. The cooperative binding of α2 with **a**1 depends on the 21-residue COOH-terminal tail of α2, which is located immediately COOH-terminal to its homeodomain (*17*, *18*). Deletion of the COOH-terminal tail renders α2 incapable of cooperative binding with **a**1 in vitro and of repressing the haploid-specific genes in vivo (*18*). This tail is required for interaction with the **a**1 partner protein only, as its absence does not affect the cooperative interaction of α2 with MCM1 (*18*). The interaction of the tail of α2 with the **a**1 protein is quite specific; for example, the tail fails to interact with α2 itself, a homeodomain closely related to **a**1 (*17*). Splicing this peptide onto the *Drosophila* engrailed homeodomain renders engrailed capable of cooperative interaction with **a**1 (*17*). Additional interactions between **a**1 and α2 are mediated by the NH_2-terminal domains of the respective proteins, which have been proposed to contact one another by way of a coiled-coil interaction (*19*). Deletion analysis of **a**1 and α2 has shown that their cooperative binding to the hsg operator requires only the homeodomain of **a**1 and the homeodomain plus the tail of α2 (*20*). These fragments, which were used for

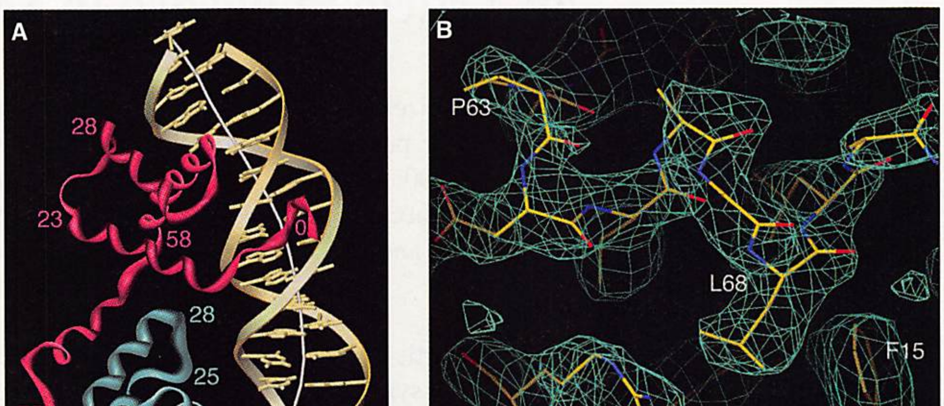

Fig. 1. Structure of the **a**1/α2–DNA ternary complex. (**A**) Overall model of the complex. The α2 protein is shown in red and **a**1 is shown in blue. Sequence numbers for the **a**1 and α2 proteins follow the same color scheme. The white line indicates the local DNA axis. This figure, as well as Figs. 3B, 4, A and C, 6, B to D, and 7 were generated with the program SETOR (*59*). (**B**) Simulated annealing omit map showing the COOH-terminal tail of α2 bound to **a**1. Residues 59 to 74 of α2 were deleted and the model was subjected to limited simulated annealing refinement in order to remove phase bias. The electron density map shown was calculated with $2F_o - F_c$ coefficients and phases from the resulting model and is contoured at 1.0 σ.

T. Li is in the Department of Biophysics and Biophysical Chemistry and C. Wolberger is in the Department of Biophysics and Biophysical Chemistry and the Howard Hughes Medical Institute, Johns Hopkins University School of Medicine, 725 North Wolfe Street, Baltimore, MD 21205–2185, USA. M. R. Stark and A. D. Johnson are in the Department of Microbiology and Immunology, University of California School of Medicine, San Francisco, CA 94143–0502, USA.

*To whom correspondence should be addressed.

the structural studies described here, bind DNA with 10-fold reduced affinity as compared with the full-length proteins (*11*, *20*). We refer to the complex formed by these fragments as the a1/α2 heterodimer. The equilibrium constant for dissociation of this a1/α2 heterodimer into monomers is 2×10^{-4} M (*20*).

We previously described the x-ray crystal structure of the α2 homeodomain bound to DNA (*6*). In the absence of its partner proteins, the α2 homeodomain binds as a monomer to nearly straight B-form DNA. Although the fragment of α2 crystallized contained the COOH-terminal tail that mediates heterodimerization with a1, the 21 residues of the tail were disordered in the structure of the α2-DNA complex. Solution nuclear magnetic resonance (NMR) studies show that the COOH-terminal tail is unstructured in solution as well, becoming ordered only upon heterodimerization with a1, when part of it forms a short α helix (*7*, *20*).

In order to uncover how a flexible peptide tail mediates specific heterodimer formation between two homeodomains, we determined the three-dimensional structure of a ternary complex containing an a1/α2 heterodimer bound to DNA. This crystal structure, determined at a resolution of 2.5 Å, shows that the a1 and α2 homeodomains bind in tandem to a 21–base pair (bp) DNA fragment. In the ternary complex, 16 residues of the COOH-terminal tail of α2 undergo a conformational change, becoming ordered and contacting the a1 homeodomain at a surface that does not participate in DNA binding. The heterodimer induces a pronounced DNA bend that is required for contacts between the two proteins. The manner in which a1 and α2 heterodimerize represents a possible mechanism by which other transcriptional regulators can associate with one another on the DNA.

Table 1. Crystallographic analysis. The purification and crystallization of the **a1**/α2–DNA complex and the method of flash-freezing the crystals have been described (*51*). The complex crystallizes in space group $P6_1$ with unit cell dimensions $a = b = 132.8$ Å and $c = 45.71$ Å. The crystals form with one complex per asymmetric unit and contain 68 percent solvent. Diffraction from these crystals extends to a maximum resolution of 2.4 Å, with diffraction along the *c* axis falling off in intensity beyond 2.7 Å. Heavy atom derivatives were prepared by substituting 5-iodouracil for thymine at base 1, 11, or 22 of the DNA (IdU^1, IdU^{11}, and IdU^{22}). X-ray diffraction data collection, processing, and multiple isomorphorous replacement (MIR) phase calculation and refinement were as described (*52*). The MIR phases were used to calculate an electron density map at 2.8 Å resolution, which was improved by one round of solvent flattening (*53*). A nearly complete model of the complex was fit to this map by means of the O graphics program (*54*). A statistically random selection of 10 percent of the total reflection data was excluded from the refinement and used to calculate the free *R* factor (R_{free}) as a monitor of model bias (*55*). The model was subjected to several rounds of positional and simulated-annealing refinement with X-PLOR (*56*). Several missing side chains and residues were added following inspection of $2F_o - F_c$ and $F_o - F_c$ maps and a phase-combined map calculated with SIGMAA (*57*). The analysis was continued with 120 cycles of positional and constrained temperature factor refinement, yielding an *R* factor at 2.8 Å resolution of 22.4 percent and an R_{free} of 29.2 percent. The model was then further refined at 2.5 Å resolution against the derivative data set, IdU^{11}. In the resolution range from 2.8 to 2.5 Å, the IdU^{11} data set contained 94 percent of the expected data; of those reflections recorded, 81 percent of the intensities were greater than 2σ. After rigid body, positional, and simulated annealing refinement, an additional five residues in the COOH-terminal tail of α2 were fit to $2F_o - F_c$ and $F_o - F_c$ maps. Simulated annealing omit maps (*58*) were calculated at many stages of the refinement to verify the placement of residues in the electron density map. Water molecules were included at the final stage of refinement, based on the presence of peaks in difference electron density maps of at least 3σ in significance. All water molecules have *B* factors of less than 50 $Å^2$ and participate in at least one hydrogen-bonding interaction. The model of the complex presented here contains 1851 atoms and 58 water molecules. The average atomic *B* factor for the proteins, excluding water molecules and the COOH-terminal tail of α2, is 39.1 $Å^2$; the average *B* factor of all atoms in the COOH-terminal tail of α2 is 60.4 $Å^2$.

	Native	IdU^1	IdU^{22}	IdU^{11}
Resolution (Å)	2.74	2.40	2.65	2.40
Measured reflections	74,037	83,570	35,860	76,841
Unique reflections	12,014	16,357	10,715	18,106
Completeness (%)	92.8	90.4	80.0	94.0
Overall $I/\sigma(I)$	9.01	11.7	10.5	14.7
R_{merge} (%)*	13.1	7.4	6.8	5.5
R_{iso} (%)†		11.6	8.2	8.3
R_{cullis}‡		0.57	0.65	0.60
Phasing power§		1.86	0.92	1.82
Mean overall figure of merit (20–2.8Å)‖		0.54		
		Refinement statistics		
Resolution range	6–2.8 Å			6–2.5 Å
R factor (%)¶	22.4			22.5
R_{free} factor (%)#	29.2			29.8
Refined geometry	*Overall*	*Protein*	*DNA*	
rmsd bond length (Å)	0.018	0.016	0.019	
rmsd bond angle (°)	1.93	1.83	2.02	

*$R_{merge} = \Sigma|I - \langle I \rangle|/\Sigma I$, *I*: observed intensity, $\langle I \rangle$: average intensity of multiple observations of symmetry-related reflections. †$R_{iso} = \Sigma|F_{pH} - F_p|/\Sigma F_p$, F_{pH} and F_p are the observed derivative and native structure factor amplitude. ‡$R_{cullis} = \Sigma||F_{pH} \pm F_p| - F_{H(calc)}|/\Sigma|F_{pH} - F_p|$. §Phasing power = $\{\Sigma|F_{pH(calc)}|^2/\Sigma[|F_{pH(obs)}| - F_{p(calc)}|]^2\}^{1/2}$, $|F_{pH(obs)}| - F_{p(calc)}|$ is the lack-of-closure error. ‖Mean figure of merit = $\langle|\Sigma P(\alpha)e^{i\alpha}/\Sigma P(\alpha)|\rangle$, α: phase, $P(\alpha)$: phase probability distribution. ¶$R = \Sigma|F_p - F_{p(calc)}|/\Sigma F_p$. #*R* factor for a subset of 10 percent of the reflection data that were not included in the crystallographic refinement.

Overview of the ternary complex. The a1/α2–DNA complex (Fig. 1A) contains the a1 and α2 proteins bound to a 21-bp fragment of bent duplex DNA. The structure of the complex was determined as described (Table 1); a representative view showing the fit of the model to the electron density map is shown in Fig. 1B. The sequence of the DNA site was derived from the sequences of 14 in vivo a1/α2 binding sites (Fig. 2C) and differs in the four central base pairs from the consensus sequence. Of a number of different DNA sequences and oligonucleotide lengths, this DNA site yielded the best crystals. The sequences of the proteins and the DNA, and the numbering scheme used to describe them, are shown in Fig. 2. The a1 and α2 homeodomains bind in a tandem orientation to one face of the DNA, burying 2300 $Å^2$ of protein and DNA surface area. The tandem binding of the two homeodomains, which had been predicted on the basis of chemical protection experiments (*16*), is in agreement with the observed pattern of DNA protection from hydroxyl radical attack and methylation in the presence of bound a1/α2 (Fig. 2D).

The α2 protein contacts the a1 homeodomain with a peptide tail located COOH-terminal to the α2 homeodomain. As compared with the structure of α2 alone bound to DNA, an additional 16 residues are ordered in the ternary complex. This COOH-terminal tail, consisting of residues 59 to 74, extends from the end of helix 3 of the α2 homeodomain (Fig. 1A). Residues 59 to 62 contain a short stretch of extended chain, followed by two turns of an amphipathic helix (residues 63 to 69), which contacts the a1 homeodomain on the face opposite to that which binds DNA. The helix in the tail of α2 packs between helices 1 and 2 of a1, with the axes of all three helices roughly parallel. The α2 tail helix is somewhat distorted, with deviations from ideal hydrogen bonding geometry at residues 64 and 65. As predicted in biochemical and NMR studies (*20*), all contacts with the a1 homeodomain are mediated by the COOH-terminal extension of α2; the homeodomain of α2 (residues 0 to 59) forms no direct contacts with the a1 protein.

The model of the ternary complex contains residues 0 to 74 of α2, including the

NH_2-terminal arm (residues 0 to 7), helices 1 (residues 10 to 23), 2 (residues 28 to 37), and 3 (residues 42 to 58), and the COOH-terminal tail (59 to 74). An additional five COOH-terminal residues, which are disordered in the structure, are not required for **a**1/α2 repression (*18*). Of the **a**1 protein, residues 8 to 56 are included in the model. The first 12 amino acids in the protein, including the NH_2-terminal arm, are disordered, as is the COOH-terminal residue of helix 3, Lys[57]. The **a**1 and α2 homeodomains, which are 21 percent identical in sequence, are similar in structure and superpose with a 1.0 Å root-mean-square difference in Cα positions (residues 8 to 57).

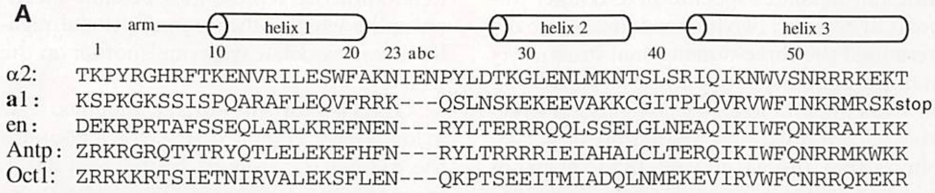

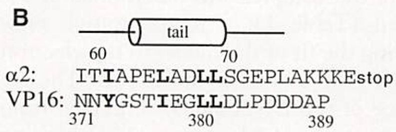

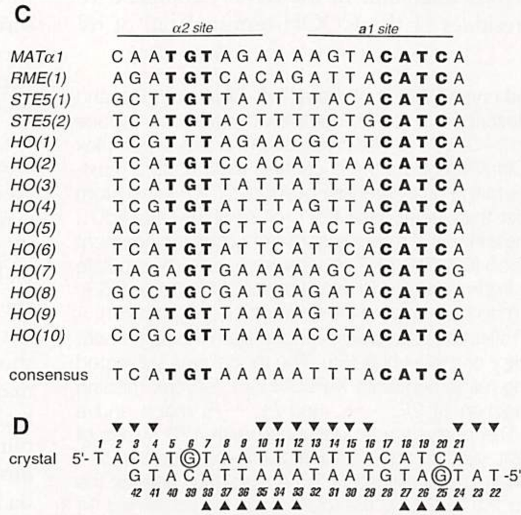

Fig. 2. (**A**) Sequence and secondary structure of the α2, **a**1, engrailed (en), *Antennapedia* (*Antp*), and Oct-1 homeodomains (*60*). The residues of the homeodomain have been renumbered from 0 to 60 in accordance with the convention established in previous studies of homeodomains (*3, 4, 6*). In this numbering scheme, residues 128 to 151 of α2 correspond to homeodomain residues 0 to 23 and residues 155 to 190 of α2 correspond to homeodomain residues 24 to 59. Residues 152 to 154 of α2, a three–amino acid insertion relative to other homeodomains, are labeled a, b, and c. The **a**1 residues 69 to 126 have been renumbered 0 to 57. (**B**) Alignment of the COOH-terminal tail of α2 with a segment of the herpes virus activator protein, VP16, which interacts with the Oct-1 homeodomain. The COOH-terminal tail of α2, residues 191 to 210, have been renumbered 60 to 79. Absolute residue numbers for VP16 are shown below the amino acid sequence. (**C**) Naturally occurring and synthetic DNA binding sites of **a**1/α2. DNA sequences are written 5′ to 3′; invariant and highly conserved bases are highlighted in bold. Sequences are shown of 14 in vivo binding sites for **a**1/α2 located upstream of haploid-specific genes (*16*); the consensus sequence is derived from the list shown. (**D**) Sequence of the double-stranded oligonucleotide used in this crystallographic study and results of in vitro chemical protection experiments (*16*). Circled guanine bases are protected from methylation by binding to DNA of the **a**1/α2 heterodimer. Triangles indicate bases that are protected from hydroxyl radical attack by **a**1/α2.

DNA structure and crystal packing. The DNA in the **a**1/α2–DNA complex contains a marked overall bend of 60° (Figs. 1A and 3). In contrast is the nearly straight DNA in the complex of α2 alone bound to DNA as discussed below, which contains a bend of 8.8° within a single homeodomain binding site and an overall bend of 7°. Our observations are in agreement with solution studies that have shown that the **a**1/α2 heterodimer introduces a bend in the DNA estimated at 100°, while α2 alone does not (*21*). The bend in the **a**1/α2 binding site occurs without dramatic local distortion or kinking of the B-DNA helix. Rather, the DNA helix is smoothly bent, most noticeably at the center of the DNA fragment and in the **a**1 half of the binding site. The bend is largely the result of a variation in base roll, which adopts negative values near the center of the DNA site and positive values in flanking base pairs (Fig. 3A). A consequence of the bend is a narrowing of the minor groove at the center of the DNA fragment, between the **a**1 and α2 proteins (Fig. 3A). The continued bending of the DNA in the **a**1 half of the site leads to a widening of the minor groove and a narrowing of the major groove. The DNA in the ternary complex bends toward the **a**1/α2 heterodimer, facilitating interactions between the two proteins. The COOH-terminal tail of α2 spans the gap between the **a**1 and α2 homeodomains at the point where the minor groove of the DNA helix is at its narrowest. Without the observed bend in the DNA, the tail of α2 could not reach its binding site on the back of the **a**1 homeodomain. The protein-protein interactions at the heterodimer interface, as well as the

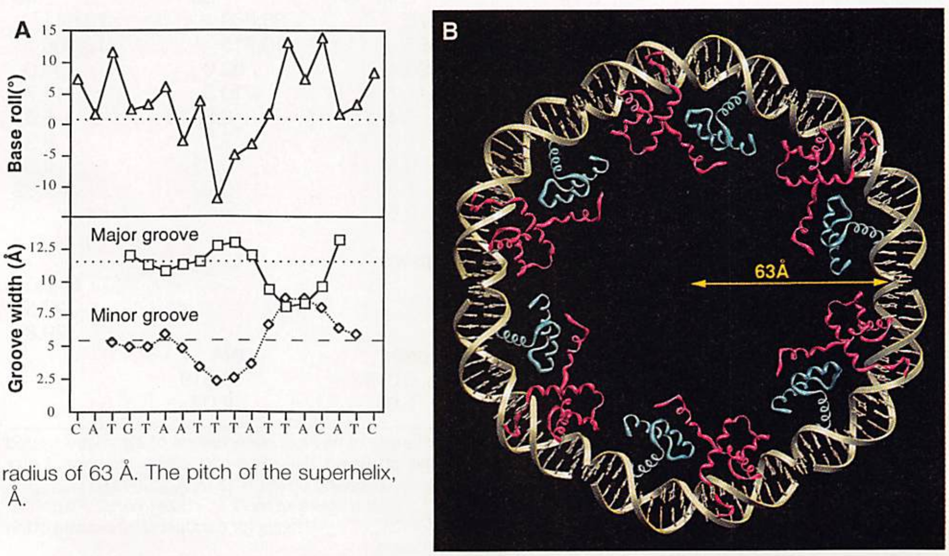

Fig. 3. (**A**) Plot of DNA parameters. A plot is shown of base roll, major groove width, and minor groove width as a function of DNA sequence; horizontal dotted or dashed lines indicate average values for B-DNA. The sequence of the top strand only is shown. Groove widths are measured as the minimum in phosphate-phosphate distance less 5.8 Å for the van der Waals radii of the phosphate groups. All parameters were calculated with the program, CURVES (*61*). (**B**) Packing of complexes in the **a**1/α2–DNA crystals; view looking down the crystallographic 6_1 axis. Adjacent complexes stack end-to-end in the crystal, with the dinucleotide 5′-ApT overhang in one complex forming base-pairing interactions with the complementary 5′-overhanging bases in the DNA of the adjacent complex. With each complex containing a 21-bp DNA fragment that has an overall bend of 60°, the stacked complexes form a superhelical spiral with a radius of 63 Å. The pitch of the superhelix, corresponding to the crystallographic *c* axis, is 45.71 Å.

contacts between **a**1 and α2 and their respective DNA subsites (both described below), probably play a role in stabilizing the bend. In addition, we observed a spine of hydration in the minor groove of the DNA, where it narrows and base roll angles are negative, and in the major groove of the DNA, where bending results in a minimum in major groove width and a maximum positive value of base pair roll angles (Fig. 3A). This hydration may contribute to the stability of the bent DNA conformation, in addition to participating in water-mediated hydrogen bonds between the proteins and the DNA bases.

The DNA bending gives rise to an unusual packing of complexes in the crystal. As has been observed in other crystals of protein-DNA complexes (*4, 6, 22–26*), the DNA stacks end-to-end in the crystal, forming a pseudocontinuous helix with Watson-Crick base pairing between the overhanging 5′-ApT at the end of one complex and the complementary unpaired bases at the end of the adjacent complex. In the **a**1/α2–DNA crystals, each successive complex bends in the same direction, resulting in a superhelical spiral of complexes that obeys the 6_1 screw symmetry of the space group (Fig. 3B). As measured from the projection shown in Fig. 3B, the radius of curvature of the DNA in the ternary complex is 63 Å. There are crystal contacts between the α2 homeodomain in one complex and the **a**1 protein in the neighboring complex that may limit the degree of bending that can occur at the ends of the DNA. The observed 60° bend may therefore represent an underestimate of the bend induced by **a**1/α2 in a single binding site embedded in a longer fragment of DNA.

Heterodimer interface. The COOH-terminal tail of α2 is unfolded in the monomer, even when bound to DNA. On interaction with the **a**1 protein, the tail of α2 folds to form a complementary surface to its binding site on the **a**1 homeodomain. The heterodimer is stabilized primarily by hydrophobic interactions, in addition to the presence of several hydrogen bonds (Fig. 4, A and B). A hydrophobic patch on the **a**1 homeodomain is formed by Val^{19} of helix 1, Val^{34} of helix 2, and Leu^{26} in the strand that connects helices 1 and 2. These three side chains are partly exposed and lie at the floor of a depression in the surface of the **a**1 homeodomain (Fig. 4, A and C). This depression is flanked at one end by a salt bridge between Lys^{23} and Glu^{30}, and at the other by Phe^{15}.

In the tail of α2, residues 63 to 69 adopt a helical conformation with three leucine side chains (Leu^{65}, Leu^{68}, and Leu^{69}) projecting from one face of the helix (Fig. 4A). In addition, Ile^{61} packs against Leu^{65} and Leu^{69} and helps to stabilize the short helix. The amphipathic helix binds to the **a**1 homeodomain, inserting the three leucine residues into the hydrophobic patch between helices 1 and 2 of **a**1 (Fig. 4, A and C). The **a**1/α2 heterodimer is further stabilized by hydrogen bonds with the **a**1 homeodomain that are mediated by main chain atoms in the COOH-terminal tail of α2 flanking the amphipathic helix (Fig. 4B). The two antiparallel helices of **a**1 and the helix contributed by the tail of α2 form a three-helix bundle, with the helix in α2 parallel to helix 2 of **a**1. The total buried surface area is 754 Å^2.

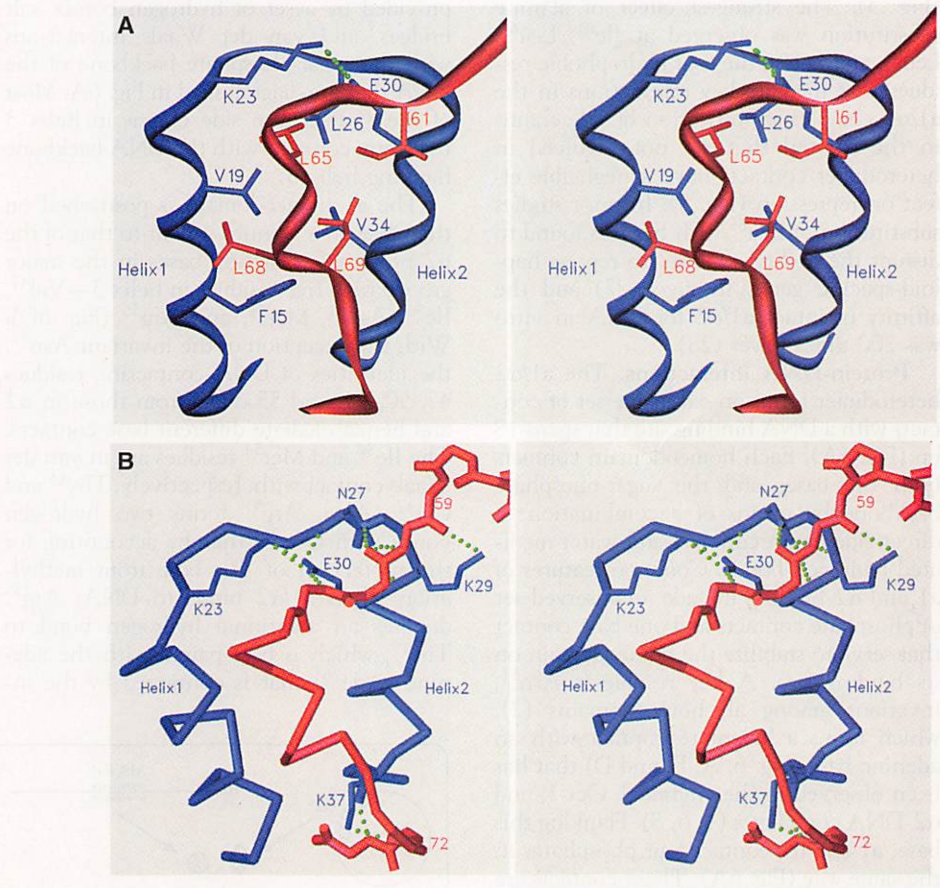

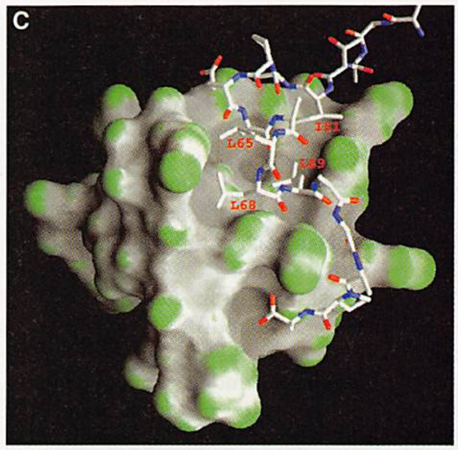

Fig. 4. (**A**) Stereo view of the **a**1/α2 heterodimer interface. The **a**1 protein is shown in blue and the α2 protein is shown in red; helix 3 of the **a**1 homeodomain has been deleted for clarity. In the **a**1 homeodomain, residues Phe^{15}, Val^{19}, Leu^{26}, and Val^{34} form a hydrophobic patch between helices 1 and 2. Residues 63 to 69 in the tail of α2 form a distorted amphipathic helix with residues Leu^{65}, Leu^{68}, and Leu^{69} exposed on one face. Ile^{61}, located NH_2-terminal to the amphipathic helix, packs against Leu^{65} and Leu^{69}. The hydrophobic face of the α2 tail forms favorable van der Waals contact with the hydrophobic patch between helices 1 and 2 of the **a**1 homeodomain, as well as with the salt bridge formed by Lys^{23} and Glu^{30}. (Additional contacts, not shown, are formed with the aliphatic side chain of Arg^{22}.) (**B**) Stereo view of the hydrogen-bonding interactions between **a**1 and α2. The main chain NH of Ala^{62} in α2 donates a hydrogen bond to the Oε of Glu^{30} in **a**1, and the second Oε accepts a hydrogen bond from the peptide NH of Asn^{27} of **a**1. The side chain of Asn^{27} in **a**1 forms a bridging contact, donating a hydrogen bond to the peptide N of Thr^{60} in α2 and capping helix 2 of **a**1 by accepting a hydrogen bond from the peptide N of Lys^{29}. The side chain of Lys^{29} donates a hydrogen bond to the carbonyl of Ile^{59}. COOH-terminal to the amphipathic helix in the α2 tail, the carbonyl of Glu^{72} hydrogen bonds with the Nζ of Lys^{37} in **a**1, while the amide N of Glu^{72} forms a hydrogen bond with the carbonyl O of Lys^{37}. (**C**) Depiction of the molecular surface of the **a**1 homeodomain, with a stick model of the COOH-terminal tail of α2. The **a**1 surface is color-coded such that the most convex part of the surface is green, the most concave part is gray, and planar surfaces are white [the figure was made with the program GRASP (*62*)].

The results of mutagenesis studies of the $\alpha 2$ protein verify the importance of the heterodimer contacts we observed. Point mutations that change a wild-type residue to alanine were introduced at various positions in the $\alpha 2$ tail and assayed for their effect on the ability of the intact $\alpha 2$ and **a**1 proteins to repress transcription in yeast (Fig. 5). The strongest effect of alanine substitution was observed at Ile^{61}, Leu^{65}, Leu^{68}, and Leu^{69}, the four hydrophobic residues that mediate key interactions in the **a**1/$\alpha 2$ complex. Substitution of side chains in the $\alpha 2$ tail that are not involved in heterodimer contacts have a negligible effect on repression (Fig. 5). In prior studies substitution of Leu^{65} with Ser was found to disrupt the ability of **a**1/$\alpha 2$ to repress haploid-specific genes in vivo (*27*) and the affinity of intact **a**1/$\alpha 2$ for DNA in vitro was 200 times lower (*28*).

Protein-DNA interactions. The **a**1/$\alpha 2$ heterodimer forms an extensive set of contacts with a DNA binding site that spans 18 bp (Fig. 6A). Each homeodomain contacts both the bases and the sugar-phosphate backbone by means of a combination of direct side chain contacts and water-mediated hydrogen bonds. Common features of **a**1 and $\alpha 2$ binding include a conserved set of phosphate contacts and one base contact that serve to stabilize the homeodomain on its binding site. A key residue is Asn^{51}, invariant among all homeodomains (*2*), which forms a bidentate contact with an adenine base (Fig. 6, A, B, and D) that has been observed in the engrailed, Oct-1, and $\alpha 2$-DNA complexes (*4*, *6*, *8*). Flanking this base, **a**1 and $\alpha 2$ contact four phosphates in the same way (Fig. 6A). These contacts are mediated by four residues that are identical in both proteins—Leu^{26}, Gln^{44}, Trp^{48}, and Arg^{53}—and by the main chain NH of residue 8. DNA sequence recognition presumably arises from contacts with the DNA bases that are mediated by side chains that differ between the two homeodomains.

The $\alpha 2$ protein contacts a total of 7 bp in either the major or minor groove. Four base pairs in the major groove are contacted by three side chains in helix 3: Asn^{51}, Arg^{54}, and Ser^{50} (Fig. 6B). Of these, Ser^{50}, which contributes to DNA binding specificity differences among homeodomains (*29–31*), forms water-mediated hydrogen bonds with 2 bp, and Arg^{54} donates hydrogen bonds to a base (Gua^{6}) and to a side chain, Asn^{51}, which contacts Ade^{38}. The Arg^{54} contact accounts for the observation that Gua^{6} is the sole guanine in the $\alpha 2$ site that is protected from methylation by **a**1/$\alpha 2$ binding. In the minor groove, 5 bp are contacted by three residues in the NH_2-terminal arm of $\alpha 2$—Arg^{4}, Gly^{5}, and Arg^{7} (Fig. 6C). Two of the base pairs contacted in the minor groove are also contacted by side chains in the major groove, thereby accounting for the high DNA sequence conservation at these positions (Fig. 2C). In addition to contacting 2 bp, Arg^{7} hydrogen bonds to a water molecule that is part of the spine of hydration observed where the minor groove narrows. Further stabilization of the $\alpha 2$ homeodomain on its binding site is provided by a set of hydrogen bonds, salt bridges, and van der Waals interactions with the sugar-phosphate backbone of the DNA that are diagrammed in Fig. 6A. Most of these arise from side chains in helix 3 that form contacts with the DNA backbone flanking helix 3.

The **a**1 homeodomain is positioned on the DNA in a manner similar to that of the $\alpha 2$ protein, contacting bases in the major groove with five residues in helix 3—Val^{47}, Ile^{50}, Asn^{51}, Met^{54}, and Arg^{55} (Fig. 6D). With the exception of the invariant Asn^{51}, the identities of DNA-contacting residues 47, 50, 54, and 55 differ from those in $\alpha 2$ and hence mediate different base contacts. The Ile^{50} and Met^{54} residues are in van der Waals contact with, respectively, Thy^{15} and Cyt^{17}. Also, Arg^{55} forms two hydrogen bonds with Gua^{26}, thereby accounting for the protection of this base from methylation when **a**1/$\alpha 2$ binds to DNA; Arg^{55} donates an additional hydrogen bond to Thy^{19}, which is base-paired with the adenine (Ade^{26}) that is contacted by the invariant Asn^{51}. The Val^{47} residue forms additional van der Waals contacts with Ade^{26}. Furthermore, 10 residues participate in contacts with the DNA backbone (Fig. 6A). The observed major groove contacts are consistent with the sequence conservation in the **a**1 subsite (Fig. 2C): All four invariant DNA positions are contacted in the major groove and two of the base pairs (Thy^{19}·Ade^{26} and Cyt^{20}·Gua^{25}) are contacted by more than one side chain.

In addition to direct side chain–DNA contacts, we see a network of five water molecules immobilized in the major groove at the interface between helix 3 and the DNA (Fig. 6D). These water molecules participate in hydrogen bond interactions with a total of 4 bp, and are stabilized by a hydrogen bond formed by one of the water molecules with the guanidinium of Arg^{46}, which also forms a salt bridge with a phosphate. Formation of this network of water-mediated contacts requires the observed local DNA curvature. An extensively hydrated interface between helix 3 and the DNA has also been observed by solution NMR in the Antennapedia-DNA complex (*32*).

Unlike that of the $\alpha 2$ homeodomain, the NH_2-terminal arm of **a**1 is disordered in the crystal. This result was unanticipated, as our present structure of the $\alpha 2$ homeodomain and earlier structural studies of homeodomains (*4–6*, *8*) show that the NH_2-

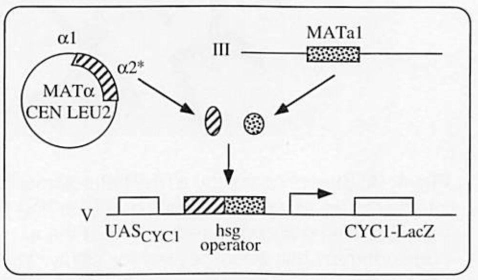

	β-gal units	Pheromone Production a-factor	Pheromone Production α-factor	Mating Behavior as a	Mating Behavior as α
vector only	45.0	+++	--	+	--
MAT α2	5.4	+	--	+	--
T58A	6.5	+	--	+	--
I59A	7.0	+	--	+	--
T60A	6.3	+	--	+	--
I61A	22.7	+	+++	+	+
P63A	7.4	+	--	+	--
E64A	7.8	+	--	+	--
L65A	44.1	+	+++	+	+
D67A	6.1	+	--	+	--
L68A	19.5	+	+++	+	+
L69A	32.4	+	+++	+	+
E72A	5.9	+	--	+	--

Fig. 5. Effects of point mutations in the COOH-terminal tail of $\alpha 2$ on **a**1/$\alpha 2$–mediated repression in vivo. Alanine was substituted for the wild-type residue at various positions in the COOH-terminal tail of $\alpha 2$. Low copy (CEN) plasmids containing the MATα locus with specific site-directed mutations in the MAT$\alpha 2$ gene ($\alpha 2^*$ in the figure) were transformed into a MAT**a** strain and repression by **a**1/$\alpha 2$ was monitored: (i) by expression of a test promoter whose expression is controlled by a single hsg operator, (ii) by the ability of transformants to produce mating pheromones, and (iii) by the ability of the transformants to mate. The mutations in the COOH-terminal tail of $\alpha 2$ are shown in the first column on the left. The second column shows the expression of a CYC-LacZ reporter construct that contains an hsg operator. In a cell carrying a wild-type MAT$\alpha 2$ gene on a plasmid, the β-galactosidase reporter gene is expressed at approximately one-ninth the level of a cell containing the plasmid vector only [this level of repression is not complete, probably because of plasmid loss—see (*28*)]. Four of the $\alpha 2$ tail mutants fail to repress efficiently the test promoter, with Leu^{65}→Ala having the strongest effect. The third and fourth columns show the production of mating pheromones by the transformants. For all of the mutants, production of **a** factor is repressed as compared to the vector control, indicating that the $\alpha 2$ mutant proteins are synthesized in the cell and can still function with MCM1 to repress the **a**-specific genes (*18*). The fourth column indicates that the four mutants that show significant derepression of the test promoter fail to repress STE12, a haploid-specific gene required for α-factor production. The fifth and sixth columns show the mating behavior of the transformants. The phenotype of the four mutants that enable the yeast to mate as α cells are consistent with a defect in **a**1/$\alpha 2$–mediated repression.

terminal arm of the homeodomain binds in the minor groove of the DNA. Chemical modification experiments that probe the protection of the DNA backbone from hydroxyl radical attack in the presence of the **a**1/α2 heterodimer are consistent with the binding of the NH$_2$-terminal arm of **a**1 in the minor groove (*16*). It is possible that the NH$_2$-terminal arm of **a**1 has been displaced from the minor groove in the **a**1/α2–DNA crystal, where the NH$_2$-terminal arm of **a**1 would be expected to bind near the junction between two double-stranded synthetic oligonucleotides. The 5′ phosphate group that would be present at that junction in a continuous DNA strand could be of importance in stabilizing binding of the NH$_2$-terminal arm of **a**1 to DNA. If there are indeed further DNA contacts formed with bases in the minor groove, some may contribute further to the observed DNA sequence preference of the **a**1 protein.

Because of the extensive set of contacts formed by the **a**1 homeodomain with DNA, it is surprising that **a**1 does not bind DNA detectably on its own. There are several possible explanations for this phenomenon. One is that DNA bending is required for the protein-DNA contacts we observe. The energy to induce and stabilize this bend might be too great for **a**1 alone, but may be facilitated by the presence of α2 on the DNA and the interaction between the α2 tail and the **a**1 homeodomain. Another explanation may be that the binding of the tail of α2 to **a**1 induces a small conformational change in the **a**1 homeodomain that increases its overall DNA binding energy. Solution NMR studies of the **a**1 homeodomain have shown that, on heterodimerization with α2, the resonances in **a**1 that are most perturbed on complex formation cor-

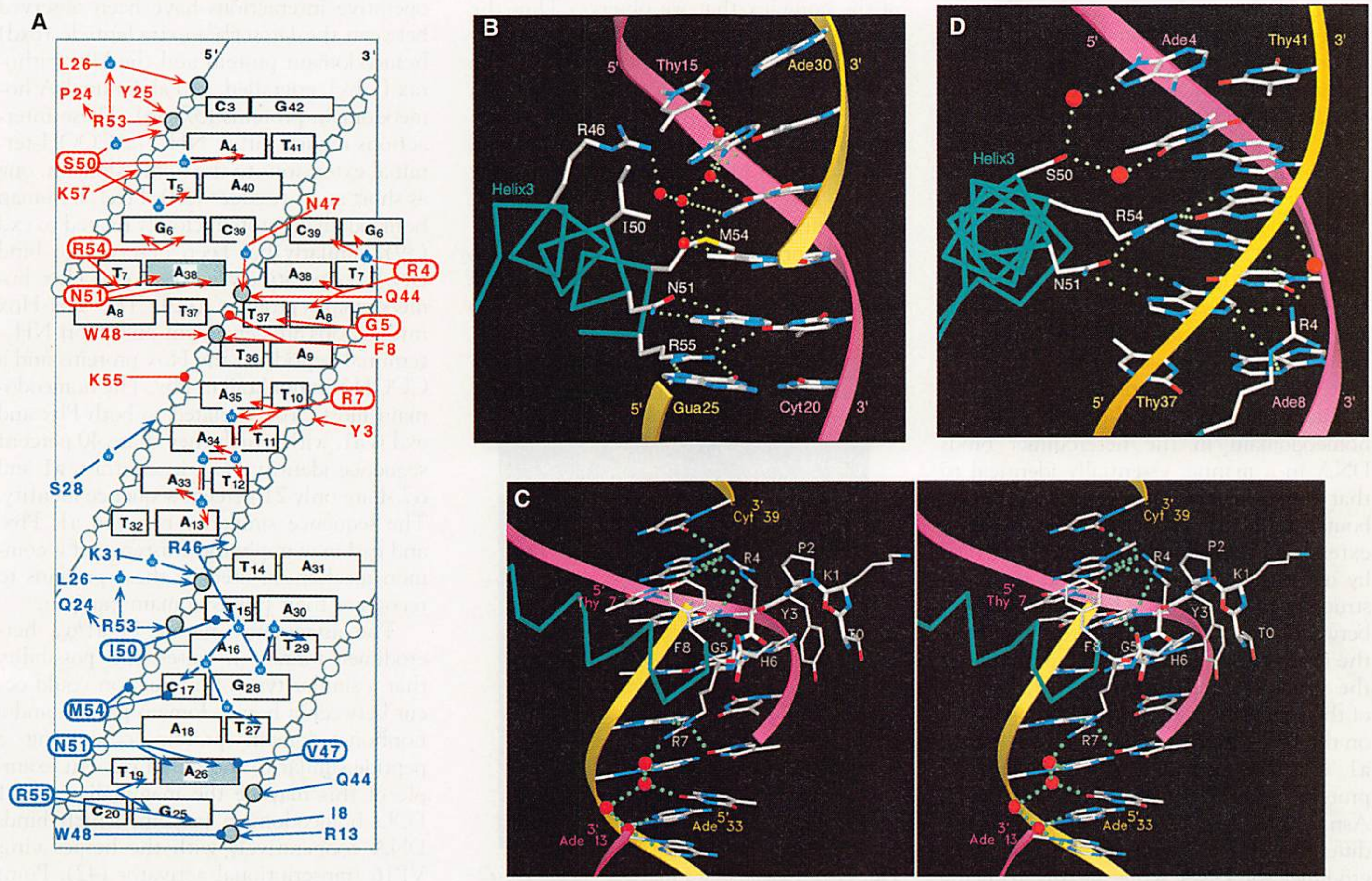

Fig. 6. Protein-DNA interactions. (**A**) Schematic diagram summarizing contacts formed by both **a**1 and α2 with the DNA. The α2-mediated contacts are shown in red; **a**1-mediated contacts are shown in blue. Residues encircled with ovals form base contacts. Hydrogen bonds and salt bridges are indicated by arrows; van der Waals interactions are indicated by lines that end in circles. Bond criteria are as follows: for hydrogen bonds, less than or equal to 3.3 Å separation of a donor-acceptor pair; van der Waals interactions, less than 4.0 Å distance between contacting groups. Residues involved in base contacts are encircled with ovals. The shaded phosphate groups and adenine bases are contacted in a conserved manner by both **a**1 and α2. The complex equilibrium constant for dissociation of the ternary complex into free **a**1, α2, and DNA is 10^{-15} M^2 for the **a**1 and α2 fragments used in this study and 10^{-16} M^2 for the intact proteins (*11, 20*). (**B**) Contacts formed between helix 3 of α2 and bases in the major groove. Asn^{51} contacts Ade^{38}, with the Oδ of the side chain accepting a hydrogen bond from the N6 of the base and whose Nδ is in contact with the N7 (dist. = 3.4 Å). Arg^{54} hydrogen bonds to the N7 and O6 of Gua^6 with its NH1, while its NH2 group forms a bridging hydrogen bond to the Oδ of Asn^{51}. Ser^{50} forms water-mediated hydrogen bonds with the N7 of Ade^4 and the O4 of Thy^5. (**C**) Stereo view of contacts between the NH$_2$-terminal arm of α2 and bases in the minor groove of the DNA. A total of five bases are contacted by three side chains in the NH$_2$-terminal arm of α2. Arg^4 contacts 2 bp directly and a third via water-mediated hydrogen bonds. The Nε of Arg^4 is within hydrogen bonding distance of the N3 of Ade^8 and the N3 of Ade^{38}, whereas the NH$_2$ contacts the Gua^6·Cyt^{39} base pair via water-mediated hydrogen bonds. The peptide NH of Gly^5 donates a hydrogen bond to the O2 of Thy^{37}, while the guanidinium group of Arg^7 donates hydrogen bonds to the N3 of Ade^{35} and the O2 of Thy^{11}. In addition, the NH$_2$ of Arg^7 helps to stabilize the spine of hydration in the minor groove. (**D**) Contacts between the **a**1 homeodomain and bases in the major groove. Ile^{50} is in van der Waals contact with the methyl of Thy^{15}, while Asn^{51} forms two hydrogen bonds with Ade^{26}, whose Oδ accepts a hydrogen bond from the N6 of the base and whose Nδ donates a hydrogen bond to the N7. The Cγ of Met^{54} is in van der Waals contact with the C6 of the Cyt^{17} pyrimidine, while the Cε is in van der Waals contact with the adjoining subdeoxyribose. The Arg^{55} side chain forms contacts with two base pairs, its NH1 donating a hydrogen bond to the N7 of Gua^{25} and its NH2 donating hydrogen bonds to the O6 of Gua^{25} and the O4 of Thy^{19}. In addition, there is a network of five bound water molecules in the major groove that hydrogen bond to the guanidinium of Arg^{46}, as well as 3 bp. Not shown in this depiction is Val^{47}, whose Cγ is in van der Waals contact with the C8 of Ade^{26}.

respond to residues that lie in portions of helices 1 and 2 and in the loop connecting them (*33*). A likely set of contacts that could be affected by a conformational change in the loop are those mediated by the invariant homeodomain residue Arg^{53}, which participates in an extensive set of contacts with the sugar-phosphate backbone, a bound water molecule, and the backbone of **a**1 in the loop between helices 1 and 2 (Fig. 6A) (*34*). Very small changes in the loop conformation could easily disrupt this network of contacts, thereby diminishing the affinity of **a**1 for DNA in the absence of α2. Since Arg^{53} is invariant among all homeodomains and mediates a conserved set of contacts in **a**1, α2, and other homeodomains, it is likely to be crucial for formation of favorable interactions between **a**1 and its DNA binding site.

In previous studies, the homeodomain was found to be positioned on the DNA in a highly conserved manner by DNA contacts that are mediated by conserved residues (*4–6, 8*). A pertinent question is whether the orientation of the homeodomain on the DNA and the contacts it forms are perturbed as a result of heterodimerization. We find that, despite the additional protein-protein interactions and the concomitant distortion in the DNA, the α2 homeodomain in the heterodimer binds DNA in a manner essentially identical to that found in the structure of α2 alone bound to DNA (Fig. 7). This similarity extends to the side chain contacts formed by α2 with its binding site and the local structure of the DNA. The few differences between the two structures are most likely the result of differences in the resolution of the structure determinations (*35*). Because of the similarity in the way α2 is positioned on the DNA in the presence and absence of **a**1, it is very surprising that a mutant α2 protein with Ala substituted for Ser^{50}, Asn^{51}, and Arg^{53} exhibits no significant difference in the affinity of the **a**1/α2 heterodimer for DNA while greatly reducing the affinity of α2 alone for DNA (*28*). It is possible, however, that this triple mutation reduces the DNA sequence discrimination of the **a**1/α2 heterodimer without impairing its affinity for the DNA.

The structure of the **a**1/α2–DNA complex shows how the binding specificity of a homeodomain can be raised by complex formation with a second protein. The heterodimerization of the α2 and **a**1 homeodomains, each with only modest affinity and specificity for DNA, results in a heterodimer that binds DNA in a highly specific manner, preferring its own binding site over random DNA by a ratio of at least 10^5 (*11*). The specificity of this interaction derives from at least three sources: the specificity of the interactions between the COOH-terminal tail of α2 and the **a**1 homeodomain, summation of the DNA sequence preferences of the individual proteins, and the precise binding site spacing imposed by the nature of the heterodimer interface. It is clear from the **a**1/α2–DNA structure that insertion or deletion of base pairs between the **a**1 and α2 binding sites would disrupt heterodimer contacts, and this observation is supported by studies of **a**1/α2 binding to altered DNA sites (*16, 35a*). A final contributing factor to ternary complex stability may be the relative deformability of a given sequence of DNA in that DNA bending is required for formation of the complex that we observe. Thus the sequence at even noncontacted bases may contribute to overall complex stability. The net result of all these considerations is a larger set of criteria that must be met for a stable **a**1/α2–DNA complex to form, and hence a much higher specificity of binding than is observed for the monomeric α2 or **a**1 proteins.

Multi-protein complex formation in transcription. The work presented above shows how the interaction between two homeodomain proteins can be mediated by a flexible tail that becomes ordered on complex formation. There are now numerous examples of cooperative interactions involving homeodomain proteins, some of which might be mediated by the same types of interactions observed in the **a**1/α2 heterodimer. The *Caenorhabditis elegans* homeodomain protein MEC-3 heterodimerizes with the UNC-86 POU domain protein, which also contains a homeodomain (*36*). This interaction is reminiscent of **a**1/α2 heterodimer formation in that it is dependent upon the 16 amino acids COOH-terminal to the MEC-3 homeodomain. Cooperative interactions have been observed between the *Drosophila* extradenticle (exd) homeodomain protein and the Ultrabithorax (Ubx), engrailed, and abdominal-A homeodomain proteins (*37–38*). These interactions require either NH_2- or COOH-terminal extensions to the homeodomain, one as short as 15 residues (*37*). Pbx1, a human homeodomain protein closely related to exd (*39*), similarly has been observed to bind DNA cooperatively with several Hox homeodomain proteins (*40*). The Pbx-Hox interactions are dependent on a short NH_2-terminal peptide in the Hox proteins and a COOH-terminal tail in Pbx. The homeodomain most closely related to both Pbx and exd is **a**1, with which they share 40 percent sequence identity (*41*); in contrast, **a**1 and α2 share only 21 percent sequence identity. The sequence similarity between **a**1, Pbx, and exd may imply the existence of a common mechanism used by these proteins to recognize their homeodomain partners.

The asymmetric nature of **a**1/α2 heterodimer formation raises the possibility that a similar type of interaction could occur between a homeodomain protein and a nonhomeodomain protein containing a peptide similar to the tail of α2. An example of this may be the mammalian Oct-1 POU homeodomain protein, which binds DNA cooperatively with the herpes virus VP16 transcriptional activator (*42*). Point mutations in Oct-1 that disrupt the Oct-1–VP16 complex are located in helices 1 and 2 of the Oct-1 homeodomain. As shown above and noted in the NMR study of **a**1/α2 (*33*), the location of the Oct-1 mutations is analogous to the region on the **a**1 homeodomain that is contacted by the tail of α2 (*43, 44*). If Oct-1 is acting as the analog of **a**1, what part of VP16 may play a role similar to the COOH-terminal tail of α2? The results of deletion and mutagenesis studies have identified a 12-residue region of VP16 responsible for interaction with the Oct-1 homeodomain (*45, 46*). This region (residues 376 to 387), which has been proposed to form an amphipathic helix, contains sequence similarity to the helix in the α2 tail that contacts **a**1 (Fig. 2B). Model-

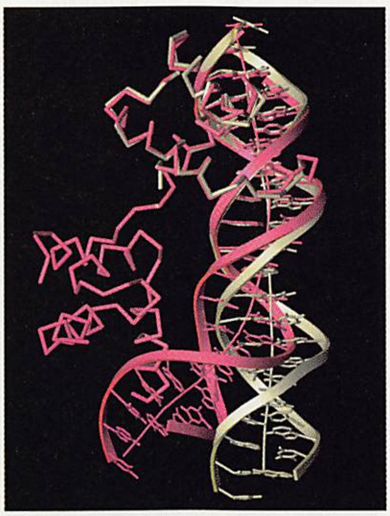

Fig. 7. Interaction of α2 with DNA in the **a**1/α2–DNA ternary complex as compared with the structure of α2 alone bound to DNA. The two structures were aligned by performing a least-squares superposition of the α2 homeodomain in the **a**1/α2–DNA complex with one of the α2 homeodomains in the structure of α2 alone bound to DNA (6). Since the latter structure contains two α2 homeodomain monomers bound to a 21-bp DNA fragment, the homeodomain chosen for the alignment is the one bound to the identical 9-bp sequence to which α2 is bound in the ternary complex. The second α2 homeodomain contained in the α2-DNA structure, which does not contact the other α2 monomer, has been omitted for clarity. The conformation of the α2 homeodomains, the local structure of the DNA, and the protein-DNA contacts are nearly identical in the two complexes. There are pronounced differences outside the α2 binding sites due to the overall 60° bend in the DNA induced by the **a**1/α2 heterodimer.

building studies show that this peptide from VP16, when folded in the conformation of the α2 tail, could pack between helices 1 and 2 of Oct-1 in a manner similar to that observed in the a1/α2 heterodimer.

It is likely that there are transcription factors from other structural classes that are also bound in protein-protein complexes by a flexible peptide that adopts a distinctive conformation only upon complex formation. There are strong parallels between the manner in which α2 interacts with a1 and the way in which it forms a complex with the MADS box protein (*47*), MCM1 (*48*, *49*). A short region NH_2-terminal to the α2 homeodomain that is unstructured in the free protein is required for cooperative binding with MCM1 (*50*). This NH_2-terminal peptide specifies complex formation with MCM1, as splicing it to the engrailed homeodomain confers on engrailed the ability to bind DNA cooperatively with MCM1 (*50*). Thus α2 has evolved as a DNA binding protein capable of interaction with two structurally distinct partners by acquiring peptide extensions both NH_2- and COOH-terminal to its DNA binding domain that specify complex formation with different partners. The presence of flexible protein-recognition peptides that extend from stably folded DNA binding domains may prove to be a general feature of the architecture of other classes of eukaryotic transcriptional regulators.

REFERENCES AND NOTES

1. W. J. Gehring *et al.*, *Cell* **78**, 211 (1994).
2. A. Laughon, *Biochemistry* **30**, 11357 (1991).
3. Y. Q. Qian *et al.*, *Cell* **59**, 573 (1989).
4. C. R. Kissinger, B. Liu, E. Martin-Blanco, T. B. Kornberg, C. O. Pabo, *ibid.* **63**, 579 (1990).
5. G. Otting *et al.*, *EMBO J.* **9**, 3085 (1990).
6. C. Wolberger, A. K. Vershon, B. Liu, A. D. Johnson, C. O. Pabo, *Cell* **67**, 517 (1991).
7. C. L. Phillips, A. K. Vershon, A. D. Johnson, F. W. Dahlquist, *Genes Dev.* **5**, 764 (1991).
8. J. D. Klemm, M. A. Rould, R. Aurora, W. Herr, C. O. Pabo, *Cell* **77**, 21 (1994).
9. M. Affolter, A. Percival-Smith, M. Müller, W. Leupin, W. J. Gehring, *Proc. Natl. Acad. Sci. U.S.A.* **87**, 4093 (1990).
10. T. Hoey and M. Levine, *Nature* **332**, 858 (1988).
11. C. Goutte and A. D. Johnson, *J. Mol. Biol.* **233**, 359 (1993).
12. A. D. Johnson, in *Transcriptional Regulation*, S. L. McKnight, K. R. Yamamoto, Eds. (Cold Spring Harbor Press, Cold Spring Harbor, NY, 1992), vol. 2, pp. 975.
13. J. C. W. Shepherd, W. McGinnis, A. E. Carrasco, E. M. De Robertis, W. J. Gehring, *Nature* **310**, 70 (1984).
14. C. Goutte and A. D. Johnson, *Cell* **52**, 875 (1988).
15. A. M. Dranginis, *Nature* **347**, 682 (1990).
16. C. Goutte and A. D. Johnson, *EMBO J.* **13**, 1434 (1994).
17. M. R. Stark and A. D. Johnson, *Nature* **371**, 429 (1994).
18. A. Mak and A. D. Johnson, *Genes Dev.* **7**, 1862 (1993).
19. C.-Y. Ho, J. G. Adamson, R. S. Hodges, M. Smith, *EMBO J.* **13**, 1403 (1994).
20. C. Phillips, M. R. Stark, A. D. Johnson, F. W. Dahlquist, *Biochemistry* **33**, 9294 (1994).
21. D. L. Smith, A. B. Desai, A. D. Johnson, *Nucleic Acids Res.* **23**, 1239 (1995).
22. A. K. Aggarwal, D. W. Rodgers, M. Drottar, M. Ptashne, S. C. Harrison, *Science* **242**, 899 (1988).
23. J. A. Anderson, M. Ptashne, S. C. Harrison, *Nature* **326**, 846 (1987).
24. S. C. Schultz, G. C. Shields, T. A. Steitz, *Science* **253**, 1001 (1991).
25. C. Wolberger, Y. Dong, M. Ptashne, S. C. Harrison, *Nature* **335**, 789 (1988).
26. J.-A. Feng, R. C. Johnson, R. E. Dickerson, *Science* **263**, 348 (1994).
27. J. Strathern, B. Shafer, J. Hicks, C. McGill, *Genetics* **120**, 75 (1988).
28. A. K. Vershon, Y. Jin, A. D. Johnson, *Genes Dev.* **9**, 182 (1995).
29. S. D. Hanes and R. Brent, *Science* **251**, 426 (1991).
30. A. Percival-Smith, M. Mueller, M. Affolter, W. J. Gehring, *EMBO J.* **9**, 3967 (1990).
31. J. Treisman, P. Gonczy, M. Vashinshtha, E. Harris, C. Desplan, *Cell* **59**, 553 (1989).
32. M. Billeter *et al.*, *J. Mol. Biol.* **234**, 1084 (1993).
33. S. M. Baxter, D. M. Gontrum, C. L. Phillips, A. F. Roth, F. W. Dahlquist, *Biochemistry* **33**, 15309 (1994).
34. Arg^{53} donates two hydrogen bonds to phosphate P4 via its Nε and NH2 groups. The NH1 group donates one hydrogen bond to the main chain carbonyl of residue 24 and a second hydrogen bond to a bound water molecule. The water, which is found in an identical position in both the a1 and α2 subsites, in turn accepts a hydrogen bond from the peptide NH of Leu^{26} and donates a hydrogen bond to phosphate P3.
35. As compared with the structure of α2 alone bound to DNA, the α2 homeodomain in the heterodimer contains five additional ordered residues in the NH_2-terminal arm, some of which mediate minor groove contacts. In addition, no water molecules were placed in the α2-DNA structure, which was determined at a resolution of 2.7 Å.

35a. Y. Jin, J. Mead, T. Li, C. Wolberger, A. K. Vershon, *Science* **270**, 290 (1995).

36. D. Xue, Y. Tu, M. Chalfie, *ibid.* **261**, 1324 (1993).
37. F. B. Johnson, E. Parker, M. A. Krasnow, *Proc. Natl. Acad. Sci. U.S.A.* **92**, 739 (1995).
38. S.-K. Chan, L. Jaffe, M. Capovilla, J. Botas, R. S. Mann, *Cell* **78**, 603 (1994); M. A. van Dijk and C. Murre, *ibid.*, p. 617.
39. J. Nourse *et al.*, *ibid.* **60**, 535 (1990); M. P. Kamps, C. Murre, X. Sun, D. Baltimore, *ibid.*, p. 547; C. Rauskolb, M. Peifer, E. Wieschaus, *ibid.* **74**, 1101 (1993).
40. C.-P. Chang *et al.*, *Genes Dev.* **9**, 663 (1995).
41. W. A. Flegel *et al.*, *Mechan. Dev.* **41**, 155 (1993).
42. S. Stern, M. Tanaka, W. Herr, *Nature* **341**, 624 (1989).
43. J. L. Pomerantz, T. M. Kristie, P. A. Sharp, *Genes Dev.* **6**, 2047 (1992).
44. J. S. Lai, M. A. Cleary, W. Herr, *ibid.*, p. 2058.
45. R. F. Greaves and P. O'Hare, *J. Virol.* **64**, 2716 (1990).
46. S. Stern and W. Herr, *Genes Dev.* **5**, 2555 (1991).
47. H. Ma, M. F. Yanofsky, E. M. Meyerowitz, *ibid.*, p. 484.
48. C. A. Keleher, C. Goutte, A. D. Johnson, *Cell* **53**, 927 (1988).
49. R. T. Sauer, D. L. Smith, A. D. Johnson, *Genes Dev.* **2**, 807 (1988).
50. A. K. Vershon and A. D. Johnson, *Cell* **72**, 105 (1993).
51. T. Li, M. Stark, A. D. Johnson, C. Wolberger, *Proteins* **21**, 161 (1995).
52. Crystals were flash-frozen and maintained at −179°C, x-ray diffraction data were collected with an *R*-AXIS II image plate detector mounted on a Rigaku RU-200 rotating anode x-ray generator, with CuKα radiation filtered by a graphite monochromator. The reflection data were processed, merged, and scaled with the *R*-AXIS software (Molecular Structure). Subsequent phase refinement and map calculations were performed with the PHASES suite of programs [W. Furey and S. Swaminathan, *American Crystallographic Association Meeting Abstracts* PA33 (1990)]. Iodine positions were located by Patterson and difference Fourier methods, and heavy atom parameters were calculated and refined to produce a set of MIR phases.
53. B. C. Wang, *Methods Enzymol.* **115**, 90 (1985).
54. T. A. Jones, J. Y. Zou, S. W. Cowan, M. Kjeldgaard, *Acta. Crystallogr.* **A47**, 110 (1991).
55. A. T. Brünger, *Nature* **355**, 472 (1992).
56. ———, *X-PLOR, Version 3.1: A System for X-ray Crystallography and NMR* (Yale Univ Press, New Haven, 1992).
57. R. J. Read, *Acta. Crystallogr.* **A46**, 900 (1990).
58. A. Hodel, S.-H. Kim, A. T. Brünger, *ibid.* **A48**, 851 (1992).
59. S. V. Evans, *J. Mol. Graph.* **11**, 134 (1993).
60. Abbreviations for the amino acid residues are: A, Ala; C, Cys; D, Asp; E, Glu; F, Phe; G, Gly; H, His; I, Ile; K, Lys; L, Leu; M, Met; N, Asn; P, Pro; Q, Gln; R, Arg; S, Ser; T, Thr; V, Val; W, Trp; and Y, Tyr.
61. R. Lavery and H. Sklenar, *J. Biomol. Struct. Dyn.* **6**, 63 (1988).
62. A. Nicholls, K. Sharp, B. Honig, *Proteins*, **11**, 281 (1991).

63. We thank M. Glover, J. Kim, M. Rould, M. Bianchet, A. Gittis, J. Klemm, and W. Weis for advice and suggestions and M. Amzel, D. Leahy, and J. Berg for comments on the manuscript. Time on a Cray supercomputer was provided by the National Cancer Institute–Frederick Biomedical Supercomputing Center. Supported by NSF grant MCB-9304526 (C.W.), the David and Lucile Packard Foundation (C.W.), and the Lucille P. Markey Charitable Trust (C.W.) and by a National Institutes of Health grant GM-37049 (A.D.J.). The coordinates have been deposited in the Protein Data Bank in Brookhaven, NY, with accession number 1YRN.

26 July 1995; accepted 13 September 1995

Elastic Properties of Flux-Line Arrays in High Transition Temperature Superconductors Probed by Two-Sided Decoration

Seokwon Yoon,* Zhen Yao, Hongjie Dai, Charles M. Lieber†

The elastic constants of magnetic flux-line lattices in copper oxide superconductors have remained uncharacterized despite their essential role in determining important phenomena such as melting. Here the absolute values of the elastic moduli of flux-line arrays have been probed by correlating the positions of individual flux lines emerging from opposite sides of $Bi_2Sr_2CaCu_2O_8$ (BSCCO) superconductors. These experiments demonstrate that the compressional and shear moduli of the flux-line lattice are three orders of magnitude smaller than the values predicted by standard models. The origin of these changes in the moduli and the general applicability of this approach to other materials are discussed. In addition, there is a remarkable correspondence between the excitations of the flux-line arrays and those of superfluid helium.

Exploiting the high-temperature superconductivity exhibited by copper oxide materials remains a great challenge to fundamental and applied research (*1*, *2*). This challenge arises in large part from the propensity of magnetic flux lines in these type-II superconductors to flow and dissipate energy in the presence of currents (*1*–*6*). To control rationally such deleterious behavior ultimately requires a fundamental understanding of the structural properties of flux-line arrays. In particular, knowledge of the elastic moduli could provide important insight into this problem because they are central to calculations of thermal fluctuations, melting, and the effects of weak pinning (*2*, *3*). Indeed, many theoretical studies of the flux-line lattice elastic moduli have been reported (*2*–*6*); however, no direct experimental evaluations are available to test these predictions.

Division of Applied Sciences and Department of Chemistry, Harvard University, Cambridge, MA 02138, USA.

*Present address: Department of Physics, Catholic University, Bucheon, Korea 422-743.

†To whom correspondence should be addressed.

Herein we report studies of the elastic properties of flux-line arrays in BSCCO superconductors done with a recently developed technique (*7*) that enables the positions of individual flux lines on both sides of a sample to be visualized and correlated. This approach is motivated by the understanding that the propagation of thermally excited fluctuations in the flux lines as they cross a sample will depend on the elastic properties of the array of flux lines (*6*, *8*). By analyzing the density and orientational correlations of the flux lines as they pass through samples, we have been able to extract the absolute values of the compressional (c_{11}), tilt (c_{44}), and shear (c_{66}) moduli for flux-line arrays in BSCCO as a function of the magnetic field *B*. These data exhibit large deviations from general theoretical predictions for anisotropic superconductors, and thus should be considered in the analyses of melting and pinning of the flux-line lattice in the copper oxide materials.

The Bitter technique has been used previously to decorate individual magnetic flux lines emerging from one surface of a superconductor (*9*–*11*). We have recently extended this technique to provide three-dimensional (3D) information simply by decorating simultaneously the two opposite sides of a sample; that is, double-sided decoration (*7*). Typical images of the same *xy* location from two sides of BSCCO samples decorated in fields of 5, 12, and 24 G are shown in Fig. 1. In these images, each flux-line position corresponds to the vertex formed by bonds drawn from the flux line to its nearest neighbors. These images show that at 12 and 24 G, the flux-line arrays are relatively well ordered and display a good correspondence of topological defects through the samples, in agreement with earlier work (*7*). At 5 G, where the flux-line array is in a highly disordered liquid-like state, there is still a good correspondence of topological defects and individual flux lines across the sample. There are, however, differences at the lattice constant scale in positions of individual flux lines and defect topologies crossing the sample, which indicate that the flux lines

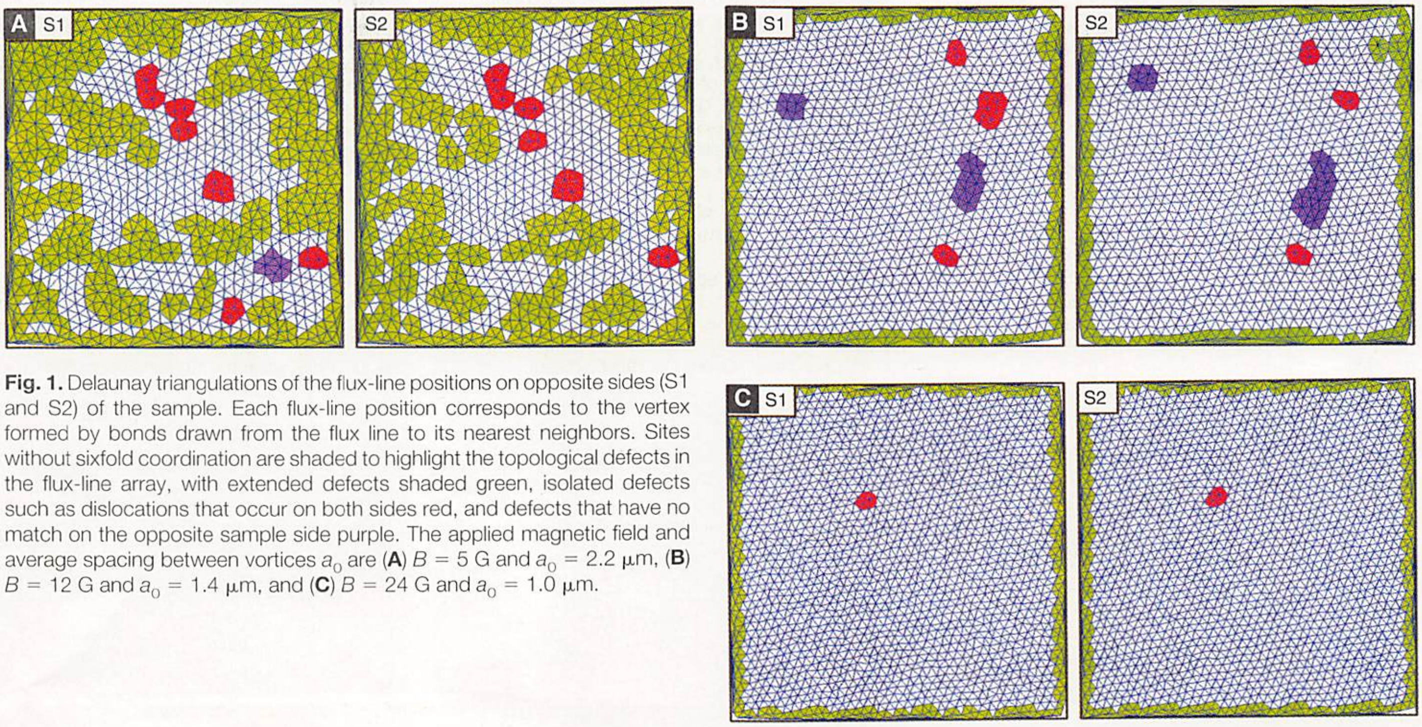

Fig. 1. Delaunay triangulations of the flux-line positions on opposite sides (S1 and S2) of the sample. Each flux-line position corresponds to the vertex formed by bonds drawn from the flux line to its nearest neighbors. Sites without sixfold coordination are shaded to highlight the topological defects in the flux-line array, with extended defects shaded green, isolated defects such as dislocations that occur on both sides red, and defects that have no match on the opposite sample side purple. The applied magnetic field and average spacing between vortices a_0 are (**A**) $B = 5$ G and $a_0 = 2.2$ μm, (**B**) $B = 12$ G and $a_0 = 1.4$ μm, and (**C**) $B = 24$ G and $a_0 = 1.0$ μm.

meander as they traverse these samples.

The central result of this paper is the quantitative evaluation of the absolute values of the elastic moduli versus magnetic field obtained from an analysis of flux-line meandering across samples. The relation between thermally excited flux-line meandering and the elastic moduli has been derived previously with a hydrodynamic model (*12*, *13*). For a sample of finite thickness L, the 3D density correlation function relevant to our two-sided decoration data is

$$S(q_\perp, L) = S_2(q_\perp)R(q_\perp, L) \qquad (1)$$

where $S_2(q_\perp)$ is the density correlation function calculated from one surface, $R(q_\perp, L) = [\cosh(L/\xi(q_\perp))]^{-1}$ measures the loss of translational order across the sample, and $q_\perp$ is the in-plane wave vector. The correlation length $\xi_\parallel(q_\perp)$ can be expressed in terms of the ratio of the compressional $[c_{11}(q_\perp)]$ and the tilt $[c_{44}(q_\perp)]$ moduli of the flux-line array

$$\xi_\parallel(q_\perp) = \sqrt{\frac{c_{44}(q_\perp)}{c_{11}(q_\perp)}}\frac{1}{q_\perp} \qquad (2)$$

and $S_2(q_\perp)$ can be expressed in terms of the product of the compressional and tilt moduli

$$S_2(q_\perp) = \frac{n_0 k_B T}{2\sqrt{c_{11}(q_\perp)c_{44}(q_\perp)}} q_\perp \qquad (3)$$

where n_0 is the average density of flux lines, k_B is the Boltzmann constant, and T is temperature (*14*). This analysis predicts that $1/\xi_\parallel(q_\perp)$ and $S_2(q_\perp)$ should go linearly to zero as $q_\perp$ goes to zero, and shows that the ratio and product of $c_{11}(q_\perp \to 0) \equiv c_{11}$ and $c_{44}(q_\perp \to 0) \equiv c_{44}$ can be obtained from the slopes of these lines.

Because $S(q_\perp, L)$ and $S_2(q_\perp)$ can be calculated directly from our two-sided decoration data, it is possible to determine c_{11} and c_{44}. Plots of $\cosh^{-1}[S_2(q_\perp)/S(q_\perp, L)]$ and $S_2(q_\perp)$ calculated from the two-sided decoration data in the disordered state at 5 G and in the more ordered state at 12 G are shown in Fig. 2. The long-wavelength (small $q_\perp$) behavior of these data exhibit the linear dependence on $q_\perp$ expected from the hydrodynamic model. The linear regions of $\cosh^{-1}[S_2(q_\perp)/S(q_\perp, L)]$ and $S_2(q_\perp)$ yield $L\sqrt{c_{11}/c_{44}}$ and $n_0k_BT/2\sqrt{c_{11}c_{44}}$ from which we obtain the absolute values of the moduli: at 5 G, $c_{11} = 1.8 \times 10^{-3}$ and $c_{44} = 1.0$ G^2, and at 12 G, $c_{11} = 8.0 \times 10^{-3}$ and $c_{44} = 4.8$ G^2 (*15*).

A similar approach can be used to measure the shear modulus c_{66} as a function of magnetic field, by determining the propagation of orientational order through the samples (*12*). Physically, the degree to which the orientation of the Bitter patterns from the two sample sides line up is indicative of how well the flux array resists shear deformations. The bond orientational correlation function $G_6(q_\perp, L)$ correlating the flux-line images from both sample sides is given by $G_6(q_\perp, L) = G_6(q_\perp)R_H(q_\perp, L)$, where $G_6(q_\perp, L)$ is the orientational correlation function calculated from a single side and $R_H(q_\perp, L) = [\cosh(L/\xi_H(q_\perp))]^{-1}$ describes the decay of flux-line orientational correlation through the sample with correlation length $\xi_H(q_\perp)$ (*16*)

$$\xi_H(q_\perp) = \sqrt{\frac{c_{44}(q_\perp)}{c_{66}(q_\perp)}}\frac{1}{q_\perp} \qquad (4)$$

Plots of $\cosh^{-1}[G_6(q_\perp)/G_6(q_\perp, L)]$ calculated from the two-sided decoration data at 5 and 12 G (Fig. 3) increase linearly with $q_\perp$ and then roll over as $q_\perp$ approaches the first reciprocal lattice vector. Using the linear slope of these plots and the values of c_{44} determined from our analyses of the density correlations, we find that values of c_{66} at 5 and 12 G are 1.4×10^{-3} and 5.0×10^{-3} G^2, respectively.

The experimental values of the elastic moduli determined at 5, 12, and 24 G are summarized in Table 1. These data show that the magnitude of c_{44} is much greater than c_{11} and c_{66} in this low–magnetic field regime. This difference between the absolute magnitudes of c_{44} versus c_{11} and c_{66} is notable because conventional models of rigid flux

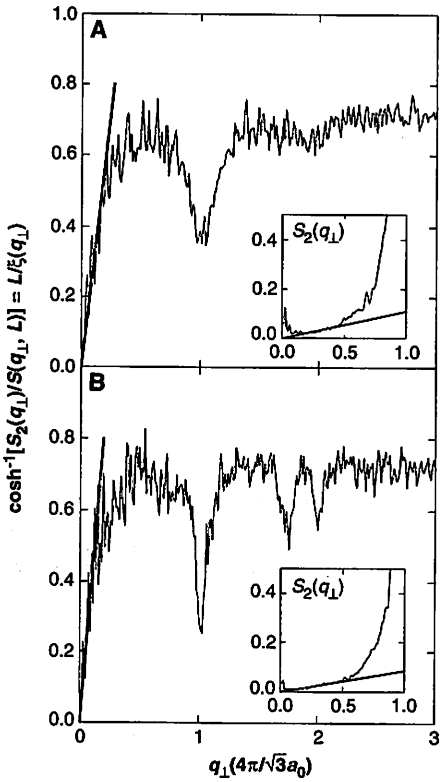

Fig. 2. Plots of $\cosh^{-1}[S_2(q_\perp)/S(q_\perp, L)] = L/\xi_\parallel(q_\perp)$ versus $q_\perp$ from the analysis of two-sided decoration data obtained in magnetic fields of **(A)** 5 G and **(B)** 12 G. The solid black lines are linear fits of the long-wavelength regime of these data; the slope of these lines equals $L\sqrt{c_{11}/c_{44}}$. The insets show the corresponding plots of $S_2(q_\perp)$ for $q_\perp$ less than the first reciprocal lattice vector. The black lines correspond to linear fits of the long-wavelength regime of the data; the slope of these lines equals $n_0k_BT/2\sqrt{c_{11}c_{44}}$. $S(q_\perp, L) = \langle\rho(q_\perp, L)\rho^*(q_\perp, 0)\rangle$ and $S_2(q_\perp) = \langle\rho(q_\perp, 0)\rho^*(q_\perp, 0)\rangle$, where $\rho(q_\perp, z)$ is the Fourier transform of the flux-line positions in a constant z cross section. The abscissa in all of these plots are in units of the reciprocal lattice vector, $4\pi/\sqrt{3}\,a_0$, where a_0 is the average spacing between vortices.

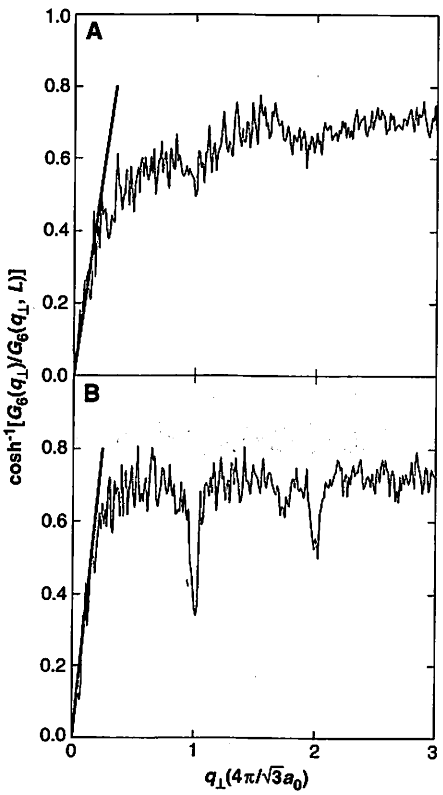

Fig. 3. Plots of $\cosh^{-1}[G_6(q_\perp)/G_6(q_\perp, L)]$ versus $q_\perp$ from the analysis of two-sided decoration data obtained in applied magnetic fields of **(A)** 5 G and **(B)** 12 G. The factor $G_6(q_\perp)$ is the 2D orientational correlation function calculated from a single (side) image, and $G_6(q_\perp, L)$ is the 3D correlation function calculated from both sample sides. The solid black lines are linear fits of the long-wavelength regime of this data; the slope of these lines equals $L\sqrt{c_{66}/c_{44}}$. The abscissa in these plots are in units of the reciprocal lattice vector, $4\pi/\sqrt{3}\,a_0$.

Table 1. Elastic moduli of the flux-line lattice in BSCCO as a function of magnetic field.

Magnetic field (G)	Elastic moduli (G²)		
	c_{11}	c_{44}	c_{66}
5	1.8×10^{-3}	1.0	1.4×10^{-3}
12	8.0×10^{-3}	4.8	5.0×10^{-3}
24	2.8×10^{-2}	8.1	9.6×10^{-3}

lines or 2D pancake vortices, which have been used extensively to treat flux lines in the high transition temperature materials, predict that they should be of comparable magnitude (2–5). The similarities and differences of these experimental data have been compared (Fig. 4) with theoretical values calculated with Ginzburg-Landau (G-L) theory (4). The elastic moduli obtained from our experiments follow the same field dependence given by the G-L theory (that is, $c_{11} \propto B^2$, $c_{44} \propto B$, and $c_{66} \propto B$), indicating that underlying physical interactions are similar. However, this analysis shows that the magnitudes of the experimental c_{11} and c_{66} are about three orders of magnitude smaller than those predicted by G-L theory, although c_{44} agrees well with theory.

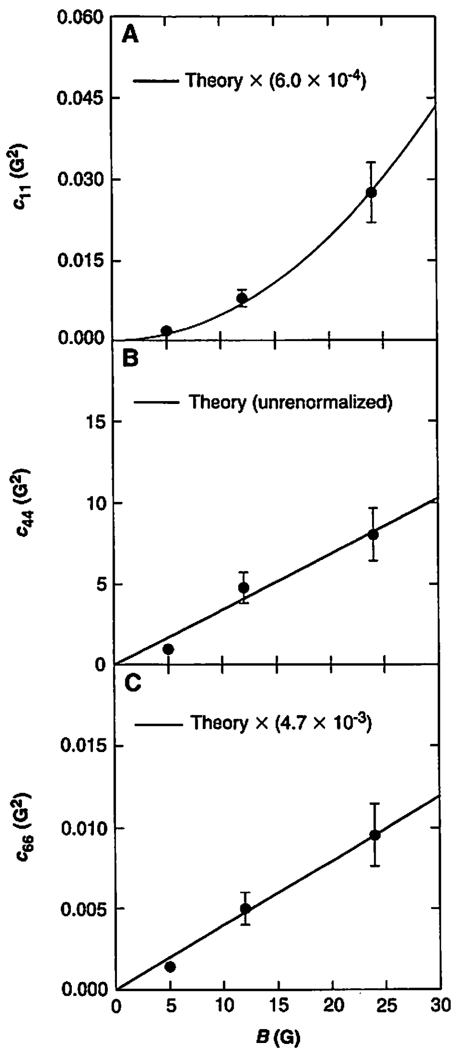

Fig. 4. Experimental values (circles) and theoretical predictions (lines) of the **(A)** compressional (c_{11}), **(B)** tilt (c_{44}), and **(C)** shear (c_{66}) moduli versus magnetic field B. The theoretical curves for c_{11} ($-B^2/4\pi$) and c_{66} ($-\phi_0 B/64\pi^2\lambda^2$) were multiplied by factors of 6.0×10^{-4} and 4.7×10^{-3}, respectively, to fit the experimental data. The theoretical fit $\phi_0 B/16\pi^2\lambda^2$ to the experimental data for c_{44} is not renormalized. The theoretical fits correspond to the long-wavelength limit of the analytical expressions for the wave vector–dependent elastic moduli (34). The value of $\lambda(T)$ used to calculate c_{44} and c_{66} is 0.62 μm and corresponds to a temperature of $0.97T_c$ (T_c, transition temperature).

The above results indicate that both c_{11} and c_{66} undergo a large downward renormalization in BSCCO. We believe that the origin of this renormalization may be thermal fluctuations. In particular, the renormalization of c_{11} can be qualitatively attributed to an entropic factor where the increased number of configurations arising from flux-line wandering and entanglement partially offsets the B^2 energy term. A theoretical analysis of the entropic and energetic contributions to c_{11} (12) and previous studies of flux-line interstitials (17) show explicitly the importance of the entropic factor, although more work is clearly needed to understand quantitatively this fascinating observation. Thermal fluctuations have also been studied previously to investigate flux-line melting (2–5), although fluctuation effects on the elastic moduli were not considered in this work (that is, the values from G-L theory were used). Hence, the large renormalization of c_{11} and c_{66} that we observe should lead to important corrections to the low-field region of the calculated flux-line lattice melting line. More generally, we believe that the two-sided decoration and analysis techniques reported herein will also have applications to studies of other copper oxide materials such as $YBa_2Cu_3O_7$, conventional superconductors, and flux-line pinning.

Lastly, the $q_\perp$-dependent spectrum of flux-line correlations is similar to the extensively studied phonon-roton excitation spectrum of superfluid ^{4}He. In superfluid ^{4}He, the wave vector–dependent excitation energy $\epsilon(q)$ increases linearly for small q, rolls over and exhibits a dip at a value of q corresponding to the average interatomic separation, and then increases again at larger q (18). The initial linear increase in $\epsilon(q)$ corresponds to phonon excitations, and the dip has been attributed to a "roton" excitation, whose microscopic origin remains controversial. These features are remarkably similar to those exhibited by our data for the disordered flux-line state in Fig. 2A. This similarity seems surprising because the flux lines are classical wiggling lines, whereas superfluid ^{4}He is a quantum liquid. However, it has been reported that the imaginary time trajectories of a 2D boson liquid (for example, ^{4}He) can be mapped onto the z-dependent positions of flux lines in a superconductor (19). By this mapping, the correlation length $\xi_{\|}(q_\perp)$ describing the decay of in-plane translation order is related to the flux-line excitation energy $\epsilon(q)$ as

$$\frac{1}{\xi_{\|}(q_\perp)} = \frac{\epsilon(q_\perp)}{k_B T} \qquad (5)$$

Hence, our Fig. 2A corresponds to a plot of $\epsilon(q_\perp)$ versus $q_\perp$ like the q-dependent excitation spectrum of superfluid ^{4}He. In the flux-line system, the linear "phonon" part of the spectrum corresponds to long-wavelength decay of density correlations along the sample z coordinate, while the roton dip corresponds to an enhanced propagation of flux-line correlation at the reciprocal lattice vector. Hence, the nature of the roton minimum, which has been controversial in superfluid ^{4}He, is in fact well defined in the flux-line system. Although more theoretical and experimental work are needed to understand the flux line–superfluid analogy, we believe that these results suggest a richness that may extend beyond the problem of flux lines.

REFERENCES AND NOTES

1. D. J. Bishop, P. L. Gammel, D. A. Huse, C. A. Murray, *Science* **255**, 165 (1992).
2. D. S. Fisher, M. P. A. Fisher, D. A. Huse, *Phys. Rev. B* **43**, 130 (1991).
3. G. Blatter, M. V. Feigel'man, V. B. Geshkenbein, A. I. Larkin, V. M. Vinokur, *Rev. Mod. Phys.* **66**, 1125 (1994).
4. D. S. Fisher, in *Phenomenology and Applications of High-Temperature Superconductors*, K. S. Bedell, M. Inui, D. Meltzer, J. R. Schrieffer, S. Doniach, Eds. (Addison-Wesley, New York, 1992), p. 287.
5. E. H. Brandt, *J. Supercond.* **6**, 201 (1993); *Phys. Rev. Lett.* **63**, 1106 (1989).
6. D. R. Nelson, in (4), p. 187.
7. Z. Yao, S. Yoon, H. Dai, S. Fan, C. M. Lieber, *Nature* **371**, 777 (1994).
8. D. R. Nelson and P. Le Doussal, *Phys. Rev. B* **42**, 10113 (1990).
9. C. A. Bolle *et al.*, *Phys. Rev. Lett.* **66**, 112 (1991).
10. I. V. Grigorieva, J. W. Steeds, K. Sasaki, *Phys. Rev. B* **48**, 16685 (1993).
11. H. Dai, S. Yoon, J. Liu, R. C. Budhani, C. M. Lieber, *Science* **265**, 1552 (1994).
12. M. C. Marchetti and D. R. Nelson, *Phys. Rev. B* **47**, 12214 (1993); *ibid*, in press.
13. The hydrodynamic model was derived originally for flux liquids. Because this model is also applicable to hexatic and crystalline flux-line arrays away from reciprocal lattice vectors, there is no loss in generality in its application to the present data (8, 12).
14. Several assumptions were made to arrive at Eqs. 2 and 3. Surface contributions to $R(q_\perp, L)$, which arise from the coulomb-like interactions between flux-line ends, have been ignored. Similarly, it is assumed that $S_2(q_\perp)$ corresponds to a 2D slice of the bulk flux-line array. For the range of $q_\perp$ evaluated in our experiments, these assumptions are believed to be reasonable (12). In addition, the contribution of flux pinning by point crystal defects was ignored because the flux-line array is frozen at a temperature close to the irreversibility line, where point pinning is believed to be weak (8).
15. The temperature relevant to the analysis of these experiments was determined from the $\cosh^{-1}[S_2(q_\perp)/S(q_\perp, L)]$ versus $q_\perp$ data. The point at which these plots deviate from linearity corresponds to $q_\perp \approx \lambda^{-1}(T)$; that is, the wave vector at which the repulsive interactions between flux lines or nonlocality in $c_{11}(q_\perp)$ becomes important. We estimate that $\lambda(T) \approx$ 0.6 μm by this criteria. The temperature obtained by extrapolating from $\lambda(0)$ to $\lambda(T)$ with the two-fluid model is $0.97T_c$ or 80 K.
16. The bond orientational correlation functions that probe orientational order across the sample and on a single side are given by $G_6(q_\perp, L) = \langle \Psi_6(q_\perp, L)\Psi_6^*(q_\perp, 0)\rangle$ and $G_6(q_\perp) = \langle \Psi_6(q_\perp, 0)\Psi_6^*(q_\perp, 0)\rangle$, respectively. The factor $\Psi_6(q_\perp, L)$ is the Fourier transform of the bond orientational order parameter $\Psi_6(\mathbf{r}) \equiv \exp[6i\theta(\mathbf{r})]$ defined at the midpoint of a "bond" connecting two

nearest flux lines in a constant z cross section (6). Both $G_6(q_\perp)$ and $G_6(q_\perp, L)$ have peaks (delta function) at $q_\perp = 0$. These peaks are effectively removed when taking the ratio of these two quantities to obtain the transfer function $R_H(q_\perp, L)$; however, we have been unable to determine reliably the small-q behavior of $G_6(q_\perp)$ alone (that is, to extract $\sqrt{c_{44}c_{66}}$ as was done in the case of 2D density correlations for $\sqrt{c_{11}c_{44}}$ because of this peak.

17. E. Frey, D. R. Nelson, D. S. Fisher, *Phys. Rev. B* **49**, 9723 (1994).
18. R. K. Pathria, *Statistical Mechanics* (Pergamon, New York, 1993).
19. D. R. Nelson, *Phys. Rev. Lett.* **60**, 1973 (1988); M. P. A. Fisher and D. H. Lee, *Phys. Rev. B* **39**, 2756 (1989).

20. We thank D. R. Nelson and M. C. Marchetti for helpful discussions. C.M.L. acknowledges support by the National Science Foundation (grant DMR 9306684) and the Materials Research Science and Engineering Center Program of the National Science Foundation (grant DMR 9400396).

10 May 1995; accepted 18 August 1995

A Class of Cobalt Oxide Magnetoresistance Materials Discovered with Combinatorial Synthesis

Gabriel Briceño, Hauyee Chang, Xiaodong Sun, Peter G. Schultz,* X.-D. Xiang*

The recent development of methods for generating libraries of solid-state compounds has made it possible to apply combinatorial approaches to the discovery of materials. A library of 128 members containing different compositions and stoichiometries of $Ln_xM_yCoO_\delta$, where Ln = Y or La and M = Pb, Ca, Sr, or Ba, was synthesized by a combination of thin-film deposition and physical masking techniques. Large magnetoresistance has been found in $La_x(Ba,Sr,Ca)_y$-CoO_δ samples, whereas Y-based samples exhibit much smaller magnetoresistive effects. The magnetoresistance of the Co-containing compounds increases as the size of the alkaline earth ion increases, in sharp contrast to Mn-containing compounds, in which the magnetoresistance effect increases as the size of the alkaline earth ion decreases.

The discovery of the magnetoresistive effect (*1*) in Mn-based perovskite oxides $(La,R)_{1-x}A_xMnO_{3-\delta}$, where R is a rare earth element and A = Ca, Sr, or Ba, has attracted considerable attention because of the potential application of these materials in magnetic storage technology. Colossal magnetoresistance (CMR), with MR ratios $\Delta R/R(0) = [R(H = 0) - R(H)]/R(H = 0)$ as large as 99.0, 99.9, and 99.99%, have been reported for polycrystalline samples of $La_{0.60}Y_{0.07}Ca_{0.33}MnO_x$ and epitaxial thin films of $La_{0.67}Ca_{0.33}MnO_3$ and $Nd_{0.7}Sr_{0.3}MnO_{3-\delta}$, respectively (*2–4*). A large number of theoretical and experimental efforts have been undertaken to understand this unexpected phenomenon and to improve the room-temperature sensitivity, $[\Delta R/R(0)]/\Delta H$, at $H = 0$ of these materials, an important factor for technical applications. The question arises whether these effects are unique to Mn-based perovskite oxides or can be found as an intrinsic property of other materials.

We have applied a combinatorial approach (*5*) to the search for more CMR materials. Our initial search for CMR compounds was around simple perovskite ABO_3 and related A_2BO_4 or $A_{n+1}B_nO_{3n+1}$ higher order structures, where A = (La, Y, or rare earth)$^{+3}$ partially substituted with (Ca, Sr, Ba, Pb, or Cd)$^{+2}$ and B = (Mn, V, Co, Ni, Cr, or Fe). In this report, we describe a specific example of the generation and screening of one such library that resulted in the discovery of a family of Co-containing CMR materials. An analysis of the effects of spin configuration and electronic structure on the MR properties of the Co- and Mn-based compounds should help to elucidate the underlying mechanism of the CMR effect. Moreover, the discovery of diverse classes of the CMR materials may help efforts to optimize these materials for eventual device applications.

A 128-member library was generated by combining sequential radio-frequency sputtering deposition of thin films with a series of physical masking steps designed to produce Y-, La-, Ba-, Sr-, Ca-, and Co-containing films (1 mm by 2 mm) with varying compositions and stoichiometries (Fig. 1). Polished (100) $LaAlO_3$ single crystals were used as substrates and La_2O_3, Y_2O_3, $BaCO_3$, $SrCO_3$, CaO, and Co were used as sputtering targets (*6*). Two identical libraries (L1 and L2) were generated simultaneously and then thermally treated under different annealing and sintering

		La				Y			
		1							8
Ba	16	1.38 0.62	1.14 0.62 ●	0.89 0.62	0.64 0.62	0.5 0.62	1.0 0.62	0.74 0.62	1.24 0.62
		1.0 0.45 ●	0.83 0.45 ●	0.65 0.45 ●	0.47 0.45	0.36 0.45	0.72 0.45	0.54 0.45	0.9 0.45
		0.73 0.33 ●	0.6 0.33 ●	0.47 0.33 ●	0.34 0.33	0.26 0.33	0.52 0.33	0.4 0.33	0.66 0.33
		0.61 0.27 ●	0.5 0.27 ●	0.39 0.27 ●	0.28 0.27 ●	0.22 0.27	0.45 0.27	0.33 0.27	0.55 0.27
Sr		1.38 0.62	1.14 0.62 ●	0.89 0.62 ●	0.64 0.62 ●	0.5 0.62	1.0 0.62	0.74 0.62	1.24 0.62
		1.0 0.45	0.83 0.45 ●	0.65 0.45 ●	0.47 0.45 ●	0.36 0.45	0.72 0.45	0.54 0.45	0.9 0.45
		0.73 0.33	0.6 0.33 ●	0.47 0.33 ●	0.34 0.33 ●	0.26 0.33	0.52 0.33	0.4 0.33	0.66 0.33
		0.61 0.27	0.5 0.27 ●	0.39 0.27 ●	0.28 0.27 ●	0.22 0.27	0.45 0.27	0.33 0.27	0.55 0.27
Ca		1.38 0.62	1.14 0.62	0.89 0.62 ●	0.64 0.62 ●	0.5 0.62	1.0 0.62	0.74 0.62	1.24 0.62
		1.0 0.45	0.83 0.45	0.65 0.45	0.47 0.45 ●	0.36 0.45	0.72 0.45	0.54 0.45	0.9 0.45
		0.73 0.33	0.6 0.33	0.47 0.33	0.34 0.33	0.26 0.33	0.52 0.33	0.4 0.33	0.66 0.33
		0.61 0.27	0.5 0.27	0.39 0.27	0.28 0.27	0.22 0.27	0.45 0.27	0.33 0.27	0.55 0.27
Pb		1.38 0.62	1.14 0.62	0.89 0.62	0.64 0.62	0.5 0.62	1.0 0.62	0.74 0.62	1.24 0.62
		1.0 0.45	0.83 0.45	0.65 0.45	0.47 0.45	0.36 0.45	0.72 0.45	0.54 0.45	0.9 0.45
		0.73 0.33	0.6 0.33	0.47 0.33	0.34 0.33	0.26 0.33	0.52 0.33	0.4 0.33	0.66 0.33
	1	0.61 0.27	0.5 0.27	0.39 0.27	0.28 0.27	0.22 0.27	0.45 0.27	0.33 0.27	0.55 0.27

Fig. 1. A map of compositions and stoichiometries ($Ln_xM_yCoO_{3-\delta}$, where Ln = La or Y and M = Ba, Sr, Ca, or Pb) of thin-film samples in libraries L1 and L2. Samples are labeled by index (row number, column number) in the text and figure legend. The first number in each box indicates x and the second y. Solid circles indicate the samples that show significant MR effects (>5%).

G. Briceño and X.-D. Xiang, Molecular Design Institute, Lawrence Berkeley Laboratory, Berkeley, CA 94720, USA.
H. Chang, X. Sun, P. G. Schultz, Molecular Design Institute, Lawrence Berkeley Laboratory, Howard Hughes Medical Institute, and Department of Chemistry, University of California, Berkeley, CA 94720, USA.

*To whom correspondence should be addressed.

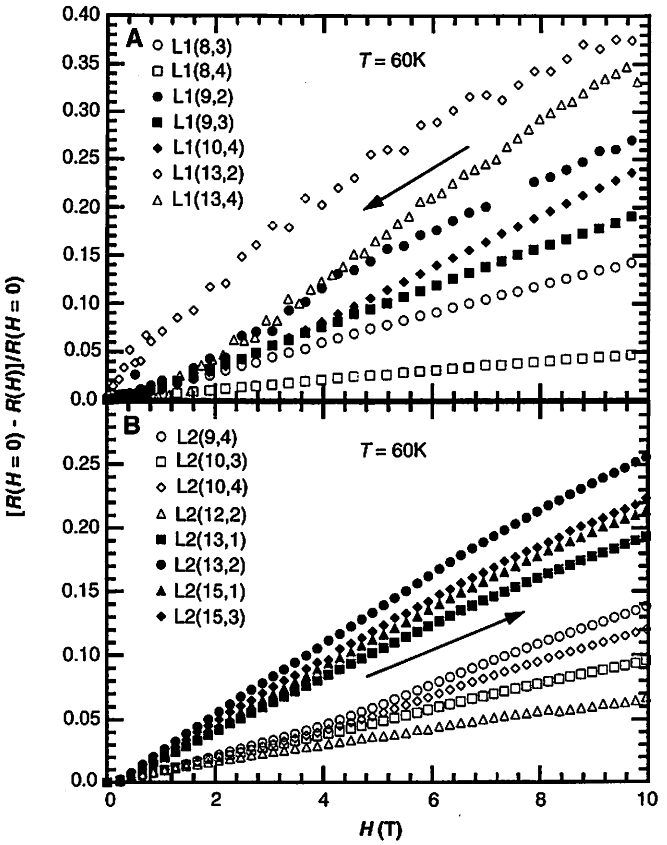

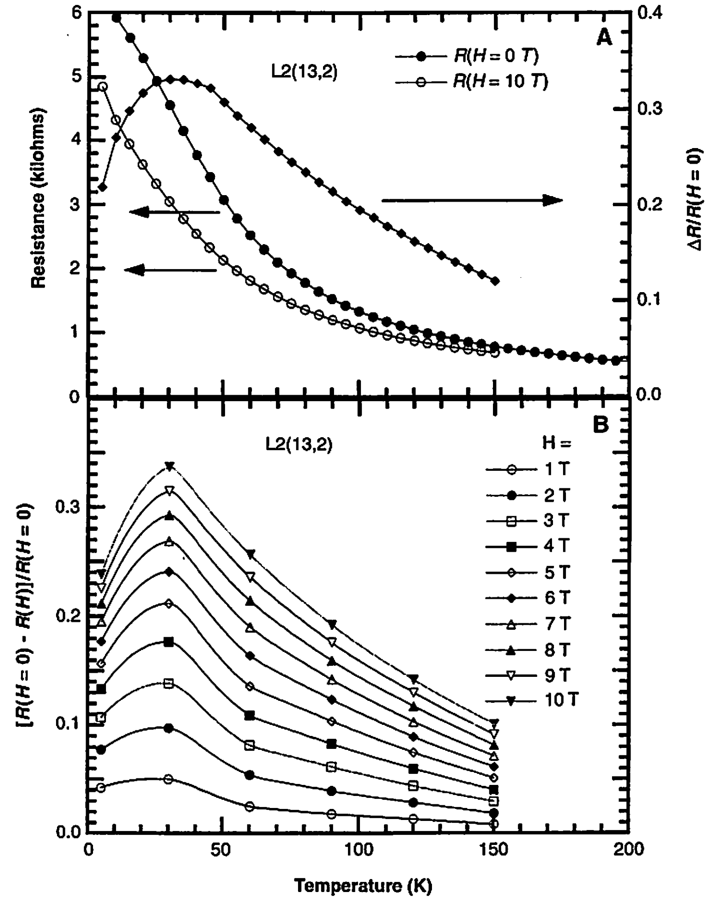

Fig. 2 (left). The MR ratios of representative samples in **(A)** L1 and **(B)** L2 as a function of magnetic field. **Fig. 3 (right).** **(A)** Resistance of sample L2(13, 2) under 0 and 10 T and the MR ratio (H = 10 T) as a function of temperature; **(B)** MR ratios of the same sample for different magnetic fields as a function of temperature. The solid lines are guides to the eye.

procedures (up to 900°C) in O_2 or air (7). Figure 1 indicates the composition and stoichiometry of each sample. The resistivity of each sample as a function of magnetic field (perpendicular to the probing current) and temperature was measured by the four-probe contact method with a computer-controlled multichannel switching system. A liquid-helium cryogenic system with a superconducting 12-T magnet was used to perform variable-temperature and -field measurements.

A number of films in the library showed a significant (>5%) MR effect (Fig. 1, solid circles). Three compounds that exhibit a large giant-MR effect have been identified: $La_xM_yCoO_\delta$, where M = Ca, Sr, or Ba. The normalized MRs of representative samples as a function of magnetic field at fixed temperature (60 K) are shown in Fig. 2; the temperature dependence of the resistance and normalized MR of a representative sample, L2(13, 2), under different fields are shown in Fig. 3. In contrast to the behavior of Mn oxide MR materials (2, 3), the MR effect increases as the size of the alkaline earth ion increases (Fig. 2).

The MR effects of the samples in library L1 are larger than those of L2, presumably because of differences in oxidation resulting from slightly different thermal treatments. The largest MR ratio measured in this library was 72%, obtained for sample L1(15, 2) at T = 7 K and H = 10 T. This value is comparable to those measured for films generated in a similar fashion in a Mn-based library (8). As with the Mn-containing materials, optimization of composition, stoichiometry, substrate, and synthetic conditions may lead to increases in the MR ratio. The corresponding Y-(Ba,Sr,Ca)-Co compounds show much smaller (<5%) MR effects.

Three bulk samples with the stoichiometry $La_{0.67}(Ba,Sr,Ca)_{0.33}CoO_\delta$ were then synthesized (sintered at 1400°C in air) for further structural study. The x-ray diffraction patterns show that the crystal structure is basically cubic perovskite with lattice constant a = 3.846, 3.836, and 3.810 Å for the Ba, Sr, and Ca compounds, respectively. Minor splittings of the intensity peaks are attributed to rhombohedral distortion from the perfect cubic perovskite structure (9).

A bulk sample of stoichiometry $La_{0.58}Sr_{0.41}CoO_\delta$ was synthesized and its magnetization was measured with a superconducting quantum interference device (SQUID) magnetometer. The sample MR as a function of magnetic field and the sample magnetization under a 1-T magnetic field as a function of temperature were measured (Fig. 4). A gradual ferromagnetic transition starts at ~200 K and saturates below 50 K. The MR ratio of this bulk sample (60%) is

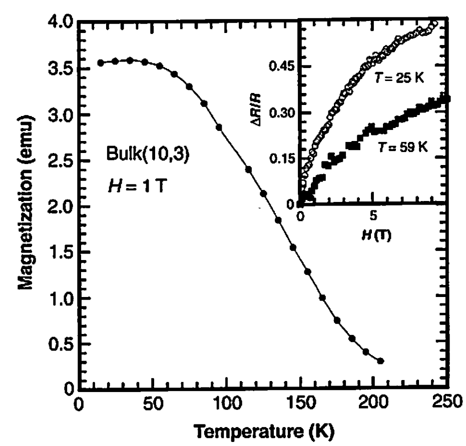

Fig. 4. Magnetization of the bulk sample $La_{0.58}Sr_{0.41}CoO_\delta$ under a 1-T field as a function of temperature. The solid line is a guide to the eye. **(Inset)** MR ratios of the sample at different temperatures as a function of magnetic field.

significantly higher than that of the corresponding thin-film sample in L1 (30%). The x-ray analysis of this sample confirmed the cubic perovskite structure with $a = 3.82$ Å.

It has been suggested (3) that the CMR effect in the Ca-doped $LaMnO_3$ system originates from "double exchange" electron-hopping processes between Mn^{3+} and Mn^{4+} neighboring sites through the O^{2-} anion between them (10). In these processes, the e_g itinerant electron conduction or hopping rate $t_{ij} = t_0\cos(\theta_{ij}/2)$, where θ_{ij} is the angle between local spin directions of electrons on neighboring sites i and j, and t_0 is the hopping rate in a perfect ferromagnetic state. The application of an external field may align the disordered local spins during a ferromagnetic transition and thereby increase electron conduction or even induce an insulator-metal transition through strong interaction between itinerant electron and local spins. In this model, the MR effect may be induced by an external field when the system is in transition toward the ferromagnetic state. In this aspect, our data are consistent with this model, that is, MR effects appear only below the Curie temperature ($T_c \sim 150$ to 200 K) and decrease below the saturation field (~30 to 40 K) (Fig. 3). However, the role of alkaline earth ion size in the MR effect remains unclear. In doped $LaMnO_3$ systems, it appears that smaller dopant size favors the MR effect (5), whereas in doped $LaCoO_3$ systems, the opposite effect is observed.

REFERENCES AND NOTES

1. See, for example, R. M. Kusters, J. Singleton, D. A. Keen, R. McGreevy, W. Hayes, *Physica B* **155**, 362 (1989); K. Chahara, T. Ohno, M. Kasai, Y. Kozono, *Appl. Phys. Lett.* **63**, 1990 (1993); H. L. Ju, C. Kwon, R. L. Greene, T. Venkatessan, *ibid.* **65**, 2108 (1994); R. von Helmolt, J. Wecker, K. Samwer, L. Haupt, K. Bärner, *J. Appl. Phys.* **76**, 6925 (1994).
2. S. Jin, H. M. O'Bryan, T. H. Tiefel, M. McCormack, W. W. Rhodes, *Appl. Phys. Lett.* **66**, 382 (1995).
3. S. Jin *et al.*, *Science* **264**, 413 (1994).
4. G. C. Xiong *et al.*, *Appl. Phys. Lett.* **66**, 1427 (1995).
5. X.-D. Xiang *et al.*, *Science* **268**, 1738 (1995).
6. Sputtering was carried out at 5 to 15 mtorr, with Ar as the sputtering gas; deposition rates were 0.1 to 1 Å s^{-1}. Film thickness was monitored with a crystal microbalance and calibrated independently with a profilometer. The uniformity of the deposited films varied less than 5% over an area ~2.5 cm in diameter.
7. Library L1 was treated as follows: heated from room temperature (RT) to 200°C, heated to 300°C over 12 hours, and cooled to RT; it was then heated to 650°C over 1 hour, heated to 850°C over 3 hours, heated to 900°C over 3 hours, and cooled to RT over 2 hours. Library L2 was treated as follows: heated from RT to 200°C, heated to 350°C over 15 hours, and cooled to RT; it was then heated to 650°C over 2 hours, heated to 740°C over 13 hours, heated to 850°C over 1 hour, heated to 900°C over 0.5 hour, cooled to 650°C over 2 hours, and cooled to RT.
8. G. Briceño, X. Sun, H. Chang, X.-D. Xiang, P. G. Schultz, unpublished material.
9. F. Askham, I. Fankuchen, R. Ward, *J. Am. Chem. Soc.* **72**, 3799 (1950).
10. C. Zener, *Phys. Rev.* **82**, 403 (1951); P. W. Anderson and H. Hasegawa, *ibid.* **100**, 675 (1955); P.-G. de Gennes, *ibid.* **118**, 141 (1960).
11. We are grateful for financial support for this work from the Laboratory Directed Research and Development Program of Lawrence Berkeley Laboratory under U.S. Department of Energy contract DE-AC03-76SF00098 and the Office of Naval Research (grant N00014-95-F-0099). G.B. acknowledges support from a University of California President's Postdoctoral Fellowship. We thank J. Torrance for helpful advice and E. Granlund and J. Wu for technical support.

25 May 1995; accepted 22 August 1995

Molluscan Diversity in the Late Neogene of Florida: Evidence for a Two-Staged Mass Extinction

Edward J. Petuch

Analyses of recent data show that Floridian molluscan diversity declined markedly during the Pliocene-Pleistocene mass extinction. This decline in diversity was seen at all trophic levels, indicating a complete collapse of the ecosystem. These findings contradict the notion that there was a species diversity stasis throughout the Pliocene-Pleistocene and that the diversity of Pliocene Florida was equivalent to that of Recent Florida. The mass extinction was a two-staged, sequential event. A similar two-staged mass extinction occurred in the Miocene, indicating that two ecological catastrophes in quick geological succession may have produced this mass extinction as well.

Studies of tropical western Atlantic Pliocene (Plio)-Pleistocene molluscan mass extinctions (1–8) have resulted in two conflicting conclusions. The main data source used to arrive at these antitheses was the rich upper Neogene molluscan fossil beds of southern Florida (deposited within the Floridian component of the Plio-Pleistocene Caloosahatchian Molluscan Province) (2, 6, 9). One conclusion (4) was that diversity (at both the generic and specific levels) decreased dramatically in Florida during late Pliocene–early Pleistocene time, producing an impoverished middle and late Pleistocene fauna and a reconstituted but less diverse Recent Floridian fauna. The other conclusion (8) was that although Plio-Pleistocene rates of extinction were high in Florida, the overall diversity (species level) has remained relatively constant from the Pliocene to the Recent. This was explained by a high rate of recruitment (origination), produced by invasion and speciation, that balanced the net loss due to extinction. Both notions, however, were hampered by incomplete museum collections and by variable reporting in the literature.

Data sources and compendia have recently become available that offer a more complete database of molluscan diversity (10, 11). When put into a new stratigraphic and geochronological scheme (12, 13), the data on macrogastropod diversity reveal patterns of extinction and faunal impoverishment. In an attempt to illustrate such patterns, I selected eight dominant macrogastropod families for analysis, with each representing a major trophic level within its respective molluscan community. Included are algal film grazers (Potamididae), sea grass and epibiont feeders (Cypraeidae), suspension and detritus feeders (Turritellidae), large general carnivores (Busyconidae), small general carnivores (Buccinidae), molluscivores (Muricidae), vermivores (Conidae), and specialized suctorial feeders (Cancellariidae). If a mass extinction truly occurred, with a corresponding drop in species diversity, it would be safe to assume that many, if not all, trophic levels within an ecosystem would suffer.

As can be seen in Table 1 and Fig. 1, all eight families reached a peak of species diversity during the middle Pinecrest Beds (PB2, units 5, 6, 7) at approximately 3 million years ago (Ma) (14). Species diversity declined at the end of Pinecrest Beds time, rose again during Caloosahatchee time, at approximately 1.5 to 2 Ma, and then dropped precipitously during the late Pleistocene (Bermont to Fort Thompson interval). With the exception of the Conidae, with five additional species, and the Potamididae, with an equivalent number of species, all other families show a much lower species diversity in Recent Florida. If all three Pinecrest Beds faunas are considered in unison, as in (8), then the total number of Pinecrest Beds species is much larger for all eight families. In the case of some families, such as the Busyconidae, the difference between the late Pliocene Pinecrest Beds and the Recent fauna is over eightfold. Other families, such as the Cypraeidae, Turritellidae, and Cancellariidae, all exhibit differences ranging from factors of 4 to over 5. The same pattern is seen at the generic level, as shown in Table 2. With the exception of the Cypraeidae (because of late Pleistocene inva-

Division of Geological Oceanography, Department of Geology, Florida Atlantic University, Boca Raton, FL 33431, USA.

sion and recruitment) (*10*), seven families are shown to have had more genera during the late Pliocene than are found in Recent Florida.

These data all indicate that the late Pliocene molluscan mass extinction was a real event, and they substantiate the findings of Stanley (*3*, *4*) and Stanley and Campbell (*1*). The sharp drop in the number of genera between the late Pliocene and Recent, particularly in such stenothermal tropical and subtropical indicator families as the Potamididae and the Conidae, also supports the extinction model of Stanley (*4*). Of all eight families, the Buccinidae seems to have suffered the greatest extinction at both the specific and generic levels, and it seems never to have fully recovered after the mass extinction. High tropical genera such as *Cymatophos* and *Trajana* all became regionally extinct after Pinecrest Beds time but have survived in the tropical Eastern Pacific. These, and many other examples, imply that abrupt cooling and an accompanying reduction in productivity (as shown by the corresponding drop in diversity in the detritivore–suspension-feeding family Turritellidae) caused this extinction event. The present data do not support the proposition of a Plio-Pleistocene species diversity stasis (*8*).

The data show that the Plio-Pleistocene mass extinction was not a single, one-time event but a two-staged, sequential event. Both extinction episodes occurred in close geochronological succession, and the extinction couplet is seen on the graph shown in Fig. 1. On the basis of the data in Tables 1 and 2, the first and strongest extinction event took place at the end of Pinecrest Beds time (PB3) and resulted in a much lowered species diversity. Although such genera as *Rhipophos*, *Extractrix*, and *Virgiconus* and many others became extinct in Florida, some groups such as *Pterorhytis*, *Acantholabia*, *Solenosteira*, and *Massyla* survived on into the Pleistocene (as new and different species). By Caloosahatchee time, climatic conditions apparently returned to those of Pinecrest Beds time, as evidenced by incipient species radiations of several main groups such as *Siphocypraea* and *Contraconus* (*10*). At the end of Caloosahatchee time (early Pleistocene) a second extinction event took place, and this acted as the "coup de grâce" for even these last remnants of the great Pliocene eastern American molluscan fauna.

This pattern of a two-staged molluscan mass extinction may not be unique to the Plio-Pleistocene event. A similar but more widely spaced couplet is seen in the middle and late Miocene of the Atlantic coastal plain. Here, a Serravalian extinction event was recently documented (*15*) and was shown to have resulted in a drop in diversity and a loss of such distinctive gastropod genera as *Ecphorosycon*, *Stephanosalpinx*, *Trisecphora*, and *Patuxentrophon*. Climatic conditions became more tropical by the early Tortonian, as evidenced by the first appearance of genera such as *Leptoconus*, and both specific and generic diversity climbed to former levels. By the late Tortonian and Messinian, however, a second extinction event occurred (6) and most pre-Serravalian survivors, as exemplified by the busyconids *Turrifulgur* and *Sycopsis*, died out. Another recent analysis of a mass extinction at the end of the Permian (*16*) has, again, revealed a similar two-staged pattern. Detailed studies of other faunal impoverishments throughout time may show that these couplets are recurrent events and that they may be typical, if not necessary, components of mass extinctions.

Table 1. Number of species in predominant macrogastropod families found in southern Floridian Plio-Pleistocene faunizones (arranged by ecology). PB1, Pinecrest Beds fauna, units 8, 9, and 10; PB2, Pinecrest Beds fauna, units 5, 6, and 7; PB3, Pinecrest Beds fauna, units 2, 3, and 4; C, Griffin Pit and Caloosahatchee fauna; BE, Bermont and Holey Land fauna; FT, Fort Thompson fauna; R, Recent fauna. Data taken from (*10*) and (*17*).

Family and ecology	Number of species in faunizones						
	PB1	PB2	PB3	C	BE	FT	R
Potamididae, algal film grazers	0	3	8	5	5	2	3
Cypraeidae, sea grass feeders*	3	13	5	3	3	1	5
Turritellidae, suspension-detritus	8	18	3	10	4	2	5
Busyconidae, general carnivores, large	15	20	7	17	6	5	5
Buccinidae, general carnivores, small	4	27	5	6	7	4	11
Muricidae, molluscivores	11	47	11	26	27	9	38
Conidae, vermivores	4	18	7	20	12	4	23
Cancellariidae, specialized suctorial	5	23	6	13	6	2	6

*Based on living relative *Cypraea mus* and paleoenvironmental inferences.

Table 2. Number of genera in predominant macrogastropod families found in southern Floridian Plio-Pleistocene faunizones, showing times of extinction (both regional and complete). P_0, total number of genera at beginning of Pinecrest Beds time; E_p, number of genera that became extinct at end of Pinecrest Beds time; E_c, number of genera that became extinct at end of Caloosahatchee time; E_b, number of genera that became extinct at end of Bermont time; E_f, number of genera that became extinct at end of Fort Thompson time; R, number of genera found in Recent Floridian neritic fauna. Data taken from (*10*) and (*17*).

Family	Number of genera					
	P_0	E_p	E_c	E_b	E_f	R
Potamididae	4	2	0	0	1	1
Cypraeidae	2	0	1	1	0	3*
Turritellidae	7	2	2	0	0	3
Busyconidae	7	0	2	0	0	5
Buccinidae	15	7	2	0	0	6
Muricidae	21	3	5	1	0	15†
Conidae	8	1	1	0	0	4
Cancellariidae	9	2	3	0	0	5‡

*The genera *Erosaria*, *Luria*, and *Macrocypraea* appear in the early and late Pleistocene. †The genera *Caribiella* and *Tripterotyphis* appear in the Recent fauna and *Trachypollia* first appears in the Bermont fauna. ‡The genus *Bivetopsia* appears in the Bermont fauna.

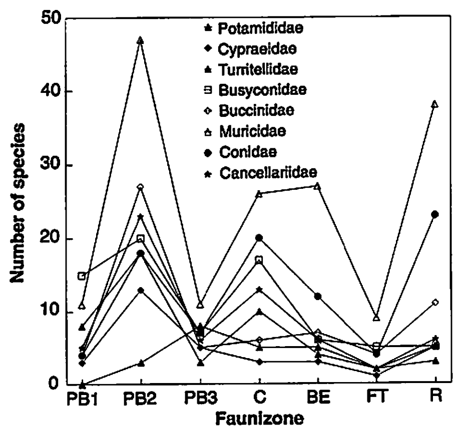

Fig. 1. Number of species in eight ecologically exclusive gastropod families, arranged geochronologically by faunizone. Data points are listed in Table 1. PB1 (3.5 Ma), PB2 (3 Ma), and PB3 (2.5 Ma) (Pinecrest Beds 1, 2, 3), late Pliocene; C (Caloosahatchee) (1.5 to 2 Ma), Plio-Pleistocene boundary and early Pleistocene; BE (Bermont) (1 Ma), middle Pleistocene; FT (Fort Thompson) (150,000 years), late Pleistocene; R, Recent Florida fauna. Dating listed under (*14*).

REFERENCES AND NOTES

1. S. M. Stanley and L. D. Campbell, *Nature* **293**, 457 (1981).
2. E. J. Petuch, *Proc. Acad. Nat. Sci. Phila.* **134**, 12 (1982).
3. S. M. Stanley, *Geology* **12**, 205 (1984).
4. ———, *Palaios* **1**, 17 (1986).
5. G. J. Vermeij and E. J. Petuch, *Malacologia* **27**, 29 (1986).
6. E. J. Petuch, *Neogene History of Tropical American Mollusks* (Coastal Education and Research Foundation, Charlottesville, VA, 1988).
7. J. B. C. Jackson, P. Jung, A. G. Coates, L. S. Collins, *Science* **260**, 1624 (1993).
8. W. D. Allmon, G. Rosenberg, R. W. Portell, K. S. Schindler, *ibid.*, p. 1626.
9. D. S. Jones and P. F. Hasson, in *The Great American Biotic Interchange*, F. G. Stehli and S. D. Webb, Eds. (Plenum, New York, 1985), pp. 325–355.
10. E. J. Petuch, *Atlas of Florida Fossil Shells (Pliocene and Pleistocene Marine Gastropods)* (The Graves Museum of Archaeology and Natural History, Dania, FL, 1994).
11. ———, in "The Neogene of Florida and adjacent regions," V. A. Zullo, W. B. Harris, T. M. Scott, R. W. Portell, Eds. (Spec. Publ. 37, Florida Geological Survey, 1993), pp. 73–85.
12. T. M. Scott in "The Plio-Pleistocene stratigraphy and paleontology of southern Florida," T. M. Scott and W. D. Allmon, Eds. (Spec. Publ. 36, Florida Geological Survey, 1992), pp. 21–25. The terms Pinecrest Beds, Caloosahatchee Formation, Bermont Formation, and Fort Thompson Formation were never formally proposed as lithostratigraphic units but are, in actuality, simply faunizones. In anticipation of a formal biozonational scheme for southern Florida, I have adopted a transitional nomenclature, referring to the previous "formations" as "faunas" within Scott's proposed "Okeechobee Formation" and within a redefined Tamiami Formation. With this scheme, the Sarasota Unit, Buckingham "Formation," the Ochopee "Member," and the Pinecrest Beds are included within the Tamiami Formation, and the Caloosahatchee "Formation," Griffin Pit Unit, Holey Land Unit, Bermont "Formation," and Fort Thompson "Formation" are included in the new Okeechobee Formation.
13. Although Allmon *et al.* (*8*) included the Pinecrest Beds as a single faunal unit, chronologically equivalent to the Caloosahatchee and Bermont Formations, recent geochronological data [D. S. Jones *et al.*, *J. Geol.* **99**, 637 (1991)] and faunal analyses (*10*) have shown that the Pinecrest Beds contain three separate sequential faunas and that the total unit is chronologically three times as large as either the Caloosahatchee, Bermont, or Fort Thompson faunizones. As shown in (*10*), Pinecrest Beds unit 10 (and the thinner units 8 and 9) contains a base set of species (essentially the same fauna as contained in the "*Ecphora* zone" of the Jackson Bluff Formation of northwestern Florida), whereas Pinecrest Beds unit 7 (and the thinner units 5 and 6) contains a separate suite of species descended from the unit 10 fauna, and Pinecrest Beds unit 3 (and also units 4 and 2) (this fauna has also been collected in the Mule Pen quarry in Naples, Collier County, Florida) contains yet another separate suite descended from the unit 7 fauna. The highly endemic Kissimmee River valley fauna is here included with the stratigraphically equivalent Pinecrest Beds.
14. On the basis of (*10*, *13*), Pinecrest Beds unit 10 is now dated at 3.5 Ma, Pinecrest Beds unit 7 at 3 Ma, Pinecrest Beds unit 3 at 2.5 Ma, the Caloosahatchee and Griffin Pit faunas at 1.5 to 2 Ma, the Bermont fauna at 1 Ma, and the Fort Thompson Fauna at 150,000 years before present.
15. E. J. Petuch, *Nautilus* **106**, 155 (1993).
16. S. M. Stanley and X. Yang, *Science* **266**, 1340 (1994).
17. R. T. Abbott, *American Seashells* (Reinhold, New York, ed. 2, 1974).

12 June 1995; accepted 16 August 1995

Geomorphically Driven Late Cenozoic Rock Uplift in the Sierra Nevada, California

Eric E. Small* and Robert S. Anderson

Geologists have long accepted that the Sierra Nevada, California, experienced significant late Cenozoic tectonically induced uplift. A flexural-isostatic model presented here shows, however, that a large fraction of the primary evidence for uplift could be generated by the lithospheric response to coupled erosion of the Sierra Nevada and deposition in the adjacent Central Valley and therefore requires less tectonic forcing than previously believed. The sum of range-wide erosion and the resultant isostatic rock uplift would have lowered Sierra mean elevation by 200 to 1000 meters since 10 million years ago and could also have increased summit elevations during the current period of relief production.

For a century, geologists have thought that the Sierra Nevada (Sierra) crest (Fig. 1) has been uplifted about 2000 m by tectonic forces in the late Cenozoic (*1–3*). This uplift event is enigmatic because it occurred 100 million years after arc-related crustal thickening in the Sierra (*4*). England and Molnar (*5*) proposed that much evidence used to infer mountain uplift, similar to that reported for the Sierra, may actually reflect either exhumation or isostatically driven rock uplift rather than tectonically driven surface uplift. In addition, they hypothesized (*6*) that much of the data interpreted as evidence for late Cenozoic uplift events could instead have been generated by global cooling, thereby challenging proposals that the reputed late Cenozoic uplift had caused global cooling (*7*).

Department of Earth Sciences and Institute of Tectonics, University of California, Santa Cruz, CA 95064, USA.

*To whom correspondence should be addressed.

Surface uplift is the change in mean elevation with respect to the geoid averaged over $>10^3$ km^2, rock uplift is displacement of individual points (rocks) with respect to the geoid, and exhumation is displacement of points with respect to the surface (*5*). These terms are related: surface uplift equals rock uplift minus exhumation. Rock uplift can be driven by tectonic forcing or by the isostatic response to exhumation. Before using any geologic data to constrain the amount of surface uplift attributable to tectonic forcing, one must first assess how much of this geologic signal was generated by exhumation and the resultant isostatically driven rock uplift. Here, we quantify what fraction of the evidence for late Cenozoic Sierra uplift was produced by these latter processes.

The primary evidence previously used to calculate the magnitude and timing of Sierra uplift was the westward tilt of markers (Fig. 2) (*1–3*), including stratigraphic horizons in the eastern Great Valley sedimentary sequence and abandoned fluvial channels filled with dated volcanic flows and alluvium along the western Sierra margin. Most studies, as well as our own, have focused on uplift north of 36.5°N because tilted markers do not exist farther south (Fig. 1). In previous studies, crestal uplift was calculated by simple linear projection of tilted markers to the crest (Fig. 2). Four assumptions were made in these studies: (i) the Sierran block rotated rigidly, (ii) there was a constant hinge line position, (iii) all tilt exceeding modern stream gradients indicates deformation, and (iv) there was no erosion (*2*, *3*). The last assumption was not explicitly stated. The tilt rate deduced from stratigraphic markers more than doubles 3 to 4 million years ago (Ma); this observation lead researchers to argue for accelerated uplift toward the present (*2*). Huber (*2*) calculated about 2000 m of crestal uplift since 10 Ma, with 1000 m of this uplift occurring since 3 Ma. This crestal uplift corresponds to a 1000-m increase in mean elevation (surface uplift) since 10 Ma if all four of these assumptions are valid. Secondary evidence used to argue for late Cenozoic uplift comes from studies of paleobotany (*8*), sediment provenance (*9*), and the depletion of deuterium in Great Basin ground water (*10*).

The tilt of western Sierra geologic markers unambiguously records differential rock uplift, with greater rock uplift occurring within the Sierra than in the adjacent Central Valley. Rock uplift could have been driven by tectonic forcing or by the isostatic response to geomorphic forcing, or both. Tilt observed at the western Sierra margin can be used to quantify tectonically driven surface uplift of the range only in the absence of exhumation (*5*), that is, when surface uplift equals rock uplift. Previous researchers have implicitly assumed that tilt indicates differential surface uplift and, therefore, that it is both tectonic in origin and has increased Sierra mean elevation. Several time-dependent tectonic mechanisms have been proposed to explain the accelerating increase in mean elevation

since 10 Ma (*11*). Debate about these mechanisms continues (*12, 13*). We hypothesize that a large fraction of the westward tilt of markers, and therefore of the differential rock uplift this tilt represents, is instead the product of upward forcing from erosion to the east and downward forcing from deposition to the west of these markers. This erosion and deposition (geomorphic forcing), and the resultant flexural-isostatic response, would certainly have lowered the mean elevation and would possibly have increased the maximum elevation of the range.

The same rock uplift that tilted markers could also have increased summit elevations. The elevation at any point will increase if erosion is slower than rock uplift, regardless of whether rock uplift is driven by erosion or tectonics. Lithospheric rigidity distributes the response to loading over a horizontal distance of 10 to 100 km; therefore, summit elevations will increase if upward lithospheric deflection from regional erosion (unloading) exceeds lowering of peaks by local erosion.

Many Sierra peaks appear to be eroding more slowly than the surrounding landscape. If true, then peak elevations could be increasing as a result of regional erosional unloading. The Sierra crest is dotted with summit flats (Fig. 1) that display slopes <10° and show no evidence of erosion by the fluvial or glacial processes that have been active in the surrounding landscape. Instead, periglacial creep is the dominant geomorphic process (*14*). The erosion of flats appears to be limited by the slow rate (*15*) at which bedrock weathering produces material transportable by this creep. Erosionally driven rock uplift only increases peak elevations during intervals of relief production, that is, when summits erode more slowly than valleys. Although it appears that Sierran relief is currently increasing because summits are capped by slowly eroding flats, no evidence suggests that flats and associated relief production have existed since 10 Ma. Because the history of relief production is unknown, we modeled the rate at which peak elevations are currently increasing as a result of erosional unloading.

We explored what fraction of the measured tilt of 10-million-year-old geologic markers could be due to the lithospheric response to geomorphic forcing. Any remaining tilt requires tectonic forcing. In our calculations, we used a one-dimensional flexural-isostatic model similar to that used in many recent studies (*16*), with loading constrained by measured Central Valley deposition and less well known magnitudes and patterns of Sierra erosion. Because the magnitude and timing of tilt is similar along the axis of the Sierra north of 36.5°N (*3*), we compared our calculated tilt to the measured tilt of a 10-million-year-old lava-filled San Joaquin River paleochannel (*2*) (Fig. 1). We also tracked changes in mean and maximum elevation along a model swath, $<z>(x)$ and $z_{max}(x)$, and changes in mean elevation over the entire model swath, $<z>_{SN}$ (*17*). Because only changes in elevation were modeled, our results are independent of both present and past topography.

The geomorphic forcing in our model has four components, of which we varied the latter three (Fig. 3): (i) Central Valley deposition, (ii) mean erosion rate, $<\varepsilon>_{SN}$, within our model swath, (iii) pattern of mean erosion rates along the swath, $<\varepsilon>(x)$, and (iv) summit flat erosion rate, ε_s. Central Valley well data were used to determine sediment thickness above an 8-million-year-old marker horizon (Fig. 3A) (*18*). We then converted this sediment thickness to a 10-million-year depositional load by assuming no deposition between 8 and 10 Ma (yielding a minimum estimate of loading during this period and, hence, a minimum estimate of related tilt), and by converting sediment thickness to rock mass using porosity-depth relations (Fig. 3B) (*19*). Apatite fission track studies indicate that $<\varepsilon>_{SN}$ over the past 15 to 30 million years has been 0.07 to 0.20 mm year^{-1} (*20*). Estimates of erosion rates from sediment mass balance and geobarometry studies in the Sierra, and from a global denudation-relief relation, support this range of values over time scales from 100 to 100 million years (*21*). We varied $<\varepsilon>_{SN}$ beyond the range suggested by these studies to illustrate fully the relation between tilt and erosional unloading. The crossing of modern and paleochannels indicates minor mean erosion at the western Sierra margin. Because no other constraints on the range-normal pattern of mean erosion rates exist, a boxcar erosional load that tapers to zero at the western range margin was used (Fig. 3B). We examined the sensitivity of our results

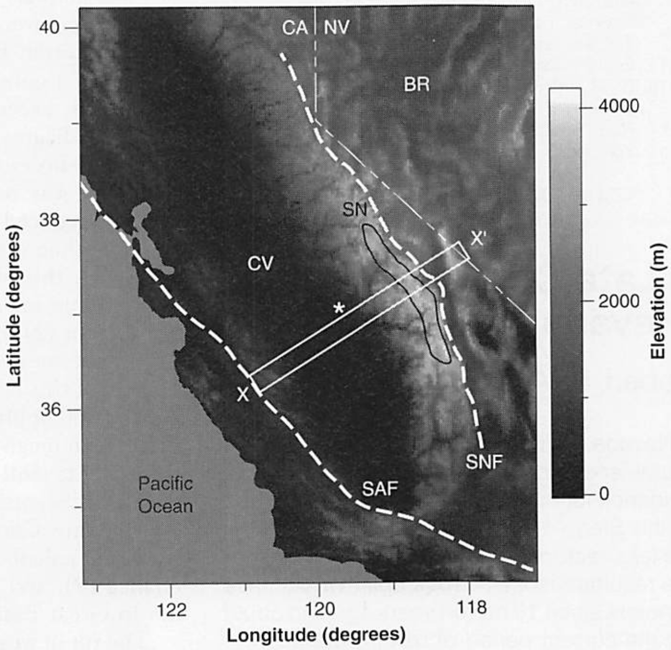

Fig. 1. Sierra Nevada topography from 30″ digital elevation model (DEM) data. The Sierra Nevada (SN) is separated from the Basin and Range (BR) province on the east by the Sierra Nevada fault system (SNF). The Central Valley (CV) bounds the Sierra on the west. Central Valley deposition does not constrain Sierra erosion because the valley has not been a closed basin continuously since 10 Ma (*31*) and has received sediment from both the Sierra and the Coast Ranges to the west. Mean and maximum elevations along a 20-km-wide range-normal swath (X-X′), from the San Andreas fault (SAF) into the Basin and Range, are shown in Fig. 3A. Tilted stratigraphic horizons and abandoned fluvial channels are common along the western Sierra margin north of 36.5°. The asterisk (*) denotes the 10-Ma San Joaquin River paleochannel. Summit flats are common at the Sierra crest (outlined area).

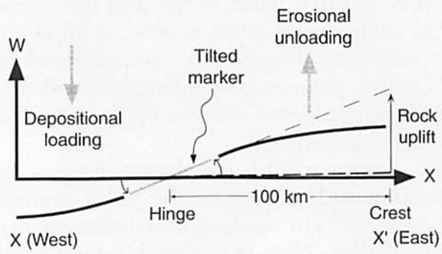

Fig. 2. Schematic of both our hypothesis for the origin of tilt of Sierra geologic markers and the method used by previous researchers to calculate uplift of the Sierra crest, after (*2*). The 10-Ma San Joaquin River paleochannel (gray line labeled "Tilted marker") is tilted 25 m/km, whereas the present stream gradient is 1 m/km through this area (thick dashed line) (*2*). Previous researchers linearly projected markers to the crest of the range to calculate uplift (thin dashed line), assuming rotation of a nearly horizontal line (thick dashed line). Upward forcing from erosion to the east and downward forcing from deposition to the west (large arrows) of markers located at the hinge line could produce the observed tilt. The resulting deformation pattern, *w*(*x*), is shown (solid line) for a case with reas onable flexural rigidity.

to three other mean erosion rate patterns (Fig. 3B). Sierra summit flats and ridgetops across the range are not datums that constrain either the magnitude or pattern of mean erosion since 10 Ma because their age and erosional history are unknown. The 10-Ma elevations at current summit flat and ridgetop locations could have been above or below the general paleotopography at that time, depending both on the pattern and magnitude of mean erosion, and on the total erosion from present summit flat and ridgetop locations since 10 Ma. As the erosion of summit flats appears to be weathering-limited (*14*), we assumed that ε_s is 0.01 mm year^{-1}, the bare granite weathering rate measured with cosmogenic radionuclides 10 km east of the Sierra crest (*15*).

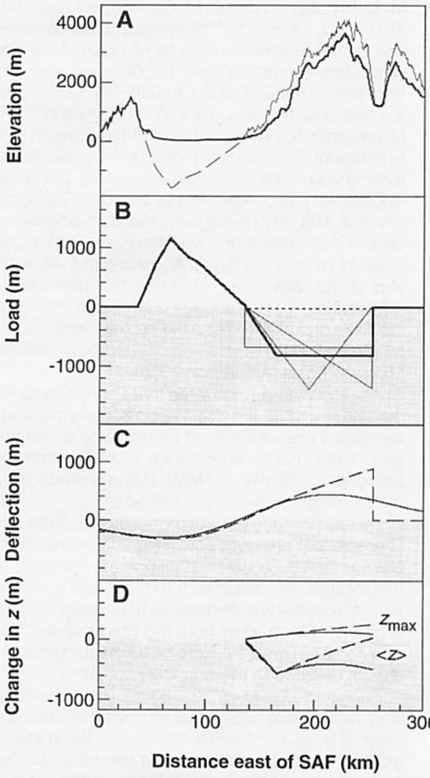

Fig. 3. (**A**) Mean (thick line) and maximum elevation (thin line) along swath X-X′ (in Fig. 1) from 3″ DEM data. The dashed line is the depth of an 8-million-year-old marker horizon in the Central Valley (*18*). (**B**) Thickness of positive depositional load in the Central Valley and of the tapered boxcar erosional load in the Sierra, with density ρ_c = 2700 kg/m^3 (thick line) (*32*). All three other erosion patterns examined (thin lines) and the tapered boxcar have equal mean erosion rates, $<\varepsilon>_{SN}$ = 0.07 mm year^{-1} for 10 million years. Where summit flats exist along the swath, local erosion lowers peaks by 0.01 mm year^{-1}, or a total of 30 m if flats have persisted since 3 Ma (dashed line). (**C**) Deflection from tapered boxcar and Central Valley loading in (B) for a continuous (solid line) and broken lithosphere (dashed line) of T_e = 30 km. The density contrast between crust and mantle is −500 kg/m^3 (we assume a mantle density ρ_m of 3200 kg/m^3). The discontinuity is the break at the Sierra Nevada fault. (**D**) Changes in mean elevation ($<z>$) for continuous (solid) and broken (dashed) lithosphere as a result of the sum of tapered boxcar erosion in (B) and the lithospheric response to this loading in (C). The sharp trough in mean elevation change (at 160 km) is caused by the corner in the tapered boxcar erosion pattern. Changes in maximum elevation (z_{max}) are due to the sum of summit flat erosion in (B) and deflection from the boxcar load in (C), for summit flats that have persisted since 3 Ma.

We modeled the lithospheric response to this geomorphic forcing as that of a thin, uniformly rigid elastic plate overlying a viscous substrate (*22*). The effective elastic thickness, T_e, and the lateral boundary conditions control the lithospheric response to distributed loads. Flexural subsidence modeling indicates that T_e in the southern Central Valley has been about 20 km over the past 10 million years (*18, 23*). We examined the sensitivity of our results to a range of T_e's bracketing this value and also performed all model runs with the lithosphere both broken and continuous across the Sierra Nevada fault (SNF), representing end-member calculations for how vertical shear and fiber stresses are transmitted across this edge of the Basin and Range province (*24*).

The tilt and elevation changes were calculated by summing erosion and lithospheric deflection, w, at every position along the model swath, x (Fig. 3). Tilted markers exist only where there has been no erosion since the marker was emplaced. Because markers are not eroded, changes in their elevation are due solely to the total local deflection since they were emplaced 10 Ma. It follows that the tilt of a marker is equal to the local gradient in deflection, dw/dx. Markers at the western Sierra margin are tilted up to the east because the deflection gradient is positive in that direction (Fig. 3C). The change in mean elevation at any section along our swath is the sum of the total mean erosion [the product of $<\varepsilon>(x)$ with an elapsed time, t, of 10 million years] and the total deflection since 10 Ma at that x position [$\Delta<z>(x) = <\varepsilon>(x)t + w(x)$] (Fig. 3D). Because eroded crust is less dense than the underlying mantle asthenosphere, the combined effects of mean erosion and deflection lower the mean elevation of the entire swath, $<z>_{SN}$. Along the Sierra crest where slowly eroding summit flats exist, the rate of change of maximum elevations is the sum of the local erosion rate, ε_s, and the deflection rate [total deflection divided by the elapsed time (10 million years)] at the crest [$dz_{max}(\text{crest})/dt = \varepsilon_s + w(\text{crest})/t$] (Fig. 3D). Upward deflection from regional unloading is greater than the lowering of summit flats by local erosion, resulting in increases in maximum elevation (Fig. 3D).

Our results show that a large percentage of the observed tilt of 10-Ma geologic markers can be generated solely by geomorphic forcing and the resulting lithospheric response (Fig. 4A). For the expected range of $<\varepsilon>_{SN}$ and T_e (gray boxes in Fig. 4), the amount of tilt produced by geomorphic forcing varies from 40 to 140% of that observed. This result suggests that tectonic forcing produced <60%, and perhaps none, of the differential rock uplift recorded by tilted markers. Previous estimates of the amount of tectonic rock uplift therefore

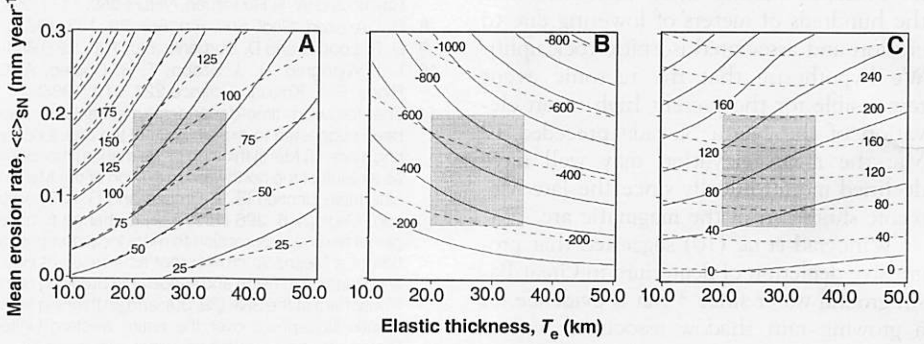

Fig. 4. (**A**) Lines of equal calculated tilt at the western Sierra margin, shown as a percent of observed tilt (*2*), due to geomorphic forcing (tapered boxcar) and lithospheric response over 10 million years, as a function of $<\varepsilon>_{SN}$ and T_e. Continuous lithosphere calculations are shown with solid lines, broken lithosphere with dashed lines [same in (B) and (C)]. A value of 100% indicates that the calculated tilt equals the observed tilt of the 10-Ma San Joaquin River channel. Values less than 100% indicate that the calculated tilt is less than the observed tilt. The shaded rectangle represents the most likely values of $<\varepsilon>_{SN}$ and T_e for the Sierra since 10 Ma [same in (B) and (C)] (*18, 20, 21*). When $<\varepsilon>_{SN}$ = 0.0, tilt is driven solely by Central Valley deposition. (**B**) Lines of equal calculated mean elevation change (in meters), $<z>_{SN}$, from the sum of modeled erosion and associated rock uplift over 10 million years, as a function of $<\varepsilon>_{SN}$ and T_e. Note that all values are negative, indicating that geomorphic forcing would lower the mean elevation since 10 Ma. (**C**) Lines of equal rate of change of maximum elevation (meters per million years) for peaks with slowly eroding summit flats (for $<\varepsilon>_s$ = 0.01 mm year^{-1}). All values are positive. For every increase of 0.01 mm year^{-1} in $<\varepsilon>_s$, the rate of peak elevation change decreases by 10 m per million years for any combination of $<\varepsilon>_{SN}$ and T_e.

appear to be too high (*1–3*). Even in the extreme minimum case of no Sierra erosion since 10 Ma ($<\varepsilon>_{SN}$ = 0.0 mm year^{-1}), the well-documented Central Valley deposition alone would still have generated about 25% of observed tilt (Fig. 4A). Modeled tilt at the western Sierra margin is similar for both continuous and broken lithosphere cases because markers recording tilt are far enough away from the SNF that the boundary condition applied there does not alter the local deflection pattern (Fig. 3C). Poor constraints on the mean erosion pattern do not detract from our conclusions because modeled tilt is insensitive to the details of this pattern, especially when $T_e \geq 25$ km. Results in Fig. 4 were generated with the tapered boxcar pattern (Fig. 3B), which either produces a minimum estimate of tilt or is within 5% of the minimum, from among the four erosion rate patterns examined for all reasonable $<\varepsilon>_{SN}$ and T_e (*25*).

Concomitant with tilting generated by geomorphic forcing is a 200- to 1000-m decrease in mean elevation of the entire model swath, $<z>_{SN}$, depending on $<\varepsilon>_{SN}$, T_e, and the lateral lithospheric boundary conditions (Fig. 4B). The modeled mean elevation decrease is less for a broken lithosphere because this boundary condition promotes a more local, rather than regional, isostatic response to erosion near the SNF and, hence, results in more rock uplift within the range. The total change in Sierra mean elevation since 10 Ma is the sum of elevation changes from geomorphic and tectonic processes. Therefore, Sierran mean elevation should have decreased over the past 10 million years unless tectonic forcing, for which there is no evidence besides tilted markers, offset the hundreds of meters of lowering due to erosion and associated isostatic rock uplift. We hypothesize that the tectonic event responsible for the present high mean elevation of the Sierra Nevada preceded 10 Ma; the mean elevation may well have declined monotonically since the late Mesozoic shutdown of the magmatic arc.

Winograd *et al.* (*10*) suggested that progressive depletion of deuterium in Great Basin ground water since 3 Ma is evidence for a growing rain shadow associated with a several hundred meter rise in the Sierra crest. Our modeling suggests that the elevations of Sierra peaks capped by slowly eroding flats are currently increasing by 30 to 200 m per million years because of geomorphic forcing and associated isostatic flexure (Fig. 4C). Unlike our tilt calculations, the modeled rate of peak elevation increase is less well constrained because it is sensitive to all input variables, in particular the lithospheric boundary condition at the SNF (*26*). For the continuous lithosphere case, which provides a minimum estimate of peak elevation increase, summit elevations would still have risen 100 to 500 m since 3 Ma (*27*) if the current rate of relief production persisted throughout this interval. It therefore seems plausible that geomorphically driven uplift of the Sierra crest could have produced the intensified orographic effect inferred from Great Basin ground water studies (*10*).

If geomorphic forcing is responsible for a large fraction of the observed tilt since 10 Ma, then accelerated tilt recorded by markers could be due to increased erosion rates rather than intensified tectonic forcing (*2*). The increase in Sierra tilt rate about 3 Ma is roughly coeval with the global cooling event responsible for Northern Hemisphere continental ice sheet growth (*28*). It seems likely that the onset of Sierra alpine glaciation also occurred about 3 Ma. This onset would have enhanced the rates of erosional unloading of the range and associated depositional loading of the Central Valley, producing the accelerated tilt rates recorded by markers. If this scenario is correct, then our results support Molnar and England's (*6*) notion that evidence being used to infer tectonic uplift may instead be an effect of, and hence evidence for, global cooling.

REFERENCES AND NOTES

1. J. LeConte, *Am. J. Sci.* **32**, 168 (1886); W. Lindgren, *U.S. Geol. Surv. Prof. Pap. 73* (1911); M. N. Christensen, *Geol. Soc. Am. Bull.* **77**, 163 (1966).
2. N. K. Huber, *U.S. Geol. Surv. Prof. Pap. 28* (1981); *Geol. Soc. Am. Bull.* **102**, 102 (1990).
3. J. R. Unruh, *Geol. Soc. Am. Bull.* **103**, 1395 (1991).
4. P. C. Bateman and J. P. Eaton, *Science* **158**, 1407 (1967).
5. P. England and P. Molnar, *Geology* **18**, 1173 (1990).
6. P. Molnar and P. England, *Nature* **346**, 29 (1990).
7. M. E. Raymo, W. F. Ruddiman, P. N. Froelich, *Geology* **16**, 649 (1988); W. F. Ruddiman and J. E. Kutzbach, *J. Geophys. Res.* **94**, 18409 (1989); M. E. Raymo and W. F. Ruddiman, *Nature* **359**, 117 (1992).
8. D. I. Axelrod, *Geol. Soc. Am. Bull.* **73**, 183 (1962).
9. D. P. Loomis and D. Burbank, *ibid.* **100**, 12 (1988).
10. I. J. Winograd, B. J. Szabo, T. B. Coplen, A. C. Riggs, P. T. Kolesar, *Science* **227**, 519 (1985).
11. The following time-dependent mechanisms have been suggested to explain uplift of the Sierra occurring since 10 Ma: (i) thinning of the mantle lithosphere as a result of the northward migration of the Mendocino triple junction [S. T. Crough and G. A. Thompson, *Geology* **5**, 396 (1977)]; (ii) a change from regional flexural suppression to more local compensation of a Mesozoic crustal root as a result of Basin and Range extension and associated breaking of the lithosphere at the SNF (*29, 30*); and (iii) thinning of the mantle lithosphere over the entire western United States, driving a Cordilleran-wide uplift event (*3*).
12. C. H. Jones and H. Kanamori, *J. Geophys. Res.* **99**, 4567 (1994).
13. E. Shalev and P. E. Malin, *Eos* **75** (fall suppl.), 584 (1994).
14. E. E. Small and R. S. Anderson, unpublished data.
15. P. R. Bierman, *J. Geophys. Res.* **99**, 13885 (1994).
16. F. Pazzaglia and T. Gardner, *ibid.*, p. 12143; H. Kooi and C. Beaumont, *ibid.*, p. 12191; and others in the same volume.
17. Swath width does not affect the model results. A swath is used, instead of a single line, because it allows illustration of the changes in both mean and maximum elevation and is also representative of the area over which tectonic and flexural processes act.
18. M. S. Rentschler and R. B. Bloch [in *Studies of the Geology of the San Joaquin Basin: Pacific Section Soc. Econ. Paleontol. Mineral.*, S. A. Graham, Ed. (Pacific section of the Society of Economic Paleontologists and Mineralogists, Los Angeles, CA, 1988), vol. 60, pp. 29–52] used the top of the Santa Margarita sequence as an 8-Ma marker horizon, based on a 6.5 to 7.5 Ma diatom zone at the base of the overlying Etchegoin formation. We used California Department of Oil and Gas oil well log summaries to determine the depth to the top of the Santa Margarita sequence in our swath.
19. J. G. Sclater and P. A. F. Christie, *J. Geophys. Res.* **85**, 3711 (1980).
20. T. A. Dumitru, *ibid.* **95**, 4925 (1990).
21. M. N. Christensen and C. M. Gilbert [*Geol. Soc. Am. Abstr. Prog.* **2**, 81 (1970)] reported mass balance–based erosion rates from the Mono Basin of 0.5 mm year^{-1} between 30,000 and 10,000 years ago, and from behind the SNF of 0.1 to 0.25 mm year^{-1} over the past several million years. W. D. Page and W. R. Noryko [*ibid.* **9**, 479 (1977)] reported a minimum erosion rate of 0.01 to 0.02 mm year^{-1} by calculating missing volume beneath a dated lava flow. Using paleobarometry, J. J. Ague and G. Brimhall [*Geol. Soc. Am. Bull.* **100**, 912 (1988)] demonstrated exhumation rates of >0.1 mm year^{-1} over the past ~100 million years for most of the Sierra. According to F. Ahnert's [*Am. J. Sci.* **268**, 243 (1970)] empirical denudation-relief relation, $<\varepsilon>_{SN}$ should be >0.2 mm year^{-1}, on the basis of present relief in the central Sierra.
22. M. Hetenyi, *Beams on Elastic Foundation* (Univ. of Michigan Press, Ann Arbor, 1946).
23. Chase and Wallace calculated that T_e in the region of our swath was 55 km (*29*). We do not use this value because it was determined by modeling of the upward force due to 60-km-thick crust beneath the Sierra, which Shalev and Malin (*13*) and others have more recently shown to be ~35 km.
24. Chase and Wallace (*29, 30*) proposed that shear and fiber stresses are not transmitted across the Sierra Nevada fault because the lithosphere is "broken" at that location. We assumed the lithosphere is continuous across the San Andreas fault; because the fault is about 140 km away from the tilted markers and about 220 km away from the Sierra crest, our results are not sensitive to this boundary condition.
25. For unreasonably low T_e (≤15 km), the wedge erosion pattern (Fig. 3B) generates less tilt than the tapered boxcar (>5% difference). For these low rigidities, most of the observed tilt can be generated by any of the erosion patterns examined (Fig. 4A).
26. Because the Sierra crest is within 10 to 20 km of the SNF, the amount of rock uplift at the crest, and therefore the rate of summit elevation increase, due to erosional unloading for the broken lithosphere case is nearly two times that of the continuous lithosphere case (Fig. 4C).
27. D. R. Montgomery [*J. Geophys. Res.* **99**, 13913 (1994)] calculated that Sierra peak elevations would rise a maximum of 200 m since 10 Ma as a result of erosional unloading. This calculation was not a true maximum for two reasons: (i) his assumed 10-Ma paleotopography was not an envelope at the elevation of the highest peaks, and therefore did not maximize erosional unloading with respect to the highest peaks; and (ii) his use of local isostatic compensation did not allow for the possibility that rapid erosion within the range could have driven elevation increases at the crest.
28. R. Tiedemann, M. Sarnthein, N. Shackleton, *Paleoceanography* **9**, 619 (1994).
29. C. G. Chase and T. C. Wallace, *Geology* **14**, 730 (1986).
30. ———, *J. Geophys. Res.* **93**, 2795 (1988).
31. A. J. Bartow, *U.S. Geol. Surv. Prof. Pap. 1501* (1991).
32. H. W. Oliver, J. G. Moore, R. F. Sikora, *Geophys. Res. Lett.* **20**, 2179 (1993).

30. We thank L. Abbott and two anonymous reviewers for constructive criticisms. Supported by the Topography and Surface Change Program of the National Aeronautics and Space Administration, a National Defense Science and Engineering graduate fellowship to E.E.S., and by a Presidential Young Investigator Award from NSF to R.S.A.

21 February 1995; accepted 27 July 1995

Pseudotachylites Generated in Shock Experiments: Implications for Impact Cratering Products and Processes

Peter S. Fiske,* William J. Nellis, Magnus Lipp, Hector Lorenzana, Masae Kikuchi, Yasuhiko Syono

Laboratory hypervelocity impact experiments in which quartz was shock-loaded from 42 to 56 gigapascals imply that type A pseudotachylites form by strain heating and contribute to the loss of strength of rocks in the central uplift of large impact structures. Shock impedance–matched aluminum sample containers, in contrast to steel containers, produced nearly single-wave pressure loading, and enhanced deformation, of silicate samples. Strain heating may act with shock heating to devolatilize planetary materials and destroy extraterrestrial organic material in an impact.

Meteorite impact is the most cataclysmic planetary geologic process operating in our solar system. During the formation of an impact crater, rocks are subjected to enormous transient pressure and deformation causing phase transitions, melting, and vaporization. Large impacts produce a transient cavity in the crust that immediately rebounds, forming a flat-floored crater with a central peak, or in the case of the largest impacts, a multi-ring basin.

Some impact-induced features that occur in rocks from both large and small craters have been synthesized in laboratory shock experiments (*1*). Other features found in abundance only in larger impact structures, such as shatter cones and pseudotachylites (a fine-grained, dark gray or black rock that resembles tachylite, a volcanic glass) (*2*), are difficult to reproduce in laboratory shock experiments, suggesting a significant dependence on scale. Although the pressures experienced by rocks in small and large impacts are comparable, the principal difference is in the amount of strain to which the rocks are subjected. Laboratory experiments have simulated the pressure but not the strain produced by impact. To investigate the origin of strain heating and the production of pseudotachylites, we have conducted a series of experiments using shock recovery systems that enable us to vary the strain experienced by the sample during shock loading. We produced glassy veins of black material in quartz that are analogous to pseudotachylites found in the central portion of large impact craters.

Pseudotachylites are bodies of melted and pulverized rock formed in situ by frictional melting and are found in large impact structures (*3*) and along some tectonic faults (*4*). Workers have identified two varieties of impact pseudotachylites that differ in size and timing of formation (*5*). Type B pseudotachylites are large dike- or sill-like masses (centimeters to several hundred meters in width and up to kilometers in length) and commonly occur along discrete faults. They are analogous to, though usually larger than, tectonic pseudotachylites and are formed by frictional heating as a result of large amounts of slip along a fault surface. Type B pseudotachylites have been produced experimentally with the use of friction-welding devices (6), demonstrating that friction melts in rock can be produced by high-speed slip along a fault surface. At the Sudbury impact structure, type B pseudotachylites (known as Sudbury Breccia) define the basin-bounding rings of the structure (*7*).

Type A pseudotachylites are smaller (<1 mm to several millimeters in width) and are found mainly in bedrock exposed in the central parts of large impact structures. They form a distinctive network of veins throughout the rock rather than occurring along discrete fault surfaces. In some cases, type A pseudotachylites are found along the surface of shatter cones (8). Martini reported that small type A pseudotachylites in quartzite from the Vredefort impact structure in South Africa contain coesite and stishovite (9). Disrupted clasts of rock containing type A pseudotachylite have also been observed in dikes of type B pseudotachylite (*5*). These features suggest that type A pseudotachylites form before type B pseudotachylites during the initial compression and excavation of the crater (*7*), but their exact mechanism of formation, and the implications for impact cratering, have not been well understood.

To achieve production of pseudotachylites, we used a sample capsule similar in geometry to those used in earlier studies (*10*) but made of aluminum instead of steel. The sample and capsule were contained by a large fixture made of a strong titanium alloy (*11*). Aluminum, with a density of 2.7 g/cm^3, has a shock impedance much closer to that of silicates (in this case quartz, density 2.65 g/cm^3) than to that of steel. The shock impedance match produces nearly a single loading pulse in the sample, rather than a reverberation or "ring-up" to high pressure, as for steel capsules. This single-wave loading produces a greater rise in temperature than the quasi-isentropic loading of a ring-up experiment and we believe more realistically approximates the single-shock pressure rise during meteorite impact. Lateral deformation of the sample takes place on release from high pressure, analogous to the deformation that occurs during the excavation stage of crater development. Despite being held in the strong Ti-alloy fixture, samples held in Al capsules undergo more than three times the radial strain of samples held in steel (*12*) and shocked to the same pressure.

We enclosed disks of synthetic high-purity cross-cut single crystal quartz [used in previous studies including (*10*)] in Al and steel capsules and shock-loaded the samples to 42 to 56 GPa (*13*) using the 6.5-m two-stage light gas gun at Lawrence Livermore National Laboratory. Samples recovered from Al capsules consisted of transparent amorphous SiO_2 cut by radial and concentric veins filled with a black glassy material (Fig. 1, A and B). The transparent regions of the sample show variable low birefringence under cross-polarized light indicating significant residual strain in the amorphous material. The regions with the highest birefringence have the densest spacing of veins. Overall, the density of veins increased with pressure. In contrast, a sample shock-loaded to 56 GPa in steel capsules was transparent throughout, showed no birefringence under cross-polarized light, and had only a few small, irregular fractures localized in the central portion of the sample (Fig. 1C). The total radial strain (*13*) of the 56-GPa sample held in Al was 60%, whereas it was only 20% for the sample held in steel and shock-loaded to the same pressure.

Analyses of the samples by x-ray diffraction and Raman spectroscopy showed that the black glass consists of a mixture of nanocrystalline Al (derived from the capsule) and Si and amorphous SiO_2. The amount of Si and Al increased with pressure, and the highest pressure sample contained 1 to 2% Si by weight (*14*). Transmission electron microscopy (TEM) images and electron diffraction patterns confirmed the presence of Si and Al crystallites, along with some crystalline Al_2O_3, and showed that the Si and Al occur as round clasts 10 to 400 nm in size in a matrix of amorphous

P. S. Fiske, W. J. Nellis, M. Lipp, H. Lorenzana, L-413, Lawrence Livermore National Laboratory, Livermore, CA 94550, USA.
M. Kikuchi and Y. Syono, Institute for Materials Research, Tohoku University, Katahira 2-1-1, Aoba-ku Sendai 980-77, Japan.

*To whom correspondence should be addressed.

SiO_2 (Fig. 2) (*15*). Raman spectra showed that the clear parts of the sample consist of diaplectic glass similar to that observed in studies of shocked quartz (*16*). The paucity of Al_2O_3 in the black glass and the absence of any detectable molecular oxygen indicates that much of the oxygen liberated by the dissociation of SiO_2 is unaccounted for. The melting of SiO_2 provides a lower limit on the temperature of the pseudotachylite in our experiments (2000 K at 1 bar), and these temperatures are similar to those required to reduce SiO_2 in soils struck by lightning (*17*).

The black glass veins made in our experiments are analogous to type A pseudotachylites found in large impact structures. Compression and development of a hemispherical transient crater cavity during meteorite impact involves bulk plastic deformation comparable to that created in these experiments but for much longer times (10^{-3} to 10^{0} s as compared with 10^{-6} s in these experiments). The rocks closest to ground zero undergo the largest amount of strain, which may explain why type A pseudotachylites are found principally in and around the central uplifts of large craters. Rebound of the crater floor and formation of the central peak or multiple rings involves significant displacement along faults rather than bulk plastic flow, explaining the production of type B pseudotachylites in discrete zones which postdate type A pseudotachylites (*7*).

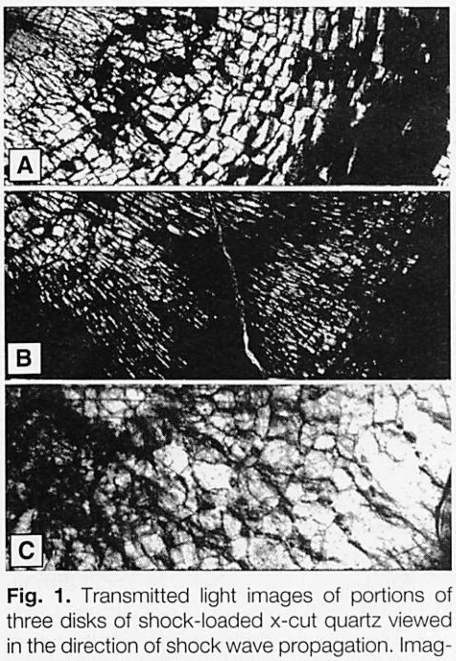

Fig. 1. Transmitted light images of portions of three disks of shock-loaded x-cut quartz viewed in the direction of shock wave propagation. Images are 7 by 2 mm. The center of each disk is in the upper left corner, and the edge is in the lower right corner. (**A**) Shock-loaded to 42 GPa in Al. The sample consists of clear regions of amorphous SiO_2 cut by radial and concentric veins filled with black glass. (**B**) Shock-loaded to 56 GPa in Al. The density of veins and the amount of crystalline Si increase with pressure. This sample contains 1 to 2% Si by weight. (**C**) Shock-loaded to 56 GPa in steel. Sample is optically clear with a few irregular fractures in the center of the disk. No Si was detected in this sample.

Plastic deformation and the production of pseudotachylites may be an important process in meteorite impacts. Our highest pressure sample contained 1 to 2% crystalline Si by weight. TEM images suggest that the Si represents roughly 10 to 20% of the volume of black glass produced. Thus, 5 to 20% of the total sample consisted of pseudotachylite melt at a minimum temperature of 2000 K. This would substantially elevate the residual temperature of the entire sample. The formation of dense networks of type A pseudotachylites in the central portions of impact structures may similarly leave the rocks substantially hotter than predicted from Hugoniot data or postshock temperature measurements of bulk materials (*18*). If strain heating is important, as these experiments imply, the central portions of large impact structures may have a substantial static thermal metamorphic overprint. Such a feature has been reported in the rocks from the Vredefort impact structure in South Africa but has been attributed to endogenic processes (*19*). Friction-induced melting may also add to the total volume of impact melt in larger craters and may explain the reported increase in the proportion of impact melt with crater size (*20*).

Shock wave profile measurements show that when quartz is shock-loaded above the Hugoniot elastic limit (12 GPa), it is virtually strengthless on release from high pressure (*21*). The formation and persistence of melt veins may be a principal contributor to the loss of strength on pressure release (*21*). If so, the formation of type A pseudotachylites during compression and crater excavation may substantially weaken the basement rock in the center of the crater.

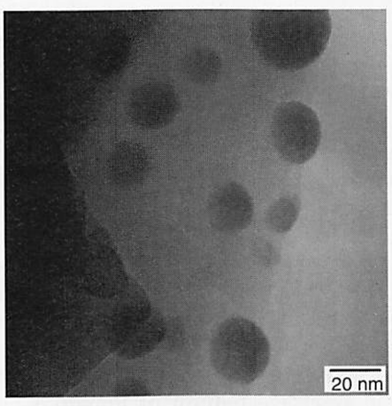

Fig. 2. Transmission electron microscope image of the black glass formed in quartz shock-loaded to 46 GPa in Al. The black glass consists of spheres of crystalline Si and Al (which appear darker) in a matrix of SiO_2 glass. Crystallites observed by TEM range in size from 20 to 400 nm.

Finally, plastic flow and the formation of pseudotachylites might affect estimates of shock devolatilization of planetary materials on the basis of shock experiments. Experiments using steel capsules (*22*) may have prevented significant strain of the sample, thus producing lower temperatures and an underestimation of the amount of shock devolatilization with pressure. Similarly, numerical modeling of cometary impacts (*23*) may underestimate the role of strain heating in the projectile and thus may overestimate the potential for delivery of organic material by impact.

REFERENCES AND NOTES

1. For a review, see B. M. French and N. M. Short, Eds., *Shock Metamorphism of Natural Materials* (Mono, Baltimore, 1968).
2. The term pseudotachylite was first used by S. J. Shand [*Q. J. Geol. Soc. London* **72**, 198 (1916)] to describe rocks from the Vredefort impact structure in South Africa.
3. For example P. S. Fiske, R. B. Hargraves, T. C. Onstott, C. Koeberl, S. Hougen, in *Large Meteorite Impacts and Planetary Evolution*, B. O. Dressler, R. A. F. Grieve, V. L. Sharpton, Eds. (Geological Society of America, Boulder, CO, 1994), vol. 293, pp. 163–176.
4. For example, R. H. Sibson, *Geophys. J. R. Astron. Soc.* **43**, 775 (1975).
5. P. Lambert, in *Multi-Ring Basins*, P. H. Schultz and R. B. Merrill, Eds. (Pergamon, New York, 1981), vol. 12A, pp. 59–78.
6. J. G. Spray, *J. Struct. Geol.* **9**, 49 (1987).
7. ______ and L. M. Thompson, *Nature* **373**, 130 (1995).
8. J. E. J. Martini, *Earth Planet. Sci. Lett.* **103**, 285 (1991).
9. ______, *Nature* **272**, 715 (1978).
10. A. J. Gratz *et al.*, *Phys. Chem. Min.* **19**, 267 (1992).
11. The alloy Ti-6%Al-4%V is 45% lighter than 304 steel and has a tensile strength 40% greater. Some of these experiments were done by chilling the sample fixture to 100 K, which caused brittle failure of the outer Ti alloy fixture during release thereby producing an effective momentum trap. See P. Cordier *et al.* [*Phys. Chem Min.* **21**, 133 (1994)] for details.
12. The total strain was determined by measuring the initial and final diameter (D) of each sample. Strain was calculated as [(final D − initial D)/initial D)].
13. Shock pressures were generated by the impact of a 2- or 3-mm-thick Cu or Al impactor at velocities up to 4 km/s. Peak shock pressures were calculated by the impedance match method for the projectiles and the sample capsules. Samples were removed, mounted in epoxy, and polished. The entire sample was recovered in every experiment. Fifteen experiments were done for this study.
14. Concentrations of Si, Al, and Al_2O_3 were estimated from x-ray diffraction scans by comparisons to standards made from quartz glass with various amounts of Si, Al, and Al_2O_3. These experiments showed that the detection limit for Al_2O_3 was 1% by weight.
15. The formation of Si has been reported in a few other shock experiments in which the chemical reaction of SiO_2 with a reducing metal was involved. C. Jammes *et al.* [*Lunar Planet. Sci.* **14**, 347 (1983)] report the presence of Si and Al_2O_3 in the products of impact experiments with Al spheres and a quartz sand target. The presence of Si and Ta_2O_5 in an 800-nm reaction layer at the interface of quartz held in Ta capsules and shocked above 67 GPa was reported by M. Kikuchi *et al.* [*J. Mat. Sci. Lett.* **6**, 97 (1987)].
16. P. F. McMillan, G. H. Wolf, P. Lambert, *Phys. Chem. Min.* **19**, 71 (1992).
17. E. J. Essene and D. C. Fisher, *Science* **234**, 189 (1986).
18. S. A. Raikes and T. J. Ahrens, *Geophys. J. R. Astron. Soc.* **58**, 717 (1979).

19. W. Schreyer, *J. Petrol.* **24**, 26 (1983).
20. R. A. F. Grieve and M. J. Cintala, *Meteoritics* **27**, 526 (1992).
21. D. E. Grady, *J. Geophys. Res.* **85**, 913 (1980).
22. For example, G. Chen, J. A. Tyburczy, T. J. Ahrens, *Earth Planet. Sci. Lett.* **128**, 615 (1994); J. A. Tyburczy, R. V. Krishnamurthy, S. Epstein, T. J. Ahrens, *ibid.* **98**, 245 (1990); A. Deutsch, I. Martinez, U. Schärer, *Eos Trans. Am. Geophys. Union* **75**, 188 (1994).
23. C. F. Chyba, P. J. Thomas, L. Brookshaw, C. Sagan, *Science* **249**, 366 (1990).
24. We thank N. Hinsey for performing the gas gun experiments. TEM work was carried out at the High Resolution Microscopy Laboratory of Tohoku University. Work at Lawrence Livermore National Laboratory was performed under the auspices of the U.S. Department of Energy under contract number W-7405-Eng-48.

12 June 1995; accepted 16 August 1995

Role of Transcriptional Activation of IκBα in Mediation of Immunosuppression by Glucocorticoids

Robert I. Scheinman,* Patricia C. Cogswell, Alan K. Lofquist,† Albert S. Baldwin Jr.‡

Glucocorticoids are potent immunosuppressive drugs, but their mechanism is poorly understood. Nuclear factor kappa B (NF-κB), a regulator of immune system and inflammation genes, may be a target for glucocorticoid-mediated immunosuppression. The activation of NF-κB involves the targeted degradation of its cytoplasmic inhibitor, IκBα, and the translocation of NF-κB to the nucleus. Here it is shown that the synthetic glucocorticoid dexamethasone induces the transcription of the IκBα gene, which results in an increased rate of IκBα protein synthesis. Stimulation by tumor necrosis factor causes the release of NF-κB from IκBα. However, in the presence of dexamethasone this newly released NF-κB quickly reassociates with newly synthesized IκBα, thus markedly reducing the amount of NF-κB that translocates to the nucleus. This decrease in nuclear NF-κB is predicted to markedly decrease cytokine secretion and thus effectively block the activation of the immune system.

Glucocorticoids (GCs) have been used for decades as clinical tools to suppress both the immune response and the processes of inflammation (*1*), yet the immunosuppressive mechanism by which these drugs act is poorly understood. GCs bind to a cytoplasmic glucocorticoid receptor (GR), a member of the steroid hormone receptor superfamily, which then translocates to the nucleus as a transcription factor (*2*). Transcriptional activation of cytokine and cell adhesion genes is critical in the activation of the immune and inflammation systems and is repressed by GCs (*3*). GC repressive elements, however, have not been found in cytokine promoters. In addition, the GR is able to repress the transcription factor AP-1 through a cross-coupling mechanism (*4*), yet AP-1 regulates only a small number of GC-sensitive cytokine promoters. GCs can also repress members of the NF-κB–Rel transcription factor family (*5, 6*). NF-κB–responsive elements are required for the function of many cytokine promoters (*7*), and NF-κB–responsive elements in the interleukin-6 (IL-6) and IL-8 promoters have been implicated in GC-mediated suppression (*5*). A major form of NF-κB is composed of a dimer of p50 and p65 (RelA) subunits, and this complex is retained in the cytoplasm by repressor molecules that contain ankyrin repeat motifs (*7*). These inhibitory molecules include the IκB family: IκBα, β, and γ, as well as the NF-κB precursor molecules p105 (NF-κB1) and p100 (NF-κB2) (*7–9*). Although a cross-coupling mechanism of inhibition exists between NF-κB and the GR (*5, 6*), it cannot fully explain the ability of GCs to inhibit NF-κB. Here it is shown that GCs induce the transcription of the gene encoding IκBα. The increase in IκBα mRNA results in increased IκBα protein synthesis, which effectively inhibits NF-κB activation.

We initiated this study by extending our analysis of the ability of the synthetic GC dexamethasone (DEX) to block the induction of NF-κB–like DNA binding activities in several cell types and by several different inducers. As shown previously (*6*), DEX blocks the induction of NF-κB by tumor necrosis factor α (TNF-α) in HeLa cells (Fig. 1A, left panel) as well as induction by IL-1 (*10*). The identity of this complex as NF-κB was determined by supershift experiments (*10*). DEX inhibited the induction of NF-κB in the monocytic cell line THP-1, mediated by TNF-α (Fig. 1A, middle panel) and by lipopolysaccharide (LPS) (*10*). DEX also inhibited the TNF-α–mediated induction of NF-κB in the murine T cell hybridoma 2B4 (Fig. 1A, right panel). In addition, thymocytes and lymph nodes derived from mice treated with monoclonal antibody (mAb) to CD3 in combination with DEX no longer express NF-κB activity as compared with mice treated with CD3 mAb alone (*11*). This effect of DEX requires protein synthesis, as it is blocked by cycloheximide (CHX) (Fig. 1A, right panel). DEX treatment results in a reduction in NF-κB–mediated gene expression as measured by transfected reporter constructs (*5, 6, 11*). Previous work indicated that the inhibition of NF-κB was the result in part of a decrease in nuclear translocation after stimulation with TNF-α.

We wanted to determine if the DEX-mediated reduction of nuclear p65 translocation, after TNF-α stimulation, correlated with an increase in IκBα. IκBα is rapidly degraded after TNF-α addition (*7, 12*) (Fig. 1B, top left panel) and this loss correlates with the appearance of nuclear p65 (Fig. 1B, bottom left panel). After 1 hour in the presence of TNF-α, IκBα protein begins to reappear as a result of the induction of gene transcription by NF-κB (Fig. 1B, top panel, lane 5). After pretreating HeLa cultures with DEX, we observed a small but measurable increase in IκBα protein (Fig. 1B, top panels; compare lanes 1 and 6). The average increase in IκBα protein was measured as 1.5-fold ($n = 10$). DEX pretreatment had no effect on cytoplasmic p65 amounts (*10*). In addition, DEX pretreatment slowed the disappearance of IκBα mediated by TNF-α. After 1 hour of TNF-α treatment, the amount of translocated nuclear p65 was reduced approximately 50% in DEX-treated cultures as compared with untreated cultures (Fig. 1B, bottom panels; compare lanes 5 and 10). THP-1 cultures induced with TNF or LPS gave similar results (*10*). We then considered whether DEX might induce other NF-κB–sequestering molecules such as the recently cloned IκBβ (*13*). HeLa cells cultured with DEX for 5 hours were compared with untreated HeLa cultures, and no differences were found in amounts of IκBβ (*10*). Whereas IκBβ is insensitive to TNF treatment, LPS induction for 2 hours is sufficient to induce release of NF-κB and IκBβ degradation (*13*). Pretreatment with DEX had no effect on either IκBβ amounts or LPS-induced IκBβ

R. I. Scheinman, P. C. Cogswell, A. K. Lofquist, Lineberger Comprehensive Cancer Center, University of North Carolina, Chapel Hill, NC 27599, USA.
A. S. Baldwin Jr., Lineberger Comprehensive Cancer Center and Department of Biology, University of North Carolina, Chapel Hill, NC 27599, USA.

*Present address: School of Pharmacy, University of Colorado Health Sciences Center, Denver, CO 80262, USA.
†Present address: Department of Biological Science, University of Idaho, Moscow, ID 80844, USA.
‡To whom correspondence should be addressed.

loss (*10*). Thus, DEX selectively increases the abundance and overall stability of the IκBα population.

In order to determine if the GC-mediated increase in IκBα protein was preceded by an increase in IκBα mRNA, Northern (RNA) blot analysis was done on mRNA derived from HeLa cultures treated with DEX for increasing periods of time. DEX induced a marked increase in IκBα mRNA abundance, which peaked by 1 to 2 hours (Fig. 2A) and in some cases remained elevated for over 20 hours (*10*). A similar pattern was observed with THP-1 cultures (*10*) and is consistent with other studies (*11*). We tested whether protein synthesis was necessary for this induction of the IκBα message. HeLa cultures were treated with DEX in the absence or presence of CHX, and IκBα mRNA amounts were compared by Northern blot analysis. CHX alone induced IκBα mRNA, as has been observed for other messages (Fig. 2B, lane 2). CHX plus DEX superinduced IκBα mRNA (Fig. 2B, lane 4), indicating that DEX does not function by inducing the synthesis of an intermediary factor which must then induce the IκBα message. These data suggest that GCs directly activate IκBα gene transcription. We tested this hypothesis by performing run-on transcription assays on HeLa and THP-1 cultures after DEX treatment for various periods of time (Fig. 2C). DEX clearly increased RNA polymerase occupancy on the IκBα gene within 15 min and for at least 2 hours. In order to quantitate the effect, we normalized the IκBα signal to an actin control, thereby measuring the increase in transcription as almost 10-fold (Table 1). We cannot discount the possibility that actin transcription may be slightly inhibited by DEX treatment, thus decreasing the amount of the induction, but the interpretation of the data remains unaffected. In addition, DEX had no effect on transcription of genes encoding c-Myc or TNF-α (*10*). TNF-α treatment, in comparison, induces both IκBα and IL-8 transcription (Fig. 2C and Table 1). No change in IκBα mRNA stability was detected as measured after actinomycin D treatment in the absence or presence of DEX (*10*). Preliminary data indicated that a IκBα promoter construct extending to position −600 was not activated by DEX (*10*), which suggests that the putative GC-responsive element is located further upstream or within the gene. Taken together, these data suggest that DEX increases IκBα protein abundance through an increase in gene transcription.

The increase in IκBα gene transcription induced by DEX was much greater than the average increase in IκBα protein abundance as measured by protein immunoblot. We thus wanted to determine if the rate of IκBα protein synthesis increased in a manner similar to that of the mRNA population. We metabolically labeled HeLa cells in the absence or presence of DEX, prepared whole-cell extracts, and immunoprecipitated with an antibody specific for either IκBα or p65. DEX induced a three- to fivefold increase in the rate of incorporation of ^{35}S-labeled methionine into the IκBα pool (Fig. 3A, compare lanes 1 and 3). The p65 antiserum immunoprecipitated almost as much labeled IκBα as did the IκBα antiserum, suggesting that the majority of newly synthesized IκBα was associated with p65 (Fig. 3A, compare lanes 3 and 4). Detection of coimmunoprecipitated p65 by the IκBα antiserum was obscured by a comigrating nonspecific band (Fig. 3A, lanes 1 to 3). In addition, the degree of incorporation of label into the p65 pool was

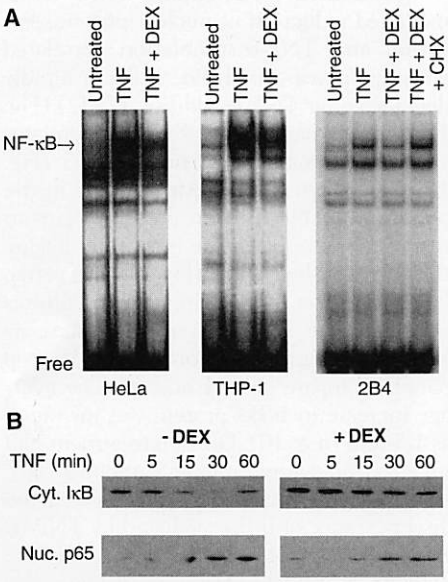

Fig. 1. DEX-mediated repression of NF-κB. (**A**) HeLa cultures were pretreated for 12 hours with 10^{-7} M DEX and stimulated for 1 hour with TNF-α (1 ng/ml). THP-1 cells and 2B4 murine T cell hybridomas were pretreated for 5 hours with 10^{-7} M DEX and stimulated for 1 hour with TNF-α (1 ng/ml). Nuclear extracts were analyzed by electrophoretic mobility-shift assay with the murine major histocompatibility complex class I NF-κB DNA binding probe UV21 as described (*6*). Data are representative of six independent experiments. (**B**) HeLa cultures were pretreated with 10^{-7} M DEX for 2 hours and stimulated with TNF-α (1 ng/ml) for periods of time shown at the top of the figure. Cytoplasmic (Cyt.) and nuclear (Nuc.) extracts were normalized for protein amounts and analyzed by immunoblotting with IκBα and p65 antibodies to peptide (obtained from Rockland, Boyertown, Pennsylvania).

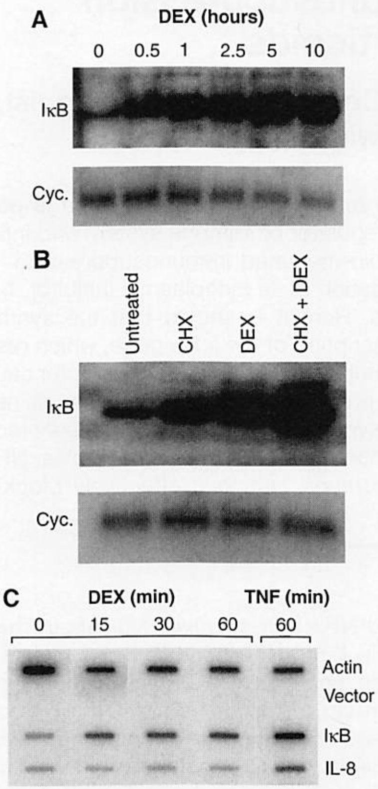

Fig. 2. DEX induces IκBα gene transcription. (**A**) Northern blot analysis of HeLa total RNA. HeLa cultures were treated for increasing periods of time with 10^{-7} M DEX and harvested for RNA. RNA was prepared as described (*17*). Equal amounts of RNA (10 μg) as determined by ethidium-stained 28*S* RNA were size separated by formaldehyde acrylamide gel electrophoresis, blotted to Zetaprobe (Bio-Rad), and processed according to the manufacturer's instructions. The blot was probed first with a *MAD-3*–IκBα complementary DNA (cDNA) (*8*) labeled by random priming. Subsequently, the blot was reprobed with a cyclophilin (Cyc.) cDNA (labeled as above) as a control RNA. Prehybridization and washing were done according to Bio-Rad's recommendations. (**B**) Cultures were treated with CHX (10 ng/ml) for 1 hour; 10^{-7} M DEX was then added to appropriate cultures for an additional 2.5 hours, and RNA was harvested and analyzed by Northern blot as described above. (**C**) Run-on transcription assays were done on cultures treated with either 10^{-7} M DEX or TNF-α (1 ng/ml) for varying periods of time as shown. Nuclei were isolated, and run-on transcriptions were done as described (*18*). The filters were exposed to a PhosphoImager (Molecular Dynamics) screen, and the bands were quantitated. IκBα and IL-8 transcription were normalized to actin transcription. The data are representative of four independent experiments.

Table 1. Fold activation of transcription normalized to actin. Number of experiments, *n*.

Condition	Average* (±SD) IκBα	Experiments (*n*)
Control	1.00 (0.07)	3
DEX (15 min)	9.88 (1.73)	2
DEX (30 min)	10.06 (3.74)	4
DEX (1 hour)	11.08 (4.66)	4
DEX (2 hours)	7.54 (0.59)	2
TNF-α (1 hour)	23.5 (17.77)	2

*Experiments such as those shown in Fig. 2C were quantitated with a PhosphoImager. Radioactivity was normalized to actin and expressed as fold increase over control.

much reduced as compared with IκBα, even though the two proteins contained similar numbers of methionines, indicating that the rate of p65 synthesis was low. These data indicate that newly synthesized IκBα is incorporated into preexisting NF-κB complexes, which is consistent with previous results (*14*). We tested this hypothesis further by labeling HeLa cultures for short periods of time and determining the efficiency of immunoprecipitation of IκB by the two antisera. After a 15-min pulse, extract was prepared and divided into identical aliquots, one of which was incubated with the IκBα antisera and the other with the p65 antisera. Once again, the IκBα signal derived from the p65 immunoprecipitation was similar to that derived from the IκBα immunoprecipitation (Fig. 3B, lanes 1 and 2). Analysis of the supernatants indicated that the antibodies accounted for all of the signal (Fig. 3B, Sup. 1 and Sup. 2). Thus, all of the surviving newly synthesized IκBα protein was rapidly associated with NF-κB. This is consistent with the observation that free IκBα is intrinsically unstable and rapidly degraded (*14*).

In the absence of DEX, TNF-α treatment results in the transient loss of IκBα, which allows NF-κB to translocate to the nucleus (*12*). We wanted to observe the effect of TNF-α treatment on the DEX-induced pool of newly synthesized IκBα associated with NF-κB. To this end, HeLa cultures were metabolically labeled in the absence or presence of DEX. TNF-α was then added and extracts were prepared at various times. The extracts were immunoprecipitated with the p65-specific antibody, and the resultant material was analyzed by SDS–polyacrylamide gel electrophoresis (PAGE). As expected, TNF-α treatment in the absence of DEX resulted in the rapid loss of p65-associated IκBα (Fig. 4A). In the presence of DEX, the amount of newly synthesized IκBα associated with p65 was greatly increased (Fig. 4A; compare lanes 2 and 6). When treated with TNF-α and DEX, the amount of newly synthesized IκBα associated with p65 remained elevated (Fig. 4A). Thus, DEX treatment stabilizes the overall association of p65 with the pool of newly synthesized IκBα even in the presence of an inducer like TNF-α.

This result could be explained either by the inhibition by DEX of the TNF-α–mediated release of NF-κB from IκBα (for example, by affecting IκBα phosphorylation) or by the induction of the reassociation of newly synthesized IκBα with newly released NF-κB. These possibilities can be distinguished by performing a pulse-chase experiment and treating HeLa cultures with TNF-α during the chase. Under chase conditions, newly synthesized IκBα protein has a much lower specific activity. Thus, if DEX blocks the TNF-α–mediated release of NF-κB, the IκBα signal should remain relatively unchanged. If, in the presence of TNF-α, newly synthesized IκBα (low specific activity) replaces preexisting IκBα (high specific activity), then the IκBα signal should sub-

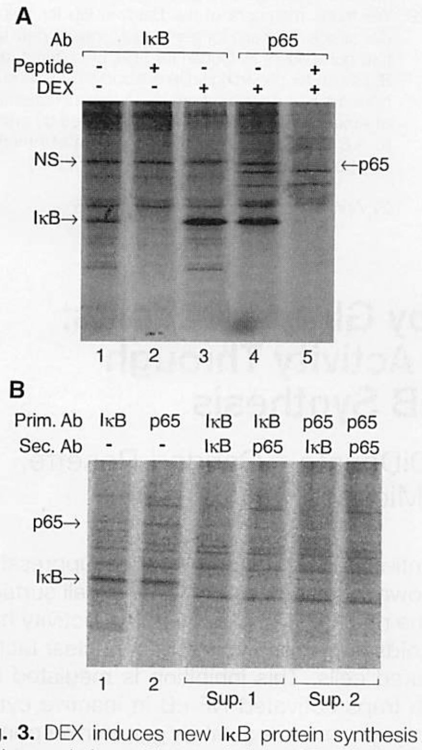

Fig. 3. DEX induces new IκB protein synthesis and association with preexisting p65. (**A**) HeLa cells were metabolically labeled for 2 hours in the absence or presence of 10^{-7} M DEX, and extracts were prepared as described (*19*). Immunoprecipitations were done overnight with 1 μl of IκBα or p65 antiserum (Ab) to peptide plus 20 μl of protein A–Sepharose (PAS) either in the absence or presence of 1 μl of competing peptide (1 mg/ml) as indicated. NS, nonspecific. Data are representative of seven independent experiments. (**B**) Six HeLa cultures were metabolically labeled for 15 min, and extracts were pooled and divided into two equal portions. Each was immunoprecipitated overnight with antiserum to peptide as above. PAS was pelleted and supernatants were collected, and each was divided into two equal portions. Supernatants derived from the IκBα immunoprecipitation (Sup. 1) and the p65 immunoprecipitation (Sup. 2) were reimmunoprecipitated as above [second antibody (Sec. Ab)]. Immunoprecipitations were analyzed as in (A).

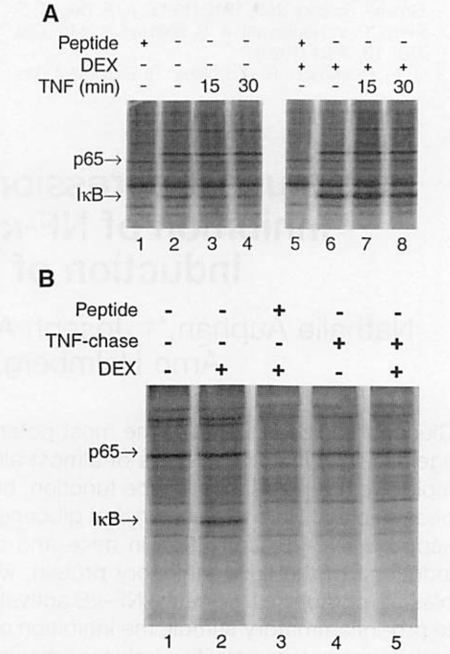

Fig. 4. Newly synthesized IκBα reassociates with preexisting NF-κB after TNF-α stimulation. (**A**) HeLa cultures were metabolically labeled in the presence or absence of 10^{-7} M DEX for 2 hours. TNF-α (1 ng/ml) was then added in the presence of carrier bovine serum albumin. Extracts were prepared by lysis in RIP buffer as described (*19*) and incubated with 1 μl of antiserum to p65 in the absence or presence of 1 μl of competing peptide as shown at the top of the panel. PAS pellets were extensively washed, and immunoprecipitated proteins were analyzed by SDS-PAGE. (**B**) HeLa cultures were metabolically labeled in the presence or absence of 10^{-7} M DEX as described above. Plates were washed with PBS and either harvested or treated with chase medium containing TNF-α (1 ng/ml). After 30 min, plates were harvested and extracts were incubated with antiserum to p65 and processed as described above.

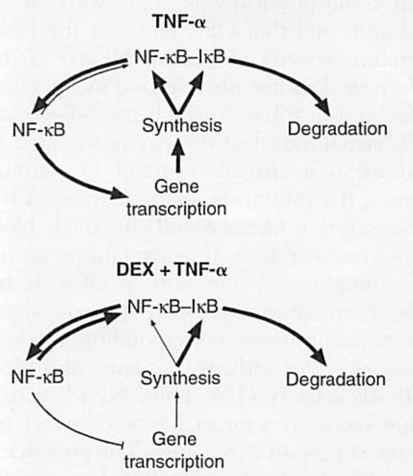

Fig. 5. A model illustrating how DEX treatment affects the NF-κB system as a whole. TNF-α induction results in the rapid degradation of IκBα and the nuclear translocation of NF-κB (upper diagram). NF-κB either reassociates with a newly synthesized IκBα molecule (thin arrow) or translocates to the nucleus. Nuclear NF-κB induces transcription of both p50 and IκBα genes, as well as effector molecules regulating the biological response. In the presence of DEX (lower diagram), IκBα synthesis is increased as a result of increased gene transcription. TNF-α–mediated nuclear translocation of NF-κB is inhibited by the reassociation of NF-κB with newly synthesized IκBα. In addition, DEX renders the remaining NF-κB that translocates to the nucleus unable to bind DNA (*5, 6*). Thick arrows represent induced pathways; thin blocked line represents an inhibited pathway.

stantially decrease. HeLa cultures were metabolically labeled in the absence or presence of DEX for several hours. The labeling medium was then replaced with chase medium containing DEX and TNF-α. Cultures were harvested and extracts were immunoprecipitated with the p65-specific antibody. Under these conditions, the IκBα signal rapidly disappeared (Fig. 4B). Thus, DEX does not appear to alter the signal transduction pathway leading to the induced dissociation of NF-κB and IκBα.

Together, these data indicate that DEX treatment induces the transcription of the IκBα gene. This induction results in the increased synthesis of IκBα protein. This increase in protein synthesis leads to the rapid turnover of IκBα protein associated with preexisting NF-κB complexes. In the presence of an activator such as TNF-α, newly released NF-κB reassociates with the DEX-induced IκBα and thus reduces the amount of NF-κB translocating to the nucleus. Additionally, newly synthesized IκBα may enter the nucleus and inhibit NF-κB DNA binding (*15*). A model of this process is shown in Fig. 5. Consistent with this model, we show that the GC-mediated inhibition of NF-κB induction by means of TNF-α is blocked by CHX (Fig. 1). Previously we and others showed that activated GR could physically associate with NF-κB subunits and that DEX represses the DNA binding activity of nuclear NF-κB (*5, 6*). Here we demonstrate a second independent mechanism through which the NF-κB and GC signal transduction systems interact. As NF-κB is a critical regulator of cytokine genes, the inhibition of the activity of this transcription factor would effectively block cytokine secretion, thus explaining an immunosuppressive function of GCs. It has also been reported recently that salicylates, at concentrations corresponding to doses prescribed for arthritis patients, also block NF-κB activity (*16*). Thus, NF-κB activation serves as a target for two distinct immunosuppressive therapies. The presence of multiple levels of interaction between the NF-κB and GC systems suggests that these interactions may have evolved to serve a physiological role in the development of the immune system and in modulation of the immune response.

REFERENCES AND NOTES

1. T. R. Cupps and A. S. Fauci, *Immunol. Rev.* **65**, 133 (1982); R. C. Haynes Jr., in *Goodman and Gilman's the Pharmacological Basis of Therapeutics*, A. G. Gilman, T. W. Roll, A. S. Nies, P. Taylor, Eds. (Pergamon, New York, ed. 8, 1990), pp. 1431–1462.
2. R. M. Evans, *Science* **240**, 889 (1988); M. J. Tsai and B. W. O'Malley, *Annu. Rev. Biochem.* **63**, 451 (1994); M. Truss and M. Beato, *Endocr. Rev.* **14**, 459 (1993).
3. K. A. Smith, *Immunol. Rev.* **51**, 337 (1980); P. J. Knudsen, C. A. Dinarello, T. B. Strom, *J. Immunol.* **139**, 4129 (1987); B. Beutler, N. Krochin, I. W. Milsark, C. Luedke, A. Cerami, *Science* **232**, 977 (1986).
4. T. K. Kerppola, D. Luk, T. Curran, *Mol. Cell. Biol.* **13**, 3782 (1993); H. Konig, H. Ponta, H. J. Rahmsdorf, P. Herrlich, *EMBO J.* **11**, 2241 (1992); R. Schule *et al.*, *Cell* **62**, 1217 (1990); H. F. Yang Yen *et al.*, *ibid.*, p. 1205; M. I. Diamond, J. N. Miner, S. K. Yoshinaga, K. R. Yamamoto, *Science* **249**, 1266 (1990); F. C. Lucibello, E. P. Slater, K. U. Jooss, M. Beato, R. Muller, *EMBO J.* **9**, 2827 (1990); C. Jonat *et al.*, *Cell* **62**, 1189 (1990).
5. A. Ray and K. E. Prefontaine, *Proc. Natl. Acad. Sci. U.S.A.* **91**, 752 (1994); N. Mukaida *et al.*, *J. Biol. Chem.* **269**, 13289 (1994); E. Caldenhoven *et al.*, *Mol. Endocrinol.* **9**, 401 (1995).
6. R. I. Scheinman, A. Gualberto, C. M. Jewell, J. A. Cidlowski, A. S. Baldwin Jr., *Mol. Cell. Biol.* **15**, 943 (1995).
7. M. Grilli, J. J.-S. Chiu, M. J. Lenardo, *Int. Rev. Cytol.* **143**, 1 (1993); P. A. Baeuerle and T. Henkel, *Annu. Rev. Immunol.* **12**, 141 (1994); U. Siebenlist, G. Franzoso, K. Brown, *Annu. Rev. Cell Biol.* **10**, 405 (1994).
8. S. Haskill *et al.*, *Cell* **65**, 1281 (1991).
9. N. R. Rice, M. L. MacKichan, A. Israel, *ibid.* **71**, 243 (1992); R. I. Scheinman, A. A. Beg, A. S. Baldwin Jr., *Mol. Cell. Biol.* **13**, 6089 (1993); F. Mercurio, J. A. DiDonato, C. Rosette, M. Karin, *Genes Dev.* **7**, 705 (1993).
10. R. I. Scheinman, P. C. Cogswell, A. K. Lofquist, A. S. Baldwin, unpublished observations.
11. N. Auphan, J. A. DiDonato, C. Rosette, A. Helmberg, M. Karin, *Science* **270**, 286 (1995).
12. K. Brown, S. Park, T. Kanno, G. Franzoso, U. Siebenlist, *Proc. Natl. Acad. Sci. U.S.A.* **90**, 2532 (1993); S.-C. Sun, P. A. Ganchi, D. W. Ballard, W. C. Greene, *Science* **259**, 1912 (1993); A. A. Beg, T. S. Finco, P. V. Nantermet, A. S. Baldwin Jr., *Mol. Cell. Biol.* **13**, 3301 (1993).
13. J. E. Thompson, R. J. Phillips, H. Erdjument-Bromage, P. Tempst, S. Ghosh, *Cell* **80**, 573 (1995).
14. N. R. Rice and M. K. Ernst, *EMBO J.* **12**, 4685 (1993).
15. F. Arenzana-Seisdedos *et al.*, *Mol. Cell. Biol.* **15**, 2689 (1995).
16. E. Kopp and S. Ghosh, *Science* **265**, 956 (1994).
17. J. J. Chirgwin, A. E. Przbyla, R. J. MacDonald, W. J. Rutter, *Biochemistry* **18**, 5294 (1979).
18. A. K. Lofquist, K. Mondal, J. S. Morris, J. S. Haskill, *Mol. Cell. Biol.* **15**, 1737 (1995).
19. HeLa cultures were metabolically labeled as follows: Cell culture plates were washed once with phosphate-buffered saline (PBS) and incubated with starve medium [Eagle's minimum essential medium (MEM) without methionine or cysteine, plus 15 mM Hepes] for 1 hour. Starve medium was replaced with fresh starve medium to which was added Express Label (NEN) to a final concentration of 200 μCi/ml. Cultures remained in a tissue culture incubator until harvest or addition of chase medium (Eagle's MEM containing 25 mM methionine and 25 mM cysteine). Cells were harvested by being scraped into ice cold PBS and lysed for 5 min on ice in RIP buffer [25 mM tris (pH 7.6), 150 mM NaCl, 2 mM EDTA, 0.5% Nonidet P-40, and 2 mM phenylmethylsulfonyl fluoride]. Membranes were removed by spinning of cells for 10 min in a microfuge at 4°C.

20. We thank members of the Baldwin lab for helpful discussion, M. Karin for generously sharing data before publication, P. Cohen for 2B4.11 cultures, and S. Ghosh for providing IκBβ antibody. R.I.S. is supported by a fellowship from the Arthritis Foundation of America. This research was supported by grants to A.S.B. from the Arthritis Foundation of America and from NIH (grants AI35098 and CA52515).

27 April 1995; accepted 9 August 1995

Immunosuppression by Glucocorticoids: Inhibition of NF-κB Activity Through Induction of IκB Synthesis

Nathalie Auphan,*† Joseph A. DiDonato,† Caridad Rosette, Arno Helmberg,‡ Michael Karin§

Glucocorticoids are among the most potent anti-inflammatory and immunosuppressive agents. They inhibit synthesis of almost all known cytokines and of several cell surface molecules required for immune function, but the mechanism underlying this activity has been unclear. Here it is shown that glucocorticoids are potent inhibitors of nuclear factor kappa B (NF-κB) activation in mice and cultured cells. This inhibition is mediated by induction of the IκBα inhibitory protein, which traps activated NF-κB in inactive cytoplasmic complexes. Because NF-κB activates many immunoregulatory genes in response to pro-inflammatory stimuli, the inhibition of its activity can be a major component of the anti-inflammatory activity of glucocorticoids.

Glucocorticoids (GCs) are physiological inhibitors of inflammatory responses and are widely used as immunosuppressive and anti-inflammatory agents (*1*). Interference with GC action or synthesis increases animal mortality after challenge with bacterial superantigens (*2*). GCs induce lymphocyte apoptosis (*1, 3*) and inhibit synthesis of lymphokines (*4*) and cell surface molecules required for immune functions (*5*). In spite of the widespread use of GCs, the molecular mechanisms that underlie their therapeutic effects are poorly understood (*1*). GCs induce target genes through the glucocorticoid receptor (GR), a ligand-activated transcription factor (*6*). GCs repress gene expression through transcriptional interfer-

Department of Pharmacology, Program in Biomedical Sciences, Center for Molecular Genetics, School of Medicine, University of California, San Diego, La Jolla, CA 92093–0636, USA.

*Present address: Centre d'Immunologie, Institut National de la Santé et de la Recherche Médicale–Centre National de la Recherche Scientifique, Marseille Laminy Case 906, 13288 Marseille, Cedex 9, France.

†These authors contributed equally to this work.

‡Present address: Institute for General and Experimental Pathology, University of Innsbruck Medical School, A-6020 Innsbruck, Austria.

§To whom correspondence should be addressed.

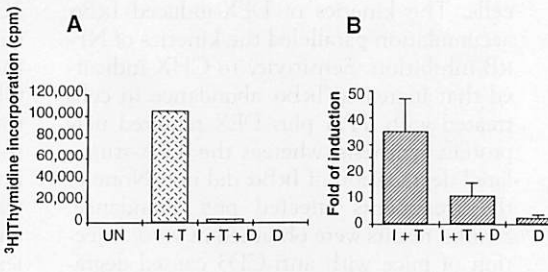

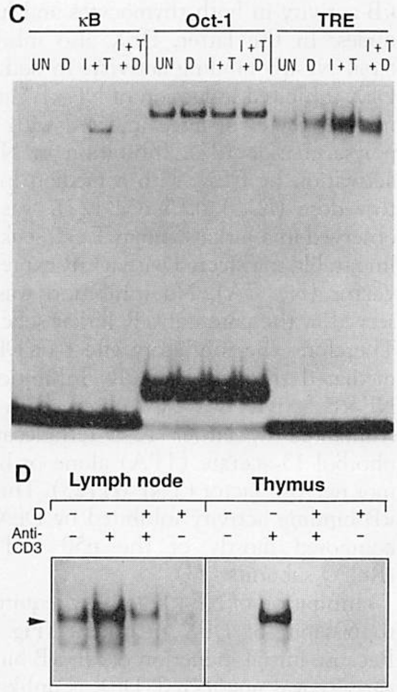

Fig. 1. Inhibition of IL-2 promoter activation by DEX correlates with decreased DNA binding of both AP-1 and NF-κB. (**A**) FJ8.1 cells (*16*) were seeded into microtiter plates (2×10^4 cells per well) and incubated for 24 hours with either medium alone (UN) or with 4 μM ionomycin (I) and TPA (T) (100 ng/ml) in the absence or presence of 1 μM DEX (D). Culture supernatants were harvested, and their IL-2 content was measured through its mitogenic effect on the T cell line HT-2 (*16*). The results shown are averages of triplicates. (**B**) FJ8.1 cells were electroporated with the IL-2–LUC plasmid (*17, 18*). After 12 hours, cells were treated as indicated above, and luciferase activity was determined 7 hours later. The results shown are averages of three separate experiments and are presented as fold of induction above basal IL-2–LUC expression. (**C**) FJ8.1 cells were treated as indicated, and after 1 hour nuclear extracts were prepared. Five micrograms of each extract were incubated with 20,000 cpm of ^{32}P-labeled κB, Oct-1, or AP-1 (TRE) binding site probes, and DNA binding activity was measured by EMSAs. The increase in AP-1 binding activity in response to DEX was not reproducibly seen and was probably the result of loading more protein in that lane. (**D**) Inhibition of NF-κB induction in T lymphocytes in vivo. BIO.BR mice (10 weeks old) were injected with (i) phosphate-buffered saline (PBS), (ii) 100 μg of CD3 monoclonal antibody (145.2c.11) in PBS, (iii) DEX-acetate (1 mg per kilogram of body weight) together with 100 μg of anti-CD3 in PBS, or (iv) DEX-acetate (1 mg/kg). In the experiment shown here, DEX (D) was administered 2 hours before anti-CD3. Two hours after anti-CD3 injection, thymuses and lymph nodes were isolated, and their cells were retrieved by being squeezed through a nylon mesh. After being washed in PBS, whole-cell extracts were prepared (*36*). Fifteen-microgram samples were incubated with the κB probe, and NF-κB binding activity was analyzed as described above.

ence between the activated GR and other transcription factors, most notably AP-1, by a mechanism likely to involve protein-protein interactions (*7, 8*). Although AP-1 is involved in lymphokine gene induction (*9*), interference with AP-1 activity cannot account for the full spectrum of immunoregulatory genes affected by GCs. Another transcription factor that activates immunoregulatory genes is NF-κB, whose predominant form is a heterodimer composed of p50 and p65 subunits (*10*). In unstimulated cells, the NF-κB heterodimer is kept as an inactive cytoplasmic complex by inhibitory proteins, such as IκBα and IκBβ (*11*). After cell stimulation, the IκBs are rapidly degraded (*12, 13*) and free NF-κB dimers translocate to the nucleus and activate target genes (*10, 14*). This process is transient and is terminated through delayed NF-κB–mediated IκBα induction (*12, 14*). Because of its role in the activation of lymphokine genes and other immunoregulatory genes, we examined whether NF-κB activity is inhibited by GCs. Here we show that GCs are potent inhibitors of NF-κB activation. This inhibition is the result of induction of IκBα expression, followed by sequestration of NF-κB dimers in the cytoplasm.

The interleukin-2 (IL-2) promoter contains cis elements required for maximal induction during T cell activation, which are recognized by AP-1, NF-κB, NF of activated T cells, and octamer-binding proteins (OBP) (*9, 15*). We investigated which of these factors mediate the inhibitory effect of the synthetic GC dexamethasone (DEX) on IL-2 production by a murine T cell hybridoma (*16*). As shown previously (*17, 18*), DEX inhibited induction of IL-2 secretion (Fig. 1A) and transcription, as measured by an IL-2–luciferase reporter plasmid (*19*) (Fig. 1B). Electrophoretic mobility-shift assays (EMSAs) (*20*) revealed that both AP-1 and NF-κB DNA binding activities were elevated in nuclear extracts of activated cells (Fig. 1C). DEX inhibited induction of NF-κB binding activity and reduced the amount of AP-1 binding activity, whereas OBP binding activity was unaffected. DEX also inhibited induction of NF-κB in mouse T lymphocytes in vivo (Fig. 1D). Administered either 2 hours before or simultaneously with anti-CD3, a potent T cell–activating monoclonal antibody (*21*), DEX inhibited induction of NF-

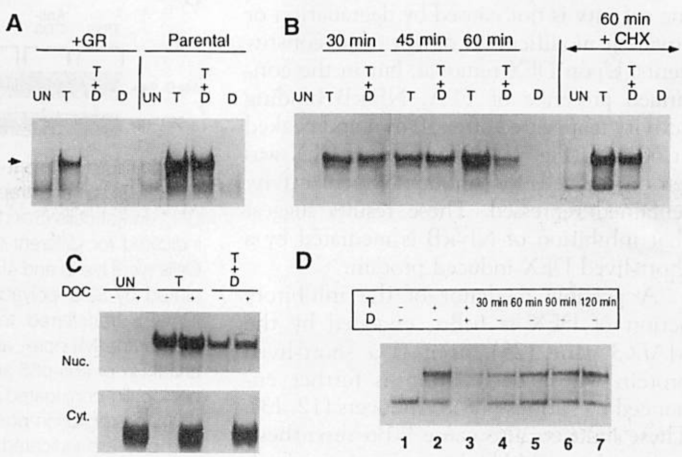

Fig. 2. Inhibition of NF-κB activation requires induction of a short-lived inhibitory protein. (**A**) A GR$^-$ subclone of Jurkat cells (parental) or Jurkat cells stably transfected with an expression vector encoding rat GR and expressing 20,000 receptors per cell (+GR) were incubated with TPA (T) (100 ng/ml), DEX (D) (1 μM), a combination of TPA plus DEX, or no further addition (UN). After 1 hour, nuclear extracts were prepared and 5-μg samples were examined for NF-κB binding activity as described above. The arrowhead indicates the NF-κB–DNA complex. (**B**) GR$^+$ Jurkat cells were treated with TPA (T), TPA plus DEX, or DEX (D) for the indicated times. Untreated (UN) and DEX-treated cells were harvested after 60 min. When indicated, cells were pretreated with CHX (10 μg/ml) for 30 min and then incubated with TPA, TPA plus DEX, or DEX in the presence of CHX. NF-κB DNA binding activity in nuclear extracts was assayed as described above. (**C**) GR$^+$ Jurkat cells were either untreated (UN) or incubated in the presence of TPA (T) or TPA plus DEX (D) as described above. After 60 min, nuclear and cytoplasmic extracts were prepared. Samples of nuclear (Nuc.) (5 μg) and cytosolic (Cyt.) (10 μg) extracts were treated with 0.8% Na-deoxycholate (DOC) and 1.2% NP-40 and analyzed for NF-κB binding activity by EMSA. (**D**) GR$^+$ Jurkat cells were incubated in medium alone (lane 1), in medium plus TPA (T) (lane 2), or in TPA plus DEX (D) (lanes 3 to 7) for 90 min. After two washes, cells treated with TPA plus DEX were divided into aliquots and incubated for the indicated times with either TPA (lanes 4 to 7) or TPA plus DEX (lane 3) for 120 min. In lanes 1 and 2, cells were maintained under the same conditions (lane 1, medium; lane 2, TPA) for another 120 min. Nuclear extracts were prepared and analyzed for NF-κB binding activity.

κB activity in both thymocytes and lymph nodes. In the latter, DEX also inhibited basal NF-κB binding activity. In addition, DEX inhibited induction of NF-κB activity in splenocytes of mice injected with lipopolysaccharide (22). Inhibition of NF-κB activation by DEX, with a median inhibitory dose (IC_{50}) of 5 nM (22), was also observed in a Jurkat human T cell leukemia line stably transfected with a GR expression vector (Fig. 2A). No inhibition was observed in the parental GR Jurkat subclone. Therefore, the inhibitory effect of DEX is mediated through the GR. Inhibition of NF-κB activity was also observed in cells stimulated by either 12-O-tetradecanoylphorbol 13-acetate (TPA) alone or by tumor necrosis factor (TNF-α) (23). The NF-κB binding activity inhibited by DEX was composed mostly of the p50 and p65 (RelA) subunits (23).

Inhibition of NF-κB activity required 45 to 60 min of DEX treatment (Fig. 2B). Because initial induction of NF-κB binding activity was unaffected, DEX is unlikely to interfere with the signaling cascade that leads to NF-κB activation. Inhibition of NF-κB activity required new protein synthesis; it was prevented by cycloheximide (CHX) (Fig. 2B). The inactive, cytoplasmic NF-κB–IκB complex dissociates after deoxycholate (DOC) treatment (24). DOC treatment of cytoplasmic extracts of DEX-treated cells revealed the same amount of NF-κB binding activity as in untreated cells (Fig. 2C). Thus, inhibition of NF-κB binding activity is not caused by degradation or covalent modification of any of its constituents. Upon DEX removal, but in the continued presence of TPA, NF-κB binding activity reappeared after 30 min and peaked at 60 min (Fig. 2D). However, if DEX was left on the cells for 5 hours, NF-κB activity remained repressed. These results suggest that inhibition of NF-κB is mediated by a short-lived DEX-induced protein.

A possible mediator of the inhibitory action of DEX is IκBα, encoded by the *MAD-3* gene (25), as it is a short-lived protein whose degradation is further enhanced by various NF-κB inducers (12, 13). These inducers also cause IkBα resynthesis by stimulating *MAD-3* transcription, a feedback response that terminates NF-κB activation (12). The effect of DEX on IκBα metabolism was examined by immunoblotting with an antibody to IκBα. Treatment with TPA led to the partial disappearance of IκBα, which reached 20% of its basal level after 30 min (Fig. 3A). At 10 and 20 min, DEX had an insignificant effect on the amount of IκBα in TPA-treated cells, but after 30 min the amount of IκBα in cells treated with TPA plus DEX was similar to that in unstimulated cells, and after 45 min it was 50% higher than in unstimulated cells. The kinetics of DEX-induced IκBα accumulation paralleled the kinetics of NF-κB inhibition. Sensitivity to CHX indicated that increased IκBα abundance in cells treated with TPA plus DEX required new protein synthesis, whereas the TPA-stimulated degradation of IκBα did not. None of the treatments affected p65 abundance. Similar results were obtained in vivo: Injection of mice with anti-CD3 caused degradation of thymic IκBα, but simultaneous administration of DEX resulted in IκBα levels similar to those in untreated animals (Fig. 3B). Examination of GR^+ Jurkat cells (26) or HeLa cells stained with an antibody to p65 by indirect immunofluorescence indicated that p65 was cytoplasmic in unstimulated cells, but after 10 min of TNF-α stimulation, most of it was nuclear (Fig. 3C). Treatment of TNF-α–stimulated cells with DEX resulted in retention of p65 in the cytoplasm. Staining with antibody to GR indicated that DEX induced nuclear translocation of GR, regardless of whether the cells were stimulated with TNF-α or not. Recently a second form of IκB, IκBβ, was molecularly cloned (27). Immunoblot analysis of HeLa cell extracts with antibodies to IκBα did not reveal any effect of DEX on IκBα expression (28).

Because DEX did not prevent IκBα degradation at early time points, the increase in IκBα abundance in DEX-treated cells is probably the result of increased IκBα synthesis. Northern (RNA) blot analysis verified this assumption and indicated that DEX treatment of GR^+ Jurkat cells, but not the GR^- parental cell line, led to sevenfold in-

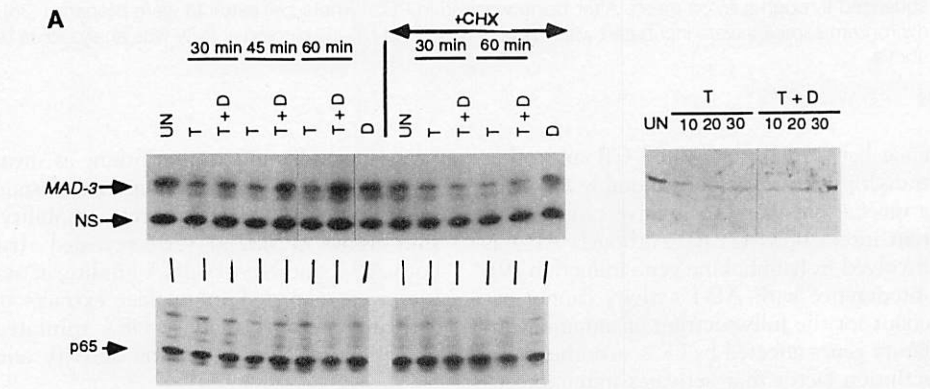

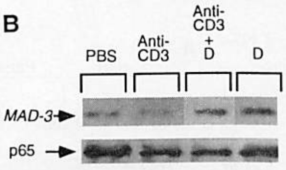

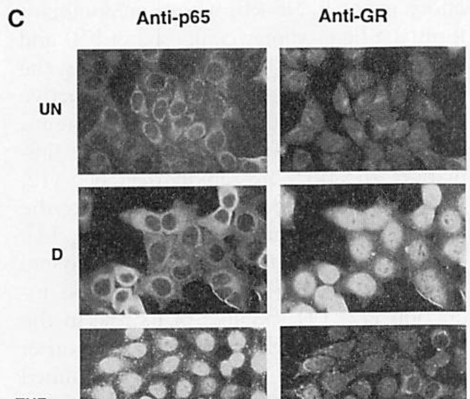

Fig. 3. DEX treatment increases the abundance of IκBα (*MAD-3*) and traps p65 in the cytoplasm. (**A**) GR^+ Jurkat cells (5×10^6 per lane) were treated as indicated for different lengths of time (in minutes). Cells were lysed and 40 μg of each lysate was separated by SDS–polyacrylamide gel electrophoresis (PAGE), transferred to a polyvinylidene difluoride membrane (Millipore), and immunoblotted with either anti-IκBα or anti-p65 and donkey anti-rabbit immunoglobulin conjugated to peroxidase as described (20). The migration positions of both *MAD-3* (IκBα) and p65 are indicated. UN, untreated; T, TPA; D, DEX; NS, a nonspecific cross-reacting protein. The levels of IκBα were quantitated with the use of a chemoluminescence-sensitive screen and a PhosphoImager and normalized to the level of the nonspecific protein. (**B**) BIO.BR mice were injected with PBS, anti-CD3, DEX (D), or anti-CD3 plus DEX, as described in the legend to Fig. 1D. After 2 hours, the thymuses were isolated and whole-cell extracts were prepared. Fifty micrograms of each extract were separated by SDS-PAGE, transferred to Immbilon P membrane, and probed with antibodies to IκBα and p65. (**C**) HeLa cells were plated on glass cover slips and were left untreated (UN) or were treated with DEX (D) for 30 min, TNF-α for 10 min, or DEX for 30 min and then TNF-α for 10 min. After treatment, the cells were fixed and the intracellular locations of p65 and GR were determined by indirect immunofluorescence with the use of anti-p65 (Pharmingen, La Jolla, California) and anti-GR, as described (37). Shown are typical fields of stained HeLa cells showing the exclusive cytoplasmic location of p65 in untreated, DEX-treated, or TNF-α–plus–DEX–treated cells and its nuclear translocation in TNF-α–treated cells.

duction of *MAD-3* (IκBα) mRNA (Fig. 4A). Stimulation of either GR$^+$ or GR$^-$ cells with TPA resulted in sixfold induction of *MAD-3* mRNA after 1 hour. Treatment with both TPA and DEX resulted in a synergistic induction (23-fold), but only in the GR$^+$ subclone. None of the treatments had a substantial effect on expression of p65 (RelA) mRNA. Induction of IκBα expression by both TPA and DEX is most likely the result of increased transcription because it was inhibited by actinomycin D (Fig. 4B). In an accompanying report (*29*), Scheinman *et al.*, who obtained similar results, demonstrate that DEX increases the transcription rate of the *MAD-3* gene. Actinomycin D also prevented DEX-induced inhibition of NF-κB binding activity (Fig. 4C).

Collectively, these results define a simple mechanism through which GCs repress NF-κB activity. Unlike previously described transcriptional interference (*8*), inhibition of NF-κB activity does not rely on direct interaction between the activated GR and any NF-κB constituent. Rather, the inhibition is based on induction of IκBα expression. Induction of *MAD-3* mRNA results in faster reappearance of IκBα in activated cells treated with DEX than in activated cells not exposed to DEX. Reappearance of IκBα correlates with termination of NF-κB activation. Even a modest increase in the amount of IκBα, not greatly exceeding its basal level in unstimulated cells, is sufficient to cause redistribution of active p65 from the nucleus to the cytoplasm, where it is sequestered as an inactive complex.

It was previously suggested that inhibition of NF-κB activation by DEX is mediated by physical interactions between the activated GR and the p65 component of NF-κB (*30*). However, those results were obtained by transient cotransfection experiments, and although it is feasible that once overexpressed the GR and p65 can directly interact, this mechanism is not necessary to explain the results described above that were obtained under physiological conditions. Furthermore, DEX treatment causes translocation of p65 from the nuclei of stimulated cells to the cytoplasm, whereas the activated GR remains nuclear. It is therefore unlikely that direct binding of GR to p65 mediates cytoplasmic sequestration of p65. Because DEX induces *MAD-3* expression in nonactivated T cells, the induction response itself does not appear to rely on direct interaction between the activated GR and NF-κB. As is consistent with other work (*31*), the simplest explanation of the current results is that newly synthesized IκBα translocates to the nucleus, where, as shown in vitro (*32*), it can sequester free NF-κB and thereby promote net dissociation of DNA-bound NF-κB. This is followed by translocation of IκBα- and p65-containing complexes to the cytoplasm. This mechanism also differs from the one proposed to explain inhibition of NF-κB activation by the relatively weak anti-inflammatory agent aspirin (*33*).

Inhibition of NF-κB activation can account for many of the immunosuppressive and anti-inflammatory activities of GCs, which are amongst the most potent anti-inflammatory agents known. NF-κB plays a central role in induction of a large number of important immunoregulatory genes, including those encoding IL-1, IL-2, IL-3, IL-6, IL-8, TNF-α, interferon γ (IFN-γ), granulocyte-macrophage colony-stimulating factor, class I and class II major histocompatibility complexes, the κ light chain, and endothelial leukocyte adhesion molecule 1 and intercellular adhesion molecule 1 (*10*). Several of these genes are also regulated by AP-1 (*9*), which synergizes with NF-κB (*34*). Because GCs inhibit both NF-κB and AP-1 activities, albeit through different mechanisms, it is no longer a surprise that they repress expression of a very wide spectrum of immunoregulatory genes. Indeed, administration of GC prevents systemic release of IL-2, IL-6, IFN-γ, and TNF-α in response to anti-CD3 or to superantigen (*2*, *35*). It is anticipated that other effective inhibitors of NF-κB and AP-1 may also turn out to be useful immunosuppressive and anti-inflammatory agents.

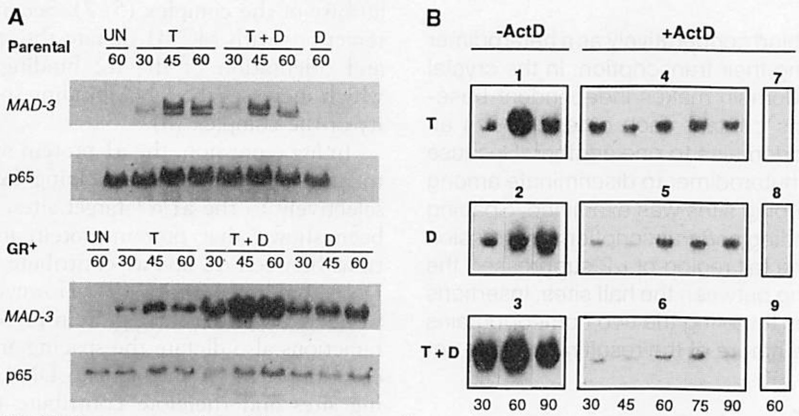

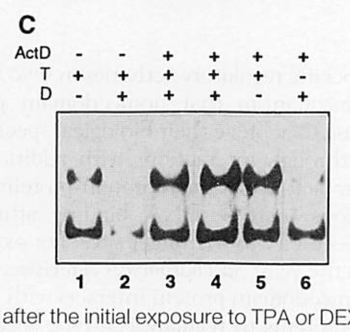

Fig. 4. DEX induces expression of the gene encoding IκBα (*MAD-3*), which is required for inhibition of NF-κB activation. (**A**) GR$^-$ (parental) and GR$^+$ Jurkat cells were treated for different lengths of time (in minutes), as indicated. Total cytoplasmic RNA was extracted and 20-μg samples were separated on a 1% agarose gel, transferred to a nylon membrane, and analyzed by hybridization to *MAD-3* (IκBα) and p65 (*RelA*) complementary DNA probes. UN, untreated; T, TPA; D, DEX. (**B**) GR$^+$ Jurkat cells were treated with TPA (T) or DEX (D) or both for different times (in minutes) as indicated. Boxes 1 to 3 show no further additions. In boxes 4 and 5, actinomycin D (ActD; 3 μg/ml), was added 15 min after the initial exposure to TPA or DEX, then cells were harvested every 15 min as indicated. In box 6, cells were pretreated with DEX for 15 min, followed by ActD, and after 15 min TPA was added. In boxes 7 to 9, ActD was added 15 min before incubation with TPA or DEX or both. Total cellular RNA was prepared and 30-μg samples were separated on an agarose gel, transferred to nylon membrane, and analyzed for the presence of *MAD-3* (IκBα) mRNA. (**C**) GR$^+$ Jurkat cells were incubated with DEX (D) for 15 min, then ActD (3 μg/ml) was either added (lane 3) or not (lane 2), and after 15 min TPA (T) was added. As a control, ActD was also added 15 min before incubation with TPA plus DEX (lane 4), TPA (lane 5), or DEX (lane 6). In addition, TPA was added alone (lane 1). Nuclear extracts were prepared, and NF-κB binding activity was examined.

REFERENCES AND NOTES

1. J. E. Parillo and A. S. Fauci, *Annu. Rev. Pharmacol. Toxicol.* **19**, 179 (1979); J. J. Cohen, in *Anti-Inflammatory Steroid Action, Basic and Clinical Aspects*, R. P. Schleimer, H. N. Claman, A. L. Oronsky, Eds. (Academic Press, San Diego, CA, 1989), pp. 111–131.
2. J. A. Gonzalo, A. González-García, C. Martínez-A., G. Kroemer, *J. Exp. Med.* **177**, 1239 (1993).
3. A. H. Wyllie, *Nature* **284**, 555 (1980).
4. P. J. Knudsen, C. A. Dinarello, T. B. Strom, *J. Immunol.* **139**, 4129 (1987); S. K. Arya, F. Wong-Staal, R. C. Gallo, *ibid.* **133**, 273 (1984); J. A. Culpepper and F. Lee, *ibid.* **135**, 3191 (1985); M. A. Collart, D. Belin, J.-D. Vassalli, P. Vassalli, *ibid.* **139**, 949 (1987); Y. Wang, H. D. Campbell, I. G. Young, *J. Steroid Biochem. Mol. Biol.* **44**, 203 (1993); B. Zanker, G. Walz, K. J. Wieder, T. B. Strom, *Transplantation* **49**, 183 (1990); B. Beutler, N. Krochin, I. W. Milsark, C. Luedke, A. Cerami, *Science* **232**, 977 (1986).
5. M. Von Knebel Doeberitz, S. Koch, H. Drzonek, H. Zur Hausen, *Eur. J. Immunol.* **20**, 35 (1990).
6. M. Beato, *Cell* **56**, 335 (1989); P. J. Godowski, D. D. Sakai, K. R. Yamamoto, in *DNA-Protein Interactions in Transcription*, UCLA Symposia on Molecular and Cellular Biology, New Series (Liss, New York, 1989), vol. 95.
7. I. E. Akerblom, E. P. Slater, M. Beato, J. D. Baxter, P. L. Mellon, *Science* **241**, 350 (1988).
8. H. F. Yang-Yen *et al.*, *Cell* **62**, 1205 (1990); C. Jonat *et al.*, *ibid.*, p. 1189; M. I. Diamond, J. N. Miner, S. K. Yoshinaga, K. R. Yamamoto, *Science* **249**, 1266 (1990); M. Pfahl, *Endocr. Rev.* **14**, 651 (1993).
9. E. A. Serfling *et al.*, *EMBO J.* **8**, 465 (1989); J.-H.

Park, K. Kaushansky, L. Levitt, *J. Biol. Chem.* **268**, 6299 (1993); P. N. Cockerill, M. F. Shannon, A. G. Bert, G. R. Ryan, M. A. Vadas, *Proc. Natl. Acad. Sci. U.S.A.* **90**, 2466 (1993).
10. M. Grilli, J. J.-S. Chiu, M. J. Lenardo, *Int. Rev. Cytol.* **143**, 1 (1993); P. A. Baeuerle, *Biochim. Biophys. Acta* **1072**, 63 (1991).
11. P. A. Baeuerle and D. Baltimore, *Science* **242**, 540 (1988).
12. S. C. Sun, P. A. Ganchi, D. W. Ballard, W. C. Greene, *ibid.* **259**, 1912 (1993); K. Brown, S. Park, T. Kanno, G. Franzoso, U. Siebenlist, *Proc. Natl. Acad. Sci. U.S.A.* **90**, 2532 (1993); R. de Martin *et al.*, *EMBO J.* **12**, 2773 (1993); T. Henkel *et al.*, *Nature* **365**, 182 (1993).
13. E. B. M. Traenckner, S. Wilk, P. A. Baeuerle, *EMBO J.* **13**, 5433 (1994); J. A. DiDonato, F. Mercurio, M. Karin, *Mol. Cell. Biol.* **15**, 1302 (1995); I. Alkalay *et al.*, *ibid.*, p. 1294.
14. A. A. Beg and A. S. Baldwin Jr., *Genes Dev.* **7**, 2064 (1993).
15. K. S. Ullman, J. P. Northrop, C. L. Verweij, G. R. Crabtree, *Annu. Rev. Immunol.* **8**, 421 (1990).
16. B. Gaugler, C. Langlet, J. M. Martin, A. M. Schmitt-Verhulst, A. Guimezanes, *Eur. J. Immunol.* **21**, 2581 (1991).
17. A. Vacca *et al.*, *Mol. Endocrinol.* **3**, 1659 (1989).
18. J. Northrop, G. R. Crabtree, P. S. Matilla, *J. Exp. Med.* **175**, 1235 (1992).
19. The IL-2–luciferase plasmid described by Northrop *et al.* (*19*) was electroporated (960 μF, 320 V) by means of a Bio-Rad gene pulser into FJ8.1 cells (25 μg of DNA per 10^7 cells).
20. Nuclear extracts of FJ8.1 cells were prepared as described [Y. Devary, C. Rosette, J. A. DiDonato, M. Karin, *Science* **261**, 1442 (1993)] and 5-μg samples were incubated with κB, Oct-1, or AP-1 binding site probes. Protein–DNA binding was examined by EMSAs,as described above [M. Garner and A. Revsin, *Nucleic Acids Res.* **9**, 3047 (1981)]
21. O. Leo, M. Foo, D. H. Saiks, L. E. Samelson, J. A. Bluestone, *Proc. Natl. Acad. Sci. U.S.A.* **84**, 1374 (1987).
22. N. Auphan, unpublished data.
23. J. DiDonato and N. Auphan, unpublished data.
24. P. A. Baeuerle and D. Baltimore, *Cell* **53**, 211 (1988).
25. S. Haskill *et al.*, *ibid.* **65**, 1281 (1991).
26. C. Rosette, unpublished data.
27. J. E. Thompson, R. J. Philips, H. Erdjument-Bromage, P. Tempst, S. Ghosh, *Cell* **80**, 573 (1995).
28. J. DiDonato, unpublished data. Antiserum to IκBβ was obtained from S. Ghosh.
29. R. I. Scheinman, P. C. Cogswell, A. K. Lofquist, A. S. Baldwin Jr., *Science* **270**, 283 (1995).
30. A. Ray and K. E. Prefontaine, *Proc. Natl. Acad. Sci. U.S.A.* **91**, 752 (1994); R. I. Scheinman, A. Gualberto, C. M. Jewell, J. A. Cidlowski, A. S. Baldwin Jr., *Mol. Cell. Biol.* **15**, 943 (1995).
31. U. Zabel, T. Henkel, M. Silva, P. A. Baeuerle, *EMBO J.* **12**, 201 (1993); D. E. Cressman and R. Taub, *Oncogene* **8**, 2567 (1993).
32. U. Zabel and P. A. Baeuerle, *Cell* **61**, 255 (1990).
33. E. Kopp and S. Ghosh, *Science* **265**, 956 (1994).
34. B. Stein *et al.*, *EMBO J.* **12**, 3879 (1993).
35. M.-L. Allegre, *et al.*, *J. Immunol.* **146**, 1184 (1991).
36. J. D. Dignam, R. M. Lebovitz, R. G. Roeder, *Nucleic Acids Res.* **11**, 1475 (1983).
37. F. Mercurio, J. A. DiDonato, C. Rosette, M. Karin, *Genes Dev.* **7**, 705 (1993).
38. We thank R. Raghow for critical reading of the manuscript, A. Baldwin for helpful discussions, C. Van Orshoven and P. Alford for expert secretarial assistance, A. M. Schmitt-Verhulst for providing the T cell hybrodoma and laboratory facilities to N.A. that were required for completion of this work, and R. Evans for the antibody to GR. Supported by NIH. N.A., J.D., and A.H. were supported by postdoctoral fellowships from the Association pour la Recherche Contre le Cancer, INSERM, NIH, and the Austrian Science Foundation, respectively. C.R. was supported by a minority research supplement from NIH.

19 June 1995; accepted 9 August 1995

Altered DNA Recognition and Bending by Insertions in the α2 Tail of the Yeast a1/α2 Homeodomain Heterodimer

Yisheng Jin, Janet Mead, Thomas Li, Cynthia Wolberger, Andrew K. Vershon*

The yeast MATα2 and MAT**a**1 homeodomain proteins bind cooperatively as a heterodimer to sites upstream of haploid-specific genes, repressing their transcription. In the crystal structure of α2 and **a**1 bound to DNA, each homeodomain makes independent base-specific contacts with the DNA and the two proteins contact each other through an extended tail region of α2 that tethers the two homeodomains to one another. Because this extended region may be flexible, the ability of the heterodimer to discriminate among DNA sites with altered spacing between α2 and **a**1 binding sites was examined. Spacing between the half sites was critical for specific DNA binding and transcriptional repression by the complex. However, amino acid insertions in the tail region of α2 suppressed the effect of altering an **a**1/α2 site by increasing the spacing between the half sites. Insertions in the tail also decreased DNA bending by **a**1/α2. Thus tethering the two homeodomains contributes to DNA bending by **a**1/α2, but the precise nature of the resulting bend is not essential for repression.

Homeodomain proteins are found in a wide range of eukaryotic organisms and form a large family of transcription factors that function in many different cellular processes (*1*). Although many homeodomain proteins bind DNA with relatively low sequence specificity in vitro, they often confer very specific regulatory activities in vivo (*2*). One mechanism that homeodomain proteins use to achieve their biological specificity is through interactions with additional protein factors (*3*). Such protein-protein interactions increase DNA binding affinity and specificity to the target sites. For example, in the yeast *Saccharomyces cerevisiae*, the α2 homeodomain protein interacts with two other proteins to regulate cell-type specific gene expression (*4*). In haploid α cells, the α2 protein acts in combination with MCM1, a MADS box protein, to bind DNA as a heterotetramer to repress **a**-specific genes (*asg*) (*5*). In **a**/α diploid cells, the α2 protein also interacts with **a**1, another homeodomain protein, to bind DNA as a heterodimer and repress haploid-specific genes (*hsg*) (*6*). Therefore, MCM1 and **a**1 contribute to the target site selection of α2.

In *asg* repression, the MCM1 protein contributes to the sequence specific binding of α2 in two different ways. First, the cooperative interactions between the two proteins increases the apparent DNA binding affinity of the complex (*5*, *7*). Second, interactions with MCM1 dictate the spacing and orientation of the α2 binding sites, which increases the DNA binding specificity of the complex (*8*).

In *hsg* repression, the **a**1 protein appears to play a similar role in helping α2 bind selectively to the **a**1/α2 target sites. It has been shown that protein-protein interactions between α2 and **a**1 contribute to the DNA binding affinity (*9*). However, we wondered whether these protein-protein interactions also dictate the spacing and orientation of the homeodomain DNA binding sites and therefore contribute to the DNA binding specificity of the complex. The crystal structure of the **a**1/α2/DNA ternary complex shows that although there are no direct contacts between the α2 and **a**1 homeodomains, the two proteins interact through a region immediately following the α2 homeodomain that forms a short α helix and makes a set of mainly hydrophobic contacts with **a**1 (*10*). This helix is tethered to the end of the third helix in the α2 homeodomain by an extended linker region (residues 59 to 63 in the crystal structure, residues 189 to 193 of the intact protein) which does not appear to be making contacts with either protein or DNA. Because both NMR and x-ray studies suggest that the linker is extended, it is possible that the linker is somewhat flexible (*10*, *11*). The **a**1 protein may therefore not de-

Y. Jin, J. Mead, A. K. Vershon, Waksman Institute and Department of Molecular Biology and Biochemistry, Rutgers University, Piscataway, NJ 08855–0759, USA.
T. Li, Department of Biophysics and Biophysical Chemistry, Johns Hopkins University School of Medicine, Baltimore, MD 21205–2185, USA.
C. Wolberger, Howard Hughes Medical Institute and Department of Biophysics and Biophysical Chemistry, Johns Hopkins University School of Medicine, Baltimore, MD 21205–2185, USA.

*To whom correspondence should be addressed.

termine the spacing between the DNA binding sites in the same manner as MCM1. We wanted to test whether the protein-protein interactions between **a**1 and α2 are rigidly fixed and whether this interaction determines the spacing of the homeodomain binding sites.

In order to test repression by **a**1/α2 sites with altered spacing, oligonucleotides with a consensus *hsg* site, similar to the one used in the crystallographic study, as well as sites with a one base insertion or deletion in the center of the site, were cloned between the UAS and TATA sequences of a *CYC1-lacZ* fusion promoter. These constructs were co-transformed into yeast with wild-type α2 and assayed for *lacZ* expression by determining β-galactosidase activity (Fig. 1A) (*12*). The first column in Fig. 1 shows the repression data for wild-type α2 protein with the wild-type *hsg* consensus site and with *hsg* sites having altered spacing between the half sites. An insertion or deletion of a single base pair between the two half sites, at a position that is not contacted by either protein, causes a large reduction in repression. In order to correlate repression in vivo with DNA binding in vitro, we assayed the binding affinities with purified **a**1 and α2 proteins in electrophoretic mobility shift assays (*13*). The binding affinity of the wild-type protein to the altered DNA site with a 1–base pair (bp) insertion is at least 100-fold weaker than to the wild-type site (Fig. 1, B and C). Deletion of base pair 11 in the operator resulted in a similar loss of DNA binding activity (*14*). This result shows that **a**1/α2 repression and DNA binding is dependent on the spacing of the two half sites and that the relative position of the sites is rigidly fixed. The failure of **a**1/α2 sites with altered spacing to repress transcription suggests a reason why all known wild-type operators have 6-bp spacing between the α2 and **a**1 half sites. In contrast, the natural α2/MCM1 binding sites have either a 4- or 5-bp spacing between the α2 and MCM1 half sites, suggesting that the spacing requirements between these proteins is more flexible than for **a**1 and α2.

Because the linker region between the α2 homeodomain and the helix that contacts **a**1 is extended, we reasoned that insertion of residues within this linker might be able to suppress the decrease in DNA binding that occurs when the **a**1 and α2 sites are moved apart. On the basis of the crystal structure of the **a**1/α2–DNA complex (*10*), we inserted either one, two, or three glycines between residues 59 and 60 of the linker region and tested how these insertions affect repression from wild-type and altered spacing sites. All of these insertions in the α2 tail were able to repress transcription from a wild-type site at approximately wild-type levels (Fig. 1A). The affinity of these mutant proteins for the wild-type DNA site is also within threefold of wild-type binding affinity (Fig. 1B). These results show that the position of the short helix in the α2 tail in relation to the α2 homeodomain is not critical for protein-protein interactions, cooperative DNA binding, and repression. It also suggests that the extended region is somewhat flexible, because it can adopt an altered conformation that accommodates the inserted glycine residues, while maintaining proper spacing between the **a**1 and α2 homeodomains binding to the wild-type consensus *hsg* site.

We next tested whether insertions in the α2 tail would suppress the defects of the *hsg* site with a single base insertion (Fig. 1A). We found that increasing the number of residues in the extended region results in greater repression from the *hsg* site with a single base insertion. An α2 protein with three glycines inserted into the extended region, α2+3Gly, restores repression to near wild-type levels. This result shows that insertions in the tail can at least partially suppress the effect of altering the spacing of an *hsq* site. These in vivo results predict that α2 proteins with insertions in the tail should bind to the altered site with higher affinity than the wild-type protein. We found that the α2+3Gly mutant bound to the *hsg*+A site with more than 25-fold higher affinity than the wild-type protein (Fig. 1C). Although this level of binding was still down fivefold from the binding affinity to the wild-type site, it shows that increasing the length of the extended region in the tail can restore binding to the altered site. These results also demonstrate that the conserved spacing observed in the wild-type sites is restricted by the length of the extended region between the α2 homeodomain and the short helix that contacts **a**1.

Biochemical and structural studies have shown that the **a**1/α2 complex produces a

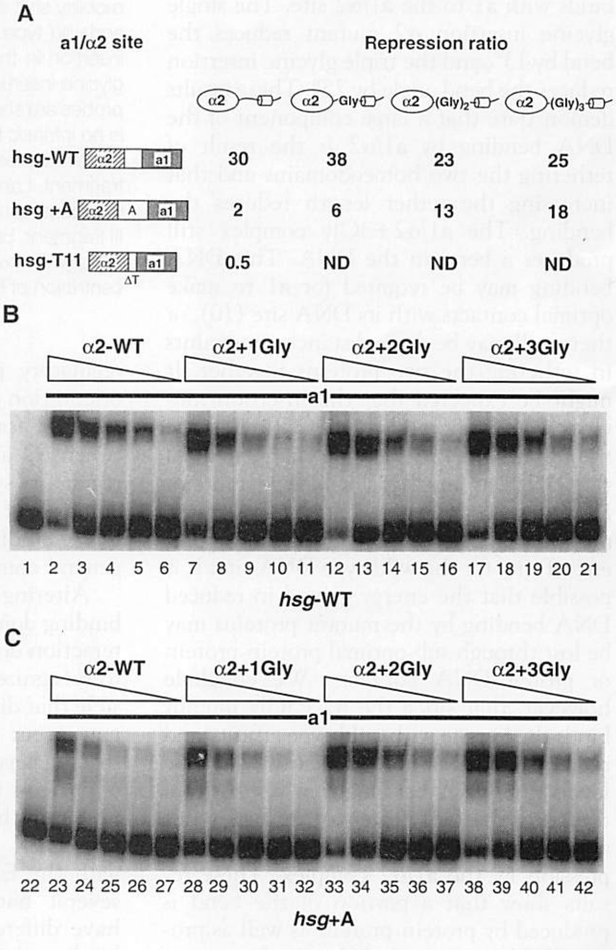

Fig. 1. Glycine insertions in the α2 tail restore the repression and DNA binding of an *hsg* operator with altered spacing. (**A**) A *CYC1-lacZ* promoter reporter vector containing a consensus wild-type (pYJ103) and altered spacing *hsg* sites (pYJ148, pYJ182) were co-transformed into a MAT**a** strain with plasmids that express either no α2 (pAV114), wild-type α2 (pJM130), or mutant α2 proteins with either one, two, or three glycines inserted into the tail (pYJ201, pYJ202, and pYJ203) and assayed for β-galactosidase activity (*12*). Values shown represent the repression ratio calculated by comparing the β-galactosidase activity in the presence and absence of α2. In the absence of α2, a *CYC1-lacZ* construct that contains a wild-type consensus *hsg* site (pYJ103) expresses an average of 335 ± 15 units of β-galactosidase activity. A strain that contains the wild-type α2 protein (pJM130) expresses 11 ± 1 units of β-galactosidase activity from the same *CYC1-lacZ* reporter plasmid (pYJ103) thereby showing ~30-fold repression of the promoter. (**B**) α2 proteins with glycine insertions in the tail bind to the wild-type *hsg* site with wild-type affinity. A labeled fragment containing the wild-type consensus *hsg* site was assayed for binding in the presence of a constant amount of **a**1 and dilutions of wild-type and mutant α2 proteins ranging by fivefold from 3×10^{-10} M (lanes 2, 7, 12, and 17) to 4.8×10^{-13} M (lanes 6, 11, 16, and 21). (**C**) Insertion in the α2 tail restores the binding of α2 to an *hsg* site with altered spacing. A labeled fragment containing the *hsg*+A site was assayed for binding in the presence of a constant amount of **a**1 and dilutions of α2 proteins ranging by fivefold from 1.5×10^{-9} M (lanes 23, 28, 33, and 38) to 2.4×10^{-12} M (lanes 27, 32, 37, and 42). Protein concentrations were normalized by Bradford assay and Coomassie-strained SDS gels.

smooth bend in the DNA that is localized in the **a**1 half site and the center region between the **a**1 and α2 sites (*10, 15*). This bending may be required for the **a**1 protein to make optimal contacts with the DNA. It may also be the result in part to tethering the two DNA binding domains together at a fixed distance such that the only way both proteins can simultaneously recognize their sites is to bend the DNA. A natural question that arises from our experiments is whether insertions in the tail reduce the DNA bending by **a**1/α2. In performing gel shift experiments of the α2 glycine insertion mutants on the wild-type *hsg* site, we noticed that the **a**1/α2 mutant complexes migrated slightly faster than the complex of the wild-type protein (Fig. 1B). This faster mobility could be the result of a decrease in DNA bending by the **a**1/α2 mutant complex. In order to test this model, we assayed the ability of these proteins to bend a wild-type *hsg* site in circular permutation experiments (Fig. 2) (*16*). As was observed in previous experiments (*15*), the wild-type α2 protein produces a bend of 100° when it binds with **a**1 to the **a**1/α2 site. The single glycine insertion α2 mutant reduces the bend by 13°, and the triple glycine insertion reduces the bend angle by 25°. These results demonstrate that a large component of the DNA bending by **a**1/α2 is the result of tethering the two homeodomains and that increasing the tether length reduces the bending. The **a**1/α2+3Gly complex still produces a bend in the DNA. This DNA bending may be required for **a**1 to make optimal contacts with its DNA site (*10*), or there still may be some distance constraints in tethering the two proteins together. It might be expected that the insertion mutants would bind with higher affinity since they do not require the same energy to bend the DNA as much as wild-type protein. However, we observe that the insertions and wild-type protein have the same apparent affinity for the wild-type DNA site. It is possible that the energy gained in reduced DNA bending by the mutant proteins may be lost through sub-optimal protein-protein or protein-DNA contacts. We conclude however, that since the α2+3Gly mutant binds the *hsg* site with wild-type affinity and represses transcription at nearly wild-type levels, the DNA bending that results from tethering the two proteins together is not absolutely required for DNA binding or repression by the **a**1/α2 complex. These results show that a portion of the bend is produced by protein-protein as well as protein-DNA contacts and that in the case of **a**1/α2, the two contributions can be partially separated.

Our results show that spacing between DNA binding domains contributes to the specificity of a complex of transcriptional regulatory proteins. Specific spacing and orientation of the DNA binding sites is also required for cooperative interactions between α2 and MCM1, as well as in other regulatory systems (*8, 18*). Spacing and orientation of the sites within a complex of DNA binding proteins may therefore be a general component of target site selection.

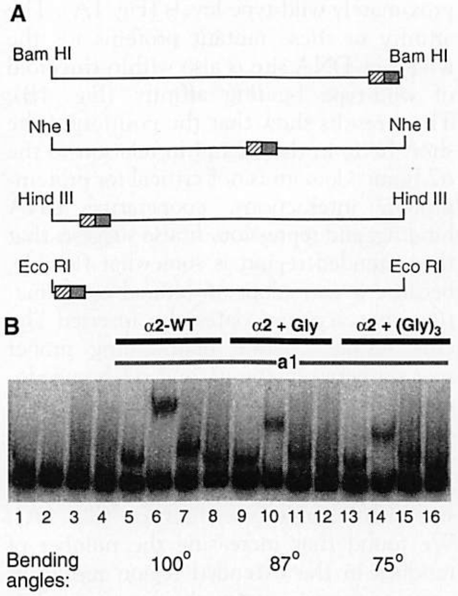

Fig. 2. Insertions in the α2 tail reduce the DNA bending caused by **a**1/α2 DNA binding. (**A**) A diagram indicates the position of the **a**1/α2 site in the 430-bp fragments used as probes in the position permutation assay (*17*). (**B**) The electrophoretic mobility shift assay shows the DNA bending by **a**1 and wild-type α2 (lanes 5 to 8), α2 with one glycine insertion in the tail (lanes 9 to 12), α2 with three glycine insertions in the tail (lanes 13 to 16). Free probes are shown in lanes 1 to 4 and indicate there is no intrinsic bending of the site in the absence of protein. Lanes 1, 5, 9, and 13 contain the Bam HI fragment. Lanes 2, 6, 10, and 14 contain the Nhe I fragment. Lanes 3, 7, 11, and 15 contain the Hind III fragment. Lanes 4, 8, 12, and 16 contain the Eco RI fragment; α2 proteins were added to a final concentration of 6×10^{-11} M.

Altering the spacing between the DNA binding domain and the protein-protein interaction domain allows the **a**1/α2 complex to recognize different target sites. It is possible that differences in sequence specificity may occur naturally, through altering the spacing between the DNA binding domains of proteins in a complex. It is interesting to note that the *Drosophila* homeodomain protein UBX, which interacts cooperatively with the EXD homeodomain protein, has several naturally occuring isoforms that have different spacing between the DNA binding domain and the YPWM protein-protein interaction motif (*19*). It is possible that in combination with EXD, these UBX isoforms may bind different target sites as a result of different spacing between the homeodomains. As other DNA binding cofactors are identified, it may become more apparent whether differences in spacing between DNA binding domains in a complex is a general mechanism used to alter target site selection.

REFERENCES AND NOTES

1. M. P. Scott, J. W. Tamkun, G. W. Hartzell, *Biochem. Biophys. Acta.* **989**, 25 (1989); W. J. Gehring, M. Affolter, T. Burglin, *Annu. Rev. Biochem.* **63**, 487 (1994).
2. T. Hoey and M. Levine, *Nature* **332**, 858 (1988); C. Desplan, J. Theis, P. H. O'Farrel, *Cell* **54**, 1081 (1988); S. Hayashi and M. Scott, *ibid.* **63**, 883 (1990); P. A. Lawrence and G. Morata, *ibid.* **78**, 181 (1994).
3. S. Stern, M. Tanaka, W. Herr, *Nature* **341**, 624 (1989); D. Xue, Y. Tu, M. Chalfie, *Science* **261**, 1324 (1993); S. Chan, L. Jaffe, M. Capovilla, J. Botas, R. S. Mann, *Cell* **78**, 603 (1994); M. A. van Dijk and C. Murre, *ibid.*, p. 617.
4. I. Herskowitz, *Nature* **342**, 749 (1989); A. D. Johnson, in *Transcriptional Regulation*, K. Yamamoto and S. McKnight, Eds. (Cold Spring Harbor Laboratory Press, Cold Spring Harbor, NY, 1992), pp. 975–1006.
5. C. A. Keleher, C. Goutte, A. D. Johnson, *Cell* **53**, 927 (1988).
6. C. Goutte and A. D. Johnson, *ibid.* **52**, 875 (1988); A. M. Dranginis, *Nature* **347**, 682 (1990); C. Goutte and A. D. Johnson, *J. Mol. Biol.* **233**, 359 (1993); *EMBO J.* **13**, 1434 (1994).
7. C. A. Keleher, S. Passmore, A. D. Johnson, *Mol. Cell. Biol.* **9**, 5228 (1989).
8. D. L. Smith and A. D. Johnson, *Cell* **68**, 133 (1992).
9. A. Mak and A. D. Johnson, *Genes Dev.* **7**, 1862 (1993).
10. T. Li, M. Stark, A. D. Johnson, C. Wolberger, *Science* **270**, 262 (1995).
11. C. L. Phillips, M. R. Stark, A. D. Johnson, F. W. Dahlquist, *Biochemistry* **33**, 9294 (1994).
12. Oligonucleotides containing glycine codons (GGT) inserted between α2 residues 189 and 190 were synthesized with Bam HI overhang (top strand) or Nhe I overhang (bottom strand). Plasmid pYJ201, pYJ202, and pYJ203, which contain one, two, or three glycines inserted between residues 189 and 190, respectively, were constructed by cloning annealed Bam HI–Nhe I fragments into pJM130, a yeast *CEN, LEU2* plasmid containing an engineered α2 gene with unique Bam HI and Nhe I sites in a 4.3-kb MATα fragment [J. Mead, H. Zhong, T. B. Acton, A. K. Vershon, in preparation]. *CYC1-LacZ* reporter plasmids were constructed by cloning oligonucleotides containing either the consensus wild-type site (pYJ103, hsg-WT: TCGATCATGTAATTAATTACATCA) or altered spacing sites (pYJ148, hsg+A: TCGATCATGTAATTAAATTACATCA; pYJ182, hsg-T11: TCGATCATGTAATAATTACATCA) into the Sal I site of pAV73, a yeast 2μ, *URA3* plasmid containing a *CYC1-lacZ* reporter promoter [A. K. Vershon, N. M. Hollingsworth, A. D. Johnson, *Mol. Cell. Biol.* **12**, 3706 (1992)]. The α2 expression plasmids pAV114, pJM130, pYJ201, pYJ202, and pYJ203 were paired with the appropriate *CYC1-lacZ* reporter vectors and cotransformed into the wild-type *MATa* strain, EG123 (*ura3, trp1, leu2, and his4*) (*5*) and the level of *LacZ* expression in three independent transformants was measured by liquid β-galactosidase assays (*8*).
13. Labeled fragments containing the *hsg* sites were synthesized by polymerase chain reaction using ^{32}P kinased primers that anneal to sequences in the *CYC1* promoter on either side of the *hsg* operator; 0.1 μg of the pYJ103, pYJ148, or pYJ182 was used as the template for 30 rounds of amplification, and the 120-bp labeled operator fragment was then gel-purified, eluted, and precipitated. The α2 protein used in this experiment is a fragment consisting of amino acid residues 123 to 210 (the entire homeodomain and COOH-terminal tail) with six histidine residues fused to the NH_2-terminus. α2 protein was expressed from plasmid pYJ195, a derivative of pET21a(+) (from Novagen) and was purified by chro-

matography on a nickel column according to the manufacturers protocols. Full-length **a**1 protein with six histidine residues fused to the COOH-terminus was expressed from plasmid pYJ173, a derivative of pET21a(+), and purified according to the protocol (Novagen). Electrophoretic mobility shift assays were performed as described (6). Reactions were incubated for 1 hour at RT and then electrophoresed on a nondenaturing 6% polyacrylamide gel with 0.5× TBE. Dried gels were exposed to a phosphor screen and the image was scanned on a Molecular Dynamics model 425 phosphorimager.

14. Y. Jin and A. Vershon, unpublished results.
15. D. L. Smith, A. B. Desai, A. D. Johnson, *Nucleic Acids Res.* **23**, 1239 (1995).
16. H.-M. Wu and D. M. Crothers, *Nature* **308**, 509 (1984).
17. In the position permutation experiment, 430-bp fragments containing the *hsg* site were generated by cutting plasmid pAJ459 (*15*), with appropriate enzymes (Bam HI, Nhe I, Hind III, or Eco RI) and filling in 5′ overhangs with [α-^{32}P]dNTPs. The labeled fragments were purified and electrophoretic mobility shift assays were performed as described above. Reaction mixes were electrophoresed on a nondenaturing 4% polyacrylamide gel with 1X TBE (90 mM tris-borate, 2 mM EDTA). Apparent DNA bending angles were calculated based on the Thompson and Landy relationship [J. F. Thompson and A. Landy, *Nucleic Acids Res.* **16**, 9687 (1988)].
18. K. Umesono, K. Murakami, C. Thompson, R. Evans, *Cell* **65**, 1255 (1991); A. M. Naar *et al.*, *ibid.*, p. 1267.
19. K. Kornfeld, R. B. Saint, P. A. Beachy, P. J. Harte, D. A. Peattie, D. S. Hogness, *Genes Dev.* **3**, 243 (1989).
20. We thank C. Abate-Shen, R. Ebright, and D. Norris for comments on the manuscript. Y.J. was supported by a Busch predoctoral fellowship and J.M. was supported by a Busch postdoctoral fellowship. This work was supported by a grant from NSF (MCB-9304526) to C.W. and NIH (GM49265) to A.K.V.

8 September 1995; accepted 22 September 1995

Titins: Giant Proteins in Charge of Muscle Ultrastructure and Elasticity

Siegfried Labeit and Bernhard Kolmerer

In addition to thick and thin filaments, vertebrate striated muscle contains a third filament system formed by the giant protein titin. Single titin molecules extend from Z discs to M lines and are longer than 1 micrometer. The titin filament contributes to muscle assembly and resting tension, but more details are not known because of the large size of the protein. The complete complementary DNA sequence of human cardiac titin was determined. The 82-kilobase complementary DNA predicts a 3-megadalton protein composed of 244 copies of immunoglobulin and fibronectin type III (FN3) domains. The architecture of sequences in the A band region of titin suggests why thick filament structure is conserved among vertebrates. In the I band region, comparison of titin sequences from muscles of different passive tension identifies two elements that correlate with tissue stiffness. This suggests that titin may act as two springs in series. The differential expression of the springs provides a molecular explanation for the diversity of sarcomere length and resting tension in vertebrate striated muscles.

During the past decade, additional filament systems formed by two giant proteins, titin and nebulin, had to be incorporated into the established view of vertebrate striated muscle as a two-filament sliding system [for reviews see (*1*)]. Progress on the molecular characterization of the titin and nebulin filaments initially was limited to histochemical approaches and electron microscopy because of the unusual sizes of these molecules, with molecular weights in the megadalton range. Native molecules of titin (*2*), also referred to as connectin (*3*), are filaments >1 μm long (*4*) that in situ extend from Z discs to M lines (*5*) (Fig. 1). The portion of titin that spans the A band (the region within the thick filament, referred to here as A band titin) is composed of regular arrangements of domains (*5*) that bind to other proteins of the thick filament (*6, 7*). This suggests that titin is involved in the regulation of the A band ultrastructure. In the I band (the region of titin that spans the thin filament), titin filaments are extensible, as revealed by immunoelectron microscopy (*5, 8*). This is likely to account for the intrinsic elasticity of vertebrate striated muscle myofibrils (*9*), because degradation of titin by radiation or proteases or its removal by extraction results in a loss of passive tension (*10*). The critical role of the titin filament for muscle structure and function cannot be unraveled without knowledge of its primary structure. Here, we determined the complete complementary DNA (cDNA) sequence of human titin. We suggest that titin specifies a sarcomeric building plan, into which tissue-specific features such as different passive tensions are provided by differential splicing.

We have previously isolated five partial titin cDNA clones from a human heart cDNA library (*6*). The partial titin cDNAs have been extended systematically into both the 5′ and the 3′ direction by anchored polymerase chain reaction (PCR) techniques. A total of 49 extensions were found to link the partial cDNAs into one 82-kb sequence contig. This contig represents the full-length coding sequence of titin expressed in the human heart, as indicated by the presence of untranslated regions at the 5′ and 3′ ends. The 81-kb open reading frame predicts a 26,926-residue protein with a molecular mass of 2993 kD. Ninety percent of the mass is contained in a repetitive structure composed of 244 copies of 100-residue repeats (Fig. 2). These repeats encode 112 immunoglobulin (Ig)-like and 132 FN3-like domains. The pool of 54 partial cardiac titin cDNAs identified 60 λ phage clones in a human genomic DNA library to which the partial cDNAs were assigned in a co-linear order. A subset of 16 phage clones was sufficient to span the 54 cardiac titin cDNAs and covered a contiguous span of 300 kb of genomic DNA. This argues against the presence of cloning artifacts and also suggests that the portion of the titin gene harboring the coding se-

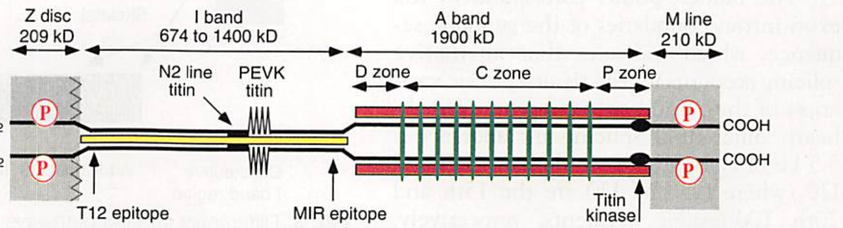

Fig. 1. Model for titin in the sarcomere. The titin filament is shown in black, the thin filament (actin) in yellow, and the thick filament (myosin) in red. The epitopes of the titin antibodies T12 and antibodies to the MIR have been mapped in the sarcomere by immunoelectron microscopy (*5, 26*); the positions of their epitopes in the titin sequence are known (*27*). Antibodies to the titin kinase domain react with the periphery of the M line (*12*). Therefore, it can be estimated which sections of the titin sequence are in the Z disc, I band, A band, and the M line. For the I band, the range of variation as predicted by the observed splice variants is indicated. The presumed extensible element of the I band, the PEVK element, is located between the N2 line titin and the second tandem Ig block (zig-zag pattern). Within the thick filament in the central C zone (green stripes), titin binds to both the C protein and myosin (*7, 8*) and is likely to specify the presence of 11 copies of the 430 Å thick filament repeat in vertebrate striated muscles. Phosphorylation of tandemly arranged Ser-Pro repeats in the Z disc and the M line titin (red P) may control integration of the titin filament into Z discs and M lines during myogenesis (*13*).

European Molecular Biology Laboratory, P.O. Box 102209, 69012 Heidelberg, Germany.

quences is ~300 kb in size.

The epitope position of the T12 titin antibody predicts that about 200 kD of titin enters the Z disc (Figs. 1 and 2). Domain architecture in the Z disc region of titin is arranged by a specialized class of Ig-like domains alternating with nonrepetitive sequences. The I band region of titin is composed of three different segments: tandem Ig-like domains, nonrepetitive sequence insertions in the central region of the I band, and a complex domain architecture near the junction of the A band and the I band. This correlates with earlier electron microscopic data that show that the I band titin has a complex fine structure (*11*). The nonrepetitive sequences in the central I band region (Fig. 2) are possibly involved in the self-association of the two or three titin strands (or half sarcomere) seen in the N2 line region. The end of the tandem Ig segment and the transition into a more complex architecture toward the A band (Fig. 2) may correspond to the junction point where titin strands branch from the thin filament to enter the thick filament (*11*).

For the A band section, where detailed ultrastructural information is available, the correlation of titin sequence and sarcomere structure is most obvious. Seven-module super-repeats correspond to the D zone titin, 11-module super-repeats to the C zone titin, and a less regular P zone region connects the A band to the M line titin (Fig. 2). The M line titin encompasses about 200 kD at the COOH-terminal end of titin (*12*). Its structure has been described in detail (*13*).

Some monoclonal antibodies specific to the I band titin distinguish between the cardiac and skeletal titins (*14*), and electrophoretic mobilities indicate that titins from different tissues have different sizes (*15*). Therefore, we compared human and rabbit titin mRNAs from different tissues. In the central part of the I band, cardiac and skeletal titins branch into distinct isoforms (Fig. 3). The branch points correspond to the exon-intron boundaries of the genomic sequence, which indicates that alternative splicing accounts for the tissue-specific variation of the I band titin structure (*16*). In heart, differential splicing includes about 3.5 kb of cDNA between domains I15 and I20 (where I15 and I20 are the 15th and 20th 100-residue segments, respectively, within the I band region of titin); in skeletal muscle, 22.5 kb of cDNA is included (Fig. 3). The inclusion of two structural motifs in different copy numbers accounts for the tissue-specific variation of I band titin mass (*17*). First, cardiac titin comprises 37 tandem Ig repeats, whereas 90 tandem Ig domains are present in the human skeletal sequence. Second, a sequence element rich in Pro (P), Glu (E), Lys (K), and Val (V) residues has a different length in cardiac and skeletal muscle (Fig. 4). The four amino acids P, E, V, and K constitute 70% of this element, and therefore we refer to it as the PEVK domain of titin. This domain comprises 163 or more residues in the cardiac titin sequence and 2174 residues in the skeletal titin sequence.

Hybridization of the 22.5 kb of skeletal cDNAs included between the I15 and I20 branch sites to blotted RNAs from different rabbit striated muscles revealed a tissue dependence of signal intensities with probes from the tandem Ig and PEVK region (Fig. 5). Different isoforms of I band titin were also detected within the same tissue. In heart, many splice variants occur within the PEVK region (Fig. 4), and two distinct isoforms of N2 line titin, N2-A and N2-B, were observed (Fig. 3). We conclude that a range of isoforms of I band titin is generated by differential splicing, which affects the length of the tandem Ig and the PEVK region of titin.

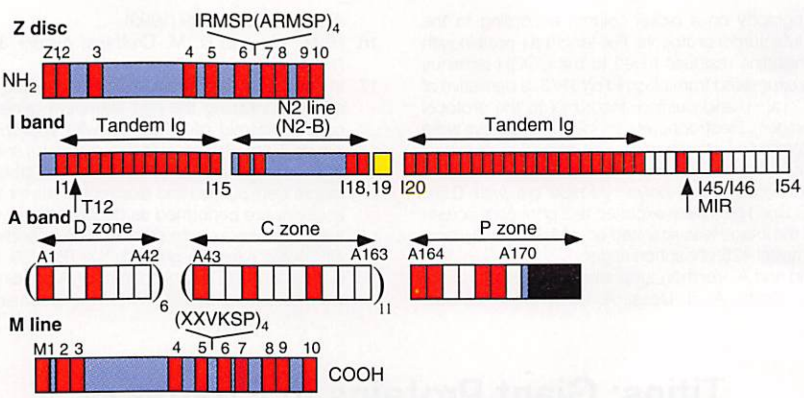

Fig. 2. Domain structure of the cardiac titin filament. The modular architecture of cardiac titin as predicted by its full-length cDNA is shown. A total of 244 copies of 100-residue repeats (indicated by vertical rectangles) are contained, of which 112 belong to the Ig (red) domain and 132 to the FN3 (white) superfamily. The 100-residue repeats are indicated by region and position regardless of whether they are Ig or FN3 domains. The titin kinase domain is shown in black, the PEVK element (N2-B 163-residue variant; see Fig. 3) in yellow. Sequences with no homology to database entries comprise 10% of the titin primary structure (blue). The epitope positions of T12 and MIR are indicated (*28*). The change in motif organization NH_2-terminal of T12 is proposed to be the Z disc–I band junction; the start of super-repeats COOH-terminal of MIR is proposed to be the beginning of the A band region of titin. Within the A band region, the D zone contains six copies of the seven-module super-repeat (A1 through A42); the C zone contains 11 copies of the 11-module super-repeat (A43 through A163). The positions of the tandemly repeated RMSP and VKSP motifs in the Z disc and M line region of titin are shown (*29*).

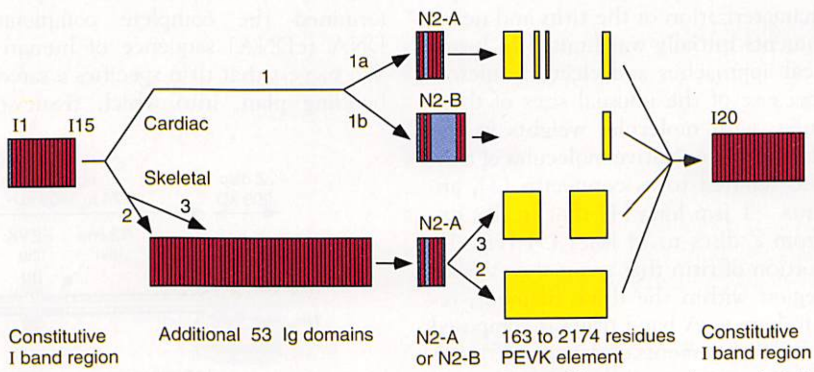

Fig. 3. Differential splicing pathways of I band titin. Comparison of human cardiac and skeletal titin cDNAs (*30*) reveals branching into distinct sequences between I15 and I20; color codes for domains are as in Fig. 2. In splicing pathway 1, for the heart, alternative splicing includes one of two distinct elements, termed N2-A and N2-B; the homology of N2-A to a partial chicken titin sequence from the N2 line region (*31*) suggests that N2-A and N2-B encode N2 line titin. Two sequenced variants of the PEVK element that are linked to the cardiac pathway N2-B encompass 163 and 181 residues (1b). N2-A–associated PEVK elements appear to be larger (1a). In splicing pathway 2, for skeletal muscle, 53 additional copies of tandem Ig domains are included, and the PEVK element is 2174 residues long. RT-PCR analysis of human tissues (*32*) with primer pairs derived from sequences from splicing pathways 1 and 2 suggests the presence of splicing pathway 2 in human soleus and diaphragm tissue. In human psoas tissue, some of the tandem Ig and PEVK sequences are excluded, and the approximate regions of excluded sequences are given (3). The human cardiac sequence submitted to the EMBL data library corresponds to pathway 1b, the skeletal I band sequence to pathway 2.

Fig. 4. The PEVK region in titin. The 2174 residues of the PEVK element from the human skeletal entry are shown (*29*). It is composed predominantly of four residues (P, pink; E, blue; K, green; V, yellow), and Pro-rich regions alternate with stretches rich in Glu residues. Analysis of cardiac cDNA clones from the PEVK region reveals multiple positions of differential splicing within the PEVK sequences (indicated by arrows), which suggests that the PEVK element can be cut in many different ways. The underlined 163 residues are shared by all sequenced cardiac clones and correspond to the N2-B–associated splice pathway (Fig. 3).

```
   1 PPEEIPPVVAPPVPLLLPTPEEKKPPPKRIEVTKKAVKKDAKKVVAKPKEMTPREEIVKKPPPPTTLIPAKAPEIIDVSSKAEEVKIMTITRKKEVQKEK
 100 EAVYEKKQAVHKEKRVFIESFEEPYDELEVEPYTEPFEQPYYEEPDEDYEEIKVEAKKEVHEEWEEDFEEGQEYYEREEGYDEGEEEWEEAYQEREVIQV
     QKEVYEESHERKVPAKVPEKKAPPPPKVIKKPVIEKIEKTSRRMEEEKVQVTKVPEVSKKIVPQKPSRTPVQEEVIEVKVPAVHTKKMVISEEKMFFASH
     TEEEVSVTVPEVQKEIVTEEKIHVAVSKRVEPPPKVPELPEKPAPEEVAPVPIPKKVEPPAPKVPEVPKKPVPEEKKPVPVPKKEPAAPPKVPEVPKKPV
     PEEKIPVPVAKKKEAPPAKVPEVQKGVVTEEKITIVTQREESPPPAVPEIPKKKVPEERKPVPRKEEEVPPPPKVPALPKKPVPEEKVAVPVPVAKKAPP
 500 PRAEVSKKTVVEEKRFVAEEKLSFAVPQRVEVTRHEVSAEEEWSYSEEEEGVSISVYREEEREEEEEAEVTEYEVMEEPEEYVVEEKLHIISKRVEAEPA
     EVTERQEKKIVLKPKIPAKIEEPPPAKVPEAPKKIVPEKKVPAPVPKKEKVPPPKVPEEPKKPVPEKKVPPKVIKMEEPLPAKVTEKHMQITQEEKVLVA
     VTKKEAPPKARVPEEPKRAVPEEKVLKLKPKREEEPPAKVTEFRKRVVKEEKVSIEAPKREPQPIKEVTIMEEKERAYTLEEEAVSVQREEEYEEYEEYD
     YKEFEEYEPTEEYDQYEEYEEREYERYEEHEEYITEPEKPIPVKPVPEEPVPTKPKAPPAKVLKKAVPEEKVPVPIPKKLKPPPPKVPEEPKKVFEEKIH
     ISITKREKEQVTEPAAKVPMKPKRVVAEEKVPVPRKEVAPPVRVPEVPKELEPEEVAFEEEVVTHVEEYLVEEEEEYIHEEEEFITEEEVVPVIPVKVPE
1000 VPRKPVPEEKKPVPVPKKKEAPPAKVPEVPKKPEEKVPVLIPKKEKPPPAKVPEVPKKPVPEEKVPVPVPKKVEAPPAKVPEVKKKPVPEKKVPVPAPKK
     VEAPPAKVPEVPKKLIPEEKKPTPVPKKVEAPPPKVPKKREPVPVPVALPQEEEVLFEEEIVPEEEVLPEEEEVLPEEEEVLPEEEEVLPEEEEIPPEEE
     EVPPEEEYVPEEEEFVPEEEVLPEVKPKVPVPAPVPEIKKKVTEKKVVIPKKEEAPPAKVPEVPKKVEEKRIILPKEEEVLPVEVTEEPEEEPISEEEIP
     EEPPSIEEVEEVAPPRVPEVIKKAVPEAPTPVPKKVEAPPAKVSKKIPEEKVPVPVQKKEAPPAKVPEVPKKVPEKKVLVPKKEAVPPAKGRTVLEEKVS
     VAFRQEVVVKERLELEVVEAEVEEIPEEEEFHEVEEYFEEGEFHEVEEFIKLEQHRVEEEHRVEKVHRVIEVFEAEEVEVFEKPKAPPKGPEISEKIIPP
1500 KKPPTKVVPRKEPPAKVPEVPKKIVVEEKVRVPEEPRVPPTKVPEVLPPKEVVPEKKVPVPPAKKPEAPPPKVPEAPKEVVPEKKVPVPPPKKPEVPPTK
     VPEVPKAAVPEKKVPEAIPPKPESPPPEVFEEPEESPSAPPKKPEVPPVRVPEVPKEVVPEKKVPAAPPKKPEVTPVKVPEAPKEVVPEKKVPVPPPKKP
     EVPPTKVPEVPKVAVPEKKVPEAIPPKPESPPPEVFEEPEEVALEEPPAEVVEEPEPAAPPQVTVPPKNPVPEKKAPAVVAKKPELPPVKVPEVPKEVVP
     EKKVPLVVPKKPEAPPAKVPEVPKEVVPEKKVAVPKKPEVPPAKVPEVPKKPVLEEKPAVPVPERAESPPPEVYEEPEEIAPEEEIAPEEEKPVPVAEEE
     EPEVPPPAVPEEPKKIIPEKKVPVIKKPEAPPPKEPEPEKVIEKPKLKPRPPPPPPAPPKEDVKEKIFQLKAIPKKKVPENPQVPEKVELTPLKVPGGEK
2000 KVRKLLPERKPEPKEEVVLKSVLRKRPEEEEPKVEPKKLEKVKKPAVPEPPPPKPVEEVEVPTVTKRERKIPEPTKVPEIKPAIPLPAPEPKPKPEAEVK
     TIKPPPVEPEPTPIAAPVTVPVVGKKAEAKAPKEEAAKPKGPIKGVPKKTPSPIEAERRKLRPGSGGEKPPDEA        2174
```

Vertebrate thick filaments are organized into D, C, and P zones (*18*). It has not been understood what regulates thick filament assembly into three structurally distinct compartments and why 11 stripes of members of the MyBpC protein family (C, H, and X protein) are bound at regular intervals of 430 Å in the C zone (*18*). The C zone titin sequence comprises 11 copies of 11-module super-repeats, which bind to the C protein in vitro (*6*, *7*). We conclude that the super-repeat architecture of A band titin can explain the global architectures present in vertebrate thick filaments. The high degree of sequence conservation in the C zone titin (*6*, *19*) correlates with the presence of C zones in all vertebrate thick filaments. In contrast to the conserved module architecture of the A band titin, the structure of I band titin depends on tissue type (Fig. 3). Also, in the M line, two distinct isoforms of titin are expressed in correlation with the M line fine structure (*20*). Therefore, we suggest that where sarcomeres have a conserved ultrastructure, the domain architecture is constant, whereas tissue-specific features are introduced into the building plan of the titin mRNA by differential splicing in regions where sarcomere ultrastructures are variable.

Comparison of the I band titin sequences from heart, psoas, and soleus muscles, each of which has different passive tensions and expresses different size classes of titin (*15*), identifies the regions that are involved in elasticity. The I band sequences have different contents both of the tandem Ig and of the PEVK segments. Previous work on the molecular basis of elasticity in titin assumed that I band titin is composed only of Ig and FN3 domains. Therefore, it was proposed that the Ig-like β barrel structures of the titin repeats (*21*) unfold to gain an increase in length of severalfold (*22*). However, the stability of expressed I band domains does not support such unfolding theories (*23*). The PEVK region might be more easily stretched than the Ig domains because the reduced complexity of the sequence together with the clusters of negative charges should prevent the formation of stable tertiary structure folds. In an extended state, the 2200-residue version of the PEVK segment could span up to 0.8 μm in vivo and account for the initial ~0.8-μm extension per half sarcomere, during which most skeletal muscles develop only little passive tension (*15*).

Therefore, the PEVK domain may account for the extensibility of the titin filament at low forces. After this extensibility has been exhausted, the stable folds of the titin's I band Ig domains will resist further extension. This would explain the rapid rise in tension toward the end of the physiological slack length of sarcomeres. The moderate levels of further extension (beyond 0.8 μm per half sarcomere) that occur in vivo in skeletal muscles may be explained by conformational changes in the tandem Ig segments, such as bending and stretching of interdomain linkers. In conclusion, we propose that the PEVK region and tandem Ig titin are two elements of differential stiffness that function in parallel as a two-spring system. This is in agreement with mechanical studies on muscle that propose a two-spring model (*15*, *24*), and with immunohistochemical studies showing a nonuniform extensibility within the I band titin (*11*, *25*).

It remains to be seen how the multiple splicing events in the I band titin are regulated. The length of the tandem Ig and the PEVK segments are correlated, presumably because the longer slack lengths of more elastic muscles necessitate longer I bands. Therefore, their splicing must be coordinated. The second giant muscle protein nebulin is thought to specify the length of the thin filament and is also expressed in variable length versions by differential splicing (*26*). The assembly plans of the I band that are specified by both molecular rulers will match only if differential splicing events controlling the size of I band titin and

Region of I band titin	Probe	H	P	G	EDL	LD	S + D + PL
Tandem Ig	P1	-	-	+	+	+	+
	P2	-	-	+	+	+	+
	P3	-	-	+	+	+	+
	P4	-	o	+	+	+	+
	P5	-	+	+	+	+	+
	P6	-	+	+	+	+	+
	P7	-	+	+	+	+	+
	P8	-	+	+	+	+	+
	P9	-	+	+	+	+	+
N2-A	P10	+	+	+	+	+	+
	P11	+	+	+	+	+	+
	P12	+	+	+	+	+	+
PEVK element	P13	+	+	+	+	+	+
	P14	-	-	+	+	+	+
	P15	-	-	+	+	+	+
	P16	-	-	o	o	+	+
	P17	-	-	o	o	+	+
	P18	+	o	+	+	o	+

Fig. 5. The type of I band titin expressed depends on the tissue. Expression of the 22.5-kb of central I band titin sequences located between I15 and I20 was monitored in a panel of striated muscle RNAs (*33*). Total RNA from the indicated muscles was blotted onto nylon membranes and hybridized to a set of probes (P1 through P18) covering the 22.5-kb region. Analyzed tissues were all from rabbit. H, heart; P, psoas; G, gastrocnemius; EDL, extensor digitorum longus; LD, longissimus dorsi; S, soleus; D, diaphragm; PL, plantaris longus. Signals were compared with a titin kinase probe, because the exon encoding this domain is expressed in all striated muscles (*20*). Expression less than 25% of the kinase control probe is indicated with a minus; for 60 to 100% of controls, with a plus; for values 25 to 60% of the control, as "o" (unspliced intermediates or splicing within the probe sequence may explain intermediate signals). The differential hybridization of tandem Ig and PEVK probes suggests that they have different lengths in different muscles.

nebulin are interdependent. Therefore, the precision and tissue specificity of the sarcomeric assembly program in vertebrates appear to necessitate coordinated splicing decisions in the titin and nebulin precursor mRNAs.

REFERENCES AND NOTES

1. K. Maruyama, *Biophys. Chem.* **50**, 73 (1994); J. Trinick, *Trends Biochem. Sci.* **19**, 405 (1994).
2. K. Wang, J. McClure, A. Tu, *Proc. Natl. Acad. Sci. U.S.A.* **76**, 3698 (1979).
3. K. Maruyama *et al.*, *J. Biochem. (Tokyo)* **82**, 317 (1977).
4. R. Nave, D. O. Fürst, K. Weber, *J. Cell Biol.* **109**, 2177 (1989); J. Suzuki, S. Kimura, K. Maruyama, *J. Biochem. (Tokyo)* **116**, 406 (1994).
5. In the microscope, striated muscle appears as a periodical array of darker and brighter stripes. The dark segment contains the thick filament (myosin) and is referred to as the A band, the bright segment contains the thin filament (actin) and is called the I band. In the center of A and the I bands, dense structures ~100 nm wide are present, referred to as M lines and Z discs, respectively. A single titin molecule spans the distance from the Z disc to the M line [D. O. Fürst, M. Osborn, R. Nave, K. Weber, *J. Cell Biol.* **106**, 1563 (1988)].
6. S. Labeit, M. Gautel, A. Lakey, J. Trinick, *EMBO J.* **11**, 1711 (1992).
7. A. Soteriou, M. Gamage, J. Trinick, *J. Cell Sci.* **104**, 119 (1993).
8. Y. Itoh *et al.*, *J. Biochem. (Tokyo)* **104**, 504 (1988).
9. A. Magid and D. J. Law, *Science* **230**, 1280 (1985).
10. R. Horowits, E. S. Kempner, M. E. Bisher, R. J. Podolsky, *Nature* **323**, 160 (1986); T. Funatsu, H. Higuchi, S. Ishiwata, *J. Cell Biol.* **110**, 53 (1990); G. Salviati, R. Betto, S. Ceoldo, S. Pierobon-Bormioli, *Am. J. Physiol.* **259**, C144 (1990).
11. T. Funatsu *et al.*, *J. Cell Biol.* **120**, 711 (1993).
12. A monoclonal antibody raised to an expressed titin kinase domain fragment stains sarcomeres in the periphery of the M line region (D. O. Fürst, unpublished material).
13. M. Gautel, K. Leonard, S. Labeit, *EMBO J.* **12**, 3827 (1993).
14. C. Hill and K. Weber, *J. Cell Biol.* **102**, 1099 (1986).
15. K. Wang, R. McCarter, J. Wright, J. Beverly, R. Ramirez-Mitchell, *Proc. Natl. Acad. Sci. U.S.A.* **88**, 7101 (1991); R. Horowits, *Biophys. J.* **61**, 392 (1993); H. L. Granzier and T. C. Irving, *ibid.* **68**, 1027 (1995).
16. B. Kolmerer and S. Labeit, unpublished material.
17. The inclusion of the 22.5 kb of sequences between I15 and I20 predicts that soleus titin is encoded by a 101-kb mRNA, encompasses 33,000 residues, and has a molecular mass of 3700 kD.
18. R. Craig, *J. Mol. Biol.* **109**, 69 (1977); ______ and G. Offer, *Proc. R. Soc. London Ser. B.* **192**, 451 (1976); M. Sjöström and J. Squire, *J. Mol. Biol.* **109**, 49 (1977).
19. A 1.8-kb cDNA probe of C zone titin strongly cross-hybridizes to a variety of vertebrate DNAs, from humans to turtles, and detects conserved fragment lengths in most mammalian species (C. Witt and H. Jockusch, unpublished material).
20. The titin exon Mex5 encoding the domain is7 is expressed in all striated muscles; the exon Mex5 is differentially expressed in correlation with M line structure (B. Kolmerer, unpublished results).
21. H. M. Holden, M. Ito, D. J. Hartshorne, I. Rayment, *J. Mol. Biol.* **227**, 840 (1992); M. Pfuhl and A. Pastore, *Structures* **3**, 391 (1995).
22. A. Soteriou, A. Clarke, S. Martin, J. Trinick, *Proc. R. Soc. London Ser. B.* **254**, 83 (1993); H. Erickson, *Proc. Natl. Acad. Sci. U.S.A.* **91**, 10114 (1994).
23. A. S. Politou, D. J. Thomas, A. Pastore, *Biophys. J.*, in press.
24. K. Wang, R. McCarter, J. Wright, J. Beverly, R. Ramirez-Mitchell, *ibid.* **64**, 1161 (1993).
25. K. Trombitas and G. H. Pollack, *J. Muscle Res. Cell Motil.* **14**, 416 (1993).
26. S. Labeit and B. Kolmerer, *J. Mol. Biol.* **248**, 308 (1995).
27. J. A. Aarli, K. Stefansson, L. S. G. Marton, R. L. Wollmann, *Clin. Exp. Immunol.* **82**, 284 (1990).
28. For the main immunogenic region (MIR) of titin, patients' sera (*27*) were used to screen a human cardiac gt11 library, and the isolated phage inserts were expressed in *Escherichia coli*. Protein immunoblots and enzyme-linked immunosorbent assays with recombinant titin antigens assigned the MIR to I45 and I46 [M. Gautel *et al.*, *Neurology* **43**, 1581 (1993)]. T12 (*5*) monoclonal antibody was used to screen a gt11 library. Positive phages were sequenced from both ends and identified a region of overlap within I2 and I3.
29. Single-letter abreviations for the amino acids are as follows: A, Ala; , C, Cys; D, Asp; E, Glu; F, Phe; G, Gly; H, His; I, Ile; K, Lys; L, Leu; M, Met; N, Asn; P, Pro; Q, Gln; R, Arg; S, Ser; T, Thr; V, Val; W, Trp; Y, Tyr; and X, any residue.
30. The cDNA sequences were obtained from commercially available cDNA libraries: human cardiac, Stratagene catalog number 936208; human skeletal, Clontech HL1124.
31. K. Maruyama *et al.*, *Biochem. Biophys. Res. Commun.* **194**, 1288 (1993).
32. For reverse transcriptase–polymerase chain reaction (RT-PCR), human RNAs were prepared essentially as described [R. J. MacDonald, G. H. Swift, A. E. Przybyla, J. M. Chirgwin, *Methods Enzymol.* **152**, 219 (1987)]. Reverse transcription was performed with Moloney murine leukemia virus RT from BRL as specified by the supplier. RT reactions were analyzed by PCR with the use of combinations of primer pairs derived from the cardiac and skeletal sequences [R. K. Saiki *et al.*, *Science* **230**, 1350 (1985)].
33. The 22.5 kb of skeletal I band titin included between I15 and I20 were amplified by PCR as a set of 18 subfragments. Total RNA was blotted on nylon membranes, cross-linked, and hybridized as described, except that temperatures were lowered to 55°C to account for the species difference of the probe and RNA [G. M. Church and W. Gilbert, *Proc. Natl. Acad. Sci. U.S.A.* **81**, 1991 (1984)]. Probes P1 through P18 were labeled randomly essentially as described [A. P. Feinberg and B. Vogelstein, *Anal. Biochem.* **13**, 6 (1983)].

34. We thank J. Trinick for his contributions in the initial stages of this project, M. Saraste, A. Pastore, B. Bullard, K. Leonard, and M. Gautel for their continuous support and encouragement, D. O. Fürst and K. Weber and C. Witt and H. Jockusch for communicating unpublished results, and the Chirugische Kinik Heidelberg for human muscle tissues from organ transplant donors. We gratefully acknowledge the financial support of the Deutsche Forschungsgemeinschaft, the European Community, the Human Frontier Science programme, and the Frauenklinik Mannheim. The 82-kb cardiac titin cDNA and the 22-kb I band titin cDNA included in soleus skeletal muscle have been submitted to the European Molecular Biology Laboratory (EMBL) data library (accession numbers AC X90568 and X90569, respectively). The coordinates of the P1 through P18 subfragments are included in the annotations to accession number X90569; the DNA is available from us. Additional information on the titin sequence and available cDNA and genomic probes can be obtained from the World Wide Web from http: //www.aaas.org/science/science.html; see "Beyond the Printed Page."

25 May 1995; accepted 18 August 1995

Requirement for Generation of H_2O_2 for Platelet-Derived Growth Factor Signal Transduction

Maitrayee Sundaresan, Zu-Xi Yu, Victor J. Ferrans, Kaikobad Irani, Toren Finkel*

Stimulation of rat vascular smooth muscle cells (VSMCs) by platelet-derived growth factor (PDGF) transiently increased the intracellular concentration of hydrogen peroxide (H_2O_2). This increase could be blunted by increasing the intracellular concentration of the scavenging enzyme catalase or by the chemical antioxidant *N*-acetylcysteine. The response of VSMCs to PDGF, which includes tyrosine phosphorylation, mitogen-activated protein kinase stimulation, DNA synthesis, and chemotaxis, was inhibited when the growth factor–stimulated rise in H_2O_2 concentration was blocked. These results suggest that H_2O_2 may act as a signal-transducing molecule, and they suggest a potential mechanism for the cardioprotective effects of antioxidants.

Evidence from both plant and animal cells suggests that H_2O_2 may act as an intracellular second messenger. Hydrogen peroxide may regulate the defense of plants against viral pathogens by serving as a small diffusible molecule to orchestrate the hypersensitive response (*1*). Salicylic acid binds to and inactivates tobacco catalase, leading to a rise in H_2O_2 concentration ($[H_2O_2]$) and the activation of gene expression (*2*). In mammalian cells, H_2O_2 has been implicated as an indirect activator of the transcription factor nuclear factor kappa B (NF-κB) (*3*). Because NF-κB modulates the expression of a variety of immune and inflammatory molecules, it would appear that a role for H_2O_2 in host defense mechanisms has been conserved from plants to animals. Similarly, H_2O_2 may function in triggering apoptosis in both plant and animal cells (*1*, *4*).

Stimulation of various mammalian cell types with either cytokines, phorbol esters, or growth factors increases the secretion of

M. Sundaresan, K. Irani, T. Finkel, Cardiology Branch, National Heart, Lung, and Blood Institute (NHLBI), National Institutes of Health (NIH), Bethesda, MD 20892–1650, USA.
Z.-X. Yu and V. J. Ferrans, Pathology Section, NHLBI, NIH, Bethesda, MD 20892–1518, USA.

*To whom correspondence should be addressed

H_2O_2 into the extracellular space (5, 6). We investigated the possibility that a parallel between nitric oxide (NO) and H_2O_2 might exist. High concentrations of these diffusible reactive oxygen intermediates play a role in host defense; however, at low concentrations, NO modulates signal transduction of endothelial and neuronal cells. To evaluate whether H_2O_2 could have a similar function in signal transduction, we studied VSMCs for which low concentrations of exogenous H_2O_2 are mitogenic (7).

PDGF stimulation of primary rat VSMCs revealed an increase in intracellular [H_2O_2] as measured by the oxidation of the peroxide-sensitive fluorophore 2′,7′-dichlorofluorescin (DCF). Microfluorometric study with confocal microscopy showed that, compared with quiescent cells, stimulation with the PDGF-AB isoform (5 ng/ml) rapidly increased DCF fluorescence by 50- to 100-fold. The PDGF-stimulated increase in [H_2O_2] is transient (Fig. 1A), with [H_2O_2] peaking within the first few minutes after growth factor addition and then returning rapidly toward basal levels. This time course is similar to that described for PDGF-induced tyrosine phosphorylation (8). Exogenously added H_2O_2 or other oxidant stresses can induce tyrosine phosphorylation in several cell types (9). We observed similar effects in VSMCs. Increasing extracellular [H_2O_2] from 0.01 to 10 mM resulted in significant increases in the total amount of tyrosine-phosphorylated proteins (Fig. 1B). To achieve the intracellular [H_2O_2] seen after PDGF stimulation required extracellular [H_2O_2] in the 0.1 to 1.0 mM range (10). This range of extracellular [H_2O_2] also appears to induce the tyrosine phosphorylation of the p42 isoform of mitogen-activated protein (MAP) kinase (Fig. 1C).

We decreased [H_2O_2] in VSMCs by increasing the amount of the peroxide-scavenging enzyme catalase. This enzyme rapidly degrades H_2O_2 to water and molecular oxygen. Infection of VSMCs with an adenovirus that encodes catalase (Ad.Cat) resulted in measurable increases in intracellular catalase activity (Fig. 2A) (11). The level of enzymatic activity was a function of the multiplicity of infection (MOI), and no increase was seen when a control adenovirus encoding the *Escherichia coli lacZ* gene (Ad.βgal) was used. Addition of purified catalase to the culture medium resulted in even greater increases in intracellular VSMC catalase activity. Because catalase is a 60-kD protein which in solution forms homotetramers, it seems unlikely that the protein simply diffuses into VSMCs. Indeed, although loading of VSMCs with catalase by addition of the purified enzyme to the medium resulted in a time-dependent increase in VSMC intracellular catalase activity, this was not observed in several other cell lines tested such as human umbilical vein endothelial cells (HUVECs) or HeLa cells (Fig. 2B). Uptake of catalase into VSMCs did not occur at 4°C, suggesting that it is an energy-dependent and perhaps receptor-mediated process (10). The increase in intracellular catalase activity was dependent on the concentration of extracellular catalase (Fig. 2C). At the highest extracellular concentration used (3000 U/ml), a 72-hour incubation resulted in a ~50-fold increase in intracellular catalase activity.

To show that the addition of exogenous catalase did not result in its nonspecific binding to the outer surfaces of VSMCs, we loaded cells with catalase and then exposed them to proteinase K. Although proteinase K (1 mg/ml) rapidly inactivated purified catalase in solution, the enzymatic activity of catalase-loaded cells was resistant to the protease (Fig. 2D). We also stimulated VSMCs loaded with catalase with PDGF and assayed for H_2O_2 levels. Catalase-loaded VSMCs had a reduced peak level of DCF fluorescence after the addition of PDGF. The relative peak DCF fluorescence seen after growth factor addition was a function of catalase concentrations (Fig. 2E).

We assessed the effect of increased intracellular catalase activity on PDGF signal transduction. PDGF-AB (5 ng/ml) induced a rapid increase in tyrosine phosphorylation of numerous proteins (Fig. 3A). As catalase activity increased, the PDGF-induced stimulation of tyrosine phosphorylation was correspondingly reduced in a dose-dependent fashion. At the highest amount of intracellular catalase activity, an amount that almost completely blocks the growth factor–induced rise in [H_2O_2], stimulation of tyrosine phosphorylation by PDGF was almost completely inhibited (Fig. 3A).

The addition of catalase even in large amounts (3000 U/ml) for prolonged periods of time (>5 days) produced no visible effects on VSMCs and did not affect viability as assessed by trypan blue exclusion, although catalase-loaded cells grew at approximately half the rate of control cells (10). In addition, although catalase-loaded cells had an attenuated response to PDGF, when the NO

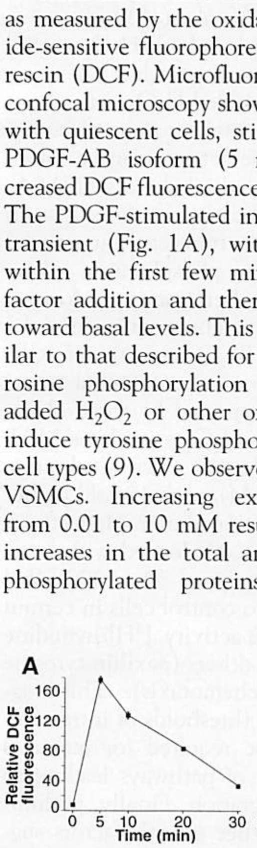

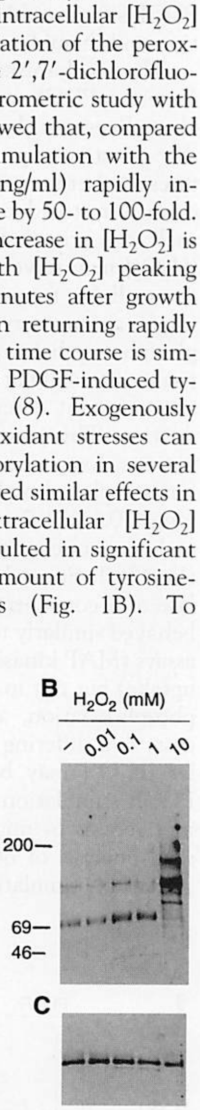

Fig. 1. Production of H_2O_2 in cells stimulated with PDGF and the effects of H_2O_2 on protein tyrosine phosphorylation. Primary VSMCs were deprived of serum for 3 days and then incubated with the H_2O_2-sensitive fluorophore DCF (17) and imaged by laser confocal microscopy before and after treatment with PDGF (5 ng/ml). (**A**) Time course of H_2O_2 generation after PDGF stimulation in relative DCF fluorescence units (scale of 0 to 256 units). Values are mean ± SEM obtained from 20 or more random cells. (**B** and **C**) Lysates were prepared from unstimulated VSMCs or VSMCs stimulated for 20 min with increasing concentrations of H_2O_2 (as indicated). Lysates were first immunoprecipitated with an antibody to phosphotyrosine and immunoblots probed with either (B) a phosphotyrosine antibody or (C) an antibody that recognizes the p44 and p42 isoforms of MAP kinase (18). Molecular sizes are indicated in (B) in kilodaltons.

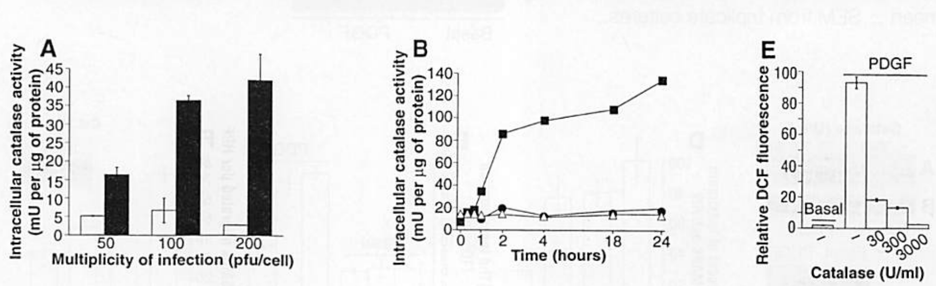

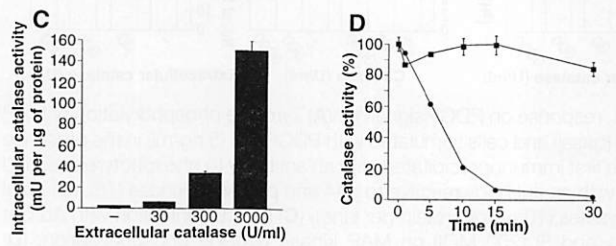

Fig. 2. An increases in intracellular catalase activity and its effects on intracellular [H_2O_2]. (**A**) Intracellular catalase activity as a function of adenoviral multiplicity of infection [recorded as plaque-forming units (pfu) per cell] (19). A catalase-containing adenovirus (Ad.Cat, black bars) or a control virus encoding the *E. coli lacZ* gene (Ad.βgal, white bars) was used. (**B**) Time-dependent intracellular catalase activity after exogenous administration of catalase to VSMCs (■), HUVECs (●), and HeLa cells (△) (20). (**C**) Intracellular catalase activity as a function of exogenous catalase concentration. (**D**) Effects of proteinase K on catalase activity (21). All measurements of catalase activity were obtained from triplicate cultures and are expressed as mean ± SEM. ■, Catalase-loaded cells; ●, purified catalase in solution. (**E**) Representative experiment demonstrating relative DCF fluorescence in unstimulated and PDGF-stimulated cells loaded with catalase. Values were obtained from 20 or more cells and expressed as mean ± SEM.

donor sodium nitroprusside (SNP) was added to the medium there was a rise in the concentration of cyclic guanosine 3′,5′-monophosphate (cGMP) equal to or greater than that of control cells (Fig. 3B). This indicates that the H_2O_2 and NO pathways are separable and that increased intracellular catalase does not have a toxic or global effect on all signal transduction pathways.

We next identified specific proteins whose growth factor–stimulated tyrosine phosphorylation was regulated by endogenous H_2O_2 release. Stimulation of VSMCs with PDGF induced an increase in the amount of tyrosine-phosphorylated p44 and p42 isoforms of MAP kinase. As intracellular catalase activity increased, both basal and PDGF-stimulated tyrosine phosphorylation of MAP kinase were inhibited (Fig. 4A). These results were not due to changes in the steady-state amount of MAP kinase protein in catalase-treated cells (Fig. 4B). Qualitatively similar results were obtained after adenoviral gene transfer. Infection with Ad.Cat (200 MOI) produced intracellular catalase activity that was equivalent to that observed with 72 hours of catalase loading at an intermediate dose (300 U/ml) of extracellular catalase (Fig. 2, A and C). Such infection with either Ad.βgal or Ad.Cat affected cell morphology and in general reduced the responsiveness of VSMCs to growth factors (*10*). Nonetheless, MAP kinase phosphorylation after PDGF addition was inhibited to a greater extent in Ad.Cat-infected compared with similarly infected Ad.βgal cells (Fig. 4C). In accordance with the amount of MAP kinase tyrosine phosphorylation, MAP kinase enzymatic activity [as assessed by phosphorylation of a myelin basic protein (MBP) substrate] varied in relation to catalase activity (Fig. 4D). Consistent with the reduction in MAP kinase phosphorylation and activity, PDGF-induced [^{3}H]thymidine incorporation was reduced in the presence of increased amounts of catalase (Fig. 4E).

Increased amounts of intracellular catalase activity also inhibited the ability of PDGF to stimulate chemotaxis of VSMCs (Fig. 4F). A ~50% reduction in migration was observed at the highest level of catalase activity. The molecular basis of PDGF-induced migration is not fully understood, but it might involve the cytoskeletal-associated protein paxillin, whose tyrosine phosphorylation is stimulated by PDGF in several cell types including VSMCs (*12*). The amount of tyrosine-phosphorylated paxillin in PDGF-stimulated lysates was decreased in cells containing high catalase activity (Fig. 4F, insert).

We tested whether other reactive oxygen intermediate scavengers would have effects similar to those of catalase. When VSMCs were treated with the chemical antioxidant *N*-acetylcysteine (NAC), we noted a concentration-dependent reduction in PDGF-stimulated DCF fluorescence (Fig. 5A). NAC caused a concentration-dependent reduction in PDGF-stimulated tyrosine phosphorylation (Fig. 5B). Similarly, millimolar amounts of NAC resulted in a reduction of PDGF-stimulated MAP kinase phosphorylation and thymidine uptake (*10*).

The mechanism by which H_2O_2 participates in PDGF signal transduction is unclear. Exogenously added H_2O_2 can reversibly inactivate protein tyrosine phosphatases, and enzymatic activity can be subsequently restored by thiol donors (*13*). As such, the growth factor–stimulated rise in [H_2O_2] may serve to transiently inactivate intracellular tyrosine phosphatases, allowing for a temporary alteration in the kinase-phosphatase balance. The magnitude of the rise in intracellular [H_2O_2] may therefore be an important determinant of signal transduction. This is supported by three observations. Exogenous H_2O_2 stimulates MAP kinase phosphorylation over a discrete range (0.1 to 1.0 mM), with 10-fold higher or lower concentrations having less effects (Fig. 1C). Second, cells loaded with catalase at a concentration of 30 or 300 U/ml behaved similarly to control cells in certain assays (MAP kinase activity, [^{3}H]thymidine uptake) but not in others (paxillin tyrosine phosphorylation, chemotaxis). This suggests that differing thresholds of intracellular [H_2O_2] may be required for maximal PDGF stimulation of pathways leading to mitogenesis or migration. Finally, preliminary analysis of other growth factors suggests that stimulation of VSMC by epider-

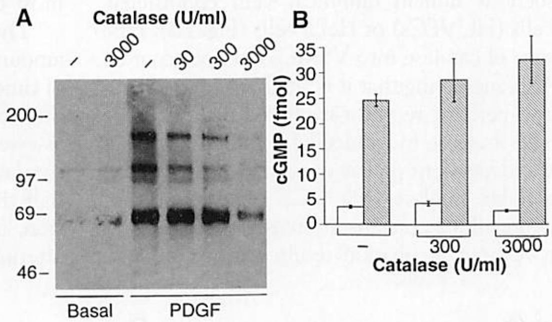

Fig. 3. Effect of increased catalase activity on VSMC signal transduction. (**A**) Immunoblots with antibody to phosphotyrosine of proteins from unstimulated (basal) and PDGF-stimulated cells treated with various amounts of catalase as indicated (*18*). Molecular sizes are shown in kilodaltons. (**B**) Amounts of cGMP 30 min after stimulation with SNP (10 mM) (striped bars) (*22*). White bars, no SNP stimulation. Values are mean ± SEM from triplicate cultures.

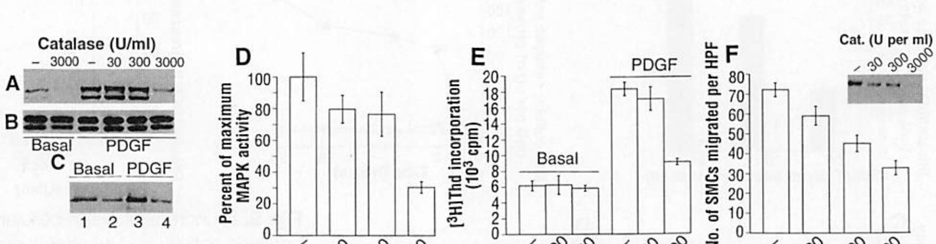

Fig. 4. Effect of inhibition of the H_2O_2 response on PDGF signaling. (**A**) Tyrosine phosphorylation of MAP kinase proteins in unstimulated cells (basal) and cells stimulated with PDGF-AB (5 ng/ml) in the presence or absence of catalase. Lysates were first immunoprecipitated with an antibody to phosphotyrosine, and then the immunoblots were probed with an antibody reactive to p44 and p42 MAP kinase (*18*). (**B**) Total MAP kinase amounts in whole-cell lysates (10 μg of protein per lane). (**C**) Effect of infection with Ad.Cat (lanes 2 and 4) or Ad.βgal (lanes 1 and 3) (200 MOI) on MAP kinase tyrosine phosphorylation. (**D**) Stimulated MAP kinase (MAPK) enzymatic activity as a function of catalase activity (*23*). Results are the mean ± SEM obtained from two separate experiments each performed in triplicate. (**E**) [^{3}H]Thymidine (Thd) incorporation in quadruplicate wells (mean ± SEM) after stimulation of cells with PDGF in the presence or absence of catalase (*24*). (**F**) Effect of intracellular catalase activity on PDGF-stimulated VSMC chemotaxis (*25*). Results are from triplicate experiments and are expressed as the number (mean ± SEM) of migrated VSMC per high-power field (HPF). (**Inset**) Amount of tyrosine-phosphorylated paxillin in PDGF-stimulated lysates as a function of catalase concentrations (*18*).

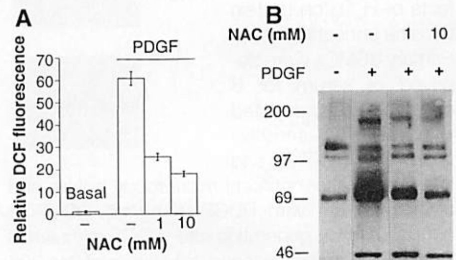

Fig. 5. Effects of the chemical antioxidant *N*-acetylcysteine (NAC) on PDGF signal transduction. (**A**) DCF fluorescence of cells either unstimulated (basal) or stimulated with PDGF as a function of NAC concentration (*26*). Values represent mean ± SEM from 20 or more cells. (**B**) Protein immunoblots of tyrosine-phosphorylated proteins from cells either untreated or treated with PDGF (5 ng/ml) in the presence of the indicated concentration of NAC.

mal growth factor, fibroblast growth factor, or angiotensin II all produce a rise in $[H_2O_2]$ with a correlation existing between the magnitude and duration of an increase in $[H_2O_2]$ and the level of tyrosine phosphorylation (*10*). These latter observations also strengthen the case that in many ways H_2O_2 fulfills the definition of an intracellular second messenger.

VSMCs appear to be unusual in their uptake of extracellular catalase. Certain cells secrete catalase, and the amount of catalase in serum increases in certain disease states (*14*). Thus, growth of VSMCs might be influenced by extracellular catalase in vivo. Recent epidemiological studies suggest a cardioprotective effect of antioxidants (*15*). Given that PDGF-induced VSMC migration and proliferation is thought to precipitate early atherogenic changes (*16*), one mechanism by which dietary antioxidants might protect against cardiovascular events is by a direct effect on H_2O_2-mediated signal transduction in VSMCs.

REFERENCES AND NOTES

1. A. Levine, R. Tenhaken, R. Dixon, C. Lamb, *Cell* **79**, 583 (1994).
2. Z. Chen, H. Silva, D. F. Klessig, *Science* **262**, 1883 (1993).
3. R. Schreck, P. Rieber, P. A. Baeuerle, *EMBO J.* **10**, 2247 (1991); R. Schreck and P. A. Baeuerle, *Trends Cell Biol.* **1**, 39 (1991).
4. D. M. Hockenbery, Z. N. Oltvai, X. Yin, C. L. Millman, S. J. Korsmeyer, *Cell* **75**, 241 (1993); D. J. Kane *et al.*, *Science* **262**, 1274 (1993); G. Haecker and D. L. Vaux, *Trends Biochem. Sci.* **19**, 99 (1994).
5. M. Shibanuma, T. Kuroki, K. Nose, *Oncogene* **5**, 1025 (1990); H. I. Krieger-Brauer and H. Kather, *J. Clin. Invest.* **89**, 1006 (1992); B. Meier *et al.*, *Biochem. J.* **263**, 539 (1989).
6. M. Ohba, M. Shibanuma, T. Kuroki, K. Nose, *J. Cell Biol.* **126**, 1079 (1994).
7. G. N. Rao and B. C. Berk, *Circ. Res.* **70**, 593 (1992).
8. L. T. Williams, *Science* **243**, 1564 (1989).
9. D. Heffetz, I. Bushkin, R. Dror, Y. Zick, *J. Biol. Chem.* **265**, 2896 (1990); F. J. T. Staal *et al.*, *Proc. Natl. Acad. Sci. U.S.A.* **91**, 3619 (1994).
10. M. Sundaresan and T. Finkel, unpublished observations.
11. S. C. Erzurum, P. Lemarchand, M. A. Rosenfeld, J.-H. Yoo, R. G. Crystal, *Nucleic Acids Res.* **21**, 1607 (1993).
12. S. Rankin and E. Rozengart, *J. Biol. Chem.* **269**, 704 (1994); E. A. Clark and J. S. Brugge, *Science* **268**, 233 (1995); H. Abedi, K. E. Dawes, I. Zachary, *J. Biol. Chem.* **270**, 11367 (1995).
13. D. Hecht and Y. Zick, *Biochem. Biophys. Res. Commun.* **188**, 773 (1992).
14. J. A. Leff *et al.*, *Free Radical Biol. Med.* **13**, 143 (1992); P. A. Sandstom and T. M. Buttke, *Proc. Natl. Acad. Sci. U.S.A.* **90**, 4708 (1993).
15. J. M. Gaziano, J. E. Manson, J. E. Buring, C. H. Hennekens, *Ann. N.Y. Acad. Sci.* **669**, 249 (1992); M. J. Stampfer *et al.*, *N. Engl. J. Med.* **328**, 1444 (1993); E. B. Rimm *et al.*, *ibid.*, p. 1450.
16. R. Ross, *Nature* **362**, 801 (1993).
17. Primary VSMCs were obtained from rat thoracic aorta by enzymatic digestion as described [J. H. Campbell and G. R. Campbell, *Vascular Smooth Muscle in Culture* (CRC, Boca Raton, FL, 1987), pp. 15–22] and were stimulated with PDGF-AB (5 ng/ml); DCF fluorescence was measured (*6*). Images were collected with a Leica Laser confocal scanning microscope, model TCD4. Relative DCF fluorescence was recorded on a scale from 0 to 256. In general, basal fluorescence averaged from 0 to 10 units, whereas stimulated fluorescence averaged from 60 to 200 units. Although DCF is oxidized by both H_2O_2 and hydroxyl radicals, the lack of fluorescence in PDGF-stimulated catalase-loaded cells suggests that the fluorescent signal after the addition of growth factor is predominantly derived from H_2O_2 (see Fig. 2E).
18. VSMCs deprived of serum for 3 days were stimulated with the indicated concentration of H_2O_2 or PDGF-AB (5 ng/ml) for 20 min, after which cells were harvested and lysed in RIPA buffer [50 mM tris-Cl (pH 7.5), 150 mM NaCl, 1% NP-40, 0.5% sodium deoxycholate, and 0.1% SDS]. Immunoprecipitation was done from 150 mg of unstimulated or stimulated cell lysate with aphosphotyrosine antibody (4G10, UBI). Immunoprecipitated proteins were divided in equal portions, and tyrosine-phosphorylated proteins from 50 mg of lysate were subjected to SDS–polyacrylamide gel electrophoresis (SDS-PAGE) (4 to 20% gels) and transferred to a nitrocellulose filter. When indicated, filters were probed with either an antibody to phosphotyrosine (RC20), a broadly reactive antibody to MAP kinase (erk1-CT, UBI), or an antibody to paxillin (P13520, Transduction Lab). Amounts of MAP kinase protein were detected from total cell lysates (10 μg per lane) by erk1-CT. Antibody binding was visualized by enhanced chemiluminescence (Tropix).
19. Adenoviral stocks were prepared and titered on 293 cells and used to infect VSMCs as described [R. J. Guzman *et al.*, *Proc. Natl. Acad. Sci. U.S.A.* **91**, 10732 (1994)]. Three days after infection, cells were deprived of serum for 3 days, then triplicate cultures were collected in buffer A [1× phosphate-buffered saline (PBS) (0.0067 M), 10 mM EDTA, 2% Triton X-100, and 0.5% deoxycholic acid] for measurement of enzymatic activity or in RIPA buffer for analysis with antibodies to phosphotyrosine.
20. Confluent VSMCs (1×10^6 cells), HUVECs [American Type Culture Collection (ATCC), Rockville, MD], and HeLa cells (ATCC) that had been deprived of serum were incubated with beef liver catalase (3000 U/ml, Boehringer Mannheim) for various times. After incubation, cells were washed twice in PBS, trypsinized, and lysed in buffer A. Catalase activity was assayed by the rate of decrease in absorbance at 240 nm by the method described by H. Aebi [*Methods Enzymol.* **105**, 121 (1994)].
21. Cells incubated with extracellular catalase (3000 U/ml) were collected, and triplicate cultures were exposed to proteinase K (1 mg/ml) in solution for various times. At the indicated time, cells were quickly sedimented and proteinase K diluted and removed. The cells were subsequently lysed in buffer A. Residual catalase activity was measured as described (*20*).
22. Confluent VSMCs with and without catalase loading were stimulated for 30 min with 10 mM SNP. Cells were subsequently lysed with 6% trichloroacetic acid (TCA). Lysates were neutralized, and equal amounts (2×10^5 cells) were used to determine amounts of cGMP by radioimmunoassay (Amersham) according to the manufacturer's recommendation.
23. Cells were stimulated with PDGF (5 ng/ml) for 20 min, and MAP kinase proteins were partially purified by phenylsepharose chromatography as described [S. Offermanns, *J. Immunol.* **152**, 250 (1994)]. Myelin basic protein (MBP) phosphorylation was used as an index of MAP kinase activity, where 100% activity represents the activity derived from PDGF-stimulated cells in the absence of catalase loading.
24. Confluent VSMCs were maintained in media without serum for 3 days and then, as indicated, stimulated with PDGF-AB (5 ng/ml). After 18 hours, cells in quadruplicate wells were incubated for 3 hours with [^{3}H]thymidine (1 mCi/ml), and TCA-precipitable counts were determined. If VSMCs were stimulated with PDGF in the presence of 0.5% serum, we noted effects on both basal and PDGF-stimulated thymidine incorporation; under serum-free conditions, effects were present only with PDGF stimulation. This was presumably because of the effects of catalase loading on residual growth factors present under 0.5% serum conditions.
25. VSMC migration was measured in response to PDGF stimulation in a mini-Boyden chamber as described [S. Biro *et al.*, *Proc. Natl. Acad. Sci. U.S.A.* **90**, 654 (1993)]. In the absence of PDGF stimulation, there was on average 10 VSMCs per high-power field.
26. A 200-mM stock of NAC was adjusted to pH 7.4 by NaOH, flash frozen, and stored in portions at −80° for up to 1 month. VSMCs were treated with the indicated amount of NAC for 8 hours before stimulation.

27. We acknowledge R. G. Crystal for providing the adenoviral constructs; M. Beaven, Y. F. Zhou, W. S. Kwon, R. Vemuri, and N. Epstein for helpful advice; S. G. Rhee and S. E. Epstein for critical review and helpful comments; and D. Koch for preparation of the manuscript. M.S. was supported by the Howard Hughes Medical Institute as an NIH Research Scholar.

1 June 1995; accepted 21 August 1995

Attenuated *Shigella* as a DNA Delivery Vehicle for DNA-Mediated Immunization

Donata R. Sizemore,* Arthur A. Branstrom, Jerald C. Sadoff†

Direct inoculation of DNA, in the form of purified bacterial plasmids that are unable to replicate in mammalian cells but are able to direct cell synthesis of foreign proteins, is being explored as an approach to vaccine development. Here, a highly attenuated *Shigella* vector invaded mammalian cells and delivered such plasmids into the cytoplasm of cells, and subsequent production of functional foreign protein was measured. Because this *Shigella* vector was designed to deliver DNA to colonic mucosa, the method is a potential basis for oral and other mucosal DNA immunization and gene therapy strategies.

Direct DNA-mediated immunization is an exciting new approach to vaccine development (*1*). We chose to exploit the ability of *Shigellae* to enter epithelial cells and escape the phagocytic vacuole as a method for directing plasmid DNA to the cytoplasm of the host cell for protein synthesis and processing for antigen presentation (*2*). To attenuate the *Shigella* vector, we made a deletion mutation in the *asd* gene encoding aspartate β-semialdehyde dehydrogenase, an essential enzyme that is required to synthesize the bacterial cell wall constituent

Department of Bacterial Diseases, Division of Communicable Diseases and Immunology, Walter Reed Army Institute of Research, Washington, DC 20307–5100, USA.

*To whom correspondence should be addressed. E-mail: dr._donata_sizemore@wrsmtp-ccmail.army.mil
†Present address: Merck Research Laboratories, Post Office Box 4, BL3-3, West Point, PA 19486, USA.

diaminopimelic acid (DAP) (*3, 4*). The resultant 15D construct, a Δ*asd* isolate of *Shigella flexneri* 2a strain 2457T, was able to maintain the eukaryotic expression vector pCMVβ (*5*) in the absence of antibiotic-selective pressure. The plasmid pCMVβ expresses *Escherichia coli* β-galactosidase under the control of the immediate early promoter and enhancer from the human cytomegalovirus (CMV) in mammalian cells; this permitted easy analysis of mammalian cell–mediated gene expression after delivery.

Strain 15D was screened to ensure that the large plasmid that is essential for bacterial invasion of mammalian cells had not been lost during the genetic manipulations. Immunoblots verified that the strain continued to express the invasion-associated IpaB and IpaC polypeptides (*6*) and thus showed no loss of the invasion plasmid. To confirm earlier observations, we tested 15D and 15D(pCMVβ) for the ability to invade cultured baby hamster kidney (BHK) cells with and without DAP supplementation during the 90 min allowed for invasion (*7–9*). Examination by light microscopy of fixed and stained chamber slides revealed that in the absence of DAP, 15D and 15D(pCMVβ) entered 13% and 10% of the cultured BHK cells, respectively. By contrast, 33% (15D) and 29% [15D(pCMVβ)] of the BHK cells contained bacteria when DAP was present during the invasion step. Although both constructs were able to invade BHK cells, the addition of DAP during the invasion step increased the number of BHK cells infected and the number of viable bacteria recovered (*9*).

To test the ability of 15D to deliver plasmid DNA, we followed intracellular bacterial viability and β-galactosidase activity (Fig. 1) over a 48-hour time course (*8, 10*). Initially, 1×10^7 to 3×10^7 viable bacteria of each strain were recovered from monolayers of BHK cells with no detectable β-galactosidase activity in cell extracts. No β-galactosidase activity could be detected in bacterial extracts that were equivalent to the total number of bacteria added. At each assay point, a loss of 1 to 1.5 log units of viable bacteria occurred with no notable difference between strains 15D and 15D(pCMVβ). However, at both the 24- and 48-hour assay points, increasing units of β-galactosidase activity were readily detected in extracts of BHK cells infected with 15D(pCMVβ). The detected β-galactosidase activity did not result from expression within the bacteria because, although no activity was measured at the first two assay points, large numbers of viable bacteria were present. In addition, an isolate of 15D(pCMVβ) that did not express IpaB and IpaC (as measured by immunoblotting) was unable to bring about β-galactosidase activity at the 24-hour assay point.

Infected monolayers of BHK cells were immunostained to examine β-galactosidase expression within individual cells (Fig. 2) (*8, 11*). No intracellular immunostaining was observed in monolayers infected with

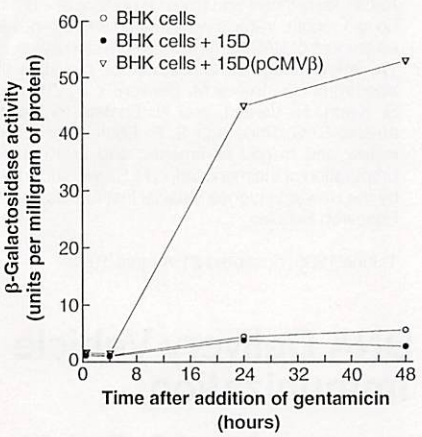

Fig. 1. Strain 15D was used as a carrier to deliver pCMVβ, a mammalian DNA expression plasmid, to BHK cells. β-Galactosidase activity (in units per milligram of protein) was determined for BHK cells alone (○), BHK cells infected with 3×10^9 15D (●), and BHK cells infected with 1×10^9 15D(pCMVβ) (▽). Determinations of β-galactosidase activity were made on an estimated 0.5×10^7 cells. Bacteria were grown as described (*8*). In this assay, DAP (50 μg/ml) was added to concentrated bacterial suspensions before these suspensions were added to flasks of semiconfluent BHK cells (~1×10^7 cells). At the indicated times, BHK cells were removed by trypsinization and washed in phosphate-buffered saline. A portion of the cell suspension was lysed with a 0.2% Triton X-100 solution, diluted, and plated on TSA Congo red DAP plates to determine the number of viable bacteria. β-Galactosidase activity was measured in the remaining cell extract by a standard biochemical assay (*10*) [units of β-galactosidase = 380 × OD_{420}/time (in minutes)]. β-Galactosidase activities were standardized to 1 mg of total protein, as determined with a BCA* protein assay kit (Pierce).

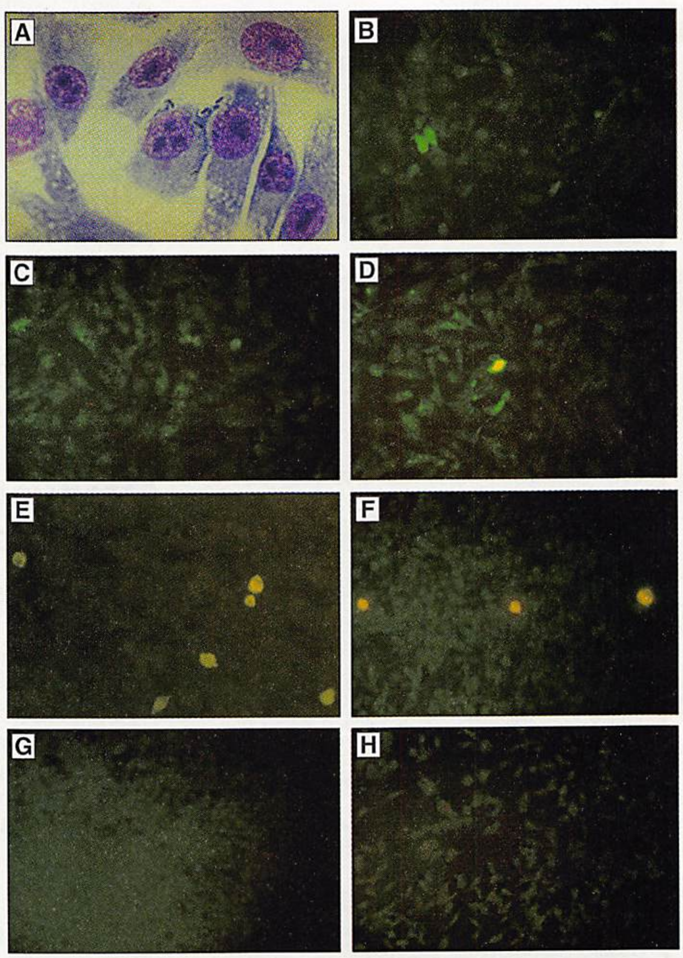

Fig. 2. Intracellular immunostaining to detect expression of β-galactosidase within BHK cells infected with 15D or 15D(pCMVβ). (**A**) A Leukostat-stained BHK monolayer infected with 15D(pCMVβ) 30 min after the addition of gentamicin-containing medium. (**B** through **H**) Immunostained infected BHK cells after the addition of gentamicin-containing medium. (B) 15D(pCMVβ), 30 min; (C) 15D, 4 hours; (D) 15D(pCMVβ), 4 hours; (E) 15D(pCMVβ), 24 hours; (F) 15D(pCMVβ), 48 hours; (G) 15D, 48 hours; (H) BHK cells alone. Three wells of a four-well chamber slide of BHK cell monolayers infected with 15D or 15D(pCMVβ) were immunostained to detect β-galactosidase expression (*8, 10, 11*). At the indicated times, washed monolayers were fixed in phosphate-buffered 4% paraformaldehyde for 5 min and then blocked with 3% goat serum (Gibco-BRL) in HBSS for 30 min. BHK cells were then permeabilized for 1 min with HBSS containing 0.1% saponin (Sigma). A monoclonal antibody to β-galactosidase (Sigma) was diluted 1:2000 in HBSS containing 0.1% saponin and applied for 30 min at 37°C in a humidified chamber. Fluorescein isothiocyanate–conjugated secondary antibody to mouse IgG (Fc-specific, Sigma) was diluted 1:32 and applied for 30 min at room temperature. Between each step, chamber slides were washed extensively with HBSS containing 0.1% saponin. A final wash step of HBSS alone was used to close permeabilized cells. Fluorescent images were visualized with a Nikon Microphot with epifluorescence attachment or with an Olympus VAN04-S with fluorescence attachment. Original magnifications, ×312.5 (A); ×62.5 (B through H).

either strain at the 30-min assay point (Fig. 2B). Only slight intracellular immunostaining was detected at the 4-hour assay point in monolayers infected with 15D(pCMVβ) (Fig. 2, C and D). By the 24- and 48-hour assay points, positive immunostaining of several cells per field was observed in monolayers infected with 15D(pCMVβ) (Fig. 2, E and F). Staining throughout the cytoplasm suggested that the plasmid DNA had been released from the bacterium into the cell cytoplasm, leading to transcription and translation by the mammalian cell. Immunostained cells also appeared to be rounded, possibly because of the presence of a large quantity of β-galactosidase protein. As measured by fluorescence-activated cell sorter (FACS) analysis, 1 to 2% of 5000 15D(pCMVβ)-infected BHK cells expressed β-galactosidase at the 24-hour assay point (*8, 10*).

Visual examination of Leukostat-stained chamber slides of 15D(pCMVβ)-infected BHK cells indicated that 28% of the cells contained one to five visually intact bacterial cells, with 1.7% containing five bacteria (Table 1). Four hours after gentamicin treatment, 26% of the cells contained visually intact bacteria, with <1% of the cells containing four bacteria. Therefore, invasion with one to five bacteria was required for foreign gene expression. Because pCMVβ is a 7164–base pair plasmid that occurs in ~500 copies per bacterial cell, each bacterium is estimated to contain $\sim 3.93 \times 10^{-9}$ μg of DNA. Thus, intracytoplasmic delivery of no more than 4×10^{-9} to 20×10^{-9} μg of DNA by *Shigella* was sufficient for expression of β-galactosidase.

To demonstrate that gene delivery was not restricted to BHK cells, we infected murine P815 cells that express H-2^d class I major histocompatibility complex (MHC) molecules with 15D(pCMVβ). As shown in Table 2, 56.25 units of β-galactosidase activity were detected in lysates from P815 cells infected with 15D(pCMVβ). Further experiments will be necessary to determine whether these cells can present *Shigella*-delivered DNA-encoded foreign antigens in the context of class I.

Studies of the ability of 15D to deliver plasmid DNA in vivo have begun in two small animal models, the guinea pig keratoconjunctival and murine intranasal models, which are used to study *Shigella* pathogenicity and immunobiology (*12, 13*). To determine whether 15D could deliver pCMVβ to the ocular surface of the guinea pig eye, we stained corneas for β-galactosidase activity and visually examined them at various times after inoculation (*12*). Varying amounts of staining were observed in the outer region of the cornea near the sclera of the right eyes that received 15D(pCMVβ), except those from day 8, in which staining was detected in only one of three corneas. Several areas typical of the staining observed in corneas that received 15D(pCMVβ) are shown in Fig. 3B. No apparent endogenous β-galactosidase activity was detected in eyes inoculated with 15D. Histology experiments will be needed to examine in greater detail the percentage of cells and cell type(s) invaded by 15D(pCMVβ) and those staining positive for β-galactosidase. In an initial experiment, spleen cells from intranasally inoculated BALB/c mice showed a moderate proliferative response to β-galactosidase protein (2.5 μg/ml) (*13, 14*). The stimulation index (*14*) was 3.6 when the inoculum was supplemented with DAP compared with 2.1 in the absence of DAP. Although preliminary, these experiments indicate that bacteria can be used to deliver plasmid DNA in vivo.

Our method for delivering functional DNA inside cells need not be restricted to *Shigella* because the invasion genes used by *Shigella* can be inserted into other bacteria such as *E. coli* (*15*). Likewise, other bacteria such as *Listeria* are able to invade cells and break out of the phagocytic vacuole into the cytoplasm (*16*). Although we have no formal proof that such a release of bacteria from the phagocytic vacuole into the cell cytoplasm is essential for DNA delivery, preliminary experiments with *Salmonella typhimurium*, which reaches the cytoplasm only with difficulty, suggest that this organism is not an efficient DNA delivery vehicle (*17*).

Any bacterial DNA delivery system will need to strike a balance between cell inva-

Table 1. Percentage of BHK cells infected and number of bacteria per BHK cell, as shown by microscopic examination. Chamber slides and bacteria were prepared as described (*8*). At least 400 BHK cells of each group were examined.

Elapsed time (hours)	BHK cells infected (%) (mean)	Bacteria per infected BHK cell (mean ± SD)	Number of BHK cells containing 1 to 6 bacteria						
			1	2	3	4	5	6	Total
			Strain 15D						
0.5	39	1.84 ± 1.2	96	47	14	14	3	3	177
4	36	1.68 ± 0.94	106	36	13	5	0	1	161
24	3.7	1	17	–	–	–	–	–	17
48	2.2	1	10	–	–	–	–	–	10
			Strain 15D(pCMVβ)						
0.5	28	1.35 ± 0.72	76	29	7	5	2	0	119
4	26	1.40 ± 0.74	95	16	4	1	0	0	116
24	3.3	1	14	1	–	–	–	–	15
48	3.8	1	18	–	1	–	–	–	19

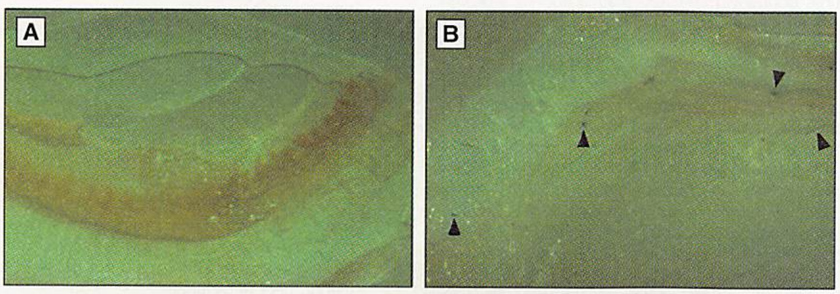

Fig. 3. Ability of 15D to deliver pCMVβ to ocular tissue. (**A**) Left cornea (15D) and (**B**) right cornea [15D(pCMVβ)], 48 hours after ocular inoculation. Arrowheads indicate areas of β-galactosidase staining.

Table 2. β-Galactosidase activity in P815 cells after infection with 15D(pCMVβ). Bacteria used to infect P815 cells were grown as described (*8*). After addition of the bacterial cultures containing DAP to the nonadherent P815 cells cultured in six-well plates, the plate was spun at 500*g* for 5 min. Bacteria and P815 cells were allowed to interact for 90 min. The cells were then extensively washed with DMEM and resuspended in DMEM containing gentamicin (100 μg/ml) for a 1-hour incubation at 37°C in the presence of 5% CO_2. The cells were again extensively washed and resuspended in DMEM containing gentamicin (20 μg/ml) for overnight culture at 37°C in the presence of 5% CO_2. β-Galactosidase activity and protein concentrations were determined at 24 hours as described (*8, 10*).

Source	β-Galactosidase (units per milligram of protein)
P815 cells	3.04
P815 cells + 15D	5.62
P815 cells + 15D(pCMVβ)	56.25

sion (with its subsequent reactogenicity) and efficiency of delivery. In the case of *Shigella*, the genes responsible for invasion also cause invasion and apoptosis of macrophages, followed by inflammation (*18*). We constructed a *Shigella* strain that was completely unable to divide in the absence of DAP. Determination of the safety of this strain awaits human trials. Preliminary experiments with a guinea pig keratoconjunctivitis challenge model indicate that a two-dose immunization regimen followed by a challenge with virulent *Shigella* 3 weeks later gave 100% protection (*12*, *14*). These results demonstrate that this highly attenuated strain, which is capable of DNA delivery, functions well in vivo.

The bacterial DNA delivery system described here has several advantages for certain applications. Delivery of DNA-encoded antigens to the mucosal immune system should permit mucosal immunization simultaneously with multiple antigens that (i) can be directed for class I presentation, class II presentation, or both; (ii) can stimulate T helper cells (T_H1 or T_H2); and (iii) can be secreted while maintaining the proper folding and conformational epitopes for immunoglobulin A (IgA) and immunoglobulin G (IgG) antibody production. Diseases that may be especially responsive to this approach include diarrheal diseases such as rotavirus, gastrointestinal diseases such as the ulcer-causing *Helicobacter pylori*, and sexually transmitted disease agents such as human immunodeficiency virus, *Neisseria gonorrhoeae*, and human papilloma virus. Suppression of autoimmunity through manipulation of immune tolerance mechanisms in the gut has been demonstrated (*19*), and if such a technique proves to be generally applicable, it should also be amenable to our approach.

Perhaps the greatest advantage of bacterial delivery of DNA for vaccination and for potential gene therapy and replacement is the ease and acceptability of oral and other forms of mucosal delivery. Likewise, because no DNA purification is required for this type of DNA vaccination (which is essentially a live, attenuated bacterial vector), vaccines can be produced for the cost of fermentation, lyophilization, and packaging. Therefore, this type of vaccination may represent, at least in part, a solution to the costs and difficulties inherent in the production and development of current vaccines.

Aside from the practical applications of bacterial DNA delivery, the relatively efficient ability of *Shigella* to transfer functional DNA containing a eukaryotic promoter into mammalian cells leads to speculation concerning the potential role of such a mechanism in evolution. Plasmids for vaccine use are designed so as to minimize the possibility of chromosomal integration, but in nature this may not be the case.

REFERENCES AND NOTES

1. J. J. Donnelly, J. B. Ulmer, M. A. Liu, *J. Immunol. Methods* **176**, 145 (1994).
2. N. High, J. Mounier, M. C. Prévost, P. J. Sansonetti, *EMBO J.* **11**, 1991 (1992).
3. K. Nakayama, S. M. Kelly, R. Curtiss III, *Biotechnology* **6**, 693 (1988).
4. A Δ*asd* derivative of *Shigella flexneri* 2a strain 2457T was constructed by polymerase chain reaction (PCR) amplification of an *E. coli asd* gene [C. Haziza, P. Stragier, J. C. Patte, *EMBO J.* **1**, 379 (1982)] incorporating Bgl II restriction sites (forward primer, 5′-Bgl II-CCCTGATAATTGCCGC-3′; reverse primer, 5′-Bgl II-CGCTTACTCCTGTATTACGC-3′) for directed cloning into a previously described vector (A. Branstrom, D. Sizemore, R. Warren, J. Sadoff, paper presented at the 33rd Interscience Conference on Antimicrobial Agents and Chemotherapy, New Orleans, 20 October 1993). Positive clones were selected with the use of *E. coli* χ6097 (3). Reverse PCR amplification was used to delete 553 base pairs of the *E. coli asd* structural gene (positions 439 to 991) (forward primer, 5′-GATCCT-CAACACATCTTCCG-3′; reverse primer, 5′-CGA-GGGCCTTTAGCGCCTCC-3′). The kanamycin resistance cassette from pUC4K-KIXX (Pharmacia) was digested with Sma I and cloned between the flanking *asd* sequences. A 2-kb fragment of the remaining *asd* gene with the internal kanamycin resistance cassette was PCR-amplified (forward primer, 5′-Sac I-CCCT-GATAATTGCCGC-3′; reverse primer, 5′-Sal I-CG-CTTACTCCTGTATTACGC-3′) and cloned into the Sac I-Sal I site of the positive selection suicide vector pCVD442 [M. S. Donnenberg and J. B. Kaper, *Infect. Immun.* **59**, 4310 (1991)], creating pSEAK. Clones were transformed into SM10λpir [R. Simon, U. Priefer, A. Puhler, *Biotechnology* **1**, 784 (1983)] and selected for resistance to ampicillin. SM10λpir(pSEAK) was conjugated with *S. flexneri* 2a strain 2457T (pAB322[Tet^r,Amp^s]) and conjugants were selected for resistance to ampicillin and tetracycline. PCR analysis of resultant isolates showed that plasmids integrating into the chromosome had recombined with the downstream portion of the *asd* fragment of pSEAK. Growth on sucrose resulted in a second recombination event [J. Quandt and M. F. Hynes, *Gene* **127**, 15 (1993)], and isolate 15C was obtained by screening the resultant isolates for resistance to kanamycin and the requirement for DAP. Hybridization and PCR analysis confirmed a deletion in *asd*. Further, the mutation could be complemented with a low-copy number plasmid carrying the *E. coli asd* gene. Isolate 15C was cured of the tetracycline resistance plasmid by fusaric acid treatment [S. R. Maloy and W. D. Nunn, *J. Bacteriol.* **145**, 1110 (1981)] to generate isolate 15D.
5. G. R. MacGregor and C. T. Caskey, *Nucleic Acids Res.* **17**, 2365 (1989).
6. J. A. Mills, J. M. Buysee, E. V. Oaks, *Infect. Immun.* **56**, 2933 (1988).
7. E. V. Oaks, M. E. Wingfield, S. B. Formal, *ibid.* **48**, 124 (1985).
8. The general assay used for these studies was adapted from those described previously for *Shigella* plaque analysis (6, 7). A single Congo red-binding positive colony (denoting the expression of plasmid-encoded *Shigella* virulence determinants) of each strain was used to inoculate overnight LB broth cultures containing DAP (50 μg/ml) (for 15D) or DAP plus ampicillin (250 μg/ml) [for 15D(pCMVβ)]. Overnight cultures were diluted 1:50 and grown to approximately mid-log phase in the presence of DAP. For chamber slide assays (Nunc) and 24-well plate assays, 200 μl of washed bacteria in Hanks' balanced solution (HBSS) with or without DAP (50 μg/ml) was added to three wells of semiconfluent BHK cells (1×10^5) at ~100:1. For flask assays, bacteria were grown as described, except that mid-log phase cultures were concentrated 10-fold and 2 ml of the bacterial solution was added to a flask of BHK cells (~1×10^7). In all assays, bacteria were allowed to interact with the BHK cells in this minimal volume for 90 min at 37°C in the presence of 5% CO_2. Nonadherent bacteria were removed by extensive washes with HBSS. Extracellular bacteria were then killed by the addition of Dulbecco's modified Eagle's medium (DMEM) with 10% heat-inactivated fetal bovine serum (BioWhittaker) and gentamicin (50 μg/ml). For plating assays, cells were lysed with a 0.2% Triton X-100 solution and appropriate dilutions were plated on tryptic soy agar (TSA) Congo red DAP plates for determination of viable bacterial counts. At the indicated times, the chamber slides were extensively washed, fixed, and immunostained or stained with a Leukostat set (Fisher) before light or fluorescent microscopy. An Instat statistical program (Graphpad, San Diego, CA) was used to calculate means, SDs, and SEs. All data presented are representative of experiments performed two or more times.
9. The ability of a Δ*asd* derivative of *S. flexneri* 2a strain 2457T to invade mammalian cells in culture was assayed to examine the requirement of DAP during the adherence and invasion step. Bacterial solutions with or without DAP were allowed to interact with BHK cells for 90 min, washed extensively, and then treated with gentamicin-containing media for 30 min before plating. In the absence of DAP, 1070 ± 404 (15D) and 1095 ± 332 [15D(pCMVβ)] viable bacteria were recovered, versus $8.2 \times 10^4 \pm 1 \times 10^4$ (15D) and $8.6 \times 10^4 \pm 3.5 \times 10^4$ [15D(pCMVβ)] when DAP was present [mean ± SE; $P = 0.024$ (Mann-Whitney test)].
10. G. R. MacGregor, G. P. Nolan, S. Fiering, M. Roederer, L. A. Herzenberg, in *Methods in Molecular Biology*, E. J. Murray and J. M. Walker, Eds. (Humana, Clifton, NJ, 1991), vol. 7, pp. 217–235.
11. B. Sander, I. Höidén, U. Andersson, E. Möller, J. S. Abrams, *J. Immunol. Methods* **166**, 201 (1993).
12. For guinea pig inoculations, 7.2×10^8 15D bacteria in a 25-μl volume were placed on the left eye and 4×10^8 15D(pCMVβ) bacteria in a 25-μl volume were placed on the right eye, as described [A. B. Hartman, C. J. Powell, C. L. Schultz, E. V. Oaks, K. H. Eckels, *Infect. Immun.* **59**, 4075 (1991)]. On days 1, 2, 6, and 8, animals were killed and each eye was removed for dissection of corneas and adjacent sclera. Whole eyes or dissected corneas were stained for β-galactosidase [J. R. Sanes, J. L. R. Rubenstein, J. Nicolas, *EMBO J.* **5**, 3133 (1986)]. After overnight development, corneas were examined under a dissecting microscope, scored for staining, and photographed. Corneas from three guinea pigs were examined on days 1, 2, and 8; corneas from two guinea pigs were examined on day 6. All animal experiments were conducted in adherence to principles stated in the *Guide for Care and Use of Laboratory Animals* (NIH publication 86-23, National Institutes of Health, Bethesda, MD, 1985).
13. L. L. Van De Verg *et al.*, *Infect. Immun.* **63**, 1947 (1995).
14. D. R. Sizemore, A. B. Hartman, A. A. Branstrom, J. C. Sadoff, in preparation. Female BALB/c mice received two intranasal inoculations of 1×10^6 15D or 15D(pCMVβ) in a 30-μl volume, 4 weeks apart. The stimulation index is the difference between the mean OD_{490} values for β-galactosidase stimulation of 15D(pCMVβ) cells and for unstimulated 15D(pCMVβ) cells, divided by the difference between the mean OD_{490} values for β-galactosidase stimulation of 15D cells and for unstimulated 15D cells (where OD_{490} is the optical density at 490 nm).
15. P. J. Sansonetti *et al.*, *Infect. Immun.* **39**, 1392 (1983).
16. D. A. Portnoy and S. Jones, *Ann. N.Y. Acad. Sci.* **730**, 15 (1994).
17. D. R. Sizemore, A. A. Branstrom, J. C. Sadoff, unpublished data.
18. A. Zychlinsky, M. C. Prévost, P. J. Sansonetti, *Nature* **358**, 167 (1992).
19. J. Sun, J. Holmgren, C. Czerkinsky, *Proc. Natl. Acad. Sci. U.S.A.* **91**, 10795 (1994).

20. We thank C. Hammack, J. Grove, R. Curtiss III, E. Oaks, A. Hartman, and individuals in the Division of Medical Audio Visual Services at Walter Reed Army Institute of Research for providing materials or technical expertise. The views expressed in this report are those of the authors and not those of the U.S. Department of Defense.

6 June 1995; accepted 14 September 1995

Speech Recognition with Primarily Temporal Cues

Robert V. Shannon,* Fan-Gang Zeng, Vivek Kamath, John Wygonski, Michael Ekelid

Nearly perfect speech recognition was observed under conditions of greatly reduced spectral information. Temporal envelopes of speech were extracted from broad frequency bands and were used to modulate noises of the same bandwidths. This manipulation preserved temporal envelope cues in each band but restricted the listener to severely degraded information on the distribution of spectral energy. The identification of consonants, vowels, and words in simple sentences improved markedly as the number of bands increased; high speech recognition performance was obtained with only three bands of modulated noise. Thus, the presentation of a dynamic temporal pattern in only a few broad spectral regions is sufficient for the recognition of speech.

The recognition of speech has been thought to require frequency-specific (spectral) cues. Spectral energy peaks in speech (formants), for example, reflect the resonant properties of the vocal tract and thus provide acoustic information on the production of the speech sound. However, efforts to identify acoustic cues that convey phoneme identity reliably under various listening conditions and with various talkers have met with only limited success (*1*). Studies that used amplitude compression (*2*) and spectral reduction (*3*) have demonstrated the robustness of speech recognition under these conditions. However, these manipulations resulted in stimuli that were still highly complex in their temporal-spectral characteristics. Even total removal of spectral cues from speech resulted in stimuli that carried a surprising amount of information on consonant identity (*4*). Work on prosthetic electrical stimulation of the auditory system by cochlear implants has refocused attention on amplitude and temporal cues, which are the principal cues transmitted by these prostheses (*5*). In our study, we preserved amplitude and temporal cues while systematically varying the amount of spectral information. This combination not only allowed us to parametrically assess the role of spectral detail in speech recognition independently of temporal cues, but also simulates the stimulation pattern of a cochlear implant (*6*).

Spectral information was removed from speech by replacement of the frequency-specific information in a broad frequency region with a band-limited noise (Fig. 1). The acoustic signal was divided into several frequency bands and the amplitude envelope was extracted from each band by half-wave rectification and low-pass filtering. Low-pass filters with cutoff frequencies of 16, 50, 160, and 500 Hz were used for envelope extraction to evaluate the effect of reducing the bandwidth of temporal envelope information. The envelope signal was used to modulate white noise, which was then spectrally limited by the same bandpass filter used for the original analysis band (*7*). Thus, temporal and amplitude cues were preserved in each spectral band, but the spectral detail within each band was removed. All bands were then summed and presented to the listeners through headphones. One, two, three, or four band processors were used, each with envelope information low-pass–filtered at 16, 50, 160, or 500 Hz, for a total of 16 conditions.

Eight normal hearing listeners (*8*) listened to 16 medial consonants (a/C/a), eight vowels (h/V/d), and simple sentences in each of the signal conditions (*9*). Consonants and vowels were presented in random order to each listener. The listeners were instructed to identify the presented stimulus by selecting it from the complete set of 16 consonants or 8 vowels. Sentences were presented once and the listeners were instructed to repeat as many words as they could. The listeners were trained on sample conditions to familiarize them with the testing environment; training continued until their performance stabilized, typically within two to three sessions, for a total of 8 to 10 hours. No feedback was provided in any of the test conditions.

Speech recognition performance on all three measures increased with the number of noise bands (Fig. 2). Changing the cutoff frequency of the envelope filter had a significant effect across all tests [$F(3,21) < 0.01$]. Paired *t* tests revealed no significant difference between the results with the 50-, 160-, and 500-Hz low-pass envelope filters, so these results were pooled for presentation in Fig. 2. A significant reduction in performance ($P < 0.01$) was observed with the 16-Hz envelope filter for consonants and sentences, but not for vowels. Thus, even under conditions of reduced spectral cues, slowly varying temporal information (<50 Hz) can yield relatively high speech recognition performance. This result is consistent with the observation of poor speech discrimination in children who have central processing disorders that disrupt temporal processing in the 20- to 50-ms range (*10*).

The specific reception of three speech features—voicing, manner, and place of articulation—was evaluated by information transmission analysis (*11*) on the consonant confusion matrix (Fig. 3). Information received on voicing and manner increased from one to two bands, to >90%, with no further improvement as the number of bands increased to three or four. Thus, binary information on the spectral distribution of energy, when combined with temporal cues, is sufficient to convey almost all information on voicing and manner. Voicing and manner have similar patterns of results as a function of the number of spectral bands, and both cues show maximum performance with only two spectral bands; these findings reinforce the hypothesis (*4*) that both categories of information, although labeled according to vocal produc-

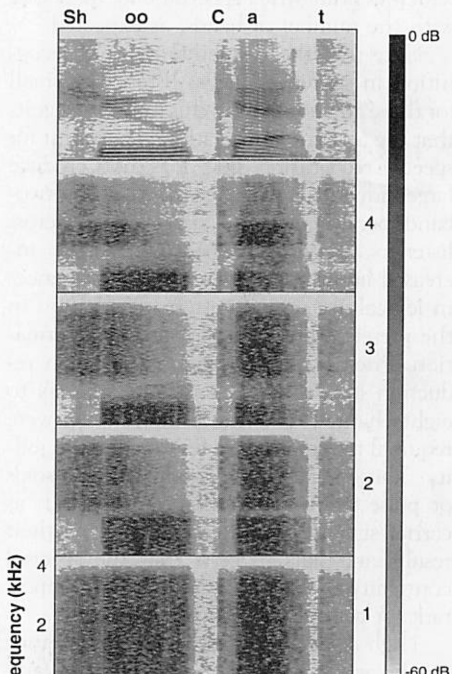

Fig. 1. Examples of spectral reduction for the speech token "shoo cat." The original narrowband spectrogram (top) shows energy as a function of frequency and time. Successively lower panels show spectrograms of the processed tokens with four, three, two, and one bands, respectively. Filter cutoff frequencies were 1500 Hz for the two-band processor, 800 and 1500 Hz for the three-band processor, and 800, 1500, and 2500 Hz for the four-band processor. All processors were low-pass–filtered at 4 kHz.

House Ear Institute, 2100 West Third Street, Los Angeles, CA 90057, USA.

*To whom correspondence should be addressed.

Fig. 2. Recognition scores for consonants (**A**), vowels (**B**), and sentences (**C**) for eight normal-hearing listeners are shown as a function of the number of noise bands. Chance performance scores in (A) and (B) are indicated by dashed lines. Results from envelope filters with frequencies of 50, 160, and 500 Hz were not significantly different and are pooled (●). Results from the 16-Hz envelope filter (△) were significantly lower than results from other envelope filter frequencies.

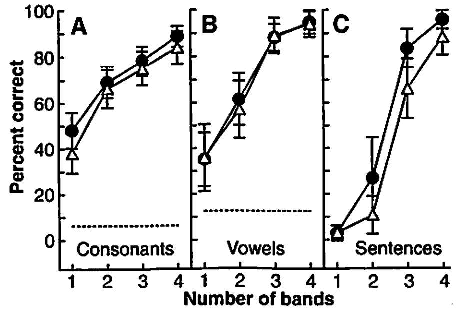

Fig. 3. Information transmission analysis for consonants. Consonant confusion matrices from eight normal-hearing listeners were summed and the aggregate matrix was analyzed in terms of the percentage of transmitted information received for medial consonant voicing (**A**), manner (**B**), and place of articulation (**C**) (*11*). Information received is shown as a function of the number of noise bands, with envelope filter frequency as a parameter (△, 16 Hz; ●, average of 50, 160, and 500 Hz).

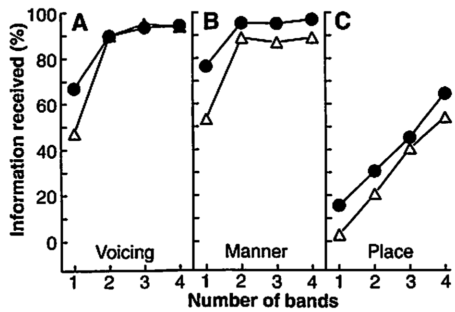

tion, are perceptually primarily related to temporal envelope information. Recognition of consonantal place of articulation, which is primarily a spectral cue, increased with the number of bands, as expected.

Note that the variability of word recognition in sentences across listeners is small for three and four bands; this finding suggests that the acoustic information is sufficient for speech recognition but does not produce large individual differences. In contrast, two-band performance is quite variable across listeners, presumably because of the increased importance of individual differences in lexical access and pattern recognition in the presence of such poor spectral information. Prior experiments on information reduction in speech (3) indicated that six to eight channels of spectral information were required for comparable levels of intelligibility. Those studies used modulated sinusoids or pulse trains rather than noise bands as carrier signals; the difference between their results and ours suggests that the spectral contiguity of temporal information is important for central pattern recognition.

High speech recognition performance can be achieved with only three time-varying bands of noise representing the complex spectral patterns of speech. Here, three bands provided a severely degraded spectral representation of vowel and consonant formants and allowed only rudimentary spectral shape information to be transmitted. No formant structure was present, and formant frequency transitions either were lost completely (if they took place wholly within one of the present analysis bands) or were conveyed as a temporal change in the relative sound level of two adjacent noise bands. The harmonic structure of voiced speech was not present in the noise-band simulations. Despite this reduced spectral content, the temporal cues were sufficient to produce 90% correct identification of words. This result indicates that minimal spectral information is required for speech recognition as long as temporal cues are available in a few contiguous spectral regions.

Speech presents a difficult pattern recognition problem for the auditory system. The message content must be retrieved from speech in a wide variety of listening conditions, including different talkers, environments, and amounts of distortion. Our results suggest that speech pattern recognition is a robust process that can make use of both spectral and temporal cues. Because impaired or absent spectral resolution often is a consequence of hearing impairment, the finding that speech recognition can be achieved with primarily temporal cues suggests alternative signal-processing strategies for auditory prostheses.

REFERENCES AND NOTES

1. K. N. Stevens and S. E. Blumstein, in *Perspectives on the Study of Speech*, P. D. Eimas and J. L. Miller, Eds. (Erlbaum, Hillsdale, NJ, 1981), pp. 1–38.
2. J. C. R. Licklider and I. Pollack, *J. Acoust. Soc. Am.* **20**, 42 (1948); J. C. R. Licklider and G. A. Miller, in *Handbook of Experimental Psychology*, S. S. Stevens, Ed. (Wiley, New York, 1951), pp. 1040–1074.
3. R. E. Remez, P. E. Rubin, D. B. Pisoni, T. D. Carrell, *Science* **212**, 947 (1981); F. J. Hill, L. P. McRae, R. P. McClellan, *J. Acoust. Soc. Am.* **44**, 13 (1968); M. R. Schroeder, *Proc. IEEE* **54**, 720 (1966); J. Allen, *IEEE Trans. Speech Audio Proc.* **2**, 567 (1994).
4. S. Rosen, *Philos. Trans. R. Soc. London Ser. B Biol. Sci.* **336**, 367 (1992); D. J. Van Tasell, S. D. Soli, V. M. Kirby, G. P. Widin, *J. Acoust. Soc. Am.* **82**, 1152 (1987); D. J. Van Tasell, D. G. Greenfield, J. J. Logemann, D. A. Nelson, *ibid.* **92**, 1247 (1992); R. L. Freyman, G. P. Nerbonne, H. C. Cote, *J. Speech Hear. Res.* **34**, 415 (1991); S. M. Rosen, A. J. Fourcin, B. C. J. Moore, *Nature* **291**, 150 (1981).
5. M. Dorman, K. Dankowski, G. McCandless, L. Smith, *Ear Hear.* **10**, 288 (1989); M. F. Dorman, L. Smith, M. Smith, J. Parkin, *J. Acoust. Soc. Am.* **92**, 3428 (1992); R. V. Shannon, F.-G. Zeng, J. Wygonski, in *The Auditory Processing of Speech: From Sounds to Words*, M. E. H. Schouten, Ed. (Mouton-DeGruyter, New York, 1992), pp. 263–274; R. V. Shannon, *Hear. Res.* **11**, 157 (1983); *J. Acoust. Soc. Am.* **85**, 2587 (1989); *ibid.* **91**, 1974 (1992); D. K. Eddington, *ibid.* **68**, 885 (1980); B. S. Wilson *et al.*, *Nature* **352**, 236 (1991).
6. S. Rosen, J. Walliker, J. A. Brimacombe, B. J. Edgerton, *J. Speech Hear. Res.* **32**, 93 (1989); M. Dorman, M. Hannley, G. McCandless, L. Smith, *J. Acoust. Soc. Am.* **84**, 5011 (1988); M. F. Dorman *et al.*, *ibid.* **88**, 2074 (1990); B. S. Wilson, C. C. Finley, D. T. Lawson, in *Models of the Electrically Stimulated Cochlea*, J. M. Miller and F. A. Spelman, Eds. (Springer-Verlag, New York, 1990), pp. 339–375.
7. The signal was digitized at a 10-kHz sampling rate and passed through a preemphasis filter to whiten the spectrum (low-pass below 1200 Hz, −6 dB per octave). The signal was then split into frequency bands (third-order elliptical IIR filters). Adjacent filters overlapped at the point at which the output from each filter was 15 dB down from the level in the pass-band. The envelope was extracted by half-wave rectification and low-pass filtering (elliptical IIR filters with cutoff frequencies of 16, 50, 160, or 500 Hz, −6 dB per octave). The envelope derived from each band was then used to modulate a white noise. The modulated noise was frequency-limited by filtering with the same bandpass filters used in the original analysis band. This last bandpass filtering reduced the modulation depth to some degree because it removed the modulation sidebands. The resulting modulated noises from each band were combined, low-pass–filtered at 4 kHz, amplified (Crown D75), and presented to the listener through headphones (TDH-49). Overall levels were calibrated from each combination of parameters to produce an average output level of 75 dBA for continuous speech.
8. All listeners participated with full informed consent. The Institutional Review Board of the House Ear Institute and St. Vincent's Medical Center approved the study protocol and the informed consent form.
9. Consonant and vowel stimuli were taken from the sound track of the Iowa audiovisual speech perception laser videodisc (R. S. Tyler, J. P. Preece, M. W. Lowder, Department of Otolaryngology, University of Iowa, 1989). The male talker was used for both vowels and consonants. Three exemplars of each token were selected randomly. Consonant confusion matrices were compiled from 10 presentations of each of the 16 medial consonants (a/C/a, for example "aba") for each listener. Vowel confusion matrices were compiled from nine presentations of each of the eight vowels in a h/V/d (for example "hood") context. Sentences were taken from the sound track of the City University of New York laser videodisc of everyday sentences (A. Boothroyd, L. Hanin, T. Hnath, Speech and Hearing Sciences Research Center, City University of New York, New York, 1985). Data were collected for 24 sentences, representing 100 key words, from each listener. The sentences were of easy to moderate difficulty and no sentences were repeated to an individual listener.
10. P. Tallal *et al.*, Eds., *Temporal Information Processing in the Nervous System* (*Ann. N.Y. Acad. Sci.* **682**, 1993).
11. G. A. Miller and P. E. Nicely, *J. Acoust. Soc. Am.* **27**, 338 (1955).

12. We thank S. Rosen, D. Van Tasell, R. Diehl, S. Nittrour, B. Wilson, S. Soli, and M. Dorman for their help and comments. Supported by National Institute on Deafness and Other Communication Disorders (NIDCD) grant RO1 DCO1526.

21 April 1995; accepted 23 August 1995

Increased Cortical Representation of the Fingers of the Left Hand in String Players

Thomas Elbert, Christo Pantev, Christian Wienbruch, Brigitte Rockstroh, Edward Taub

Magnetic source imaging revealed that the cortical representation of the digits of the left hand of string players was larger than that in controls. The effect was smallest for the left thumb, and no such differences were observed for the representations of the right hand digits. The amount of cortical reorganization in the representation of the fingering digits was correlated with the age at which the person had begun to play. These results suggest that the representation of different parts of the body in the primary somatosensory cortex of humans depends on use and changes to conform to the current needs and experiences of the individual.

Evidence has accumulated over the past two decades that indicates that alterations in afferent input can induce plastic reorganizational changes within the adult mammalian central nervous system (*1*). Changes in the relation between peripheral sensory fields and their central representations have been observed for the somatosensory (*2*), visual (*1, 3, 4*), and auditory systems (*5*), and comparable changes also have been found for motor systems (*6*). In many of these experiments, the removal of afferent input from a cortical region resulted in an "invasion" by a neighboring area whose innervation remained intact. For example, the cortical region representing a digit before amputation in owl monkeys could be activated after amputation by tactile stimulation of an intact adjacent finger (*7*). The changes noted were of the order of a few millimeters. More extensive plastic changes have recently been observed after the abolition of input from larger portions of the body—for example, with somatosensory deafferentation of an entire forelimb in macaque monkeys (*8*) and upper extremity amputation in humans (*9–11*).

In addition, it has been shown in studies with owl monkeys that a prolonged increase of tactile stimulation to the distal pad of one or two phalanges results in a greatly increased cortical representation specific to that portion of the fingers (*12, 13*). Evidence has also been reported that suggests an increased cortical representation of the index finger used in reading by blind Braille readers (*14*).

Violinists and other string players provide a good model for the study of the effects of differential afferent input to the two sides of the brain in humans. During their practice or performance, the second to the fifth digits (D2 to D5) of the left hand are continuously engaged in fingering the strings, a task that involves considerable manual dexterity and enhanced sensory stimulation. At the same time, the thumb grasps the neck of the instrument and, although not as active as the fingers, engages in relatively frequent small shifts of position and pressure. The right hand, which manipulates the bow, participates in a task involving much less individual finger movement and fluctuation in tactile and pressure input. Here, we present data from magnetic source imaging that indicates that the cerebral cortices of string players are different from the cortices of controls in that the representation of the digits of the left hand is substantially enlarged in the cortices of string players.

Nine musicians (six violinists, two cellists, and one guitarist) who had played their instruments for a mean period of 11.7 years (range, 7 to 17 years) served as subjects for our study. Six nonmusicians served as controls (*15*). The mean age for both groups was 24 ± 3 years. Before our investigation, the musicians kept a diary for 1 week, recording the amount of time practiced per day (mean 9.8 ± 8.4 hours per week), and had estimated the amount of time spent practicing during the previous month and year (10.8 ± 8.8 hours per week).

During the experimental session, somatosensory stimulation was delivered to the first digit and, in separate runs, to the fifth digit of either hand. Stimulation consisted of light superficial pressure applied by means of a pneumatic stimulator with the use of standard, nonpainful stimulation intensity (*9, 16, 17*). The data (Fig. 1) indicate that the center of cortical responsivity for tactile stimulation of the digits of the left hand was shifted in musicians as compared to that in controls, while at the same time the strength of response increased. The topographic shift was toward the midsagittal plane, which, along the surface of the postcentral gyrus, is toward the region

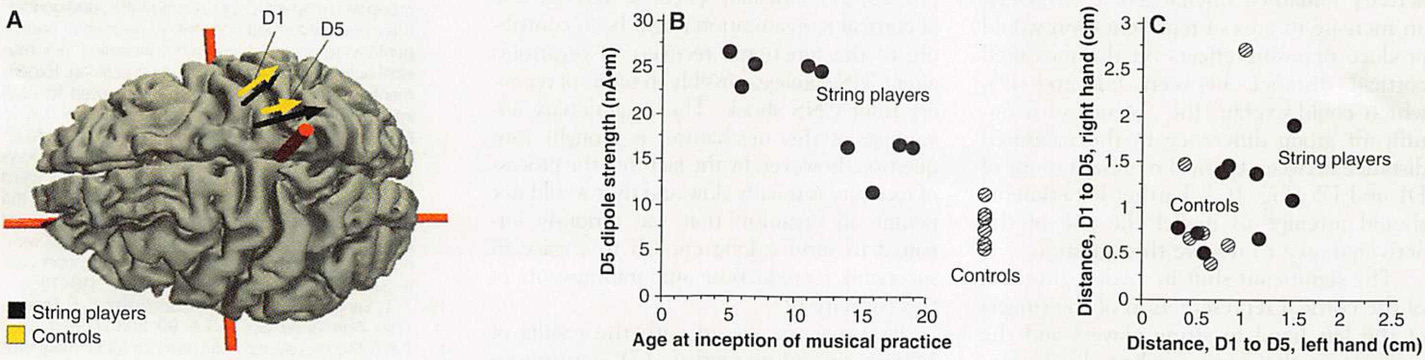

Fig. 1. (**A**) Equivalent current dipoles elicited by stimulation of the thumb (D1) and fifth finger (D5) of the left hand are superimposed onto an MRI (magnetic resonance imaging) reconstruction of the cerebral cortex of a control, who was selected to provide anatomical landmarks for the interpretation of the MEG-based localization. The arrows represent the location and orientation of the ECD vector for each of the two digits averaged across musicians (black) and controls (yellow). The length of the arrows represents the mean magnitude of the dipole moment for the two digits in each group. The average locations of D5 and D1 are shifted medially for the string players compared to controls; the shift is larger for D5 than for D1. The dipole moment is also larger for the musicians' D5, as indicated by the greater magnitude of the black arrow. (**B**) The magnitude of the dipole moment as a function of the age of inception of musical practice; string players are indicated by filled circles, control subjects by hatched circles. Note the larger dipole moment for individuals beginning musical practice before the age of 12. (**C**) Scatterplot of the Euclidean distances (in centimeters) between the cortical representations of D1 and D5. This distance for the musicians' left hands was greater than that in controls, but this difference is not statistically significant.

of the cortex that represents the palm of the hand (*18*). For D5 (little finger) of the left hand, the shift was 0.7 cm (t = 3.6, P < 0.01, degrees of freedom = 13); for D1 (thumb), the shift was 0.5 cm (t = 3.3, P < 0.01). This shift of D5 was significantly greater than the shift of D1.

Correspondingly, the analysis of variance (ANOVA), which included data from both hemispheres (*18*), showed an interaction of group (a factor in ANOVA) and digit [$F(1,13) = 4.78$, $P < 0.05$]. This effect was dependent on the side on which stimulation was given: There were no significant shifts for the digits of the right hand of the musicians compared to those of the controls. The dipole moment, which is presumed to be an index of total neuronal activity, also increased for the stimulation of the digits of the left hand of musicians compared to the left hand of controls [ANOVA interaction of group and side of stimulation, $F(1,13) = 5.54$, $P < 0.05$]. The increase was larger for D5 (t = 5.4, P < 0.01) than for D1 [t = 2.0, P < 0.1; ANOVA interaction of group and digit, $F(1,13) = 4.81$, $P < 0.05$] (*19*).

There was a correlation between the age at which the string players began studying their instruments and the magnitude of the change in the dipole moment of D5 compared to that in controls (r = 0.79, P = 0.01) (Fig. 1B). The relation between the amount of practice and the cortical measures was not significant. The increase of the dipole moment of both D1 and D5 in the string players indicates that an extended cortical network responds to tactile stimulation. If the active area expands, the point location determined by an equivalent dipole model will shift inward. Given the spherical geometry of the head, measurements of the D1 and D5 representations would approach each other if the center of activity remained unchanged. Conversely, an increase in area of representation would produce opposing effects on the measured cortical distance between D1 and D5, which could explain the absence of a significant group difference in the measured distance between cortical representations of D1 and D5 (Fig. 1C). Further experiments should attempt to model the size of the activated area to resolve this question.

The significant shift in medial direction of the cortical representation of the fingers of the left hand in string players and the increase in the corresponding dipole moments suggest that the cortical territory occupied by the representation of the digits increased in string players as compared with that in controls. Two alternate interpretations of our data should be taken into account. First, it could be argued that individuals with a genetically determined large representation of the left hand digits make superior string players and therefore are more likely to continue with musical training once they have begun. However, in research with animals, use-dependent enlargements of portions of the somatosensory map in cortical area 3b have been clearly demonstrated under conditions of increased use generally similar to those in this study (*12, 13*). In either case, the relatively larger representations of individually important digits could have the role of enhancing the particular needs of a string player in an adaptive manner.

A second alternative explanation of our results is that they are a consequence of a shift in cortical responsivity combined with an intensification of the response. However, we think a more plausible explanation is that the cortical territory of the left-hand digits has expanded. This is more plausible because (i) there is a correlation between amount of cortical reorganization and age [or stage of central nervous system (CNS) maturation] at which musical practice began and (ii) the equivalent current dipole (ECD) shift follows the one direction that is consistent with the expansion interpretation.

Related work (*10*) has shown that there is a strong correlation in humans with upper extremities amputated between extent of cortical reorganization and amount of phantom limb pain experienced. Although phantom limb pain is a maladaptive result of nervous system injury, our results demonstrate the functional relevance of cortical reorganization, similar to results reported in the context of the visual system (*3*) and auditory system (*12, 20, 21*). One may speculate that one role of cortical reorganization might be to contribute to the functional recovery of organisms after CNS damage, possibly in terms of recovery from CNS shock. The evolutionary advantage of this mechanism is brought into question, however, by the fact that the process of recovery is usually slow and thus would not permit an organism that was seriously impaired to survive long enough to engage in successful reproduction and transmission of this capacity (*22*).

However, in accord with the results of Merzenich and co-workers (*7*), continuous plastic reorganization of cortical space that permits rapid reallocation of available CNS circuitry would confer an obvious practical advantage. The possible contribution of cortical reorganization to recovery of function after CNS injury might thus be an adventitious result that "piggy backed" onto a mechanism, which permitted the much more critically important plastic processes associated with learning, physical growth during maturation, and adjustment to current environmental demands. The role of this mechanism in the recovery of function would become important only when protecting an individual with CNS damage would artificially prolong survival long enough for extensive cortical reorganization to work.

T. Elbert and B. Rockstroh, Department of Psychology, University of Konstanz, D-78434 Konstanz, Germany. E-mail: Thomas.Elbert@Uni-Konstanz.de
C. Pantev and C. Wienbruch, Biomagnetism Center, University of Münster, D-48129 Münster, Germany.
E. Taub, Department of Psychology, University of Alabama at Birmingham, Birmingham, AL 35294, USA.

REFERENCES AND NOTES

1. J. H. Kaas, *Annu. Rev. Neurosci.* **14**, 137 (1991).
2. A. Mogilner *et al.*, *Proc. Natl. Acad. Sci. U.S.A.* **90**, 3593 (1993); M. M. Merzenich *et al.*, *Neuroscience* **8**, 33 (1983); S. A. Clark, T. Allard, W. M. Jenkins, M. M. Merzenich, *Nature* **332**, 444 (1988); J. Kalaska and B. Pomeranz, *J. Neurophysiol.* **42**, 618 (1979); D. D. Rasmusson, *J. Comp. Neurol.* **205**, 313 (1982); A. M. Kellohan and G. S. Doetsch, *Somatosens. Res.* **2**, 49 (1984); J. T. Wall and C. G. Cusick, *J. Neurosci.* **4**, 1499 (1984); J. T. Wall *et al.*, *ibid.* **6**, 218 (1986).
3. C. Darian-Smith and C. D. Gilbert, *Nature* **368**, 737 (1994).
4. C. D. Gilbert and T. N. Wiesel, *ibid.* **356**, 150 (1992); F. Rösler, B. Röder, M. Heil, E. Henninghausen, *Cognit. Brain Res.* **1**, 145 (1993).
5. G. H. Recanzone, C. E. Schreiner, M. M. Merzenich, *J. Neurosci.* **13**, 87 (1993); D. Robertson and D. R. F. Irvine, *J. Comp. Neurol.* **282**, 456 (1989); D. R. F. Irvine, R. Rajan, L. Z. Wize, P. Heil, *Soc. Neurosci. Abstr.* **17**, 1485 (1991).
6. L. G. Cohen, S. Bandinelli, T. W. Frindley, M. Hallet, *Brain* **114**, 615 (1991); J. N. Sanes, S. Suner, J. F. Lando, J. P. Donaghue, *Proc. Natl. Acad. Sci. U.S.A.* **85**, 2003 (1988).
7. M. M. Merzenich *et al.*, *J. Comp. Neurol.* **224**, 591 (1984).
8. T. P. Pons *et al.*, *Science* **252**, 1857 (1991).
9. T. Elbert *et al.*, *Neuroreport* **5**, 2593 (1994).
10. H. Flor *et al.*, *Nature* **375**, 482 (1995).
11. T. T. Yang *et al.*, *Neuroreport* **5**, 701 (1994).
12. G. H. Recanzone, M. M. Merzenich, W. M. Jenkins, A. Grajski, H. R. Dinse, *J. Neurophysiol.* **67**, 1031 (1992).
13. W. M. Jenkins, M. M. Merzenich, M. T. Ochs, T. Allard, E. Guíc-Robles, *ibid.* **63**, 82 (1990).
14. A. Pascual-Leone and F. Torres, *Brain* **116**, 39 (1993).
15. Controls were either students or university employees who worked in an academic environment and had no experience playing string instruments. They were selected to be comparable to the experimental group with respect to age, social status, and gender. After giving informed consent, experimental participants were briefly interviewed concerning their musical activities and their history of practicing. Experimental participants were also interviewed to elicit information regarding their usual manual activities: None of the controls engaged in manual tasks to an unusual extent other than typing on computer keyboards. Each of them used both hands for word processing or other computer operations. Two of the musicians were found to have a tendency toward ambidexterity, but all other test participants were right-handed (Edinburgh handedness questionnaire) [R. C. Oldfield, *Neuropsychologia* **9**, 97 (1971)].
16. T. T. Yang, C. C. Gallen, B. J. Schwartz, F. E. Bloom, *Proc. Natl. Acad. Sci. U.S.A.* **90**, 3089 (1993).
17. A BTi-Magnes system was used for MEG (magnetoencephalographic) recordings. The sensor array was positioned over one of the two hemispheres (C3 or C4) in a fixed irregular order. At each site, 1000 stimuli were delivered at an average rate of 0.5 Hz (the interval between stimulus onsets was 500 ± 50 ms). Stimulation site sequence varied according to a fixed irregular order across test participants. Within the range of 30 to 75 ms, a first major peak was identified in each of the evoked wave forms. The mean latencies were 46.2 ± 7.9 ms for left D1, and 48.1 ± 7.2 ms for right D1; for left D5, the mean

latency was 52.2 ± 8.3 ms, and for right D5 52.8 ± 7.5 ms. The difference between musicians and controls for latency was not significant. For each evoked magnetic field, a single ECD model (best fitting local sphere) was fitted and the medians of the dipole moment and the dipole location were computed from a selection of points within a 20-ms time segment (11 sampling points) around the maximal rms (root mean square across the 37 channels) within the range of 30 to 75 ms. Points were selected if they met the following requirements: (i) rms indicating a signal-to-noise ratio >3; (ii) a goodness of fit of the ECD model to the measured field >0.95; and (iii) a minimal confidence volume of the ECD location <300 mm^3.

18. For all cortical measures, an ANOVA with the between-subject factor group (musicians versus controls) and the within-subject factors digit (D1 versus D5) and side of stimulation (left versus right) was computed first. ANOVAs for subsets of the data or *t* tests were used to resolve interactions.
19. Given a constant direction of the equivalent current dipole, the dipole moment indicates the total strength of cortical polarization—that is, the number of neurons involved during a cortical response. If this number increases, the dipole moment also increases. Any active focal area can be modeled by an equivalent current dipole. Each dendritic current flow contributes to this dipole moment according to the formula

$$\text{dipole moment} = (\text{conductivity}) \times (\text{cross section of the dendrite}) \times (\text{potential difference along the dendrite})$$

S. J. Williamson and L. Kaufman [in *Auditory Evoked Magnetic Fields and Electric Potentials*, F. Grandori, M. Hoke, G. L. Romani, Eds. (Karger, Basel, 1990), pp. 1–39] assume the diameter of an apical dendrite to be 4 μm, the intracellular conductivity to be about 0.25 S/m, and the potential difference to be about 10 mV. With the use of these assumptions, about 30,000 dendrites would be necessary to produce a dipole moment of 10 nA·m. If conductivity and potential difference are not different in musicians and controls, the magnification of the dipole moment in response to finger stimulation of the left hand in musicians can be explained if approximately twice as many cells were activated in musicians than were activated in the controls.
20. G. H. Recanzone, M. M. Merzenich, J. Schreiner, *J. Neurophysiol.* **67**, 1071 (1992).
21. N. M. Weinberger *et al.*, *Concepts Neurosci.* **1**, 91 (1990).
22. We are indebted to T. Pons for this observation.
23. We appreciate the assistance of S. Hampson, B. Lütkenhöner, and O. Steinsträter. Supported by the Deutsche Forschungsgemeinschaft.

25 May 1995; accepted 13 September 1995

Circle No. 34 on Readers' Service Card

Circle No. 46 on Readers' Service Card

PRINCIPLES *of* SOUND RETIREMENT INVESTING

AT THIS RATE, YOUR FUTURE IS LOOKING BETTER AND BETTER.

High rates can make a big difference when you're saving for the future. So you may appreciate the fact that TIAA is currently offering one of the highest rates of return among guaranteed annuities anywhere — 7%.[1]

Of course, that's not surprising. TIAA's net rate of return has beaten the industry average every year for the past 47 years.[2]

7%

Strong returns and solid ratings

TIAA's traditional annuity guarantees your principal and a specified interest rate, backed by TIAA's claims-paying ability, so you can rest assured your savings are secure.

It also provides the potential for additional growth through dividends—which we've declared every year since 1948.

What's more, TIAA has received the highest marks from all four of the industry's leading rating agencies for its stability, sound investments, claims-paying ability and overall financial strength. That's a distinction held by only a handful of companies nationwide.[3]

TIAA's rates are just the half of it

TIAA-CREF also provides potential for growth and diversification through the CREF variable annuity and its seven different investment accounts.

And behind it all — top financial management, a wide range of ways to receive income, and personal service you can count on today, throughout your career, and on into retirement. No wonder over 1.7 million people in education, research, and related fields trust America's largest retirement system,[4] TIAA-CREF, to help them expand their horizons.

Maybe it's time you took a closer look at TIAA-CREF. Call us at 1 800 842-2776 to learn how the security, flexibility, and growth opportunities we offer can help you set your sights on a comfortable and rewarding tomorrow.

TIAA CREF

Ensuring the future for those who shape it.℠

[1]Retirement Annuity premiums received from July 1, 1995, through September 30, 1995, will be credited with a 7% effective annual interest rate through February 29, 1996. The corresponding rate for SRAs and Rollover IRAs is 6.5%. Both include a guaranteed minimum rate of 3% plus dividends that are declared for one year at a time and are not guaranteed for future years. [2]American Council of Life Insurance, *Investment Bulletin,* 1995. [3]A++ (Superior) from A.M. Best Co., Aaa from Moody's Investors Services, AAA from Standard & Poor's, and AAA from Duff & Phelps. These are ratings of insurance companies only, so they do not apply to CREF. [4]Based on assets under management.

CREF certificates are distributed by TIAA-CREF Individual & Institutional Services. For more complete information, including charges and expenses, call 1 800 842-2733, ext. 5509, for a prospectus. Read the prospectus carefully before you invest or send money. Date of first use: 9/95

Circle No. 54 on Readers' Service Card

DNA BINDING
C. Murphy
E. Kool / N. Shimamoto

MEMBRANE RECEPTORS
H. Vogel
C. Bargmann / Y. Umezawa

MODIFIED PROTEINS
T. Cass
L. Regan / C. Govardhan

WHOLE CELLS AND SYSTEMS
M. Lerner
R. Zare / H. McConnell

COLLOIDAL, MACROMOLECULAR & POLYELECTROLYTE SOLUTIONS

COLONY HARBORTOWN
VENTURA, CA
FEBRUARY 11 – 16, 1996

Rudolf Klein, *Chair*
Timothy P. Lodge, *Vice Chair*

COLLOIDAL SUSPENSIONS I
P. N. Pusey
S. Fraden / D. Grier / G. Nägele

COLLOIDAL SUSPENSIONS II
B. Ackerson
M. Medina-Noyola / D. Weitz

COLLOID-POLYMER MIXTURES
A. Gast
D. Frenkel / W. Poon

POLYMERS
C. Han
T. Lodge / T. Perkins / K. Schweizer

POLYMERS UNDER SHEAR
D. Pine
N. Balsara / J. Israelachvili

LIVING POLYMERS
J. Candau
F. Lequeux / P. Schurtenberger

APPLICATIONS
H. Yu
C. de Kruif / J. Stokes

THE COFFEE RING
P. Chaikin
T. Witten

MEMBRANES, PROTEINS
P. Pincus
V. Bloomfield / S. Safran

POLYELECTROLYTES,THEORY
K. Kremer
J. Joanny / Y. Kantor

POLYELECTROLYTES, EXPERIMENT
K. Schmitz
S. F'rster / I. Noda

BIOPHYSICAL ASPECTS
R. Pecora
J. Marko / M. Schurr

GENERAL DISCUSSION
R. Klein
M. Fixman

POSTERS
T. Lodge

COMPOSITES

DOUBLETREE HOTEL
VENTURA, CA
JANUARY 7 – 12, 1996

Dodd Grande, *Chair*
Lawrence T. Drzal, *Vice Chair*

ADVANCES IN THERMOSET MATRIX COMPOSITES
L. Boogh / P. R. Ciriscioli

HIGH TEMPERATURE POLYMER MATRIX COMPOSITES
J. W. Connell / J. McGrath

RECYCLING OF STRUCTURAL COMPOSITES
R. E. Allred

MATERIALS AND PROCESSES FOR HIGH TEMPERATURE CERAMIC BASED COMPOSITES
J. P. Dunkers / S. S. Sternstein

STRUCTURAL BEHAVIOR OF COMPOSITES – DAMAGE MECHANISMS AND ISSUES OF SCALE
F. K. Chang / T. Peijs / M. Spearing

STRUCTURAL BEHAVIOR OF COMPOSITES – MICROMECHANICS AND MECHANISMS
C. Galiotis / M. R. Wisnom

PROCESS MODELLING AND ADVANCED PROCESSES
M. Rommel / S. W. Tsai / R. Evans

DRUG CARRIERS IN MEDICINE AND BIOLOGY

HOLIDAY INN
VENTURA, CA
FEBRUARY 25 – MARCH 1, 1996

Theresa Allen & Randall Mrsny, *Co-Chairs*
R. Duncan & P. Thorpe, *Vice Chairs*

DRUG RESISTANCE
R. Borchardt
S. Cole / B. Sikic

ANTISENSE AND GENE THERAPY
L. Mayer
A. Kabanov / A. Smith / N. Usman

POLYMERS IN ANTI-CANCER APPROACHES
H. Ringsdorf
D. Jones / H. Maeda

LIPOSOMAL THERAPIES
D. Papahadjopoulos
I. Bakker-Woudenberg / R. Mannino / F. Martin

BIOLOGICAL ISSUES OF DRUG DELIVERY
A. Oliff
M. Inoue / W.C. Shen

TARGETING TO TUMORS
R. Duncan
R. Duncan / C. Hellerqvist / R. Jain / P. Thorpe

IMMUNOCONJUGATE THERAPIES
P. Thorpe
A. Jones / P. Trail

POLYMER APPLICATIONS
A. Hoffman
J. Cassidy / M. Sefton / E. Wintermantl

DEBATE: CAN DRUG CARRIERS BE AN EFFECTIVE APPROACH FOR THE TREATMENT OF SOLID TUMORS?
R. Reisfeld / J. Weinstein
R. Duncan / I. Hellstrom / D. Jones / F. Martin / L. Mayer / R. Nayar / A. Oliff

ELECTROCHEMISTRY

DOUBLETREE HOTEL
VENTURA, CA
JANUARY 14 – 19, 1996

Janet Osteryoung, *Chair*
Owen Melroy, *Vice Chair*

SENSORS
H. Silverman
G. Swain / C. Ribes / L. Bachas

PHOTONS
P. Sherwood
D. Scherson / J. Pemberton / J. Turner

CORROSION
F. Mansfield
H. Issacs / R. Alkire

ELECTRON TRANSFER
R. deLevie
C. Chidsey / M. Sluyters-Rehbach

BATTERIES
K. Bullock
D. Fauteux / W. Smyrl

FUEL CELLS
R. Paur
S. Swathirajan / T. Mason

ADSORBATES
H. Gray
E. Bowden / K. Niki

SURFACES
J. Gordon
J. Switzer / U. Stimming

OPEN SESSION
O. Melroy

IMMUNOCHEMISTRY AND IMMUNOBIOLOGY

HOLIDAY INN
VENTURA, CA
FEBRUARY 4 – 9, 1996

David Raulet, *Chair*
Diane Mathis, *Vice Chair*

LYMPHOCYTE DEVELOPMENT: PART I
D. Mathis
B. Malissen / D. Schatz

LYMPHOCYTE DEVELOPMENT: PART II
F. Alt
K. Georgeopoulos / M. Oettinger

CELL DEATH IN THE IMMUNE SYSTEM
S. Nagata
Y. Lazebnik / C. Thompson / T. Mak

NONCONVENTIONAL RECOGNITION BY T CELLS
K. Fisher-Lindahl
M. Brenner / H. R. MacDonald

RECOGNITION BY NATURAL KILLER CELLS
E. Long
W. Seaman / L. Lanier / D. Raulet

COSTIMULATION OF LYMPHOCYTES
J. Bluestone
A. Sharpe / G. Kelsoe

ANTIGEN PRESENTATION TO T CELLS
A. Lanzavecchia
P. Peterson / D. Zaller / R. Germain

AIDS
A. McMichael
D. Trono / G. Shaw

SIGNAL TRANSDUCTION / TRANSCRIPTIONAL ACTIVATION
G. Crabtree
V. Tybulewicz / D. Littman / R. Perlmutter

ISOTOPES IN THE PHYSICAL AND LIFE SCIENCES

HOLIDAY INN
VENTURA, CA
FEBRUARY 11 – 16, 1996

Judith Klinman, *Chair*
Tak Ishida, *Vice Chair*

PHYSICAL CHEMISTRY OF ISOTOPES
M. Wolfsberg
M. W. Lee / A. van Hook

TUNNELING IN BIOLOGIC SYSTEMS
R. Schowen
S. Hammes-Schiffer / D. Northrop / C. Hynes

ISOTOPE EFFECTS IN BIOLOGIC RADICAL GENERATING SYSTEMS
B. Barry
J. Babcock / J. Kozarich

ENZYMATIC H-TRANSFER CATALYSIS
M. Kreevoy
D. Silverman / P. Frey / W. Bachovchin

ISOTOPES IN ATMOSPHERIC GEOSCIENCE
S. Tyler
P. Quay / M. Thiemens

SESSION TITLES ARE INDICATED IN BOLDFACE, *Discussion Leaders in Italics,* and Speakers in Regular type.

ISOTOPE EFFECTS AS PROBES OF MECHANISM
M. Saunders
K. Westaway / H. Schwarz / F. Romesberg

ISOTOPIC FRACTIONATION IN BIOLOGIC SYSTEMS
A. Mildvan
J. Markley / V. Anderson / H. L. Schmidt

HEAVY ATOM EFFECTS IN BIOLOGICAL SYSTEMS
G. Gebauer
A. Giesemann / M. Cleland / V. Schramm

DINOSAUR PALEOBIOLOGY
J. Bigeleisen
Y. Kolodny / R. Barrick

MAGNESIUM IN BIOCHEMICAL PROCESSES

DOUBLETREE HOTEL
VENTURA, CA
JANUARY 28 – FEBRUARY 2, 1996

Michael E. Maguire, *Chair*
J. A. S. McGuigan, *Vice Chair*

MEASUREMENT OF FREE MAGNESIUM CONCENTRATIONS IN BLOOD AND SERUM: IMPLICATIONS FOR CLINICAL TREATMENT AND BASIC RESEARCH
J. McGuigan
U. Spichiger / B. Altura / R. Elin

ABSORPTION, DISTRIBUTION AND ELIMINATION OF MAGNESIUM
C. De Rouffignac
H. Classen / C. DeRouffignac / G. Quamme

COMPARTMENTATION AND BUFFERING OF MAGNESIUM
R.D. Grubbs
R.D. Grubbs / J. Melvin / A. Romani

MAGNESIUM AND MYOCARDIAL INFARCTION: CLINICAL TRIALS RESULTS AND IMPLICATIONS
H. Karppannen
R. Collins / E. Antmann / M. Egger

INFORMAL DISCUSSION GROUP: EFFECTS AND EPIDEMIOLOGY OF MG2+ ON ISCHEMIC HEART DISEASE,
R. Neutra

CELLULAR EFFECTS OF MAGNESIUM
M. Tatibana
M. Tatibana / W. Weglicki / Karin Nelson

FREE MAGNESIUM AND ITS ACTIONS
E. Murphy
E. Murphy / J. Cowan / A. Dolphin / M. Horie

MAGNESIUM CARRIERS IN NORMAL AND DISEASE STATES
P. Flatman
P. Flatman / T. G,nther / J. Vormann / K. Beyenbach

MAGNESIUM IN NEUROTRAUMA AND EPILEPSY
M. Johnston
M. Johnston / Ian Reynolds / John Swann / Tracy MacIntosh

INFORMAL DISCUSSION GROUP: MG2+, CHANNELS, AND EXCITABILITY IN EPILEPSY AND ECLAMPSIA
K. Nelson / M. Johnston

MAGNESIUM TRANSPORT AND MAGNESIUM RECEPTORS IN PATHOGENESIS
M. Maguire
E. Nemeth / M. Maguire / E. Groisman

MARINE NATURAL PRODUCTS

DOUBLETREE HOTEL
VENTURA, CA
FEBRUARY 25 – MARCH 1, 1996

William Gerwick, *Chair*
J. Cardellina, *Vice Chair*

BIOACTIVE AGENTS FROM MARINE ORGANISMS
R. Andersen / V. Bernan

PHARMACEUTICAL DRUG DEVELOPMENT FROM MARINE ORGANISMS
K. Yamada / F. Valeriote / M. Munro / T. Higa / R. Kaba

MARINE CHEMICAL ECOLOGY
W. Fenical / W. Boland / J. Davies / V. Paul / N. Lindquist

TECHNIQUES IN STRUCTURE ELUCIDATION
G. Crooks

METALS IN BIOLOGY

DOUBLETREE HOTEL
VENTURA, CA
JANUARY 21 – 26, 1996

Stephen J. Lippard, *Chair*
Joann Sanders-Loehr, *Vice Chair*

A LOOK TO THE FUTURE
R. Holm
G. Petsko

CYTOCHROME OXYDASES
G. Babcock
N. Blackburn / S. Ferguson / R. Gennis

MODELS FOR OXYDASES
K. Karlin
J. Collman / J. Sanders / W. Tolman

METAL DNA PROCESSING AND REPAIR
T. OíHalloran
J. Barton / D. Rindge / G. Verdine

METAL CHANNELS AND NEUROSCIENCE SIGNAL TRANSDUCTION
J. Berg
J. Falke / G. Yellen

METAL-BINDING BIOMOLECULES AND METALLORECOGNITION
J. Groves
F. Diederich / C. Fierke / C. Meares

METAL MOBILIZATION
E. Stiefel
D. Kurtz, Jr. / P. Lindley

RADICALS AND COFACTORS
J. Caradonna
R. Finke / M. Ludwig / M. Newcomb / K. Wieghardt

METHODOLOGY IN BIOINORGANIC CHEMISTRY
B. Hoffman
S. Cramer / S. Dunham / H. Gray / E. Solomon

GRADUATE RESEARCH SEMINAR: BIOINORGANIC CHEMISTRY (NEW)

HOLIDAY INN
VENTURA, CA
JANUARY 25 – 28, 1996
(THURSDAY - SUNDAY)

Edward H. Ha, *Chair*

MODELS FOR METALLOBIOMOLECULES
John Groves

DNA AND TNA INTERACTIONS WITH TRANSITION METAL COMPLEXES
David Sigman

MULTINICLEAR METALLOPROTEINS-Mn
Vincent Pecoraro / James Penner-Hahn

MULTINUCLEAR METALLOPROTEINS-Ni
Marcetta Darensbourg

MULTINUCLEAR METALLOPROTEINS-Fe
Steven Watton / Don Kurtz

MULTINUCLEAR METALLOPROTEINS-Cu
William Tolma

MULTINUCLEAR METALLOPROTEINS-Cu,Zn,V AND Heme
Joan Valentine

MOLECULAR & IONIC CLUSTERS

IL CIOCCO
BARGA, ITALY
MAY 5 – 10, 1996

Udo Buck / Mark Johnson, *Co-Chairs*
Roger Milller, *Vice Chair*

SOLVATION IN LARGE SYSTEMS
J. Jortner
A Apkarian / R. B. Gerber / W. C. Lineberger

QUANTUM LIQUID CLUSTERS
S. Stringari
J. P. Toennies / G. Scoles

SPECTROSCOPY OF SIZE-SELECTED NEUTRAL AND IONIC CLUSTERS
V. Buch
J. P. Maier / D. Clary / F. Huisken

REACTIONS IN IONIC CLUSTERS
E. Schlag
O. Cheshnovsky / V. E. Bondybey

EXCESS ELECTRONS IN CLUSTERS
J. Lisy
R. E. Continetti / A. A. Viggiano

SMALL NEURAL COMPLEXES
P. Brechignac
M. Lester / N. Halberstadt / G. Chalasinski

METAL ATOM SOLVATION
J. Farrar
M. A. Duncan / C. P. Schulz

CLUSTER-SURFACE INTERACTIONS
T. Nagata
G. Ewing / A. Terasaki / U. Even

TERTIARY STRUCTURE
R. Miller
M. T. Bowers / K. Kaya

MOLECULAR CYTOGENETICS

IL CIOCCO
BARGA, ITALY
APRIL 21 – 26, 1996

David Ward, *Chair*
Thomas Cremer, *Vice Chair*

ADVANCES IN MOLECULAR CYTOGENETIC METHODS
D. Ward
A. Raap / M. Speicher

INSTRUMENTATION AND IMAGE ANALYSIS
H. Tanke
L. van Vliet / J. Piper / J. Mullikin

GENOMIC AND CHROMOSOMAL EVOLUTION
P. Heslop-Harrison
J. Wienberg / J. Korenberg

COMPARATIVE GENOMIC HYBRIDIZATION
P. Lichter
D. Pinkel / O. Kallioniemi / T. Reid

CHROMOSOME STRUCTURE
H. Willard
U. Laemmli / G. Bernardi

FUNCTIONAL ORGANIZATION OF THE NUCLEUS: CHROMOSOMES AND TRANSCRIPTION
T. Cremer
D. Spector / R. van Driel

FUNCTIONAL ORGANIZATION OF THE NUCLEUS: DNA-REPLICATION, IMPRINTING AND DNA-REPAIR
R. Laskey

SESSION TITLES ARE INDICATED IN BOLDFACE, *Discussion Leaders in Italics,* and Speakers in Regular type.

CLINICAL MOLECULAR CYTOGENETICS
M. Ferguson-Smith

RARE EVENT DETECTION
J. Gray

MOLECULAR EVOLUTION (NEW)

COLONY HARBORTOWN
VENTURA, CA
JANUARY 28 – FEBRUARY 2, 1996

William R. Atchley, *Chair*
Walter M. Fitch, *Vice Chair*

EARLY EVOLUTION
B. Schopf
F. Doolittle / M. Hasegawa

GENOME AND ORGANELLE EVOLUTION
D. Hudson
P. Tucker / J. Palmer / J. Doebley

NON-TREE-LIKE EVOLUTION
R. Milkman
W. Fitch / Speaker TBA

EVOLUTION OF DEVELOPMENT ANDY CLARK
R. Raff / D. Tautz / W. Atchley

EXPERIMENTAL PHYLOGENETICS
J J Bull
D. Hillis

MOLECULAR POPULATION GENETICS
M. Goodman
M. Ruvolo / C. Aquadro / D. Powers

STATISTICAL INFERENCE
B. Weir
N. Goldman / Speaker TBA

VIRAL EVOLUTION
M. Kidwell
P. Sharp / S. Wessler

PATTERN AND FUNCTION
J. Thorne
N. Maizels / M. McClure

MYELIN

IL CIOCCO
BARGA, ITALY
APRIL 28 – MAY 3, 1996

David Colman, *Chair*
Bruce D. Trapp, *Vice chair*

OLIGODENDROCYTE PRECURSORS EXPLAINED
R. Miller / W. Richardson
R. Bansal / C. French-Constant / J. Grinspan / B. Zalc

SIGNAL TRANSDUCTION MECHANISMS
M. Chao
Y. Hannum / W. Lesslauer

DISORDERS OF MYELINATED AXONS
J. Griffin
T. Brushart

MYELIN DEGENERATION AND REGENERATION
J. Salzer
M. Bunge / W. Thompson / M. Filbin

EVOLUTION AND CONSCIOUSNESS
G. Jeserich
S. Nona / R. Gould / K. Uyemura

NEW TRANSGENIC MODELS
I. Duncan / K. Ikenaka
K. Nave / A. Messing / W. Stoffel / D. Weinstein / P. Braun

THE NODE OF RANVIER
B. Barres
M. Ellisman / P. Shrager / B. Trapp / V. Bennett / K. Smith

CONTROL OF MYELINATING CELL TYPES
S. Pfeiffer
R. Lazzarini / R. Bunge / A. Mudge / L. Pedraza / D. DíUrso / A. Nishiyama

ORGANIC THIN FILMS

HOLIDAY INN
VENTURA, CA
JANUARY 28 – FEBRUARY 2, 1996

John F. Rabolt, *Chair*
Avi Ulman, *Vice Chair*

SELF ASSEMBLED MONOLAYERS
G. Scoles / G. Poirier / G. Ferguson

ORGANIC AND POLYMERIC LEDíS
J. C. Scott / M. Galvin

LANGMUIR-BLODGETT FILMS
C. Knobler / G. Fuller

PATTERN FORMATION IN THIN ORGANIC AND POLYMERIC FILMS
A. Balazs

LIQUID CRYSTALLLINE ALIGNMENT FOR FLAT PANEL DISPLAYS
D. Johansmann / N. Abbott

TECHNIQUES FOR THIN FILM CHARACTERIZATION
B. Lotz

ORIGIN OF LIFE

HOLIDAY INN
VENTURA, CA
JANUARY 7 – 12, 1996

Gerald Joyce, *Chair*
John D. Rummel, *Vice Chair*

ORIGINS OF LIFE ON EARTH
A. Kanavarioti
S. Miller / A. Weiner

POLYMERS OF LIFE
A. Schwartz
A. Eschenmoser / L. Orgel / J. Ferris

CHEMICAL SELF-REPLICATION
G. Joyce
G. von Kiedrowski / J. Rebek

RNA-BASED EVOLUTION
A. Ellington
J. Szostak / D. Bartel / M. Yarus

ORIGIN OF THE CELL
J. Rummel
P. L. Luisi / W. F. Doolittle

DEEP MOLECULAR PHYLOGENY
M. Sogin
P. Gogarten / N. Pace / G. Olsen

EARTHíS EARLIEST BIOSPHERE
A. Knoll
J. W. Schopf / D. DesMarais

EXOBIOLOGICAL EXPLORATION OF MARS
J. Kerridge
J. Farmer / P. Christensen / C. McKay

A PLANETARY BASIS FOR LIFE
W. Irvine
R. Brown / J. Kasting

OXYGEN RADICALS IN BIOLOGY

DOUBLETREE HOTEL
VENTURA, CA
FEBRUARY 11 – 16, 1996

Kelvin J. A. Davies, *Chair*
Catherine Rice-Evans / Matthew B. Grisham, *Vice Chairs*

OXYGEN RADICALS & AIR POLLUTION
W. A. Pryor / C. E. Cross
C. E. Cross H. J. Forman / D. J. Massaro / K. B. Adler

HEALTH BENEFITS OF PLANT-DERIVED ANTIOXIDANTS
C. Rice -Evans / M. E. Haberland
P. M. Bramley / W. Schuch / W. Bors / D. Leake.

DEBATE: 1 DO CAROTENOIDS ACT AS ANTIOXIDANTS IN VIVO?

DEBATE 2 ARE THE FLAVONOID CONSTITUENTS OF FOODS RELEVANT ANTIOXIDANTS IN VIVO?
C. Rice-Evans / F. Ursini
L. Packer / N. Krinsky

OXYGEN RADICALS & AGING
H. Warner / M. Vuillaume
R. S. Sohal / L. E. Rikans / V. J. Cristofalo / C. Finch /
J. S. Valentine / G. T. Baker III
C. Epstein / R. Weindruch

OXYGEN RADICALS, INFLAMMATION, AND ISCHEMIA/REPERFUSION INJURIES
M. B. Grisham / J. ViÒa
D. Wink / T. Manning
P. Kubes / A. Sevanian
J. M. S. Davies / M. Maiorino
S. Wahl / H. Nick

OXYGEN RADICALS, GROWTH ARREST, APOPTOSIS & CANCER
B. T. Mossman / G. Poli
E. Cadenas / C. Pasquier / A. Azzi . D. R. Crawford

CONFERENCE PLENARY LECTURE
K. J. A. Davies
S. Orrenius

PEPTIDES, CHEMISTRY & BIOLOGY OF

DOUBLETREE HOTEL
VENTURA, CA
FEBRUARY 18 – 23, 1996

Charles M. Deber / John A. Smith, *Co-Chairs*

CHEMICAL / BIOLOGICAL INTERFACES
C. M. Deber
P. G. Schultz / S. K. Burley

NOVEL SYNTHETIC APPROACHES
J. P. Tam
D. H. Rich / B. Imperiali / K. B. Sharpless / M. Goodman

RECEPTOR-LIGAND INTERACTIONS
T. K. Sawyer
T. Reisine / T. Somers / P. W. Schiller

COMBINATORIAL DRUG DISCOVERY
A. M. Felix
J. Baldwin / E. M. Gordon / R. Tung / R. A. Houghten

PEPTIDE TEMPLATES
K. D. Kopple
A. F. Spanola / V. J. Hruby / M. R. Ghadiri

PEPTIDE DESIGN
T. M. Kubiak
A. Hamilton / J. Chmielewski / D. F. Veber / J. A. Wells

PEPTIDES IN IMMUNOBIOLOGY AND INFLAMMATION
J. A. Smith
M. M. Davis / H. L. Ploegh / D. K. Miller

PEPTIDES AS STRUCTURAL MODELS
M. Bodanszky
N. Kallenbach / C. Woodward / P. T. Lansbury, Jr. / T. A. Keiderling

SESSION TITLES ARE INDICATED IN BOLDFACE, *Discussion Leaders in Italics,* and Speakers in Regular type.

PINEAL CELL BIOLOGY

DOUBLETREE HOTEL
VENTURA, CA
FEBRUARY 4 – 9, 1996

Mark Rollag, *Chair*
Steven M. Reppert, *Vice Chair*

RETINA AS MODEL FOR PINEAL
C. Craft
M. Iuvone / C. Green

PINEALOCYTE SIGNAL TRANSDUCTION
C. Chik
Y. Morita / S. Dryer / H. Korf /R. Baler

PINEALOCYTE TRANSCRIPTIONAL REGULATION
P. Voisin
P. Sassone-Corsi / D. Klein

MELATONIN ACTION
D. Blask
W. Warren / P. Morgan / C. Mahle / R. Reiter

MELATONIN ACTION IN HUMANS
J. Arendt
I. Zhdanova / A. Lewy

PINEALOCYTE ENTRAINMENT
Y. Morita
Y. Fukada / M. Max / M. Zatz / R. Barrett

RETINA-PINEAL LINKAGE
G. Brainard
I. Morgan / J. Mikkelsen

MELATONIN RECEPTORS
V. Cassone
M. Dubocovich / S. Reppert / M. Becker-Andre

MELATONIN ANALOGS
S. Reppert
B. Guardiola-Lemaitre / D. Sugden

PROLACTIN

COLONY HARBORTOWN
VENTURA, CA
FEBRUARY 4 – 9, 1996

Ameae Walker, *Chair*
Nelson D. Horseman, *Vice Chair*

THE RELATIVE ROLES OF PRL AND GH IN PROLIFERATION AND DIFFERENTIATION WITHIN THE MAMMARY GLAND
D. Kleinberg / D. Flint / J. Rosen / B. Vonderhaar / S. Galosy

PROLACTIN AND RELATED MOLECULE SIGNALING
B. Groner / Y.-F. Wang / H. Rui / S. Frank

PROLACTIN-RECEPTOR INTERACTIONS
K. Young / A. Gertler / C. Ormandy

PROLACTIN IN THE IMMUNE SYSTEM
M. Dardenne / K. Kelly / S. Walker / A. Buckley

REGULATION OF PROLACTIN RELEASE
I. Clarke / K. Gregerson / M. Lorenson

PROLACTIN AND BEHAVIOR
J. Buntin / R. Bridges

REGULATION OF PROLACTIN AND GENE EXPRESSION
R. Day / A. Guttierez-Hartman / J.-M. Boutin / F. Stanley

CLINICALLY IMPORTANT EFFECTS OF PROLACTIN AND RELATED MOLECULES
D. Linzer / A. Klibanski /

BANQUET LECTURE
C. Nicoll

SENSORY TRANSDUCTION IN MICROORGANISMS

COLONY HARBORTOWN
VENTURA, CA
JANUARY 21 – 26, 1996

John Parkinson, *Chair*
Steven Block, *Vice Chair*

MEET THE ORGANISMS
S. Parkinson
S Parkinson / G. Sprague / J. Van Houten / R. Bourret

RECEPTORS I: STIMULUS DETECTION
J. Spudich
K. Hellingwerf / J. Spudich / M. Manson / P. Devreotes

RECEPTORS II: TRANSMEMBRANE SIGNALING
J. Hazelbauer
C. Kung / J. Falke

RECEPTORS III: SIGNALING AND ADAPTATION
P. Devreotes
G. Ordal / J. Stock

CIRCUITS I: KINASES AND PHOSPHATASES
R. Dahlquist
R. Firtel / M. Simon

CIRCUITS II: SIGNAL PROCESSING
K. Borkovich
K. Borkovich / J. Dunlap / D. Fraga / J. Armitage

RESPONSES I: MOTILITY
S. Block
C. Aizawa / Howard Berg / J. Spudich / J. Howard

RESPONSES II: MOVEMENT CONTROL
J. Segall
G. Gerisch / M. Eisenbach / P. Matsumura

RESPONSES III: COMMUNICATION & DEVELOPMENT
J. Adler
R. Losick / D. Kaiser

SERUM AMYLOID A: FROM AMYLOIDOSIS TO ATHEROSCLEROSIS (NEW)

DOUBLETREE HOTEL
VENTURA, CA
FEBRUARY 1 – 4, 1996
(THURSDAY – SUNDAY)

Jean D. Sipe / Frederick C. de Beer, *Co-Chairs*

SAA GENE FAMILY: STRUCTURE AND DIVERSITY
F.C. de Beer
A.S.Whitehead / P. D. Gorevic

REGULATION OF SAA GENE EXPRESSION
W.S.L.Liao
P. Woo / W.S.L. Liao / A. Ray

SAA AS AN APOLIPOPROTEIN: IMPLICATIONS IN ATHEROSCLEROSIS I
A.M. Fogelman
C. Banka / A.M. Fogelman

SAA AS AN APOLIPOPROTEIN: IMPLICATIONS IN ATHEROSCLEROSIS II
G. Getz
A.J. Lusis / L.L. Bausserman / M. Navab

SAA IN AMYLOIDOSIS I: CURRENT PERSPECTIVES
M.D. Benson
M. Kindy / J. Liepnieks

SAA FUNCTION
J.D. Sipe
J.J. Oppenheim / L.D. Loose

SAA IN AMYLOIDOSIS AND ATHEROSCLEROSIS: FUTURE IMPLICATIONS
R. Kisilevsky
B. Kluve-Beckerman / R. Kisilevsky

SPIROCHETES, BIOLOGY OF

HOLIDAY INN
VENTURA, CA
JANUARY 21 – 26, 1996

Alan Barbour, *Chair*
Sheila Lukehart, *Vice Chair*

EVOLUTION AND GENETICS OF SPIROCHETES I
I. Saint Girons
R. Zuerner / M. Roberts / C. Hughes / S. Samuels

ECOLOGY AND VECTOR BIOLOGY OF SPIROCHETES
P. Greenberg
L. Margulis / B. Olsen / D. Fish / D. Hampson

PROTEIN EXPRESSION AND GENE REGULATION
M. Norgard
J. Dunn / P. Rosa / D. Haake

VIRULENCE FACTORS OF SPIROCHETES I
L. Stamm
R. Cevenini / A. Weinberg / V. Tryon

HOST RESPONSES TO SPIROCHETES
S. Lukehart
J. Weis / M. Simon / E. Fikrig /R. Montgomery

INTERACTIONS OF SPIROCHETES WITH HOST CELLS
M. Lovett
B. Guo / M. Klempner / R. Isaacs / U. Munderloh

EVOLUTION AND GENETICS OF SPIROCHETES II
S. Norris
Y. Yanagihara / I. Schwartz / S. Casjens

VIRULENCE FACTORS OF SPIROCHETES II
J. Benach
N. Charon / B. Adler / D. Blanco / J. Radolf

THROMBOLYSIS

HOLIDAY INN
VENTURA, CA
FEBRUARY 18 – 23, 1996

Douglas E. Vaughan, *Chair*
Katharine Hajjar / Hans Pannekoek, *Vice Chairs*

FIBRINOLYSIS AND VASCULAR DISEASE
K. Robbins
A. Hamsten / M. Reidy / M. B. Grant

GENETIC MANIPULATION AND FIBRINOLYSIS IN MICE
P. Carmeliet
J. Degan / D. Ginsburg / S. Strickland

FIBRINOLYTIC REGULATION
D. Loskutoff
S. Kojima / W. D. Schleuning

STRUCTURE/ FUNCTION OF FIBRONOLYTIC PROTEINS
H. Pannekoek
P. J. Declerk / D. Lawrence / E. Madison

THROMBOLYTIC THERAPY
D. Collen
B. Credo / T. Love

CELLULAR RECEPTORS AND FIBRINOLYSIS
K. Hajjar
J. Menell / H. Chapman / F. Blasi

ANGIOGENESIS AND CANCER
B. M. Mueller
E. Rosen / M. S. Pepper / M. S. OíReilly

NEW APPROACHES TO FIBRINOLYSIS
B. Sobel
B. Gerard / D. Eitzman / J. M. Stassen

SESSION TITLES ARE INDICATED IN BOLDFACE, *Discussion Leaders in Italics,* and Speakers in Regular type.

PLEASE DO NOT SEND PAYMENT WITH THIS APPLICATION

GRC

application *mail early*

GORDON RESEARCH CONFERENCES *frontiers of science*

DEADLINE FOR RECEIPT OF APPLICATION IS SIX WEEKS PRIOR TO THE CONFERENCE

PLEASE PRINT OR TYPE

Please return to: Conference Application, Gordon Research Conferences,
University of Rhode Island, P.O. Box 984, West Kingston, RI 02892-0984 USA (mail)

or Conference Application, Gordon Research Center, 3071 Route 138,
Kingston, RI 02881 USA (delivery)

Fax: (401) 783-7644 Phone: (401) 783-4011/3372 E-mail: app@ grcmail.grc.uri.edu

Conference Location

Name of Conference Date of Conference

Information as you would like it to appear on your badge.

Name

Organization

Business Address

City State

Country Code

Phone Fax

E-mail

Please check: I work in ☐ Academic Institution – if predominantly undergraduate, please check here ☐
☐ Government Agency ☐ Industrial Corporation

Please check: ☐ Chair ☐ Vice Chair ☐ Discussion Leader
☐ Speaker ☐ Poster Presenter ☐ Attendee

IMPORTANT

Previous Conferences Attended: ☐ None ☐ 1-5 ☐ 6-10 ☐ 10+

Your Position? ☐ Graduate Student ☐ Postdoc ☐ Research Scientist
☐ Professor ☐ Research Director ☐ Program Manager ☐ Other

Are you personally involved in research activities in the subject area of the Conference? ☐ Yes ☐ No

How many papers have you published during the past 3 years in the subject area of the Conference? ____

You are invited to submit an abstract for a poster presentation at the Conference: many Chairs find abstracts very useful in making decisions concerning admission to their Conferences. **Applications are referred to the Conference Chair in accordance with the established regulations. Following the Chair's acceptance, the registration card will be sent to you. Please complete it and return it immediately with payment of the Fixed Fee**

INDICATE YOUR PARTICULAR ACTIVITIES WHICH JUSTIFY FAVORABLE CONSIDERATION OF YOU AS A PARTICIPANT AND CONTRIBUTOR TO THIS CONFERENCE (REQUIRED FOR POSTER PRESENTERS AND ATTENDEES). USE ADDITIONAL PAGE OR POSTER ABSTRACT, IF NECCESSARY.

GORDON RESEARCH CONFERENCES ADMITS SCIENTIFICALLY-QUALIFIED CONFEREES OF ANY SEX, AGE, COLOR AND NATIONAL ORIGIN

The recording of lectures by tapes, etc. and the photography of slide material are prohibited. Printed references to Gordon Research Conference papers and discussion is not permitted. Authors are requested to omit references to the Conferences in any publiction. Guests are not permitted to attend the conference lectures and discussion sessions. Each member of the Conference agrees to these regulations when registration is accepted.

Signature Date

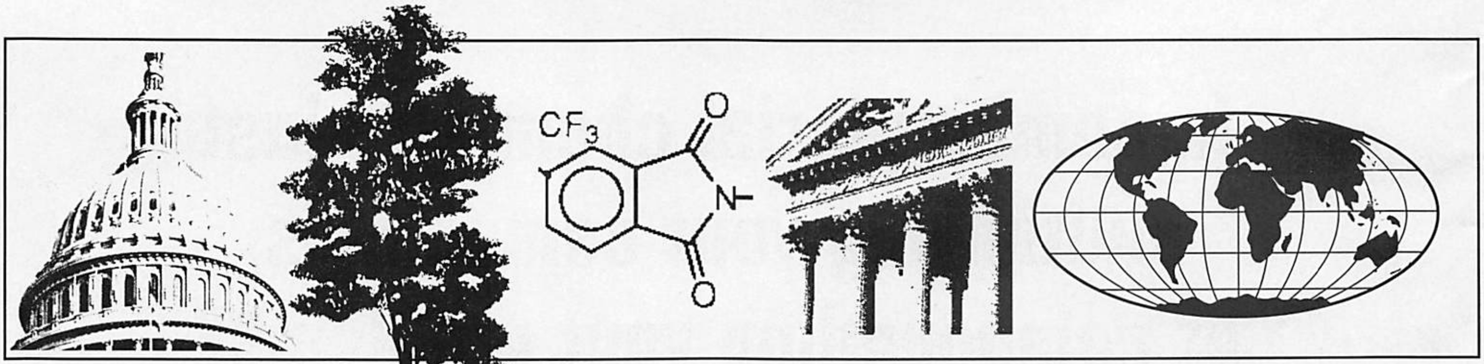

1996-97

AAAS Fellowships for Scientists and Engineers

Applicants should be postdoctoral to midcareer scientists and engineers, from any physical, biological, or social science or any field of engineering. The programs are designed to provide each Fellow with a unique public policy learning experience; to make practical contributions to the more effective use of scientific and technical knowledge in the U.S. government; and to demonstrate the value of science and technology in solving important societal problems. All Fellows participate in a rigorous orientation on the relevant congressional and executive branch operations and foreign affairs plus a year-long seminar series on issues involving science, technology, and public policy. The new, year-long Environmental program, as well as the Congressional, Diplomacy, and Technology Policy programs, begin in September 1996, and the summer Environmental program begins in June 1996. All grant-funded programs are subject to continued support.

All application deadlines are January 15, 1996.

For additional program information and application instructions, write:
Fellowship Programs/Directorate for Science and Policy Programs
AAAS
1333 H Street, NW,
Washington, DC 20005
202/326-6600 Fax: 202/289-4950
Internet: science_policy@aaas.org

American Association for the Advancement of Science

Congressional

AAAS Congressional Science & Engineering Fellows Program

Fellows spend one year on Capitol Hill working with Members of Congress or congressional committees as special assistants in legislative and policy areas requiring scientific and technical input. Two fellowships will be offered, with annual stipends of $40,000.

Technology policy

AAAS-Critical Technologies Institute Science & Engineering Fellows Program

Fellows spend one or two years, working at the Critical Technologies Institute, providing expertise in industrial research and development, technology transfer, international competitiveness, and related issues. At least one Fellow will be selected. Applicants must have a minimum of five years industrial experience, as midlevel or senior executives. Stipends are negotiable, depending on qualifications and experience. Applicants must be U.S. citizens. An additional fellowship opportunity may be available at the White House Office of Science and Technology Policy.

Environmental

AAAS/EPA Environmental Science & Engineering Fellows Programs

Fellows work at the U.S. Environmental Protection Agency—either on issues relating to risk assessment, in a new one-year program, or on a variety of research projects for 10 weeks in the summer. The Fellows assist EPA in assessing the significance of long-range environmental problems. The stipend for the one-year program is $40,000; for the summer program it is $950 a week. Applicants must be U.S. residents. Five Fellows will be selected for the year-long program; 10 for the summer program.

Diplomacy

AAAS Science, Engineering, & Diplomacy Fellows Program

Fellows work in international affairs on scientific and technical subjects for one year, either in foreign policy at the U.S. Department of State or in international development for the U.S. Agency for International Development. One Fellow will be selected at State and approximately 12 Fellows will be selected at USAID. The annual stipend varies with experience, starting at approximately $45,000. Applicants must be U.S. citizens.

Book Reviews

Ants on the Run

Army Ants. The Biology of Social Predation. WILLIAM H. GOTWALD, JR. Comstock (Cornell University Press), Ithaca, NY, 1995. xviii, 302 pp., illus., + plates. $39.95 or £31.50. Cornell Series in Arthropod Biology.

Army ants have long enjoyed an exaggerated reputation for ferocity, perhaps no better exemplified than in Carl Stephenson's classic story, "Leiningen versus the Ants," in which a Brazilian plantation owner—later played by Charlton Heston in the movie adaptation, *The Naked Jungle*—attempts to fend off a ravenous horde: "Ten miles long, two miles wide—ants, nothing but ants! And every single one of them a fiend from hell." In his engaging but more objective account, William Gotwald demonstrates that hyperbole is hardly necessary—mythology aside, army ants provide one of the more intriguing spectacles of social life in the insect world.

A key trait of the "true army ants" (members of the subfamilies Aenictinae, Dorylinae, and Ecitoninae) is their mobilization of large numbers of workers during the search for prey, as distinct from the initiation of mass recruitment after food has been located, a much more common occurrence in ants. In consequence they are able to prey upon large arthropods, social insect colonies, and even the occasional small vertebrate. So efficient is this group predation that local resource depletion occurs, and army ants are notable for their high frequency of colony movement. In the more derived species such emigration is cyclic and closely synchronized with the stages of brood development. Army ants have also achieved enormous colony sizes, exceeding a million workers in some species, all issuing from a single, wingless and grotesquely modified queen. Colony division involves a complicated form of fission or budding, which leads to intranidal conflict over the survival and reproduction of queens and to peculiar selection pressures on dispersing males, who must breach a barrier of alien workers in order to gain access to a mate. Finally, there is a remarkable retinue of symbionts—including mites, millipedes, beetles, flies, and antbirds—that have evolved to exploit various resources associated with army ant colonies, and many of these symbionts have become obligate camp-followers.

Such striking biological phenomena provoke fundamental questions about the functional organization of army ant colonies, the ecological effects of their depredations, and the evolutionary origins of army ants and their associated fauna. Gotwald does an excellent job of summarizing the existing state of knowledge, and he presents useful introductions to some of the general issues that arise from a consideration of group predation by social insects. His coverage of foraging behavior, colony emigration, and the natural history of army ant guests and predators is particularly detailed. Topics with an evolutionary flavor, such as the phylogenetic relationships between army ants and their allies and the operation of kin selection during colony fission, are given less satisfactory treatment. Speciation and coevolution, processes of potential interest in organisms with an army ant lifestyle, receive almost no mention.

As Gotwald emphasizes, most information on army ants comes from studies on a handful of large and conspicuous species that forage above ground. The vast majority of the 300-odd known species are small, elusive, subterranean ants, and we remain profoundly ignorant about most aspects of their biology. There are also significant gaps in our systematic knowledge of these ants. For the Old World taxa, on which Gotwald's work has focused, we lack even a serviceable species-level taxonomy, and for both the Old and the New World army ants there is no robust phylogenetic framework for the comparative analysis of biological traits. Even such a fundamental question as whether the three subfamilies of army ants constitute a monophyletic group remains unresolved. Gotwald suggests that they are polyphyletic, but it is a vague assertion unaccompanied by a specific hypothesis of relationships. Some recent cladistic studies, which Gotwald cites briefly, tend to support the opposite conclusion.

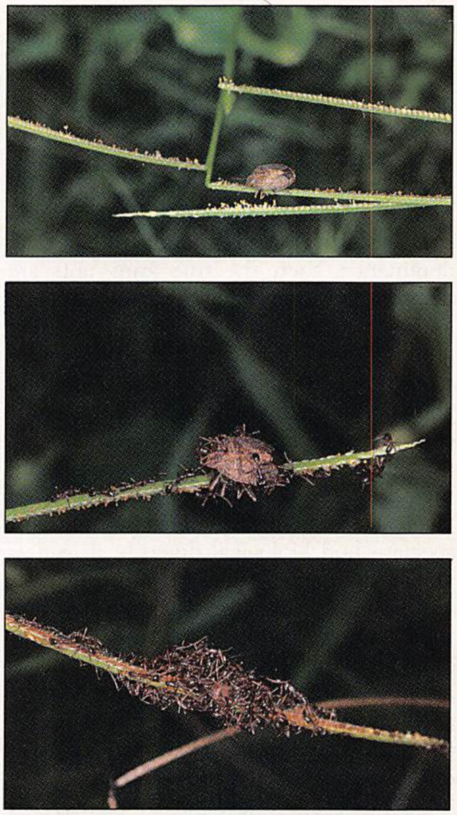

"A stinkbug attempts to escape a driver ant attack by climbing vegetation [top]. Although the stinkbug releases a defensive secretion, the ants are not deterred [center] and soon overwhelm it [bottom]." [From *Army Ants*]

Noting the convergent development of group predation and nomadism in several other ant taxa besides the true army ants, Gotwald argues that the army ant adaptive syndrome is "enormously successful." To make a proper historical assessment of this claim, however, we need to know how many times the constellation of army ant

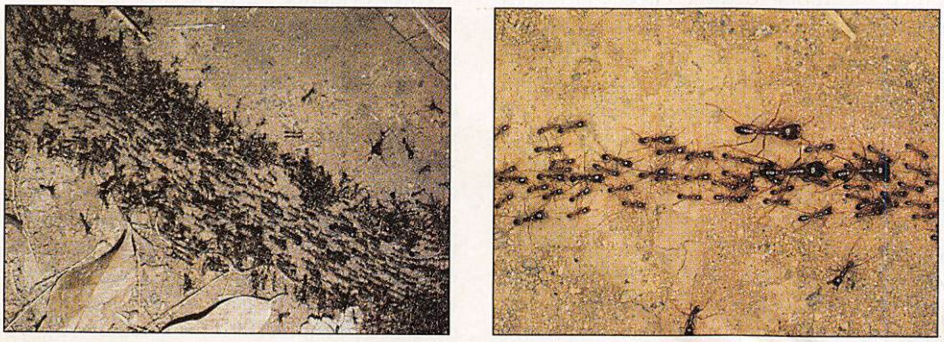

"Although driver ant foraging columns may be relatively small [as at left], it is not unusual for raiding columns to achieve a density of 13 individuals per square centimeter [right]." [From *Army Ants*]

traits has arisen and to compare the success of these lineages with that of their sister groups. The relevant phylogenetic tests have not been carried out, but it seems quite possible that the army ant groups are no more successful, with respect to net diversification (that is, contemporary species richness), than their generalist sister groups. If success is measured in terms of ecological dominance, then the true army ants are demonstrably important in many tropical and subtropical habitats, but the other groups—the army ant "wannabes"—are more limited in distribution, diversity, and abundance, and their ecological significance remains unclear.

The book concludes with an appeal for increased efforts toward conservation of tropical ecosystems where most army ant species—and biological diversity in general—reside. Despite their large colony sizes and seeming invincibility, army ants and their obligate symbionts are especially vulnerable to habitat fragmentation. This is because population (as opposed to colony) sizes are rather low and because the queens, as wingless individuals reproducing by colony fission, are very poor colonizers of isolated pieces of landscape. In reality, our rampages endanger army ants much more than their activities pose a threat to human life or limb.

Philip S. Ward
Department of Entomology,
University of California,
Davis, CA 95616, USA

The WAM Report

Dynamics and Modelling of Ocean Waves. G. J. KOMEN, L. CAVALERI, M. DONELAN, K. HASSELMANN, S. HASSELMANN, AND P. A. E. M. JANSSEN. Cambridge University Press, New York, 1994. xxii, 532 pp., illus. \$59.95 or £40.

That water waves are generated by wind was known to the ancients and proclaimed by such polymaths as Leonardo da Vinci and Benjamin Franklin, but scientific prediction of these phenomena has been attempted only in the past 50 years. The complete problem comprises two, essentially distinct parts: the prediction of the wind field, which is the province of meteorologists, and the prediction of the resulting response of the ocean surface, which is the province of oceanographers. The present monograph, which appears as the final report of the WAM (Wave Modelling) group, provides a state-of-the-art survey of the latter problem. The title page lists six authors, but 35 scientists from 12 nations are listed as "contributors" and the WAM-group list comprises 71 individuals. This is manifestly an international effort.

The first predictive model, developed by Sverdrup and Munk (1943–1947) in response to the need for sea and swell forecasts for the Allied invasion of North Africa, was based on empirical relations between characteristic parameters of the wave and wind fields and antedated the statistical description of the problem by Pierson, Neumann, and James in 1955. The starting point for subsequent models, including those covered in the volume under review, is the Boltzmann-like transport equation.

$$\frac{\partial F}{\partial t} + \mathbf{v} \cdot \nabla F = S_{in} + S_{nl} + S_{ds},$$

which governs the evolution of the surface-wave field in space ($\mathbf{x}$) and time (t); $F = F(f, \theta; \mathbf{x}, t)$ is the two-dimensional spectral density in frequency f and direction of propagation θ, $\mathbf{v} = \mathbf{v}(f, \theta)$ is the group velocity, S_{in} is the input from the wind, S_{nl} is the nonlinear transfer through wave interactions, and S_{ds} is the dissipation. This approach became practical only in the early 1960s with the theoretical studies of Phillips (1957) and Miles (1957), which provided a basis for the representation of S_{in}, and the discovery of resonant interactions by Hasselmann (1960) and Phillips (1960), which provided the basis for the representation of S_{nl}; the representation of S_{ds} was, and remains, empirical, with turbulence as an ineluctable antagonist.

Models based on the equation given above have been described as first-, second-, or third-generation, in which nonlinear interactions are, respectively, neglected, described in simplified parametric form, or incorporated within the limits of current knowledge and computing power. First-generation models failed to describe the nonlinear transfer of energy from higher frequencies, where wind generation is more efficient, to lower frequencies, where dissipation is weaker, and yielded rather misleading results. Second-generation models, which incorporated these effects, although not always successfully, were described in *Ocean Wave Modeling* by the SWAMP (SeaWave Modelling Project) Group, which I reviewed in *Science* (**229**, 377) in 1985 with the conclusion that "Future ('third generation') models, already under development, will incorporate more sophisticated parameterizations of S_{nl} and may exploit our theoretical knowledge to its present limits, after which the lack of a rational model of dissipation and the effects of finite, variable depth are likely to present barriers to further progress."

The present volume fulfills that promise, and, although the barriers remain, they may now be better described as impediments. Moreover, whereas the SWAMP book was primarily a progress report on second-generation models, Komen *et al.* provide full expositions of the basic fluid dynamics, numerical modeling, and incorporation of global satellite measurements. The development is not seamless, but, considering the number of contributors, the principal authors have done an admirable job of assembling a coherent whole and of providing a firm base for the exploration of the many challenging problems that remain.

John Miles
Institute of Geophysics and Planetary Physics,
University of California at San Diego,
La Jolla, CA 92093–0225, USA

Visual Perception

Image and Brain. The Resolution of the Imagery Debate. STEPHEN M. KOSSLYN. MIT Press, Cambridge, MA, 1994. x, 516 pp., illus. \$45 or £38.50.

Kosslyn's *Image and Brain* is a *tour de force* in the analysis of visual perception and imagery, looked upon from all possible perspectives. It is an examination of work done during the past 15 years on visual imagery by a variety of methods, from chronometric measurements to computer models to functional brain imaging, bringing a systematic approach to bear on this multitude of data to delineate the issues of brain mechanisms underlying visual perception and imagery. The scheme adopted posits a number of systems and subsystems (for example for edge detection and for encoding motion relations) that process specific kinds of information and that together make for an apparently seamless operation of visual perception and imagery. This analytical approach is open-ended, in the sense that more processing stations can be adduced if need or evidence for them arises; it is flexible, so that rearrangements in processing order are allowed for; and it is powerful, so that it can be applied rigorously to complex data. The net result is a coherent theory of visual perception and imagery in which results obtained by a diversity of methodologies—observations in normal and brain-damaged people, neuroimaging, neurophysiological experiments, and computer modeling—can be accommodated and used to explore and fill in gaps in our account of observed phenomena. This calculus of processes, as it were, that Kosslyn develops can be applied to diverse situations. An excel-

lent example is its application to the case of a particular brain-damaged patient, as detailed on pages 276–282. The analysis here shows not only what the processing deficits may be in the patient but also what tests should be done to elucidate the situation. This brings home another point, namely that empirical findings can rarely be interpreted without a theoretical framework. *Image and Brain* offers a framework for making sense of hugely diverse data on visual perception and imagery that also leads to testable hypotheses and predictions, keeping it on solid evidential ground and enabling it to evolve as a more and more sophisticated instrument.

Thus the approach expounded in *Image and Brain* is a great analytical tool. But is this how the brain works? The explanation of a complex system's behavior rests heavily on the interaction of its components (W. Bechtel, *Can. J. Philos. Suppl.* 20, 133 [1994]), and brains abound in contextually conditional states of affairs. Hence one can hardly give a global answer to this question; at best the answer can differ according to the particular processing system or systems involved.

Moreover, though the approach of *Image and Brain* has the merit of being rigorous and logical, the mechanisms used by the brain to actually solve a problem may not rely on a comparably logical series of steps. Specifically, I am referring to the possibility of "smart" mechanisms (S. Runeson, *Scand. J. Psychol.* 18, 172 [1977]). An example is the polar planimeter, a physical device that can measure the area of an irregular shape without using any logical steps that one would ordinarily employ for that purpose, such as using a fine grid. If measuring an area were important for survival, it is possible that evolutionary pressure could have resulted in a neural operation that could likewise have been implemented by a neural network without following logical steps. Similar considerations hold for the motor system, where solutions to pressing problems could have been arrived at by a long evolutionary process of trial and error rather than by a succession of logical steps (A. P. Georgopoulos *et al.*, *Science* 237, 301 [1987]). For example, movements of the arm involve movements of the joints, which are brought about by torques applied at the joints produced by contractions of muscles. To derive these torques, given the desired trajectory of hand in space, is a very tedious process of solving what is known as the inverse kinematics problem. Imagine the magnitude of this problem when, for example, the movement trajectories of four limbs have to be coordinated in time and space in a locomoting quadruped. And yet, the spinal cord can accomplish that feat alone. One can write down the logical steps in a series of box diagrams or in a mathematical solution of this problem, but from the fact that the problem is solved by the spinal cord it does not follow that it was solved in that particular way. It is much more plausible to suppose that the spinal cord has evolved as a neural network solving this problem without the benefit of mathematical or logical sequences. I believe that the answer to the question of how the brain actually does it lies somewhere in between, in that different processing subsystems may be involved in a given function but a number of them may implement "smart" mechanisms. But "smart" mechanisms are usually invented or discovered rather than arrived at by a logical process and therefore are much more difficult to find and identify. Keeping our eyes open is the smart thing to do.

As the book's title suggests, the theory developed in *Image and Brain* has far-reaching implications, with regard to the imagery debate. This debate during the 1970s and '80s focused on whether visual mental images are internally represented exclusively by language-like "propositional" representations or in part by "depictive" representations. In a depictive representation, shape is represented by points in a space: each point corresponds to a point on the object, and intervening points in the space correspond to intervening points on the object. The experimentally established fact that many cortical visual areas are topographically organized shows that the representations in these areas are depictive. Another recent finding is that "higher" visual areas have feedback connections to "lower," topographically organized areas. Therefore, it is reasonable to suppose, as Kosslyn proposes, that visual mental images are patterns of activation in topographically organized areas that are produced via these feedback connections. Evidence for shared mechanisms in imagery and perception is obviously relevant to the debate about the nature of images: if images share brain areas with perception, and these areas are hard-wired (that is, topographically organized) to represent shape depictively in perception, it follows that these areas represent shape depictively in imagery. This hypothesis is further supported by evidence that imagery not only activates homologous topographically organized areas in the human brain but is impaired when these areas are damaged. In summary, the central issue of the imagery debate can now be stated in concrete terms: do areas of the brain that depict visual information represent visual mental images? "Yes" is an educated answer. How are patterns of activation in these areas formed, manipulated, and used during imagery? With its schematic approach *Image and Brain* addresses these questions in a precise and challenging, yet enjoyable, way.

Apostolos P. Georgopoulos
Brain Sciences Center,
Veterans Affairs Medical Center,
Minneapolis, MN 55417, USA

Vignette: Proper Precautions

On the tiny dashboard monitor, they had a view looking straight down at the powerful body of a Tyrannosaurus rex, as it moved up the game trail toward them. Its skin was a mottled reddish brown, the color of dried blood. In dappled sunlight, they could clearly see the powerful muscles of its haunches. The animal moved quickly, without any sign of fear or hesitation.

Staring, Thorne said, "Everybody in the car."

—From *The Lost World*, a novel by Michael Crichton (Knopf)

Books Received

Aquaculture Development. Progress and Prospects. T. V. R. Pillay. Wiley, New York, 1994. x, 182 pp., illus. $59.95.

Behavioral Design. Nicholas S. Thompson, Ed. Plenum, New York, 1995. xvi, 334 pp., illus. $85. Perspectives in Ethology, vol. 11.

Publishers' Addresses

Below is information about how to direct orders for books reviewed in this issue. A fuller list of addresses of publishers represented in *Science* appears in the issue of 26 May 1995, page 1220.

Cambridge University Press, 110 Midland Ave., Port Chester, NY 10573–4930. Phone: 800-872-7423; 914-937-9600. Fax: 914-937-4712.

Comstock Press, P.O. Box 6525, Ithaca, NY 14851–6525. Phone: 800-666-2211 (outside NY state); 607-277-2211. Fax: 800-688-2877; 607-277-6292.

MIT Press, 55 Hayward St., Cambridge, MA 02142. Phone: 800-356-0343; 617-625-8569. Fax: 617-258-6779. E-mail: mitpress-orders@mit.edu.

Products & Materials

Antibodies

Antibodies to human tumor necrosis factor (TNF)–α and TNF-β are part of a line of research products that includes eight growth

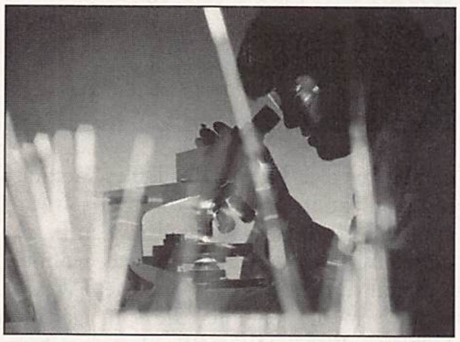

factor products in the TNF family, recombinant human and mouse TNF-α, and recombinant human TNF-β. **Sigma BioSciences. Circle 135.**

The nm23-H1 gene product, also known as nucleoside diphosphate kinase A, is a possible mediator of cancer cell invasion and metastasis. Monoclonal antibody 37.6 reacts specifically with it in formalin-fixed, paraffin-embedded or frozen tissue sections. **BioGenex. Circle 136.**

Ki-67 antigen is a widely studied marker of cell proliferation, but until recently it has been reliable only in fresh or frozen tissues. Clone MIB-1 identifies the antigen in formalin-fixed, paraffin-embedded tissue sections. **BioGenex. Circle 137.**

■

HPLC System Test Kit

The new HPLC System Test Kit provides a quick and easy way to test the performance of a high performance liquid chromatography (HPLC) system. The kit includes a C18 column and both isocratic and gradient test mixes. Use the kit at the beginning of a method to establish that the instrument is functioning properly and to establish a chromatogram fingerprint. When variation in the chromatogram occurs, simply use the test column on the system. Any deviation from the fingerprint indicates a system-related problem, whereas reproduction of the fingerprint chromatogram indicates a column or method failure. **Phenomenex. Circle 138.**

■

Capillary Electrophoresis Kit

The eCAP dsDNA 20,000 kit for DNA analysis, teamed with the P/ACE Capillary Electrophoresis System, delivers automated, reproducible, and quantitative results in minutes, providing an attractive alternative to the traditional agarose slab gel method for DNA analysis of large fragments up to 20,000 base pairs. Qualitative and quantitative characterization of a DNA fragment from a plasmid digest or polymerase chain reaction amplification can be done immediately without prior sample preparation, including desalting. **Beckman Instruments. Circle 139.**

■

Tetrameric Avidin Resin

TetraLink Tetrameric Avidin Resin can be used to tightly bind biotinylated proteins for applications including preparation of affinity resins for the purification of antibodies. The strong affinity of the avidin-biotin interaction allows release of biotinylated molecules only under strongly denaturing conditions. The resin can be used in conjunction with the PinPoint in vivo biotinylation systems, which produce biotinylated fusion proteins. The base support for TetraLink is a rigid methacrylate, polymeric gel filtration matrix that tolerates high flow rates and centrifugal forces in batch operation. **Promega. Circle 140.**

■

Multiple Format Microplate Reader

The Spectra Image reads any clear plate that fits within a 96-well plate footprint, including 6-, 24-, 48-, and 384-well plates. A special adapter is also available for terasaki plates and culture dishes. In addition to performing all standard photometer functions, the Spec-

Newly offered instrumentation, apparatus, and laboratory materials of interest to researchers in all disciplines in academic, industrial, and government organizations are featured in this space. Emphasis is given to purpose, chief characteristics, and availability of products and materials. Endorsement by *Science* or AAAS is not implied. Additional information may be obtained from the manufacturers or suppliers named by circling the appropriate number on the Readers' Service Card and placing it in a mailbox. Postage is free.

tra Image can display an image of plate contents and save it for future use. On-board software offers curve fit, kinetics, and data reduction. The instrument can also be controlled through Microsoft Excel. **Tecan. Circle 141.**

■

DNA Ligation Kit

The Rapid DNA Ligation Kit eliminates overnight ligation incubations. The kit performs high-efficiency, blunt, and sticky-end DNA fragment ligations in under 5 min at ambient temperature, cutting a day out of cloning experiments. All reagents required for ligation are supplied with the kit, so there is no need for preparation of buffers and addition of adenosine triphosphate and Mg^{2+}. **Boehringer Mannheim. Circle 142.**

■

Cell Purification Method

A new density perturbation technique allows the easy separation of cells on the basis of the immunological identity of the cell surface with the aid of antibody-coated nonmagnetic beads. Accubeads are significantly less expensive than magnetic beads and can give similar separations. The new method has a broad range of applications, for example, the separation of subsets of tissue culture cells and peripheral blood cells. **Accurate Chemical and Scientific. Circle 143.**

■

Genome Database CD-ROM

The Genome Interactive Database (GID), available on CD-ROM, is a collection of five interactive databases: GENATLAS, CEPH, CEPH/GENETHON, GENETHON, and GENSET. GID includes information about localizing genes and markers, the probes available for finding them, restriction fragment length polymorphisms, microsatellites, oligonucleotides for developing a sequence, the access number for a sequence bank, bibliographic references and abstracts from Medline, and more. **John Libbey Eurotext. Circle 144.**

■

Bacterial Lysates Without Centrifugation

The new QIAfilter cartridge is a filter designed to replace the centrifugation step after alkaline lysis of bacterial cells. Neutralized bacterial lysates are cleared in seconds, reducing plasmid purification time by up to 1 hour. The cartridge completely removes small-sized sodium dodecyl sulfate precipitates that cannot be separated by conventional centrifugation. **Qiagen. Circle 145.**

Image Analysis Software

BioMax ID Image Analysis Software is designed to analyze nucleic acid and protein electrophoresis gels. It provides molecular weight and mass data in Macintosh and Windows environments. Acquired images

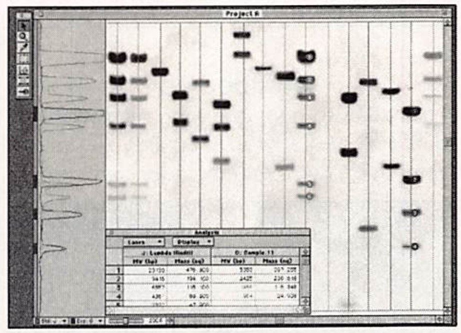

can be saved as TIFF or PICT files, facilitating publication or export to other software applications. Images for analysis can be acquired using a TWAIN compliance scanner, a digital camera that supports the TWAIN acquire mode, or any TIFF image file. **Eastman Kodak Scientific Imaging Systems. Circle 146.**

■

Literature

Vision is a bi-annual magazine aimed at scanning electron microscope users. **Leica. Circle 147.**

1995 CMS Histology and Cytology Catalog features 63 pages of equipment and supplies. Highlights include microtomes and tissue processors, immunostaining systems, and automatic slide stainers. **Curtin Matheson Scientific. Circle 148.**

Spectrolinker XL-1000 UV Crosslinker describes an instrument that covalently binds nucleic acids to membranes in less than 30 s, 240 times faster than vacuum oven baking. Applications include crosslinking of DNA and RNA by covalently binding nucleic acids to nylon or nitrocellulose membranes after Northern (RNA), Southern (DNA), slot, or dot blotting; eliminating polymerase chain reaction contamination; nicking ethidium bromide–stained DNA in agarose gels; gene mapping for creating cleavage-inhibiting thymine dimers; ultraviolet sterilization; and more. **Spectronics. Circle 149.**

A recent issue of *VIEWS* newsletter features an article on the sizing of DNA fragments by capillary electrophoresis. Other articles include "Methods for the Characterization of Synthetic Peptides" and "DNA Analysis Using Capillary Electrophoresis." **Perkin Elmer. Circle 150.**

POSITIONS OPEN

UNIVERSITY OF Miami

EVOLUTIONARY BIOLOGIST

The Department of Biology, University of Miami, invites applications for a tenure-track position at the level of **ASSISTANT PROFESSOR**. We seek an evolutionary biologist with strong quantitative skills. Preference is for a botanist using physiological, genetical, or ecological approaches who will contribute to existing departmental strengths in evolution, behavior, ecology, and tropical biology. Ph.D. degree required. The successful candidate will be expected to develop an innovative, externally funded research program, and to participate in teaching at the undergraduate and graduate levels. Applicants should send curriculum vitae, representative reprints, and summary of research interests, and arrange to have three letters of reference sent to: **William A. Searcy, Chair, Search Committee, Department of Biology, P.O. Box 249118, University of Miami, Coral Gables, FL 33124-0421**, by 7 December 1995.

The University of Miami is an Equal Opportunity/Affirmative Action Employer.

FACULTY POSITIONS—ZOOLOGY WEBER STATE UNIVERSITY (WSU)

The Department of Zoology invites applications for two tenure-track positions at the **ASSISTANT** or **ASSOCIATE PROFESSOR** level starting in September 1996. The Ph.D. is required. 1) Aquatic Ecologist with skills in fisheries: teaching responsibilities include general zoology, aquatic ecology and ichthyology. 2) Vertebrate Physiologist: teaching responsibilities include human physiology, human anatomy, and upper division classes, e.g. cell physiology and courses in specialty area. Research program involving undergraduates is expected. Send cover letter, statement of teaching philosophy and research interests, curriculum vitae, and one to three reprints. Have letters of reference sent to: **Dr. Samuel Zeveloff, Chair, Department of Zoology, c/o Human Resources, Weber State University, Ogden, Utah 84408-1016. Telephone: 801-626-6165; FAX: 801-626-7445.** Information about WSU is available on the World Wide Web (**http://WWW.WEBER.EDU**). Deadline: 1 December 1995. *Affirmative Action/Equal Opportunity Employer.*

FACULTY POSITIONS CELL AND MOLECULAR BIOLOGY

Applications are invited for tenure-track positions, at the level of **ASSISTANT PROFESSOR**, in the Department of Cell and Molecular Biology at Northwestern University Medical School. Candidates must have a Ph.D. or equivalent degree, postdoctoral experience, and research experience in cell and molecular biology. The department is particularly interested in individuals with a strong record of productivity in the areas of cytoskeleton/cell motility, nuclear architecture and function, or biological structure using high resolution microscopic techniques. Applicants will be screened with respect to their ability to carry on vigorous, independent research and to participate in departmental teaching programs. Send a complete curriculum vitae and a brief description of research interests to: **Dr. Robert Goldman, Chair, Department of Cell and Molecular Biology, Northwestern University Medical School, 303 East Chicago Avenue, Chicago, IL 60611.**

Northwestern University is an Equal Opportunity/Affirmative Action Educator and Employer and invites applications from all qualified individuals. Applications from women and minorities are especially sought.

Physiology—Creighton University School of Dentistry is seeking a Physiologist for a full-time, tenure-track position at the **ASSISTANT/ASSOCIATE PROFESSOR** level within the Department of Oral Biology. Position is available July 1, 1996.

Position qualifications include Ph.D. or equivalent. Primary responsibilities include teaching and research. Extensive facilities are available for collaborative research. Send curriculum vitae and names of three references to: **Dr. Joseph J. Keene, Jr., Chair, Department of Oral Biology, Creighton University School of Dentistry, 2500 California Plaza, Omaha, NE 68178.** *An Affirmative Action/Equal Opportunity Employer.*

POSITIONS OPEN

SEDIMENT BIOGEOCHEMISTRY MICROBIAL ECOLOGY REMOTE SENSING/GIS ASSISTANT OR ASSOCIATE RESEARCH FACULTY POSITION

The University of Georgia (UGA) Marine Institute on Sapelo Island, an institution with a 40-year history of coastal research, invites applications for a state-funded **RESEARCH FACULTY** position. We seek an individual with either outstanding potential or demonstrated expertise to develop a rigorous and dynamic research program. Preference will be given to candidates whose research is field- and process-oriented and in any of the following areas of estuarine research: Sediment Biogeochemistry; Microbial Ecology; Remote Sensing/GIS. The natural estuarine environments on Sapelo Island, especially the extensive salt marshes and sand beaches, offer an uncommon opportunity to conduct field-oriented studies without concern for uninvited human disturbances. The resident research faculty at the Marine Institute have no teaching obligations, but may hold adjunct appointments in academic departments, including the newly-formed Department of Marine Sciences, on the main campus of UGA. The position is available as early as 1 July 1996. Salary will be commensurate with experience and qualifications. Interested individuals should send a curriculum vitae, statement of research interests, and the names and addresses of three potential referees to:

Dr. James J. Alberts, Director
UGA Marine Institute
Sapelo Island, GA 31327
Application deadline is 15 December 1995

The University of Georgia is an Equal Opportunity/Affirmative Action Employer.

ASSISTANT PROFESSOR

The Signal Transduction Laboratory of the Biotherapy Program at the University of Minnesota is seeking two faculty members to fill an annual, renewable, non-tenured **ASSISTANT PROFESSOR** position. Applicants should hold a Ph.D. or an equivalent degree and have expertise in the area of molecular biology and signal transduction. Laboratory space and adequate funds are available to allow the establishment of an outstanding research program. Applicants should submit: a curriculum vitae, reprints of selected publications, and the names, addresses and telephone numbers of three individuals whom the applicant has asked to submit letters of recommendation by November 1, 1995 to: **Search Committee c/o Dr. F. M. Uckun, University of Minnesota, Box 356 UMHC, 420 Delaware Street SE, Minneapolis, MN 55455.**

The University of Minnesota is an Equal Opportunity Educator and Employer.

ACADEMIC POSITION

ASSISTANT PROFESSOR. The Department of Chemistry and Biochemistry of The University of Texas at Austin solicits applications for a tenure-track assistant professorship beginning September 1, 1996. Exceptional candidates whose research training and interests are in areas of biochemistry and experimental physical chemistry are especially encouraged to apply. Review of applications will begin on November 1, 1995, and applications received after December 1, 1995, may not receive consideration. Candidates who have demonstrated outstanding research ability and show promise in teaching should forward a curriculum vitae, short descriptions of research plans, and three letters of reference to: **Search Committee, Department of Chemistry and Biochemistry, The University of Texas at Austin, Austin, TX 78712.** *Equal Opportunity/Affirmative Action Employer.*

ENDOWED CHAIR

The Department of Anesthesia, together with the Department of Cellular and Molecular Pharmacology at the University of California, San Francisco, seeks an outstanding investigator for an endowed chair, the first William K. Hamilton **PROFESSOR** of Anesthesia. The person will be responsible for research training of academic anesthesiologists and graduate students. Experience in basic cellular and molecular approaches relevant to anesthesia and pharmacology required. Send curriculum vitae and three reference letters by October 31, 1995 to: **Jeanine P. Wiener-Kronish, M.D., UCSF, Anesthesia and Cellular and Molecular Pharmacology, Box 0624, M-917, San Francisco, CA 94143-0648.** *University of California, San Francisco is an Equal Opportunity and Affirmative Action Employer.*

UNIVERSITY OF CALIFORNIA AT BERKELEY
Department of Chemistry
Faculty Position in Chemistry

The Chemistry Department at the University of California at Berkeley solicits applications for a position as **ASSISTANT PROFESSOR** of Chemistry, beginning in the fall of 1996, pending budgetary approval. Creative and energetic candidates in synthetic and physical chemistry, particularly materials chemistry, who show exceptional promise for research and teaching are specifically sought, although truly outstanding persons in any area of chemistry will be considered. Individuals selected for this position will be expected to establish an outstanding research program. Candidates should send a curriculum vitae, a proposed research program, and arrange to have three letters of recommendation sent to: **Chairman, Faculty Recruiting Committee 67, Department of Chemistry, University of California, Berkeley, CA 94720-1460.** The deadline for receipt of applications is December 1, 1995. *The University of California is an Equal Opportunity/Affirmative Action Employer.*

ASSISTANT PROFESSOR of Biology—The University of Pittsburgh at Bradford invites applications for a tenure-track position beginning fall 1996. Applicants must have Ph.D. in some aspect of plant biology. Preference given to candidates with demonstrated teaching effectiveness, research experience, and a broad background in plant sciences. The successful candidate will be expected to teach courses in introductory biology, botany, genetics, ecology, and in area of expertise. Other duties include directing undergraduate research, academic advising, and developing collaborative interdisciplinary teaching programs.

Pitt-Bradford, Pennsylvania's public liberal arts college, is located in the Allegheny Mountains of northwestern Pennsylvania. Numerous outdoor recreational activities are found in the region. The metropolitan life of Toronto, Pittsburgh, and Buffalo is within a one to three hour drive.

Send curriculum vitae, letter of application stating teaching experience and research interests, official transcripts, and three letters of reference by November 30, 1995, to: **Dr. John S. Chandler, Biology Search Committee, University of Pittsburgh at Bradford, Bradford, PA 16701-2898.** *Affirmative Action/Equal Opportunity Employer.*

DEPARTMENT OF PATHOLOGY
CHAIR

The Bowman Gray School of Medicine is seeking a **CHAIR** for the Department of Pathology. This senior investigator will be charged with developing strong, nationally visible programs in cancer research and in neuroscience and cardiovascular disease research. He or she will be expected to maintain strong existing programs in undergraduate and graduate education as well as to provide the vision to lead a large, successful, academic-based Pathology Department through the changing environment of managed care. Please send curriculum vitae, funding history, and the names of five references to:

Dr. Joseph Jorizzo
Chairman—Search Committee
Department of Dermatology
Bowman Gray School of Medicine
of Wake Forest University
Medical Center Boulevard
Winston-Salem, NC 27157

Affirmative Action/Equal Opportunity Employer.

GROSS ANATOMIST

The Division of Preclinical Medical Education of the New York College of Osteopathic Medicine invites applications for the position of **ASSISTANT PROFESSOR** of Anatomy. Primary teaching responsibilities in Human Gross Anatomy. The ability to teach either Histology or Neuroanatomy is desirable. Applicants must have a Ph.D., experience teaching Human Gross Anatomy in a medical school environment, and a strong record of research and publications. 25% teaching and 75% research time. Research interests should complement the department's existing strengths in vertebrate paleontology and evolutionary biology. Deadline for receipt of applications is December 15, 1995. Please submit curriculum vitae and details of teaching/research experience, grant track record, and three references to: **Dr. Arnold L. Nagler (Associate Dean) and Dr. Nikos Solounias (Associate Professor of Anatomy), NYCOM, Old Westbury, NY 11568.** *Equal Opportunity/Affirmative Action Employer.*

ASSOCIATE/FULL PROFESSOR
Cell or Developmental Biology

The University of Iowa invites applications from cell or developmental biologists for the position of **ASSOCIATE** or **FULL PROFESSOR** in the Department of Biological Sciences. The successful candidate must have significant experience directing a strong, independent research program with high visibility in the research community, and the capacity to forge strong intra-university collaborations in research programs and centers. Teaching responsibilities will be in the area of cell or developmental biology. Preference will be given to applicants with research interests in vertebrate development or molecular cytology, but outstanding researchers in related areas are encouraged to apply. Please send curriculum vitae with a statement of research interests and names of three references to: **Dr. David R. Soll, Cell and Development Search Committee, Department of Biological Sciences, University of Iowa, 138 Biology Building, Iowa City, IA 52242-1324.** *The University of Iowa is an Equal Opportunity/Affirmative Action Employer. Women and minority candidates are encouraged to apply.*

CHILDREN'S HOSPITAL
UNIVERSITY OF CINCINNATI
Director, Developmental Biology

Applications are invited for the position of **DIRECTOR** of Developmental Biology and Albert Sabin Professor of Pediatrics to lead a well-established program in molecular and developmental biology. Candidates will be expected to direct their own outstanding research program, lead the Division of Developmental Biology (a 10 member Ph.D. faculty with primary focus to the molecular biology of mammalian development), participate in a well-established graduate program in developmental biology and interact with research activities in developmental sciences at the Children's Hospital Research Foundation and the University of Cincinnati College of Medicine. Candidates will have an M.D. and/or Ph.D. degree and an internationally recognized program in developmental molecular biology. Outstanding support facilities are available for the Director and the program. Send a letter of interest and curriculum vitae to: **Jeffrey A. Whitsett, Associate Chair of Pediatrics, c/o Search Committee, Children's Hospital Medical Center, Division of Pulmonary Biology, 3333 Burnet Avenue, Cincinnati, OH 45229-3039.** *Children's Hospital Medical Center is an Affirmative Action/Equal Opportunity Institution. Women and minorities are encouraged to apply.*

FACULTY POSITION
Ben-Gurion University of the Negev
Faculty of Health Sciences

The Faculty of Health Sciences invites applications for Alon Fellowship candidates leading to tenure-track **FACULTY POSITIONS** in Basic Medical Sciences. Candidates should utilize modern approaches in the following areas: microbiology, virology, human genetics, biochemistry, molecular biology, molecular oncology, molecular neurobiology, developmental biology, and immunology. A Ph.D. and/or M.D. degree and at least two years of postdoctoral training are required. Excellence in research will be of prime importance in the decisions of the Search Committee. Candidates are expected to develop independent research programs. Curriculum vitae, publication list, selected reprints, statement of research plans, and three letters of recommendation addressed to **Professor S. Segal, Dean** should reach the **Office of the Dean, Faculty of Health Sciences, Ben-Gurion University of the Negev, P. O. Box 653, 84105 Beersheva, Israel,** by November 15, 1995. **FAX: 972-7-277342.**

Department of Psychology, University of Illinois at Urbana-Champaign (UIUC), **ASSISTANT PROFESSOR**, Psychopharmacologist. The Department of Psychology of the University of Illinois at Urbana-Champaign invites applications for a full-time tenure-track faculty position beginning fall 1996. Candidates holding the Ph.D. degree and conducting research in any area of psychopharmacology/neuropharmacology that has a relationship to behavior will be considered. Teaching is at both undergraduate and graduate levels. Salary is dependent on qualifications and experience. For full consideration, a curriculum vitae, representative reprints, a statement of research interests, and three letters of recommendation should be sent by 31 January 1996 to: **William Greenough, Psychology Department, University of Illinois, Beckman Institute, 405 North Mathews, Urbana, IL 61801. Telephone: 217-333-4472.** *UIUC is an Affirmative Action/Equal Opportunity Employer.*

UNIVERSITY OF CHICAGO
Department of Organismal Biology and Anatomy

The Department of Organismal Biology and Anatomy seeks applicants for a **TENURE-TRACK** position beginning July 1, 1996. We expect to fill this position at the level of assistant professor, but individuals at a higher rank will also be considered. The Department seeks an individual who will develop an outstanding research program in, or overlapping with, the areas of developmental biology, biomechanics and physiology, or neurobiology, to build on the Department's existing strengths in these areas. We seek individuals studying organismal function in an integrative context. Teaching responsibilities will include undergraduate and graduate coursework. Applicants should submit a curriculum vitae, summary of research interests, and four letters of reference to: **OBA Search Committee Chair, University of Chicago, 1025 East 57th Street, Chicago, IL 60637.** Review of applications will commence 1 December 1995; however, applications will be accepted until the position has been filled.

The University of Chicago is an Affirmative Action/Equal Opportunity Employer. Women and members of minority groups are strongly encouraged to apply.

Morehead State University seeks applications from talented and innovative individuals to **CHAIR** the Department of Biological and Environmental Sciences. The twelve-month, tenure-track position will be available July 1, 1996. The Department Chair provides academic/administrative leadership for B.S. degrees in biology, environmental science, medical technology, and a M.S. degree in biology. Additional responsibilities include oversight for departmental budget, class scheduling, faculty/staff recruitment and evaluation, promotion of scholarly activities, and service involvement. The Chair will also advise and teach undergraduate and/or graduate students, and work with personnel across the University. Qualifications: Ph.D. in one of the department disciplines from a regionally accredited institution. Minimum of seven years full-time university teaching experience. Demonstrated proficiency in teaching, scholarly activity, service, leadership, and strong interpersonal and communication skills. Candidate should have qualifications appropriate for rank of professor with tenure. To ensure consideration, submit letter of application, résumé, statements of teaching and administrative philosophies, transcripts for the terminal degree, and names, addresses, and telephone numbers of five references by November 17, 1995, to: **Office of Human Resources, Attn: Chair. Biological and Environmental Sciences, Morehead State University, HM 101, Morehead, KY 40351.** *MSU is an Affirmative Action/American Disabilities Act/Equal Opportunity Employer. The University has a strong commitment to the principles of diversity and seeks a broad spectrum of candidates including women, minorities, and individuals with disabilities.*

Biologist. Tenure-track **ASSISTANT PROFESSOR** to begin 16 August 1996. We seek a biologist using modern approaches to study the structure and function of animal cells and tissues. Establishment of a strong, independent research program and direction of graduate students is expected. Will teach histology or cytology and participate in a team-taught introductory biology course. Ph.D. required and postdoctoral experience desirable. Send curriculum vitae, three representative reprints, and statements of teaching and research interests, and have three letters of recommendation sent to: **Chair, Biologist Search Committee, University of North Dakota, Grand Forks, ND 58202-9019.** Review of applications will begin on November 15, 1995 and continue until the position is filled. *The University of North Dakota is an Affirmative Action/Equal Opportunity Employer.*

NMR Spectroscopists. As part of a major commitment to the development of structural biology at the University of Pennsylvania, the Department of Biochemistry and Biophysics invites applications for tenure-track positions in NMR spectroscopy at the **ASSISTANT, ASSOCIATE AND FULL PROFESSOR** levels. Applicants should have demonstrated expertise and accomplishments in modern multidimensional NMR with a strong background in protein and/or nucleic acid structure, dynamics, and function. Please forward curriculum vitae and a statement of background and future scientific intentions, and have three letters of recommendation sent to: **Ruth Keris, Department of Biochemistry and Biophysics, 414 Anatomy-Chemistry Building, University of Pennsylvania School of Medicine, Philadelphia, PA 19104-6059.** *The University of Pennsylvania is an Affirmative Action/Equal Opportunity Employer. Applications from women and minorities are encouraged.*

POSITIONS OPEN

FACULTY POSITION IN MICROBIOLOGY
Southern Illinois University
at Carbondale

Applications are invited for a tenure-track position in the Department of Microbiology at the level of **ASSISTANT PROFESSOR** commencing August 16, 1996. In addition to establishing a strong research program, teaching microbiology to both graduate and undergraduate students is expected. Preference will be given to a microbiologist who works on the molecular biology/molecular genetics of pathogenic microorganisms or viruses; or the molecular biology/molecular genetics of host-pathogen interactions, including host responses to pathogens. The applicant must hold an earned doctorate in microbiology or a related field and must have postdoctoral research experience. The applicant must display evidence of research accomplishments in microbiology and the ability to establish an independently funded research program in microbiology. Salary, research facilities and start-up funds will be competitive. Applications will be accepted until December 1, 1995, or until the position is filled. Applicants should submit a letter of application, a brief proposed research plan, curriculum vitae, and arrange to have three confidential letters of recommendation sent to: **Dr. Douglas Fix, Chair, Microbiology Search Committee, Department of Microbiology, Southern Illinois University at Carbondale, Carbondale, IL 62901-6508.** *Southern Illinois University at Carbondale is an Equal Opportunity/Affirmative Action Employer.*

THE OHIO STATE UNIVERSITY
Faculty Positions in Molecular Neurobiology

Applications are invited for two tenure-track faculty positions at the **ASSISTANT, ASSOCIATE** or **FULL PROFESSOR** level. The successful candidates will join the seven current faculty in new laboratories at the Neurobiotechnology Center. The new faculty members will be expected to apply molecular biological approaches to address significant problems in neurobiology, with one position emphasizing the use of vertebrate model systems including zebrafish. A transgenic mouse facility and other excellent support facilities are available in the Neurobiotechnology Center. The Ohio State University has made a major commitment to establish an outstanding interdisciplinary program in molecular neurobiology, which is a focus area for further development under a Molecular Life Science initiative. Applicants should submit a curriculum vitae, statement of research plans, and arrange to have three letters of reference sent to: **Chair, Molecular Neurobiology Search Committee, Neurobiotechnology Center, The Ohio State University, 206 Rightmire Hall, 1060 Carmack Road, Columbus, OH 43210.** Deadline for receipt of applications is December 15, 1995. *The Ohio State University is an Equal Opportunity/Affirmative Action Employer. Women, minorities, Vietnam-era veterans, disabled veterans and individuals with disabilities are encouraged to apply.*

BETH ISRAEL HOSPITAL
HARVARD MEDICAL SCHOOL
DEPARTMENTS OF PATHOLOGY

The Harvard Department of Pathology at Beth Israel Hospital seeks well-qualified applicants (Ph.D., M.D./Ph.D. or M.D.) for one or possibly two **ASSISTANT** or **ASSOCIATE PROFESSOR** positions as part of an expansion of our basic research program in tumor biology into new laboratory space. At minimum, candidates should have completed three to five years of relevant postdoctoral experience and should have the capability of directing an independent research program in an academic setting in areas of tumor biology such as tumor stroma and its generation, angiogenesis, the tumor microvasculature, tumor invasion or metastasis. Candidates are expected to participate in the teaching activities of the department, i.e., medical students, residents, graduate students and postdoctoral fellows. Major areas of interest include angiogenesis and stroma generation, parenchymal-stromal interactions and VPF/VEGF and its receptors and wound healing. Applicants should send curriculum vitae, a statement of research interests, and three references to: **Harold F. Dvorak, M.D., Chief, Department of Pathology, Beth Israel Hospital, 330 Brookline Avenue, Boston, MA 02215.** *Beth Israel Hospital and Harvard Medical School are Equal Opportunity/Affirmative Action Employers. Women and minorities are encouraged to apply.*

POSITIONS OPEN

ENDOWED CHAIR

University of North Carolina at Greensboro (UNCG) announces a search for the Marie Foscue Rourk **PROFESSOR** of Chemistry, a new, endowed position. The position will be filled by a person with a strong chemistry background whose research interests are in any area of biological chemistry. We are looking for an individual who currently holds the rank of Associate Professor or Professor; the appointment will be made at the full professor level with tenure. The successful candidate will have a record of teaching, publication, and grant awards that merits appointment to the Marie Foscue Rourk Professorship. Teaching at both the undergraduate and graduate levels is expected. The Department of Chemistry at UNCG offers the B.A., B.S. (ACS certified), and the M.S. degrees. A B.S. degree program in biochemistry is being planned. The Professor is encouraged to collaborate with faculty in other departments, such as Biology, and in Ph.D.-granting areas, such as Foods and Nutrition. He or she will also be involved in hiring new faculty in the biochemistry area. Salary and support for research from the endowment are negotiable. Please sent curriculum vitae, a synopsis of current and planned research activities, and arrange for three letters of recommendation to be sent to: **Dr. M. F. Farona, Head, Search Committee, Department of Chemistry, UNC-Greensboro, Greensboro, NC 27412.** Applications must be received by December 1, 1995. *Equal Employment Opportunity/Affirmative Action: Women/Minorities/Veterans/Disabled.*

BIOLOGICAL SCIENCES
MESA STATE COLLEGE

Invites applications for an **ASSISTANT PROFESSOR**, tenure-track position available August 1996. Ph.D. in Biology required. Teaching assignment will include introductory and upper division courses, 12 credit hours per semester. Preference will be given to candidates with significant coursework and/or research in microbial ecology. Send curriculum vitae, statement of teaching and research interests, all college transcripts, and names of three references to: **Robert E. Kribel—Dean, School of Natural Sciences and Mathematics, Mesa State College, P. O. Box 2647, Grand Junction, CO 81502.** Deadline January 17, 1996. *Mesa State College is an Affirmative Action/Equal Opportunity Employer. Mesa State College is a drug-free workplace. All employees of the College must agree to abide by our drug free policy as a condition of employment.*

MOLECULAR MODELING
IMAGE RECONSTRUCTION
SOFTWARE SUPPORT

The University of Virginia ITC—Academic Computing Health Sciences (ACHS) Center invites applications for a Professional **FACULTY** position (non-tenure-track) to provide support for molecular modeling and three-dimensional imaging. Individuals with training at the M.S. or Ph.D. level in molecular modeling, x-ray crystallography, three-dimensional image reconstruction, or low-light fluorescence detection are encouraged to apply. The individual will collaborate with faculty on modeling and imaging projects, participate in graduate courses on protein structure and image analysis, and support molecular modeling and image acquisition/analysis software. Send a complete curriculum vitae, representative publications, and three letters of reference to: **Ross Wayland ITCACHS, Health Sciences Center Box 555, University of Virginia, Charlottesville, VA 22908. FAX: 804-982-4030; Email: rlw@virginia.EDU.** Review of applicaitons is ongoing; applications should be completed by November 15, 1995. *The University of Virginia is an Equal Opportunity/Affirmative Action Employer.*

ASSISTANT PROFESSOR OF BIOLOGY

TENURE-TRACK beginning August 20, 1996. Animal Physiology. Teaching includes animal and human physiology as well as participation in an introductory core course for majors. Must participate actively in undergraduate and Master's level research. Ph.D. required and postdoctoral experience desired. Screening of applicants will begin December 15, 1995. Send letter of application, résumé, transcripts, and three letters of recommendation to: **Dr. John DePinto, Department of Biology, Bradley University, Peoria, IL 61625.** *Equal Opportunity/Affirmative Action Employer.*

POSITIONS OPEN

Biochemist/Williams College—The Chemistry Department invites applications for a tenure-eligible position at the **ASSISTANT PROFESSOR** level for fall 1996. (Senior appointment possible in exceptional circumstances.) This will be an initial appointment for a three-year term with teaching assignments in biochemistry and introductory chemistry. A semester teaching load normally includes complete responsibility for one course and two laboratory sections, and supervision of student research projects. Candidates should have the Ph.D. or completed dissertation by September 1996 (postdoctoral experience is preferred) and a strong commitment to teaching at the undergraduate level and developing a productive research program. Williams College is a highly selective, coeducational liberal arts institution of approximately 230 faculty and 2000 undergraduates, located in northwestern Massachusetts. The Chemistry Department, with ten faculty members and 30 to 35 majors each year, is accredited by the ACS and has excellent facilities for teaching and research. A new 40-million dollar science complex will be completed in the year 2000. *The College is actively working to increase the ethnic and gender diversity of its science majors and seeks an individual who can help us meet these goals.* Send résumé, undergraduate and graduate transcripts, description of research projects for undergraduates, and three letters of recommendation to: **Professor John W. Thoman, Jr., Chair, Department of Chemistry, Williams College, Williamstown, MA 01267,** by November 30, 1995. *Williams is an Equal Opportunity/Affirmative Action Employer.*

Biology—Two tenure-track positions at the **ASSISTANT** or **ASSOCIATE PROFESSOR** level: Illinois College, a Phi Beta Kappa, church-related college in West Central Illinois, seeks candidates with broad interests in biology who have completed the Ph.D. and have a strong commitment to undergraduate teaching in a liberal arts college. Preference will be given to applicants who have experience in directing student research and advising pre-professional students. This growing department of biology currently has 100 majors.

One applicant should be prepared to teach courses in botany, an advanced field biology course in his or her area of specialization, and alternate teaching of the freshman introductory biology course. A small field station is located near the campus, and opportunities for field work with various governmental agencies are available.

One applicant should be prepared to teach cell/molecular biology, genetics, and an advanced course in his or her area of specialization.

Send application, curriculum vitae, transcripts, and the names, addresses and telephone numbers of three references to: **Dr. Elaine Chapman, Department of Biology, Illinois College, Jacksonville, IL 62650.** Screening of applications will begin November 1, 1995. *Illinois College is an Affirmative Action/Equal Opportunity Employer.*

ASSISTANT/ASSOCIATE PROFESSOR

The University of Illinois College of Medicine at Rockford seeks to add a tenure-track **ASSISTANT/ASSOCIATE PROFESSOR** of microbiology to its diversified Department of Biomedical Sciences. The specific research area is open, although it is expected to involve studies at the molecular level. Contribution to the virology section of a team-taught course in medical microbiology is expected. Submit curriculum vitae, a short statement of research interests, and the names, addresses and telephone numbers of three references to: **Dr. Fu-Li Yu, Professor and Head, Department of Biomedical Sciences, University of Illinois College of Medicine at Rockford, 1601 Parkview Avenue, Rockford, IL 61107.** Review of applications will begin December 1, 1995, and continue until the position is filled. *The University of Illinois is an Affirmative Action/Equal Opportunity Employer.*

The University of Iowa Department of Internal Medicine is seeking **FACULTY** for positions in a new program focusing on the cell and molecular biology of inflammation. Qualifications include Ph.D. degree. Expertise in the cell biology of phagocytes, endothelial cells, complement, and leukocyte-endothelial cell interacting and the ability to be an independent investigator with an established research program competitive for NIH and other external funding are desirable. Salary is based on the academic level of entry and on the applicant's qualifications and responsibilities. Candidates should submit curriculum vitae to: **Randall Jordison, Assistant to the Chairman, Department of Internal Medicine, SE309 GH, The University of Iowa, Iowa City, IA 52242.** *The University of Iowa is an Equal Opportunity and Affirmative Action Employer. Women and minorities are strongly encouraged to apply.*

POSITIONS OPEN

ASSISTANT PROFESSORS

The Department of Zoology and Physiology at Louisiana State University anticipates two tenure-track **ASSISTANT PROFESSOR** positions, "Pending Final Approval." The openings, starting August, 1996, are in any area of (1) Vertebrate Physiology, but with special consideration given to those who work in the areas of endocrinology or neurobiology using non-mammalian models, and (2) Cell Biology, but with special consideration given to those who use molecular techniques in conjunction with other approaches to study cytoskeletal regulation/molecular motors, signaling events or trafficking, protein targeting/ modification. Ph.D. or equivalent degree in a biological science and postdoctoral experience required. Successful applicants are expected to develop a strong, independent research program with extramural support and have a commitment to excellence in undergraduate and graduate instruction. Candidates should submit a statement of research interests and teaching philosophy, curriculum vitae, and the names of three references by December 5, 1995, or until the position is filled, to: **Chairman, Department of Zoology and Physiology, Louisiana State University, Baton Rouge, LA 70803-1725.** *LSU is an Equal Employment Opportunity/ Affirmative Action Employer.*

American University In Cairo (AUC). Applications are invited for one faculty opening at the **ASSISTANT, ASSOCIATE, or FULL PROFESSOR** level for a biologist to teach, in English, General Biology and a section of the core curriculum's required course in Scientific Thinking. Preference will be given to specialists in environmental biology and/or botany. Ph.D. required. AUC particularly seeks applicants with a demonstrated record or strong promise of excellence in teaching. Scholarly/research experience or potential is expected. Normal teaching load is nine hours per semester. Two-year appointment (renewable) begins September 1996. Rank, salary according to qualifications and experience. For expatriates, housing, roundtrip air travel, plus schooling for up to two children included. Write with curriculum vitae to: **Dr. Andrew Kerek, Provost, The American University in Cairo, 866 United Nations Plaza, Suite S-517, New York, NY 10017,** preferably before November 30, 1995. *AUC is an Equal Opportunity Employer.*

ASSISTANT PROFESSOR MOLECULAR BIOLOGY

The Department of Physiology in the School of Medicine, Southern Illinois University of Carbondale, anticipates, contingent upon availability of funds, a fiscal year, tenure-track faculty position in the general area of eukaryotic molecular biology starting August 16, 1996. This is a 12-month appointment with a competitive salary, excellent facilities, and substantial start-up funds. An earned doctorate degree is required, and postdoctoral experience indicating potential to conduct externally funded, independent research is preferred. The Department has an established graduate program, and active research interests in the areas of reproductive biology, neurobiology, and cell signaling. Applicants must be willing to participate in the teaching activities of the Department, which may include respiratory physiology to medical students, and training of undergraduate and graduate students in physiology. Additional departmental information can be obtained via the WWW address:**http://www.som.siu.edu.**

Deadline for applications is January 15, 1996, or until the position is filled. Applicants should send a cover letter including a brief statement of research and teaching interests, curriculum vitae, selected reprints, and three letters of reference to:

Dr. Andrzej Bartke
Molecular Biology Search Committee
Department of Physiology, School of Medicine
Southern Illinois University at Carbondale
Carbondale, IL 62901-6512

Southern Illinois University at Carbondale is an Equal Opportunity/Affirmative Action Employer.

POSTDOCTORAL POSITION available immediately to study recombination and regulation of gene expression in EBV-transformed mammalian B cells. Please send curriculum vitae, statement of research accomplishments and interests, and names of three references to: **Dr. Nancy Maizels, Department of Molecular Biophysics and Biochemistry, Yale University School of Medicine, 333 Cedar Street, New Haven, CT 06520-8024.**

UNIVERSITY OF TOLEDO
Tenure-Track Assistant Professorships in Biology

The Department of Biology at the University of Toledo has potential openings for two tenure-track **ASSISTANT PROFESSORSHIPS** beginning in the fall of 1996. The Department offers B.A., B.S., M.S., and Ph.D. degrees. A new life sciences research complex, plant sciences facility, and Lake Erie Research Center are under construction. Successful candidates will be expected to participate in both undergraduate and graduate instruction as well as develop an externally funded research program that complements existing departmental strengths. A Ph.D. and relevant postdoctoral experience are expected. Salary and set-up are competitive. Applications filed by November 30, 1995 will receive priority.

Position I will be filled with an Ecologist/Environmental Biologist. Candidates are sought whose research interests focus on the plant-soil interface, below ground terrestrial processes, or ecological modeling. Position II will be filled with a Cell/Molecular Biologist. Particular interest will be given to candidates who apply modern molecular techniques to the study of developmental systems. Interested candidates should send a letter of application, curriculum vitae, statement of teaching and research interests, and the names and addresses of at least three references to:

Chair, Search Committee
Department of Biology
University of Toledo
Toledo, OH 43606-3390

The University of Toledo is an Affirmative Action/Equal Opportunity Employer. Women and members of other under-represented groups are encouraged to apply.

ASSISTANT/ASSOCIATE PROFESSOR
Division of Rheumatology and Clinical Immunology

The Department of Medicine, University of Pittsburgh School of Medicine, invites applications for three tenure-track positions at the **ASSISTANT** or **ASSOCIATE PROFESSOR** level. Candidates must have an M.D., M.D./Ph.D., or Ph.D., postdoctoral research experience, and a well-developed plan for an independent basic or clinical research program. Applications are invited from individuals with training in the areas of molecular immunology, immunogenetics or related basic sciences with a strong interest in the basic mechanisms of autoimmunity and from individuals with training in clinical epidemiology or health services research. Applicants should submit curriculum vitae, a statement of research interests and plans, selected reprints, and a list of three references to: **Timothy M. Wright, M.D., Chief, Division of Rheumatology and Clinical Immunology, University of Pittsburgh School of Medicine, Suite 502, Kaufmann Building, Pittsburgh, PA 15213. Telephone: 412-692-4343.** *University of Pittsburgh is an Affirmative Action/Equal Opportunity Employer.*

MOLECULAR-CELLULAR BIOLOGIST

A **POSTDOCTORAL POSITION** to study cis- and trans-acting mechanisms and the role of DNA conformation in transcriptional regulation of growth factor (bFGF) and neurotransmitter (tyrosine hydroxylase) genes in adrenal medullary cells. Requires experience in DNA construction, mutagenesis, and DNA-protein binding assays. Send curriculum vitae, a summary of research experience, and references to: **Dr. Michal K. Stachowiak, Laboratory of Molecular Neurobiology, Barrow Neurological Institute, Mercy Health Care Arizona, 350 West Thomas Road, Phoenix, AZ 85013.** *Equal Opportunity Employer.*

PREDOCTORAL TRAINEESHIPS

The University of Montana's Organismal Biology and Ecology Graduate Program (OBE) has five **PREDOCTORAL TRAINEESHIPS** in Conservation and Environmental Biology for fall 1996 through the NSF-funded Training-WEB Project. Stipends are $14,100, plus tuition. *Trainees must be US citizens or permanent residents* and be admitted to the OBE Program. Contact: **The Training-WEB Secretary, Division of Biological Sciences, The University of Montana, Missoula, MT 59812. Telephone: 406-243-5222; Email: jmclark@selway.umt.edu.** *Women and members of minority groups are encouraged to apply. Equal Employer Opportunity/Affirmative Action.*

CHAIRPERSON, Department of Cell Biology, Neurobiology and Anatomy. The University of Cincinnati College of Medicine invites applications and nominations for the Francis Brunning Endowed Professorship and Department Chair. The department is composed of 22 full-time faculty with significant extramural grant support; has a long history of excellence in basic science research/medical education; and houses two large interdisciplinary graduate programs: cell biology and neuroscience.

We seek an individual with an internationally recognized research program, demonstrated leadership, and a strong commitment to biomedical education. Outstanding individuals with established and well-funded research in cellular neuroscience- or cell biology are encouraged to apply. Nominations/inquiries/applications (include curriculum vitae and three references) to: **John C. Winkelmann, M.D., Search Committee Chair, University of Cincinnati Medical Center, Department of Internal Medicine, Cincinnati, OH 45267-0508. Telephone: 513-558-2195. Email: John.Winkelmann@UC.EDU or FAX: 513-558-6703.** *Affirmative Action/Equal Opportunity Employer. Women, Minorities, Disabled, Veterans encouraged to apply.*

ASSISTANT PROFESSOR BIOCHEMISTRY
Oregon State University

The Department of Biochemistry and Biophysics announces a full-time, **TENURE-TRACK** position (nine-month). Qualifications include: outstanding quality of research as demonstrated by postgraduate and postdoctoral research productivity; desire to teach general biochemistry and related subjects. The appointee is expected to develop an active, extramurally supported research program. Research area open, but must be a biochemical area that complements and extends existing faculty interests. To apply, send a letter of interest; a curriculum vitae; a concise statement of research plans; two papers; names and addresses of three professional references; and have the three reference letters sent to: **Philip N. McFadden, Biochemistry and Biophysics, 2011 ALS, Oregon State University, Corvallis, OR 97331-7305.** Completed applications received by November 21, 1995 will be assured of consideration. *Oregon State University is an Affirmative Action/Equal Opportunity Employer, and is responsive to dual-career couples.*

DUKE UNIVERSITY DEVELOPMENTAL BIOLOGIST
Developmental, Cell, and Molecular Biology (DCMB) Group

We invite applications for a tenure-track position at the **ASSISTANT PROFESSOR** level from candidates investigating mechanisms of development in higher eukaryotes. The DCMB Group is a consortium of faculty with common interests in the Departments of Botany and Zoology. The appointment will be in the Department of Zoology. Please submit a curriculum vitae, names and addresses of three referees, description of current and future research interests, and a statement of teaching experience and interests to: **David R. McClay, Department of Zoology, Box 90325, Duke University, Durham, NC 27708-0325.** The committee will begin considering applications on November 15, 1995.

Duke University is an Affirmative Action/Equal Opportunity Employer.

LOUISIANA STATE UNIVERSITY
Department of Biochemistry
Postdoctoral Researcher

The Department of Biochemistry at Louisiana State University seeks applicants for the position of **POSTDOCTORAL RESEARCH ASSOCIATE** to conduct research in eleostearic acid synthesis in plants. Candidates must have a Ph.D. in Biochemistry or a related field. Experience in purification of enzymes and in DNA cloning and gene expression is required. Preference will be given to applicants with knowledge in fatty acids synthesis. Research will be conducted at the USDA's Southern Research Center in New Orleans, Louisiana. Send curriculum vitae, academic transcripts, and three letters of recommendation to:

Dr. Ding S. Shih
Postdoc Search
Room 322 Choppin Hall
Louisiana State University
Baton Rouge, LA 70803
Telephone: 504-388-5146; FAX: 504-388-5321

Application deadline: October 30, 1995

An Affirmative Action/Equal Opportunity Employer.

POSITIONS OPEN

IMMUNOLOGIST/MOLECULAR BIOLOGIST

Corixa Corporation is a new biotechnology company dedicated to the development of T cell vaccines and therapies for cancer and infectious diseases. Corixa is seeking Ph.D. **SCIENTISTS** in Immunology and Molecular Biology. Candidates should have two to three years of postdoctoral experience in molecular/cellular immunology pertinent to defining immunogenic human CTL epitopes or gene cloning. Successful candidates will share responsibility with other company scientists to discover T cell based vaccine candidates in the setting of oncology and infectious disease. Emphasis is on the use of recombinant DNA technology to modify human APC functions and the production of CTL, including discovery of antigen targets. Competitive salary and benefits, including equity options. Please send curriculum vitae, statement of research interests, and names of three references to: **Corixa Corporation, 1124 Columbia, Suite 464, Seattle, WA 98104. FAX: 206-667-5715.** *An Equal Opportunity Employer.*

RESEARCH POSITION

BIOLOGICAL SCIENCE/ENGINEERING Ph.D. Practical, applications-oriented, versatile, creative, self-directed, publications, excellent writer, strong microbiology and chemistry. All phases contract R&D from proposal writing to development of product. Independent and team work. Send résumé, publication list, salary requirement and names of three references to: **Human Resources, SymBiotech, Inc., 8 Fairfield Boulevard. Wallingford, CT 06490.**

SMITHSONIAN INSTITUTION FELLOWSHIP PROGRAM

GRADUATE STUDENT, PREDOCTORAL, POSTDOCTORAL, AND SENIOR FELLOWSHIPS in animal behavior, ecology, and environmental science, including an emphasis on the tropics; earth sciences and paleobiology; evolutionary and systematic biology; history of science and technology. Tenable in residence at the Smithsonian facilities. Stipends and tenure vary. Deadline: January 15 annually. Contact: **Office of Fellowships and Grants, 955 L'Enfant Plaza, Suite 7000, Desk S, Washington, DC 20560. Telephone: 202-287-3271.** *An Equal Opportunity Employer.*

CELLULAR AND MOLECULAR ENDOCRINOLOGY

A POSTDOCTORAL FELLOWSHIP and a **RESEARCH ASSISTANT PROFESSORSHIP** are available to study the mechanisms governing pituitary hormone secretion as they relate to the differentiation and transdifferentiation of growth hormone and prolactin producing cells. Both rodent and bovine model systems are utilized. We currently study these processes at the single, living cell level by employing a broad spectrum of molecular and cellular strategies that include (but are not limited to) combinations of the following techniques: reverse hemolytic plaque assays for quantifying hormone secretion, video imaging of cells transfected with luciferase-promoter constructs for assessing gene expression in real time, and microinjection (cytoplasmic and nuclear) for selectively introducing modulators of gene expression and hormone secretion. Postdoctoral experience and an extensive background in molecular biology are required for the more senior position. Salary and benefits are highly competitive and commensurate with experience. Send curriculum vitae and names and telephone numbers of three references to: **Dr. L. Stephen Frawley, Department of Cell Biology and Anatomy, Medical University of South Carolina, 171 Ashley Avenue, Charleston, SC 29425-2204. Telephone: 803-792-3526. FAX: 803-792-0664.** *Women and minorities are encouraged to apply. An Equal Opportunity/Affirmative Action Employer.*

POSTDOCTORAL POSITION (Ph.D. or M.D.) is immediately available to map and clone tumor suppressor gene(s) involved in brain tumors. Experience in molecular biology techniques is required. Salary and conditions are in accordance with national standards. Related work: *Nature Med.*, 1:686, 1995/*Cancer Res.*, 54:640, 1994; 54:2322, 1994; 54:2098, 1994; 55:2995, 1995. Please FAX curriculum vitae to: **Adrian Merlo and Rodney Scott, Brain Tumor Research/Cancer Genetics, Department of Research, University of Basel, CH-4031 Basel, Switzerland. FAX: +41-61-265-7138 or Email: Scott@ubaclu.unibas.ch.**

POSITIONS OPEN

DIRECTOR, Cytogenetics Laboratory: The Division of Human Genetics of the Children's Hospital Research Foundation (CHRF) seeks a ABMG Clinical Cytogeneticis certified or eligible M.D. or Ph.D. to direct its service and research activities. Responsibilities include amniotic cells, CVS, blood and tumor karyotype and FISH analyses, and development of research program. Academic rank determined by qualifications. Send curriculum vitae, bibliography and three letters of recommendation to: **Gregory A. Grabowski, M.D., Director, Division of Human Genetics, CHRF, 3333 Burnet Avenue, Cincinnati, OH 45229-3039.** *Children's Hospital Medical Center is an Affirmative Action/Equal Opportunity Institution. Women and minorities are encouraged to apply.*

POSTDOCTORAL POSITION

POSTDOCTORAL POSITION available immediately for a recent Ph.D. or M.D. who is interested in cell-cycle control, signal transduction and their relation to ionizing radiation and DNA damage. Strong molecular biology background with experience in yeast, biochemistry and/or cell biology are desired. Clinical Fellows interested in pursuing a career in biomedical research are encouraged to apply. Send curriculum vitae, career interest and letters of recommendation to: **Dr. Tim J. Yen, c/o Human Resources Department, Fox Chase Cancer Center, 7701 Burholme Avenue, Philadelphia, PA 19111.** *Equal Opportunity Employer.*

HARVARD MEDICAL SCHOOL HUMAN GENE THERAPY

Two **POSTDOCTORAL POSITIONS** to develop anti-tumor chimeric IgTCR-modified T cells for therapy. 1) Excellent molecular biology skills and/or retroviral vector experience. 2) Expertise in immunology and (optimally) mouse models; medical, veterinary or pathology background a plus. Send résumé, description of prior research, and names of at least two references by **FAX: 617-632-0998** to: **R. P. Junghans, Ph.D., M.D., Director, Biotherapeutics Development Lab.**

Outstanding **POSTDOCTORAL** opportunity to investigate the molecular mysteries of voltage-gated ion channels. Requires Ph.D. or M.D. and experience with molecular biological or electrophysiological techniques. Excellent research and living environment. Applicants should send curriculum vitae, description of previous research experiences, and names of three references to: **Dr. Brett Adams, Department of Physiology and Biophysics, The University of Iowa, Iowa City, IA 52242-1109. FAX: 319-335-7330; Email: Brett-Adams@Uiowa.edu.** *The University of Iowa is an Equal Opportunity/Affirmative Action Employer. Women and Minorities are strongly encouraged to apply.*

POSTDOCTORAL POSITION available immediately to work in NIH-funded project on cloning and expression of *hem* genes. Requires a relatively recent Ph.D. with two years of molecular biological experience. Background in genetics and/or heme-biochemistry preferred. Interested individuals should submit a résumé, publications, certified transcripts and licenses, and have at least two letters of recommendation sent to: **Dr. Debabrata Majumdar, Department of Biology, Norfolk State University, Norfolk, VA 23504, U.S.A. Telephone: 804-683-2543, FAX: 804-683-8817.**

POSTDOCTORAL POSITIONS MOLECULAR BIOLOGY OF HIV

Positions are available immediately to study determinants of HIV infectivity and analyze HIV accessory gene product. A background in biochemistry and molecular biology is desirable. Send curriculum vitae and names of three references to: **Mario Stevenson, Ph.D., Program in Molecular Medicine, University of Massachusetts Medical Center, 373 Plantation Street, Worcester, MA 01605.** *An Equal Opportunity/Affirmative Action Employer.*

RESEARCH ASSOCIATE position available in a program focused on immunology of human melanoma with emphasis on immunotherapy. Background in molecular immunology required to participate in a program to analyze HLA antigen expression by melanoma cells, to develop new types of immunogenes for immunotherapy and/or analyze patient's immune response. Send curriculum vitae, names of three references to: **Dr. S. Ferrone, Department of Microbiology and Immunology, New York Medical College, Valhalla, NY 10595.**

Northwestern University

Department of Neurobiology and Physiology

Two tenure-track faculty positions are available in the area of

Molecular and Cellular Neurobiology

The Department expects to hire one new faculty member with interests in the area of molecular or cellular neuroendocrinology or neuropharmacology. For the second position, candidates working in molecular or cellular neurobiology, including (but not restricted to) the areas of signal transduction, development, plasticity and learning, will be considered. These positions are expected to be filled at the junior level, but outstanding senior candidates will also be considered. Faculty are expected to maintain a strong independent research program, and to participate in graduate and undergraduate teaching. Northwestern University's main campus is located in an attractive setting along the shores of Lake Michigan. *Women and members of minority groups are especially encouraged to apply. Northwestern University is an AA/EOE employer.* Applicants should send a curriculum vitae and statement of research interests by December 1 and have at least three letters of reference sent to the address below. Applicants should specify for which position they are applying.

David Ferster, Ph.D., Jon Levine, Ph.D.
Search Committee
Department of Neurobiology and Physiology
Northwestern University
2153 North Campus Drive
Evanston, IL 60208

THE CENTER FOR ENVIRONMENTAL RESEARCH AND CONSERVATION
COLUMBIA UNIVERSITY IN THE CITY OF NEW YORK

The Center for Environmental Research and Conservation (CERC)–a consortium of Columbia University, The American Museum of Natural History (AMNH), The New York Botanical Garden (NYBG), Wildlife Preservation Trust International, and The Wildlife Conservation Society–announces the establishment of the following four new faculty positions. CERC is a multidisciplinary center aimed at promoting education, training, and research in biodiversity conservation by integrating the knowledge and methods of both the biological and social sciences. Appointments will be joint with a relevant department at Columbia and will be five-year positions at the **ASSISTANT PROFESSOR** level. Each candidate is expected to teach at least one core course in the undergraduate (Environmental Biology) or graduate (Ecology and Evolutionary Biology) curriculum of CERC as well as seminars in his/her area of expertise as it relates to conservation and biodiversity studies. Each candidate is also expected to maintain a vigorous research program supported by extramural funding. A willingness to develop integrative and multidisciplinary research and teaching is essential. Opportunities for field research exist in CERC affiliate institutions in Asia, South America, Biosphere 2, and other locations worldwide. For terms beginning with the academic year 1996-97, applications are invited in the following fields:

Community Ecologist: A community ecologist is sought with research and teaching activities focused on nutrient cycling, plant/animal interactions, and/or restoration biology within terrestrial ecosystems. Ability to teach advanced ecology, community ecology, biometry, and related courses desirable. The candidate for this position will work in close collaboration with researchers at Columbia's Lamont-Doherty Earth Observatory and Biosphere 2.

Plant Systematist: A botanist/mycologist with a strong taxonomic publication record is sought to conduct research and teach plant and fungal systematics. Candidates should be familiar with higher level taxa systematics questions, a variety of phylogenetic methods, as well as holding expertise in a specialized group. This position will be affiliated with NYBG.

Animal Systematist: A zoologist with a strong taxonomic publication record is sought to conduct research and teach invertebrate and vertebrate systematics. Candidates should be familiar with higher level taxa systematics questions, a variety of phylogenetic methods, as well as holding expertise in a specialized group. This position will be affiliated with AMNH.

Population Biologist: A population biologist is sought to teach conservation biology, population biology, biometry, and related courses. Specialization in small metapopulation dynamics, demographic or genetic dynamics, and their policy implications would be particularly desired.

Applications, including a curriculum vitae, a statement of research and teaching interests, and three letters of recommendation, will be accepted until December 1, 1995, or until suitable candidates are found. Send to: Dr. Don J. Melnick, Director, Center for Environmental Research and Conservation, Columbia University, Low Library, 535 West 166th Street Room 405, New York, NY 10027. http://www.columbia.edu/cu/cerc/

Columbia University is an Equal Opportunity/Affirmative Action Employer and strongly encourages applications from women and minorities.

FACULTY POSITION, U.C.L.A. PLANT MOLECULAR BIOLOGY

The newly formed Department of Molecular, Cell and Developmental Biology, would like to add to existing strength in Plant Molecular Biology by hiring two individuals with proven research and teaching accomplishment in the area of Plant Cell, Molecular or Developmental Biology. One appointment will be at a relatively junior level (starting Assistant through mid-Associate Professor level). The second appointment would be made in connection with our search for a Chair of the Department of Molecular, Cell and Developmental Biology. Successful candidates' research programs will be expected to use molecular and genetic techniques to address questions of fundamental importance for plant cell and developmental biology. The candidates will participate in teaching undergraduates in an integrated life sciences curriculum at both the lower and upper division levels. Applicants should send their c.v., a concise research statement indicating future plans as well as the current program, and a brief statement of teaching interests and experience to: Plant Molecular Biology Search Committee the Department of Molecular, Cell and Developmental Biology, Box 951606, U.C.L.A., Los Angeles, CA 90095-1606. Candidates for a junior position should have three letters of recommendation sent to the same address. Candidates for the senior position should include names of three potential references. The committee will start considering candidates by October 20, 1995. U.C.L.A. is an affirmative action/equal opportunity employer. *Women, minorities, and persons with disabilities are encouraged to apply.*

Junior and Senior Faculty Positions in Biochemistry

THE DEPARTMENT OF CHEMISTRY & BIOCHEMISTRY of the University of Maryland at College Park seeks to fill two positions, one at the Assistant Professor (Tenure Track) level, and one at a Senior level. The Senior position will be in the Division of Biochemistry, which is in the process of growing substantially from its current faculty; most of whom are young with active programs in enzymology, DNA recombination, catalytic RNA, antimicrobial peptides, DNA-protein interactions, atomic force microscopy, and membrane function. Candidates should be in an area that broadens this range of programs, and have an exceptional record of research accomplishment as well as being at a stage of expanding productivity. Although a senior candidate is preferred, junior candidates will also be considered.

The Asst. Prof. position will be joint with the **CENTER FOR AGRICULTURAL BIOTECHNOLOGY (CAB)**, with laboratory space, tenure, and teaching duties in Biochemistry. CAB is a component of the U of MD Biotechnology Institute and is a multidisciplinary research center emphasizing plant-microbe interactions, insect molecular genetics, vaccine development, protein modification, and biochemical engineering. It will soon occupy a newly constructed and equipped research building on the U of MD College Park campus. Candidates for this joint position should be in an area that is clearly compatible with contemporary biotechnology, with interests in protein structure and/or function being particularly desirable. They must also demonstrate exceptional promise of being able to establish and maintain a funded research program. Candidates for both positions should expect to attract graduate students from the Molecular and Cellular Biology program as well as the Biochemistry program. To apply, send resume (including a description of research plans) and arrange for 3 letters of reference to be sent to: **Prof. J. Norman Hansen, Chair; Biochemistry Search Committee, Dept. Chem & Biochem, UMCP, College Park, MD 20742.** For best consideration, application should be complete by December 1, 1995. *The University of Maryland at College Park is an Equal Opportunity/Affirmative Action Employer. Women and minorities are encouraged to apply.*

FACULTY POSITION IN MOLECULAR & CELL BIOLOGY

The Center for Advanced Biotechnology and Medicine (CABM) and the Department of Pharmacology at UMDNJ-Robert Wood Johnson Medical School are seeking applicants for a tenure-track faculty position. Applicants should have a strong record of publication in molecular and cell biology. The successful candidate will occupy new laboratory space in the CABM building and join a growing, interactive, and highly productive life-sciences community on the Busch Campus, where there are many opportunities for research collaboration and participation in several graduate programs. The position is highly competitive with regard to start-up funds, laboratory space, salary and benefits. Please send a CV, publications, and a summary of research activities and plans, along with names and addresses of 3 references to: **Drs. Aaron J. Shatkin and Leroy F. Liu, 679 Hoes Lane, Piscataway, NJ 08854-5638.** UMDNJ-Robert Wood Johnson Medical School is an Affirmative Action/Equal Opportunity Employer, M/F/D/V, and a member of the University Health System of New Jersey.

POSITIONS OPEN

UNIVERSITY OF MICHIGAN

A **POSTDOCTORAL POSITION** is available immediately in an exciting research environment to investigate signal transduction in the context of autoimmunity. Experience in cellular and molecular immunology is required.

Send curriculum vitae and names of three references to: **Dr. Joseph Holoshitz, Director, University of Michigan Specialized Center of Research in Rheumatoid Arthritis, 200 Zina Pitcher Place, Kresge I R4550, Ann Arbor, MI 48109-0531. FAX: 313-763-8974; Email: jholo@umich.edu.**

POSTDOCTORAL POSITION immediately available to study the Physical Biochemistry of protein nucleic-acid interactions, helicases, and SSB proteins. Experience in fluorescence spectroscopy preferred. Send current curriculum vitae and three reference letters to: **Dr. W. M. Bujalowski, Department of Human Biological Chemistry & Genetics, The University of Texas Medical Branch at Galveston, Galveston, TX 77555-1053.** *Equal Opportunity Employer/Minorities/Female/Disabled/Veteran. UTMB hires only individuals authorized to work in the US.*

DEPARTMENT OF BIOCHEMISTRY
UNIVERSITY OF UTAH

A **POSTDOCTORAL FELLOWSHIP** is available to participate in structural studies of the interaction of histone H1 with chromatin. The ideal candidate will be one who has a strong background in biochemistry or molecular biology, but who is also open to learning physical techniques including x-ray crystallography. The various departments involved in the life sciences provide a thriving scientific environment with good opportunities for interactions. Salt Lake City is a cosmopolitan city surrounded by beautiful areas for outdoor activities. Please contact: **V. Ramakrishnan, Department of Biochemistry, University of Utah School of Medicine, 50 North Medical Drive, Salt Lake City, UT 84132. Telephone: 801-585-6001. Email: V.Ramakrishnan@m.cc.utah.edu.** *The University of Utah is an Affirmative Action/Equal Employment Opportunity Employer.*

POSTDOCTORAL POSITION in cellular/molecular neurobiology available for individual interested in using state of the art electrophysiological and molecular biological techniques to study the roles of excitatory amino acids and second messenger/protein kinase systems in modulation of synaptic transmission and neuronal function in mammalian brain. A strong background in cellular and/or molecular neurobiology is preferred. Send curriculum vitae, three references, and statement of research interests to: **Dr. P. Jeffrey Conn, Department of Pharmacology, Emory University School of Medicine, Atlanta, GA 30322.** *Emory University is an Equal Opportunity/Affirmative Action Employer.*

POSTDOCTORAL POSITION in neuropharmacology available immediately to study the role of nitric oxide in neuroinflammatory diseases. A background in biochemical, cellular or molecular pharmacology is preferred. Salary and benefits commensurate with NIH guidelines. Send letter, curriculum vitae, and names of three references to: **Dr. K. M. K. Boje, Department of Pharmaceutics, H517 Cooke, School of Pharmacy, University of Buffalo, Buffalo, NY 14260.** *An Affirmative Action/Equal Opportunity Employer.*

POSTDOCTORAL POSITION available immediately to study *Pneumocystis carinii* lipid biochemistry and metabolism. Biochemistry, parasitology or microbiology, and lab animal experience desired. Please send curriculum vitae, and the names and telephone numbers of three references to: **Dr. Edna S. Kaneshiro, Department of Biological Sciences, University of Cincinnati, Cincinnati, OH 45221. FAX 513-556-5280.** *An Affirmative Action/Equal Opportunity Employer.*

POSTDOCTORAL POSITIONS, Harvard Medical School: Fully funded positions are currently available in two project areas: to study the regulation, role, and function of new tyrosine kinase and phosphatase genes in hematopoiesis; and human retorvirology with particular focus on gene therapy for HIV. Ph.D. and/or M.D. with a background in cell biology/hematopoiesis/molecular biology/virology preferred. Please submit curriculum vitae and three references to: **Jerome E. Groopman, M.D., Division of Hematology/Oncology, Harvard Medical School, New England Deaconess Hospital, One Deaconess Road, Boston, MA 02215. FAX: 617-424-6237.**

POSITIONS OPEN

POSTDOCTORAL POSITIONS
Transcription Initiation and Activation

Available immediately to study prokaryotic transcription (*E. coli* RNA polymerase and activators) or eukaryotic transcription (yeast and human RNA polymerase II; human general transcription factors). Prior experience in transcription desirable. Prior experience in at least two of the following required: site-directed mutagenesis, protein purification, protein chemistry, analysis of protein-nucleic acid interaction, and analysis of protein-protein interaction. Send curriculum vitae, summary of research experience, and names and addresses of three references to: **Richard H. Ebright, Waksman Institute, Rutgers University, New Brunswick, NJ 08855. FAX: 908-445-5735.**

TWO POSTDOCTORAL RESEARCH FELLOWSHIPS

MOLECULAR BIOLOGIST—the research will focus on the molecular biology of Alzheimer's disease and other disorders related to aging. Work will involve genetic studies of Alzheimer's disease, gene cloning, gene expression, functional studies, and transgenic mouse technology. Applicants should have a strong background in molecular biology, biochemistry, or molecular genetics. Interested individuals should send curriculum vitae and three letters of recommendation to: **Gerard D. Schellenberg, Geriatric Research Education and Clinical Center, Seattle Veterans Affairs Medical Center, 1660 South Columbian Way, Seattle, WA 98108.** *Affirmative Action, Equal Opportunity Employer.*

POSTDOCTORAL POSITION to study role of the winged helix transcription factors (hepatocyte nuclear factor 3 and homologs) in cell-specific gene expression via transgenic mouse models and examine their embryonic expression patterns (see *Dev. Biol.* 166:195, 1994; *Mol. Cell. Biol.* 15:1364, 1995; *Cell Growth & Differen.* 6:879, 1995). Preference will be given to applicants with knowledge of developmental biology and use of transgenic mouse technology. Please send curriculum vitae, names and telephone numbers of three references to: **Dr. Robert Costa, University of Illinois at Chicago, College of Medicine, Department of Biochemistry (M/C 536), 1819 West Polk Street, Chicago, IL 60612-7334. FAX: 312-413-0364.** *University of Illinois at Chicago is an Affirmative Action/Equal Opportunity Employer.*

COLLEGE OF AGRICULTURAL SCIENCES
PENN STATE

One-year **POSTDOCTORAL POSITION** available immediately to produce and characterize transgenic potato plants containing the antisense construct for an O_3-induced ACC synthase gene identified in our laboratory. Experience in plant transformation and regeneration is required. Send résumé and the names of three references to: **Dr. Eve J. Pell, Penn State University, Department of Plant Pathology, 210 Buckhout Laboratory, University Park, PA 16802; FAX: 814-863-7217 or Email: EJP@PSU.EDU.** *An Affirmative Action/Equal Opportunity Employer. Women and minorities encouraged to apply.*

POSTDOCTORAL POSITIONS

Immediate openings are available to conduct basic studies on the molecular mechanisms and organelle-specific signals in the regulation of terpenoid and sterol production in animals. The candidates, with Ph.D. or M.D. degrees, should have strong background in molecular/cell biology as well as biochemistry. Send curriculum vitae and names of three references to: **Dr. Ishaiahu Shechter, Uniformed Services University of the Health Sciences (USUHS), Department of Biochemistry, 4301 Jones Bridge Road, Bethesda, MD 20814-4799. Telephone: 301-295-3550.** *Equal Opportunity Employer/Affirmative Action.* Application deadline 30 November 1995.

POSTDOCTORAL POSITION available to study human cytomegalovirus glycoproteins that function in tissue tropism and pathogenesis in polarized epithelial cells and neurons. Previous research experience in molecular and cellular biology desirable. Interested candidates should submit curriculum vitae and names of three references to: **Dr. Lenore Pereira, University of California San Francisco, HSW-604, San Francisco, CA 94143-0512.** *An Equal Opportunity/Affirmative Action Employer.*

POSITIONS OPEN

POSTDOCTORAL POSITIONS
ARKANSAS CANCER RESEARCH CENTER

POSTDOCTORAL POSITIONS are available as part of a multidisciplinary program in B cell neoplasia at the University of Arkansas for Medical Sciences. Specific areas include identification of genes associated with cell-mediated cytolysis for gene and immunotherapy, and regulation of tumor growth and apoptosis by cytokines and oncogenes. Ph.D.s and/or M.D.s with experience in molecular biology, cell biology and/or immunology are encouraged to apply. Send curriculum vitae and names of three references to: **Dr. Jacki Kornbluth, Division of Hematology/Oncology, University of Arkansas for Medical Sciences, 4301 West Markham–Slot 508, Little Rock, AR 72205. FAX: 501-686-8165; Email: jkornbluth@acrc.uams.edu.** *Affirmative Action/Equal Opportunity Employer.*

SENIOR LABORATORY TECHNICIAN

The Department of Biochemistry at the Uniformed Services University of the Health Sciences (USUHS) is seeking to hire a Biological Science Laboratory Technician (Biochemistry). The duties as Senior Laboratory Supervisor will be to perform research in the field of lipid metabolism and atherosclerosis; help in training students, technicians and other staff; and maintain laboratory equipment and inventory. The candidate, with an academic degree in Biological Sciences (preferably Molecular and/or Cell Biology), needs good oral and written communications skills, knowledge of a variety of biochemical and molecular biology laboratory techniques, knowledge of procedures for handling radioactive and biohazardous materials, and ability to plan and execute experimental protocols. Salary range thirties to mid forties. Excellent benefits. Send curriculum vitae, (Preferred) or Optional Form 612, or Standard Form 171, along with the names of three references to: **Dr. Ishaiahu Shechter, Uniformed Services University of the Health Sciences (USUHS), Department of Biochemistry, (95-128) 4301 Jones Bridge Road, Bethesda, MD 20814-4799. Telephone: 301-295-3550.** *Equal Opportunity Employer/Affirmative Action.* Applications must be postmarked by 30 November 1995. *U.S. citizenship required.*

FUNDS DEVELOPMENT OFFICER

The Uniformed Services University of the Health Sciences (USUHS) is seeking to hire a **FUNDS DEVELOPMENT OFFICER.** The candidate will head an office of information resources for both extramural and intramural research funding. Candidates are required to have knowledge of grants and funding processes and medical/scientific terminology. Incumbent should have proficient oral and written communication skills as well as presentation ability. Salary range low forties to mid fifties. Excellent fringe benefits. Applicants must request a copy of job announcement (95-129). **Telephone: 301-295-3550.** Application deadline 30 November 1995. *Equal Opportunity Employer/Affirmative Action. U.S. citizenship required.*

RESEARCH ASSOCIATE. Research in the identification of insulin-sensitive genes in newborn mammals. Must use euglycemic hyper-insulinemic clamp model to investigate insulin-sensitive genes. Must be familiar with arterial catheterization and physiologic adjustment of blood glucose levels of new born mammals during hypoglycemia. Prepare tissues for extraction of metabolites, enzymes and messenger RNA. Screen genomic libraries to identify species specific insulin responsible genes and perform Northern blots. Direct neonatology metabolic laboratory—responsible for day-to-day and long-term planning of all research projects, supervise newborn animal research, radiation experiments, micro-method assays and molecular biology experiments. Ph.D. in natural science required and two years of experience in molecular biology with a focus in insulin resistance/sensitivity. Research/experience must include euglycemic hyper-insulinemic clamp model, catheterization and physiologic adjustment of blood glucose levels, extraction of metabolites, enzymes and messenger RNA, screening of genomic libraries, Northern blots. $47,500 per year, 40 plus hours per week. *Applicants must have unrestricted authority to work for any U.S. employer.* Send two copies of résumé and evidence of research experience, citing Number 940171 to: **Travis Bartel, Alien Labor Unit, 201 East Washington Avenue, Madison, WI 53702.**

DEAN - SCHOOL OF VETERINARY MEDICINE

University of California, Davis

The University of California, Davis, invites applications and nominations for the position of Dean of the School of Veterinary Medicine and Director of the Division of Agriculture and Natural Resources Programs (Veterinary Medicine).

The Dean is the chief academic and administrative officer of the School responsible for leadership of the School in the areas of teaching, research, and professional service; developing and managing resources; representing the School to the campus and University administration; and interacting with the veterinary community and governmental leaders at local, state and national levels.

Qualifications include a D.V.M. or equivalent degree, a distinguished record of teaching and research, and demonstrated leadership and administrative abilities. We seek candidates who have a deep commitment to academic excellence; who understand the challenges posed by changes in the national veterinary environment; and who will be able to lead the School in its continuing development and in fulfilling its mission as part of a major land-grant university.

Salary will be commensurate with experience and qualifications. The starting date will be September 1, 1996, or as negotiated.

Applications and nominations should be received by December 1 to ensure full consideration. The position will remain open until filled. Applications, including a cover letter, curriculum vitae, and the names, addresses, and telephone numbers of five references, should be sent to:

Chancellor Larry N. Vanderhoef
Office of the Chancellor
University of California
Davis, CA 95616-8558

An Equal Opportunity--Affirmative Action Employer

RESEARCH ROUNDTABLE

DIRECTOR

The National Research Council (NRC), the principal operating arm of the National Academy of Sciences, the National Academy of Engineering, and the Institute of Medicine, a non-profit, non-governmental organization located in Washington, D.C., invites applicants for the position of Director of the Government-University-Industry Research Roundtable (GUIRR). GUIRR is one of the major units of the NRC. GUIRR comprises senior officials in the federal government, universities, and industry, and its staff is part of the NRC. The incumbent plans and oversees a broad range of programs related to policy and other issues relating to the nation's research emphasizing key issues of common interest to government, universities, and industry.

The GUIRR Director, working with the Chair and members of the Roundtable and its Executive Committee, will develop an agenda for the late 1990's and beyond. The incumbent is responsible for all scientific, financial, and administrative operations of the unit, in coordination with cognizant GUIRR project chairs, and subject to staff coordination by the Director of the NRC Policy Division and the Executive Officer of the NRC.

Applicants should have the following qualifications: Ph.D. degree or equivalent, preferably with an emphasis directly related to science policy and/or public policy, ten or more years experience related to GUIRR's field of interest; demonstrated administrative/supervisory experience, preferably in a volunteer organization; demonstrated capacity to conceive, design, and execute policy studies; demonstrated writing, analytic, and oral communication skills; ability to interact effectively with senior leaders in government, academia, and industry. Highly desirable traits include demonstrated familiarity with U.S. institutions of higher learning and their policies and workings; demonstrated familiarity with academic and non-academic research, and first-hand familiarity with the corporate sector, especially with respect to corporate support for and utilization of research.

Please send resume in confidence to: **NRC, GUIRR/ED, NAS 242(SC), 2101 Constitution Avenue, NW, Washington, DC 20418.** All resumes must be received by **October 20, 1995.** EOE

NAS NAE IOM NRC

BATES COLLEGE
LEWISTON, MAINE 04240
Program in Environmental Studies

Announcement of Position

Bates College invites applications for a tenure track position in Environmental Studies at the level of assistant professor, beginning September 1996.

Candidates must have a Ph.D. or appropriate terminal degree in Environmental Studies or a closely related field, with demonstrated interdisciplinary teaching and research interests in environmental studies. A strong commitment to undergraduate education and a research program involving undergraduate students are expected. Bates College is inaugurating a new interdisciplinary program and major in Environmental Studies during the 1996-97 academic year; the new faculty member will play a leading role in the development of the major.

Applicants should submit a cover letter along with a 1 or 2 page statement of research objectives and teaching interests, curriculum vitae including publications, academic transcripts, and the names, addresses, e-mail, and fax numbers of three references. All material should be sent to:

Environmental Studies Search
c/o Secretarial Services
2 Andrews Road, 7 Lane Hall
Bates College
Lewiston, Maine 04240
DEADLINE: December 1, 1995

BATES COLLEGE VALUES A DIVERSE COLLEGE COMMUNITY AND SEEKS TO ASSURE OPPORTUNITY THROUGH A CONTINUING AND EFFECTIVE AFFIRMATIVE ACTION PROGRAM. WE WELCOME APPLICATIONS FROM WOMEN AND MINORITIES.

POSITIONS OPEN

DUKE UNIVERSITY
CELL/MOLECULAR BIOLOGY

POSTDOCTORAL POSITION: Investigate the gene regulation of antioxidants and proinflammatory cytokines in models of lung injury and repair. Approaches include quantitative RT-PCR, differential display, and gene transfection. Please submit a curriculum vitae with references to: **Rodney Folz, M.D., Ph.D., Duke University Medical Center, Box 3177, Durham, NC 27710. Telephone: 919-684-2513; FAX: 919-684-3067.** *Equal Opportunity Employer.*

POSTDOCTORAL POSITIONS available to study genes that determine the yeast replicative life span, their human homologs and age-responsive promoter elements (*Genetica*, 91:35, 1993; *J. Biol. Chem.*, 269:15451, 1994; *J. Biol. Chem.*, 269:18638, 1994). Experience in molecular techniques essential and in yeast genetics helpful. Send curriculum vitae with bibliography and names, telephone and fax numbers of three references to: **Dr. S. Michal Jazwinski, Department of Biochemistry and Molecular Biology, Louisiana State University Medical Center, 1901 Perdido Street, New Orleans, LA 70112.** *Affirmative Action/Equal Opportunity Employer.*

POSTDOCTORAL POSITION to study inhibitors of cellular adhesion molecule expression and effects upon inducing an inflammatory response. Previous experience with mammalian cell culture, animal handling, and the isolation of murine endothelial cells desired. Send curriculum vitae, a statement of experience, and the names, addresses, and telephone numbers of three references to: **Dr. Glenn Hoke, Dyad Pharmaceutical, 9110 Red Branch Road, Suite K, Columbia, MD 21045. FAX: 410-715-9195.**

POSTDOCTORAL FELLOWSHIP
University of Hawaii
Department of Zoology

Opening available immediately for a **POSTDOCTORAL FELLOW** to work as part of a research team investigating the comparative physiology and molecular biology of invertebrate transport proteins. Position involves application of molecular biological techniques to elucidate gene sequences of plasma membrane transport proteins occuring in specific invertebrate epithelial cells. Qualifications: Ph.D. in the Biological Sciences with demonstrated expertise in molecular biology and an ability to work independently and communicate well. Submit résumé, including list of publications and education, and names and addresses of at least three references to: **Professor Gregory A. Ahearn, Department of Zoology, University of Hawaii, Honolulu, HI 96822.** Deadline for applications: 15 November 1995.

FELLOWSHIP IN
EXPERIMENTAL NEURO-ONCOLOGY

Two one to two year **FELLOWSHIPS** in Experimental Neuro-Oncology are offered for qualified M.D., Ph.D., and M.D./Ph.D. applicants interested in a research career in Neuro-Oncology. Individuals will work with and in the laboratory of a specific scientist within the Neuro-Oncology Program of the Mayo Comprehensive Cancer Center, Rochester, Minnesota. The areas of potential investigation include, but are not limited to, signal transduction, molecular genetics, developmental pharmacology, and experimental epidemiology. Interested individuals should send copies of their curriculum vitae and bibliography and two letters of reference to: **B. P. O'Neill, M.D., Department of Neurology, Mayo Clinic, 200 First Street SW, Rochester, MN 55905.** *Mayo Foundation is an Affirmative Action and Equal Opportunity Educator and Employer.*

POSTDOCTORAL FELLOW

A **POSTDOCTORAL POSITION** is available immediately to study the molecular biology of the NF-kB/Rel signaling pathway in T cell activation. Experience in protein biochemistry and molecular immunology desired. Send curriculum vitae and three letters of recommendation to: **Dean W. Ballard, Ph.D., Department of Microbiology and Immunology, Vanderbilt University School of Medicine, 815 Light Hall, Nashville, TN 37232-0295.**

Vanderbilt University is an Equal Opportunity/Affirmative Action Employer.

POSITIONS OPEN

A position is available immediately for an imaginative and ambitious **POSTDOCTORAL** to work on a project involving AFM and Electron Microscopy of cell junctions, in particular the formation of gap junctions. The successful candidate will have a recent Ph.D. in Molecular/Cell Biology or Physical Sciences and will be interested in developing skills in Microscopy and Cell Biology. The laboratory is well equipped and the environment provides many opportunities for growth. The starting salary is $24,000 plus benefits. Send curriculum vitae and names of references to: **Prof. Jean-Paul Revel, Division of Biology 156-29, Caltech, Pasadena, CA 91125. Email: revelj@romeo.caltech.edu; FAX: 818-795-0609.** *Caltech is an Equal Opportunity/Affirmative Action Employer. Women, minorities, veterans and disabled persons are encouraged to apply.*

Laboratory for Biomaterials Research/Department of Chemistry at Rutgers University has openings for **POSTDOCTORAL ASSOCIATES** with expertise in synthesis, polymer science, or tissue engineering. Starting salary: $30,000 plus excellent benefits. Outstanding prior research accomplishments and proficiency in English required. Send résumé, current U.S. visa status, and names of three references to: **Wright-Rieman Laboratories, P.O. Box 939, Piscataway, NJ 08855-0939.** *Equal Opportunity Employer.*

POSTDOCTORAL POSITIONS
Molecular Regulation of Hepatic Gene Expression

Two **POSTDOCTORAL POSITIONS** are available to study molecular mechanisms mediating effects of insulin on hepatic gene expression. One postdoctoral investigator will characterize novel DNA/protein complexes and DNA/protein interactions by methylation interference, affinity labeling, and Southwestern blotting/cloning. Another investigator will examine the role of signaling pathways in mediating insulin effects via defined response sequences, using kinase assays and transfection models. Send curriculum vitae and names and telephone numbers of three references to: **Dr. Terry Unterman, Endocrine Section (M/C 640), Department of Medicine, University of Illinois College of Medicine at Chicago, 840 South Wood Street, Chicago, IL 60612. FAX: 312-455-5877.**

RESEARCH ASSOCIATE position available immediately to study the molecular/biochemical mechanisms of regulated cell growth differentiation in myeloid cells and therapeutic drug carriers tumor cells. Candidates with a background in molecular biology biochemistry, interested in pursuing a career in the area of cancer biology in a translational research oriented laboratory, should send a résumé, names and addresses of three references to: **Dr. Gabriel Lopez-Berestein, Department of Bioimmunotherapy-Box 60, University of Texas M. D. Anderson Cancer Center, Houston, TX 77030, U.S.A. FAX: 713-796-1731.** *The University of Texas M. D. Anderson Cancer Center is an Equal Opportunity Employer and a smoke free workplace. This program encourages application from women and minorities.*

POSTDOCTORAL RESEARCH ASSOCIATE position is available for NIH-funded research for a recent Ph.D. graduate to study the role of insulin like growth factor signaling on growth and differentiation pathways in malignant myogenic cells. Applicants should have a strong background in molecular pharmacology and molecular/cell biology techniques. Send curriculum vitae with names of three references to: **Dr. P. Houghton, Department of Molecular Pharmacology, St. Jude Children's Research Hospital, 332 North Lauderdale, Memphis, TN 38105-2794.** *Equal Opportunity/Affirmative Action Employer.*

RESEARCH ASSOCIATE

An active laboratory examining the mechanism of altered wound healing seeks a **RESEARCH ASSOCIATE** to assist with the performance of molecular analysis for the evaluation of the regulation of wound healing. The candidate should be experienced in trauma injury models, techniques of apoptosis, and the detection and regulation of growth factors. Experience with routine techniques to detect RNA and protein levels is required. Candidate must be a Ph.D. This position offers great potential for obtaining grant support from the Shriners of North America. Please send curriculum vitae to: **Business Manager, Department of Surgery, PO Box 670558, Cincinnati, OH 45267-0558.**

POSITIONS OPEN

MBL
MED BIOTECH LABORATORIES
KAMPALA, UGANDA

Three **RESEARCH ASSOCIATE POSITIONS** in Molecular Parasitology are available to clone and characterize lipid modification enzymes of *Onchocerca volvulus* as possible targets of drug development, and to identify and clone genetic markers of ivermectin resistance in parasitic nematodes. Two positions require two to three years of experience in the techniques of screening gene libraries, cloning and expression in bacteria and other expression systems, DNA sequencing, PCR, RNA, PCR finger printing heteroduplex analysis, and RFLPs. One position will require training in biochemistry with experience in enzymology. Send résumé and the names of three references to: **Dr. Thomas G. Egwang, MBL, P.O. Box 9364, Kampala, Uganda. FAX: 256-41-268251.**

POSTDOCTORAL/SCIENTIST position to join a multidisciplinary program to study receptors and subsequent signaling events regulating exocrine secretion by a long-overlooked epithelial cell type, glandular mucous cells. Research will use molecular biological and other contemporary biochemical and microscopic techniques. Position and salary are commensurate with experience. Send curriculum vitae and three letters of recommendation to: **David J. Culp, Ph.D., University of Rochester, School of Medicine and Dentistry, Box 611, Rochester, NY 14642.** *The University of Rochester is an Equal Opportunity/Affirmative Action Employer.*

Infectious Diseases **FELLOWSHIP**: Research Training in Infectious Diseases/Geographic Medicine—Unexpected opening at Case Western Reserve University (CWRU) for qualified M.D. fellowship applicant in NIH-sponsored research training program for 1996 through 1997. Areas of research include mycobacterial diseases, parasitic infections, antimicrobial resistance, molecular retrovirology, and bacterial host defense. *U.S. citizenship or permanent residency required.* Send curriculum vitae and letters of reference to: **W. Henry Bloom, M.D., Case Western Reserve University, 10900 Euclid Avenue, Cleveland, OH 44106-4984.** *CWRU is an Equal Opportunity/Affirmative Action Employer.*

ELECTRON MICROSCOPIST

The Scripps Research Institute (TSRI), the nation's largest not-for-profit biomedical research institution, has an immediate opening for an **ELECTRON MICROSCOPIST** to provide assistance for investigators who use the Institute central facility.

A qualified candidate will have a bachelor's and/or Master's degree in a Biological or Biomedical Science with at least five years of experience performing EM procedures with many, if not all, of the following: negative stain, thin-sections, immunolabeling, freeze-fracture, rotary-shadowing, and cryo sectioning.

TSRI offers a challenging environment and an outstanding benefits package. Qualified candidates please send your résumé as soon as possible to: **The Scripps Research Institute, Ref. AMSCD106, 10666 North Torrey Pines Road, La Jolla, CA 92037. FAX: 619-554-6668.** *We value and support diversity in our workforce/Affirmative Action/Equal Opportunity Employer.*

MEETING

NATO ADVANCED STUDY INSTITUTE (ASI)
The Physiological Ecology of Harmful Algal Blooms
(Co-sponsored by SCOR and the IOC)
27 May to 6 June 1996 at the Bermuda Biological Station for Research

Objectives: Assess present understanding of fundamental physiological and ecological issues underlying harmful algal blooms ("red tides"); identify inadequacies, impediments, and areas for future research; and advance and disseminate new approaches and technologies. Further information and application forms can be obtained from the ASI Director: **Donald M. Anderson, Biology Department, MS 32, Woods Hole Oceanographic Institution, Woods Hole, MA 02543 U.S.A. FAX: 508-457-2134; Email: danderson@whoi.edu.** Application deadline: 1 January 1996.

THE ROCKEFELLER FOUNDATION
POSTDOCTORAL POSITION IN AGRONOMY - MEXICO

The Rockefeller Foundation seeks a postdoctoral agronomist with experience in soil fertility/organic matter management for a program supporting research to improve smallholder, maize-based, agricultural systems in Mexico. The selected candidate will be assigned to a national research institute or university in Mexico that is a grantee of the Foundation.

In Mexico, traditional systems are based on slash-and-burn. With increased pressure on land, fallow periods are short or non-existent and soil fertility is being depleted. Growing maize intercropped or in rotation with legumes (cover crops, green manures, aboneras, slash/mulch systems) apparently has good potential for restoring soil fertility and contributing to a more sustainable and productive agriculture. Such systems, with their multiple variations - are being adopted by farmers in some regions in Central America and Mexico but their effects on labor requirement, soil fertility, soil organic matter, nutrient cycling, weeds, pests, and disease dynamics have not been fully investigated. The program aims at assessing the sustainability of these systems, and improving their productivity and stability through high quality, targeted research.

The successful candidate must be willing to live and conduct field work in the tropics, have excellent academic records, and proficiency in Spanish. She/he will help evaluate research ideas and priorities, contribute to the formulation and implementation of a research agenda responsive to farmers' needs, promote collaboration and coordination among different projects, and participate in the implementation of research activities within a network of local an international scientists from different disciplines.

Interested candidates should send a letter by November 15, 1995, indicating why they are qualified for and interested in the position, enclosing a current curriculum vitae (including academic transcripts), and arrange for three or more letters of reference to be sent to: Mexico Postdoctoral Search, Agricultural Sciences Division, Rockefeller Foundation, 420 Fifth Avenue, New York, NY 10018-2702.

The Rockefeller Foundation is an Equal Opportunity/Affirmative Action Institution

THE ROCKEFELLER FOUNDATION
POSTDOCTORAL POSITION IN AGRONOMY - MALAWI

The Rockefeller Foundation seeks a postdoctoral agronomist for a Foundation-funded program on soil fertility research and development work in Malawi. Over 80% of the Malawian population relies on maize as a staple food, and the crop is planted on approximately 70% of arable smallholder land. The selected candidate will work closely with members of one subgroup of an interdisciplinary Maize Productivity Task Force recently set up by the Government of Malawi which has a mandate to develop and implement policies aimed at increasing maize yields in Malawi.

The aim of the group is to "develop and implement strategies to increase maize production by integrating and increasing production and management of organic matter for resource poor smallholder farmers in Malawi." The Organic Matter Group consists of a small but well-qualified group of scientists, extension specialists drawn from the Malawi Government, Bunda College of Agriculture at the University of Malawi, development projects, NGOs and the International Center for Research Agroforestry.

The successful applicant will have an excellent academic record, developing-country field work experience and the ability to work co-operatively as a member of a research team. Experience in designing and implementing on-farm trials is essential. Field exposure to participatory farmer methods and a disposition to working with communities is highly desirable. The agronomist will work as a member of a team to help develop innovative ideas to help increase crop productivity on depleted smallholder soils. The team is assessing legume and biomass producing species, soil fertility management practices, agroforestry, intercropping systems, and socio-economic constraints to adoption.

The position will be based at Chitedze Research station outside Lilongwe, the capital of Malawi, and will require extensive field work throughout Malawi. The Lilongwe Office of The Rockefeller Foundation will provide local logistical support for the post but the appointee will work under the guidance of the ICRAF's Project leader for the Malawi-ICRAF Agroforestry Project.

Interested candidates should send a letter by November 15th, 1995, indicating why they are qualified for and interested in the position, enclosing a current curriculum vitae (including academic transcripts), and arrange for three or more letters of reference to be sent to: Malawi Postdoctoral Search, Agricultural Sciences Division, The Rockefeller Foundation, 420 5th Avenue, New York, NY 10018-2702.

The Rockefeller Foundation is an Equal Opportunity/Affirmative Action Institution

THE UNIVERSITY OF CALIFORNIA, IRVINE SCHOOL OF BIOLOGICAL SCIENCES ANNOUNCES 3 FACULTY OPENINGS

UCI's School of Biological Sciences has 75 full-time faculty members conducting innovative research in areas such as molecular, cellular and developmental biology, neurobiology, biochemistry, genetics, ecology and evolutionary biology. Together with the basic science departments of the College of Medicine, we operate several well regarded graduate programs. Adding to our successful recruitment of four new faculty members last year, we currently have three tenure-track positions which will require selected candidates to develop and maintain active research programs and to participate in undergraduate and graduate teaching. For each faculty opening, interested candidates should submit a curriculum vita, a description of previous and planned research, a statement of teaching experience, and the names and addresses of three references to the attention of the persons listed below BY DECEMBER 15, 1995.

Department of Developmental and Cell Biology

Assistant Professor

CELL BIOLOGY - Tenure Track

The successful candidate will be expected to develop and maintain an active, funded research program on signal transduction and/or cell-cell signaling, and to participate in teaching cell biology at both graduate and undergraduate levels. Preference will be given to applicants who will strengthen the cell biology research activities in the department. Research interests in the department include molecular genetics, developmental biology, cell biology, and molecular neurobiology. Send materials to: Dr. Peter J. Bryant, Department of Developmental and Cell Biology, UCI, Irvine, CA 92717-2300.

Department of Psychobiology

Assistant Professor

LEARNING AND MEMORY - Tenure Track

Current departmental research emphasizes plasticity with a focus on problems of learning and memory, interactive neuroscience and aging/neurodegeneration. The successful candidate will be a neurobiologist working at the molecular, cellular, systems or behavioral levels in the area of learning and memory. We anticipate the candidate's research will complement current Departmental research programs and have a manifest relationship to some behavioral endpoint. Send materials to Dr. H.P. Killackey, Department of Psychobiology, UCI, Irvine, CA 92717-4550.

Department of Molecular Biology and Biochemistry

Assistant/Associate Professor

STRUCTURAL BIOLOGY - Tenure Track

The successful candidate will have a background in macromuscular crystallography in the study of fundamental biological problems. Facilities at UCI include high field NMR, state-of-the-art x-ray diffraction equipment, and excellent computing facilities including access to the UCSD Super Computing Center. Send materials to: Dr. Thomas Poulos, Department of Molecular Biology and Biochemistry, UCI, Irvine, CA 92717-3900.

****

Located 6 miles from the ocean in Orange County, UCI is in the center of a flourishing high technology and cultural center. As one of nine University of California campuses, UCI is among the most respected institutions of higher education in the country. We are an equal opportunity employer committed to excellence through diversity.

ANNOUNCEMENT

RESEARCH INQUIRIES INVITED

The Smokeless Tobacco Research Council, Inc. invites inquiries regarding grant applications.

The Council sponsors independent research into questions of smokeless tobacco and health. Research support is through a program of grants-in-aid.

Grant applications are evaluated by the Scientific Advisory Board to the Council and will be judged solely on the basis of scientific merit and relevance.

Deadlines for submission of grant applications are December 31st for July 1st funding and June 30th for January 1st funding. Address inquiries or requests for applications to:

The Smokeless Tobacco Research Council, Inc.
420 Lexington Avenue, New York, NY 10170
Telephone: 212-697-3485
FAX: 212-986-8631